Zinc biogeochemical cycle in the Tasman Sea: Potential role for phytoplankton communities

"Debout sur le zinc"

by

Marie SINOIR, MAS in Marine biogeochemistry

Submitted in fulfilment of the requirements for the Degree of

Doctor of Philosophy in Quantitative Marine Science

(A joint CSIRO and UTAS PhD program in quantitative marine science)

University of Tasmania

April 2013

Zinc biogeochemical cycle in the Tasman Sea: Potential role for phytoplankton communities

Marie SINOIR, PhD in Marine biogeochemistry

April 2013

Declaration of originality

"This thesis contains no material which has been accepted for a degree or diploma by the University or any other institution, except by way of background information and duly acknowledged in the thesis, and to the best if my knowledge and belief no material previously published or written by another person except where due acknowledgement is made in the text of the thesis, nor does the thesis contain any material that infringes copyright."

Authority of Access

"This thesis may be made available for loan and limited copying and communication in accordance with the Copyright Act 1968."

Statement regarding published work contained in thesis

"The publishers of the paper comprising Chapter Two hold the copyright for that content, and access to the material should be sought from the respective journal. The remaining non published content of the thesis may be available for loan and limited copying and communication in accordance with the Copyright Act 1968."

Marie Sinoir, April 2013

Acknowledgements

My first and biggest thanks go to my four supervisors who took the time to share their knowledge in the good and the bad moments of this PhD. They've always found the way to bring me up and support me during those 3 years and a half and, by doing so, helped me find the confidence, the energy and the courage to keep this experience going. Many thanks Drs Andrew R. Bowie (Utas, ACE-CRC, IMAS), Mathieu Mongin (CSIRO Hobart Laboratories), Edward C. V. Butler (AIMS) and Christel S. Hassler (Université de Genève).

I'd like to thank the Quantitative Marine Science program (Institute for Marine and Antarctic Studies: IMAS and CSIRO Marine and Atmospheric Research Laboratories: CMAR) to provide the funding and scholarships for this work. This research was also partly supported by the Australian Climate and Ecosystem CRC (ACE-CRC). I'd like to thank Drs. Denbeigh Armstrong and Heidi Auman, graduate research manager of the Quantitative Marine Science program for their time answering all the questions and worries during those three years.

I'd also like to address a particular thanks to Dr. Michael Ellwood (University of Canberra) for sharing his knowledge on zinc speciation and his enthusiasm in every little good news I had during the 6 weeks in Canberra. Thanks to Claire, Moneesha, Aimee, Kelly and Steve too for their delicate attentions and help to make things easier during this time.

A particular thanks to Robin, Lesly and Val from Utas.

Thanks to my family, specially my parents, for giving me the opportunity to travel so far and experience something different at the other side. A big thought

to both my grand dads, I'm glad I made it back in France this last summer and really relieved I was able to see both of you.

Thanks to Skye, Jess, Veronique, Amélie, Melody, Narissa, Louiza, Celeste, Polly, Lucy, Alexis, Anthea, Craig, Pru, Tim(s), Mark, Jeanette, Ros…all of you made things so much easier, sharing good, bad, office or personal life. We increased the collection of postcards in the office for the next generations of PhD students and shared so many good times with wines, café, brekkies and others… Many thanks to Lucia and Erica, my two little monsters who helped me once a week to forget science. I had lots of fun going back to child games and songs with you. Many thanks to Sue, Lyn, Shelah, Tessa, Norman and many others. The time shared helped me keep on going while sharing laughing Monday afternoons!

I'd like to address a particular warm thanks to Laurent, Camille, Juliette and Nicolas. Laurent, new year and nice book to write, thanks for your support, particularly in these last months, we could thank Skype too, it deserved it! Juliette, I'm finishing on your birthday, how's that!!

"One day baby, we'll be old, Oh baby, we'll be old, and think of all the stories that we could have told" —Asaf Avidan, Reckoning Song—

Abstract

Zinc (Zn) plays an essential role in metabolic and structural functions for marine phytoplankton, being required in nearly 300 enzymes and proteins including carbonic anhydrase and alkaline phosphatase. The concentration of total dissolved Zn in the open-ocean is typically in the nanomolar (0.1-10 nmol L^{-1}) range, 98 % of which is complexed by natural strong organic ligands.

In January and February 2010, the Primary productivity Induced by Iron and Nitrogen in the Tasman Sea (PINTS) cruise covered a north to south transect from the oligotropic Tasman Sea to the productive waters of the subantarctic Southern Ocean. For this thesis, samples for chemical analyses and laboratory-based cultures were collected to assess the relationship between phytoplankton growth and zinc bioavailability and speciation in this region.

The pennate diatom *Nitzschia closterium* and the coccolithophorid *Emiliania huxleyi* were cultured at low free Zn concentrations ($[Zn^{2+}]$ = 1.5 x 10^{-12} M and $[Zn^{2+}]$ = 1.5 x 10^{-14} M) to mimic the range of free Zn encountered in marine systems. Both species were able to maintain their photosynthetic activity and growth at the low $[Zn^{2+}]$ applied. However, while *E. huxleyi* grew at these low concentrations, *N. closterium* seemed to accelerate its uptake with specific and efficient transporters and access complexed Zn.

In the Tasman Sea, total dissolved Zn was observed at 0.02 to 0.19 nmol L^{-1} (at 15 m depth) and 0.02 to 0.11 nmol L^{-1} (at 150 m) along the north-south transect studied, below the range reported for other open-ocean regions. Measurements with Anodic Stripping Voltammetry (ASV) on four selected profiles from the Tasman Sea established the concentrations of labile Zn (0.6 to

500 pmol L^{-1}) and Zn-complexing ligands (0.23 to 4.19 nmol L^{-1}) for the first time in the Tasman Sea. Zn speciation was dominated by complexation to organic ligands (59 to 98%) with the highest percentages in surface. These ligands were closely related to the phytoplankton assemblages found in the studied region (Chlorophytes ~ Haptophytes > Diatoms).

The links between chemistry and biology were studied with a simple conceptual ZnPPZZD model. It was parameterised with information gained in the experimental phases of this work, such as the difference of uptake response observed for the two species and range of concentrations measured. The model showed the concentration of ligands and zinc speciation played an important role in the structure of the conceptual phytoplankton assemblages. Further work is required to assess if ligands are produced by the organisms to enhance their uptake or if the chemistry of Zn strongly influences the community for a specific region.

CONTENTS

CHAPTER ONE

Preamble

1.1 General concepts and definitions concerning trace elements chemistry and role:

Nutrients present in seawater are separated into two classes which are empirically defined based on their respective concentrations (Bruland and Lohan, 2003). Macronutrients or major nutrients are present at concentrations greater than 10 µmol kg^{-1}, or ~1ppm by weight. Three major nutrients are present in seawater, nitrogen (N) present under 5 redox states, orthophosphates (PO_4^{3-}) are the major species of phosphorus (P) in seawater and silicic acid (Si), of which the major bioavailable species is orthosilicic acid $Si(OH)_4$ (Table 1a). These macronutrients are essential for respiration and photosynthesis, basic metabolism but also structural functions. They are assimilated in the surface layer by marine microorganisms, phytoplankton and other microorganisms such as viruses and bacteria.

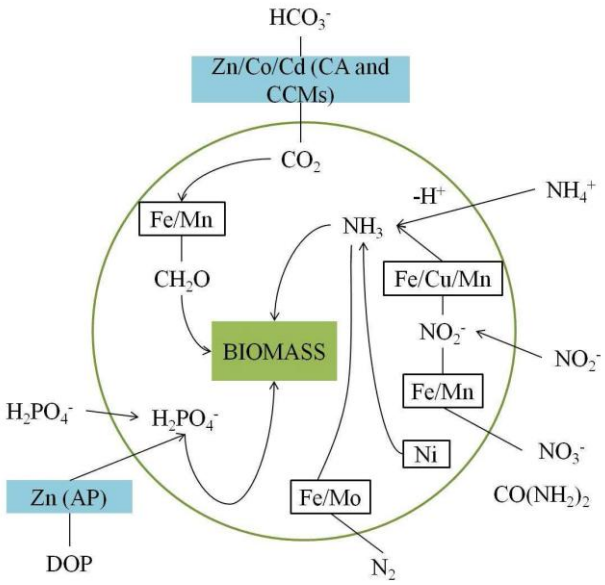

Fig. 1: Example of selected biological role of trace metals for a phytoplankton cell. Zinc roles have been highlighted. CA: carbonic anhydrase; CCMs: Carbon concentration mechanisms; AP: alkaline phosphatase. Adapted from Morel and Price 2003.

Table 1: Range of total dissolved concentrations, average concentration in the open ocean and residence time of macronutrients and selected trace elements. Data for the water column are presented and selected from Bruland and Lohan (2003) and www.mbari.org/chemsensor/summary.html (23.08.2012)

a. Macronutrients:

Macronutrients	Average concentration	Residence time (years)
N_2	590 µmol kg^{-1}	
NO_3	30 µmol kg^{-1}	3 000
PO_4 (Phosphate)	2 µmol kg^{-1}	69 000
Si (Silicium)	99.7 µmol kg^{-1}	20 000
Carbon (C)	2.25 mmol kg^{-1}	83 000

b. Trace elements:

Trace elements	Range of concentrations	Mean ocean concentration	Residence time (years)
Co	4 to 300 pmol kg^{-1}	20 pmol kg^{-1}	340
Mn	0.06 to 5 nmol kg^{-1}	360 pmol kg^{-1}	60
Fe	0.02 to 0.2 nmol kg^{-1}	540 pmol kg^{-1}	500 (10 d to 1 y in surface waters, Croot *et al.* 2004)
Cd	1 to 1000 pmol kg^{-1}	620 pmol kg^{-1}	50 000
Cu	0.5 to 4.5 nmol kg^{-1}	2.4 nmol kg^{-1}	5000
Zn	0.05 to 9 nmol kg^{-1}	5.4 nmol kg^{-1}	50 000
Ni	2 to 12 nmol kg^{-1}	8.2 nmol kg^{-1}	6 000
Mo	105 nmol kg^{-1}	—	760 000

Trace elements, micronutrients or trace metals in seawater (typically first-row transition metals, e.g. iron, manganese, zinc, cobalt) are present in lower concentrations than the major nutrients by several orders of magnitude. Bruland and Lohan (2003) defined the range of concentrations between 10 µmol kg^{-1} for the highest and 0.5 fmol kg^{-1} for the lowest (*e.g.* Table 1b). These micronutrients are very important for different metabolic and structural functions of these organisms, mainly as the metal centre in various enzymes (Fig. 1). However, in surface waters, the combination of intense biological activity, strong chemical reactivity of these trace elements (adsorption or desorption on particles), transport to depth (scavenging and sinking) and irregular external inputs imply a quicker turnover for trace elements in surface waters (*e.g. for Fe*: Sarthou *et al.* 2003, Croot *et al.* 2004, Sarthou *et al.* 2007). This rapid cycling in comparison to macronutrients can partially explain the pronounced gap and decoupling between macro and micronutrients concentrations. It is essential to determine and quantify their role for the open ocean ecosystem and impact on phytoplankton community in addition to their eventual coupling with macronutrients cycles, especially in a changing ocean (Morel 2008).

Interactions, or feedback effects, between trace elements and phytoplankton have been studied and described in several papers (Morel *et al.* 1991, Sunda and Huntsman 1992, Gonzalez-Davila 1995, Whitfield 2001, Morel and Price 2003, Sunda 2012). The combination of extremely low concentrations, bioavailability and important biological roles of trace elements for phytoplankton usually evokes the notion of limitation or co-limitation (Arrigo *et al.* 2005, Saito *et al.* 2008). The limitation concept concerns the impact of environmental factors —biotic or abiotic— on phytoplankton growth, usually leading to a decrease in their growth rate and the reduction of the development of the different

phytoplankton communities (Arrigo, 2005; Saito *et al*., 2008). With evolution, changing global conditions and exposure to diminished concentrations of trace metals, organisms have developed mechanisms to be able to access such resources and grow (Sunda and Hunstman 1992, 1995; Strzepek and Harrison 2004; Saito *et al*. 2011). A classic example of such mechanisms is the metal inter-replacement, which leads to complicated metal-metal interactions. However, such interactions between trace metals are ambiguous for the phytoplankton community as they may induce both competitive and synergetic effects (Bruland *et al.* 1991; Whitfield 2001; Peers *et al*. 2005; Maldonado *et al*. 2006; Fig. 2). The case of Zn, Co and Cd interaction is a classic advantageous metal-metal interaction for most species able to adopt it. However, interactions between manganese —Mn— and copper —Cu— provoke a growth inhibition by lowering the uptake of one essential metal due to a competitive effect with the other metal (Sunda and Huntsman, 1998).

Most of the micronutrients exhibit lower free concentrations in the surface waters not only because of the intense biological activity but also because of their high degree of complexation with organic or inorganic strong ligands present in the water column (Vraspir and Butler 2009, Hirose *et al*. 2011). These ligands affect the bioavailability of trace metal, increasing or reducing their accessibility for the phytoplankton. The bioavailability concept can simply be defined as the chemical form that can be assimilated by the phytoplankton. These chemical forms vary from one microelement to the other and can be organic, inorganic complexes or the free ion present in seawater (Saito *et al.* 2008). However, observations are complicated due to the variable nature of ligands. It seems that those ligands form complexes that are either kinetically labile enough to be available for the phytoplankton or non-bioavailable and create a loss

of trace elements throughout the sinking of particle (Morel and Price 2003). Thus, trace element bioavailability is a sophisticated concept to define (Hassler *et al.* 2012) due to the different nature of ligands and phytoplankton species. The importance of the ligands origin has been demonstrated in several studies (Gerringa *et al.* 2008; Benner 2011; Ibisanmi *et al.* 2011; Schlosser *et al.* 2012). In the case of organic ligands, such as humic substances (humic and fulvic acids), complexation effects range from enhanced to reduced biouptake (Campbell *et al.* 2002; Hirose 2007). Aside from these organic ligands, inorganic ones are present in seawater. In the presence of inorganic ligands (*e.g.* Cl^-, CO_3^{2-}, SO_4^{2-}), bioavailability of trace elements is still relatively poorly understood.

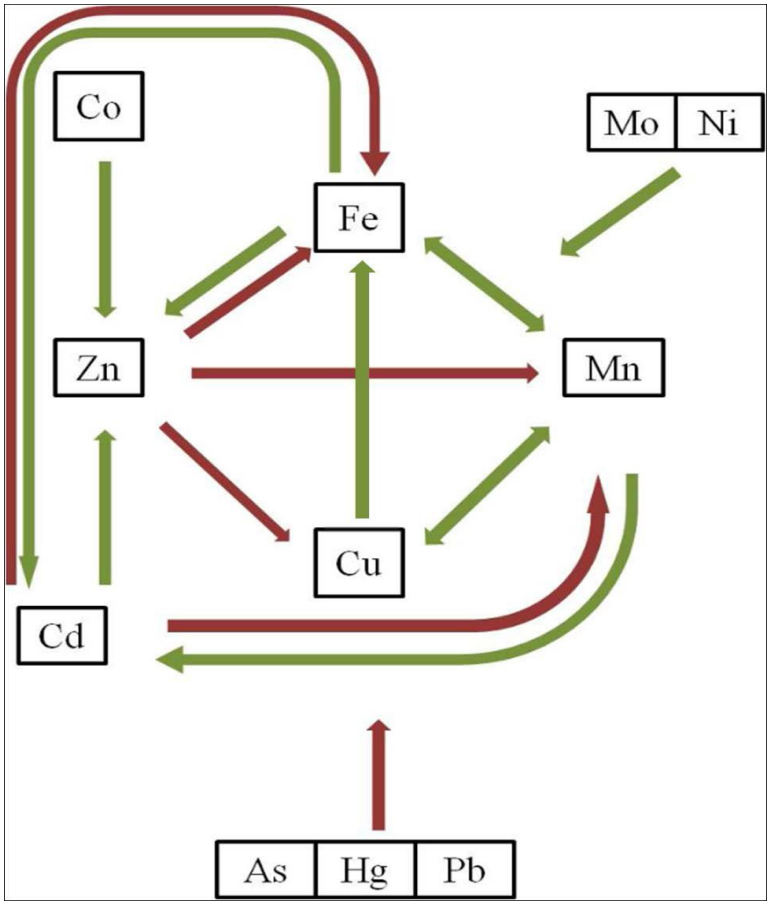

Fig. 2: Interactions between trace elements for a phytoplankton cell, in red the deleterious interactions and in green the advantageous interactions. Adapted from Bruland *et al.* 1991 and Whitfield 2001.

The first trace element intensively studied in the ocean was iron (Fe). The heightened interest in Fe came from the discovery of its importance for the biological pump and its relation to absorption of carbon by the ocean. This was called the 'iron hypothesis' by Martin *et al. (*1990*a*). Fe is a limiting micronutrient in areas where macronutrients are in high concentrations, but remain under-utilised; and therefore, chlorophyll concentrations are lower than expected. These regions are referred to as High Nutrient Low Chlorophyll (HNLC) areas — such as the Southern Ocean (Martin *et al.* 1990*b*, Löscher *et al.* 1995, De Baar *et al.* 1997, Tagliabue *et al.* 2012) and the Pacific (Kolber *et al.* 1994) and typically ~ 40% of the open ocean.

The increasing chemical and biological data, together with the development of model tools, has allowed Fe to be included in global biogeochemical models to interpret and predict biogeochemistry of HNLC areas (IRONEX II: Archer and Johnson 2000; HAMOCC5: Aumont *et al.* 2003; SWAMCO-4: Pasquer *et al.* 2005). These global biogeochemical models decisively showed that Fe availability limited growth rate in the HNLC regions. They were crucial in confirming the importance of studying trace elements in their global cycles. In light of the importance of Fe *speciation* in seawater, new models are now being developed to also take into account this complexity (Tagliabue and Arrigo 2006; Fan and Dunne 2011; Tagliabue and Völker 2011).

With advances in research and, in part, in understanding the chemistry and role of the oceans, other elements appear to be influential, too, regarding primary productivity. Morel *et al.* (1994) were first to mention the possible role of zinc (Zn) in limiting phytoplankton and to introduce, in the same manner as Martin *et*

al. (1990), the 'zinc hypothesis'. However, there is still a large gap between iron research and that of other trace elements as a search on Scopus (http://www.scopus.com: 27. 08. 2012) data base reveals. The number of papers on Fe ligands in seawater (144) far surpasses those on Zn ligands (44). In the same manner, a global search on Fe and Zn biogeochemistry in seawater gives 118 and 23 papers for Fe and Zn, respectively. The main difference between Fe and Zn is that Zn is one of the most difficult trace elements to measure due to its high risk of contamination (Fahrbach *et al.* 2011). Reliable data on Zn concentrations and speciation are becoming available and allow a more precise determination of Zn biogeochemistry in various regions. The combination of culture experiments and chemical data show that Zn would fit more accurately with co-limitation. Zn affects oceanic productivity when its concentrations are extremely low, but in accordance with factors such as light, carbon or other nutrients' concentration (Muller *et al.*, 2003; Sunda and Hunstman, 2005; Saito *et al.*, 2008). Indeed, studies have shown that there are regions of the ocean that are not limited in Fe but still have low micronutrients' concentrations and limited Chl *a* (Sargasso Sea: Shaked *et al.* 2006; Wisniewski-Jakuba *et al.* 2008 and parts of the Southern Ocean: Hassler *et al.* 2012). This combination of conditions has also suggested a place for Zn in determining the phytoplankton assemblages in the different regions studied.

In this work, Zn's biogeochemical role was studied in the Tasman Sea. The predicted sensitivity of this waterbody to temperature rise (Hobday *et al.* 2008) and its socio-economic importance to Australia and New-Zealand reinforce the relevance of studying this region. Several studies also highlighted the sensitivity of this region to dust deposition and the impact of these sporadic

and localised inputs of trace metals on primary production (Calvo *et al.* 2004, Marx *et al.* 2008, McGowan and Clark 2008, Mongin *et al.* 2011). Moreover, a recent study underlined the increased productivity of this region in the last decade with inputs from the Australian desert (Matear *et al.* 2012, in press). This region is of prime interest in a changing ocean as this study revealed an increase of the carbon sequestration over the last decade.

The work conducted during this PhD aims to bring new data and understanding of Zn's role in this region and the response of phytoplankton to its low concentrations. The quantification and qualification of this role in the Tasman Sea demanded, first, to review the current knowledge on Zn biogeochemistry in seawater (Sinoir *et al.* 2012). In this review, knowledge and gaps of the current research were identified and potential paths for advancement addressed. The scope of the following chapters is based on this review and covers biological, chemical and modeling aspect to better understand Zn biogeochemical cycle in the Tasman Sea. In chapter three, two species present in the Tasman Sea were grown and cultured to study their Zn requirement and response to the low free ion concentration found in the same region. Although Zn is a required element for living organisms, its speciation in seawater affects organisms' ability to access to it. Different analytical methods for Zn determination allow measurement of its speciation in seawater (van den Berg, C. M. G. 1985; Bruland 1989; Donat and Bruland 1990). In chapter four, Zn speciation was measured using voltammetry (ASV) technique across a north- south transect in the Tasman Sea from samples taken during the PINTS voyage (January 2010). The final work and chapter was done by gathering all data obtained during this work to create a ZnPPZZD type conceptual model driven by the hypothesis that Zn chemical speciation partially drove the phytoplankton community. This chapter is a preliminary

work on integrating zinc speciation in a global model. The main discussion, chapter six, summarizes the results obtained in the previous chapters, discusses in further details outputs obtained with the model and opens on perspectives for future work and orientations.

1.2 References:

Archer, D. E., and Johnson, K. (2000), A Model of the Iron Cycle in the Ocean, *Global biogeochemical. cycles*, **14.**

Ardelan, M. V. , Steinnes, E., Lierhagen, S., and Linde, S. O. (2009). Effects of experimental CO_2 leakage on solubility and transport of seven trace metals in seawater and sediment, *Science of The Total Environment*, **407**, 6255-6266.

Arrigo, K. R. (2005). Marine microorganisms and global nutrient cycles, *Nature*, **437**, 349-355.

Aumont, O., Maier-Reimer, E., Blain, S., and Monfray, P. (2003). An ecosystem model of the global ocean including Fe, Si, P colimitations, *Global biogeocheical. cycles*, **17,** *doi:* 10.1029/2001gb001745.

Benner, R.(2011). Loose ligands and available iron in the ocean. *Proceedings of the National Academy of Sciences*, **108,** 893-894.

Bruland, K. W., and Lohan, M. C. (2003). Controls of Trace Metals in Seawater, in 'Treatise on Geochemistry', pp. 23-47 (Pergamon, Oxford).

Bruland, K. W. (1989). Complexation of zinc by natural organic ligands in the central north pacific. *Limnology and Oceanography* **34**, 269-285.

Bruland, K. W., Donat, J. R., and Hutchins, D. A. (1991). Interactive Influences of Bioactive Trace Metals on Biological Production in Oceanic Waters. *Limnology and Oceanography*, **36,** 1555-1577.

Calvo, E., Pelejero, C., Logan, G. A., and de Deckker, P. (2004). Dust-induced changes in phytoplankton composition in the Tasman Sea during the last four glacial cycles. *Paleoceanography*, **19**

Campbell, P. G. C., Errécalde, O., Fortin, C., Hiriart-Baer, V. P., and Vigneault, B. (2002). Metal bioavailability to phytoplankton– applicability of

the biotic ligand model, *Comparative Biochemistry and Physiology Part C: Toxicology & Pharmacology*, **133**, 189-206.

Croot, P. L., Streu, P., and Baker, A. R. (2004) Short time residence time for iron in surface water impacted by atmospheric dry deposition from Saharan dust events. *Geophys. Res. Lett.*, **31**, doi: 10.1029/2004GL020153.

De Baar, H. J. W., De Jong, J. T. M., Nolting, R. F., Timmermans, K. R., Van Leeuwen, M. A., Bathmann, U., Rutgers Van Der Loeff, M., and Sildam, J. (1999). Low dissolved Fe and the absence of diatom blooms in remote Pacific waters of the Southern Ocean. *Marine Chemistry,* **66,** 1-34.

Delille, B., Harlay, J., Zondervan, I., Jacquet, S., Chou, L., Wollast, R., Bellerby, R. G. J., Frankignoulle, M., Borges, A. V., Riebesell, U., and Gattuso, J. P. (2005). Response of primary production and calcification to changes of pCO_2 during experimental blooms of the coccolithophorid *Emiliania huxleyi*, *Global Biogeochemical Cycles*, **19**, doi:10.1029/2004GB002318.

Donat, J. R., and Bruland, K. W. (1990). A comparison of two voltammetric techniques for determining zinc speciation in Northeast Pacific Ocean waters. *Marine Chemistry* **28**, 301-323.

Doney, S. C., Fabry, V. J., Feely, R. A., and Kleypas, J. A. (2009). Ocean acidification: the other CO_2 problem, *Annual Review of Marine Science*, **1**, 169-192.

Fan, S-M., and Dunne, J. P. (2011). Models of iron speciation and concentration in the stratified epipelagic ocean, *Geophysical Research Letters*, **38**, L15611, doi:10.1029/2011GL048219.

Fahrbach, E., de Baar, H. J. W., Garçon, V. C., and Provost, C. (2011). Introduction to physics, carbon dioxide, trace elements and isotopes in the Southern Ocean: The Polarstern expeditions ANT-XXIV/3 (2008) and

ANT-XXIII/3 (2006). *Deep Sea Research Part II: Topical Studies in Oceanography,* **58,** 2501-2508.

Gerringa, L. J. A., Blain, S., Laan, P., Sarthou, G., Veldhuis, M. J. W., Brussaard, C. P. D., Viollier, E., and Timmermans, K. R. (2008). Fe-binding dissolved organic ligands near the Kerguelen Archipelago in the Southern Ocean (Indian sector). *Deep Sea Research Part II: Topical Studies in Oceanography,* **55,** 606-621.

González-Dávila, M. (1995). The role of phytoplankton cells on the control of heavy metal concentration in seawater, *Marine Chemistry,* **48**, 215-236.

Hirose, K. (2007). Metal-organic matter interaction: Ecological roles of ligands in oceanic DOM. *Applied Geochemistry,* **22,** 1636-1645.

Hirose, K., Saito, T., Lee, S. H., and Gastaud, J. (2011). Vertical distributions of the strong organic ligand in the twilight zone of Southern Hemisphere Ocean particulate matter. *Progress in oceanography,* **89,** 108-119.

Hobday, A. J., Poloczanska, E. S., and Matear R .J. (eds) (2008), *Implications of climate change for Australian fisheries and aquaculture: a preliminary assessment*, Report to the Department of Climate Change, Canberra

Ibisanmi, E., Sander, S. G., Boyd, P. W., Bowie, A. R., and Hunter, K. A. (2011). Vertical distributions of iron-(III) complexing ligands in the Southern Ocean. *Deep Sea Research Part II: Topical Studies in Oceanography,* **58,** 2113-2125.

Kolber, Z. S., Barber, R. T., Coale, K. H., Fitzwater, S. E., Greene, R. M., Johson, K. S., Lindley, S., and Falkowski, P. G. (1994). Iron limitation of phytoplankton photosynthesis in the equatorial Pacific Ocean. *Nature,* **371,** 145-149.

Löscher, B. M., De Baar, H. J. W., De Jong, J. T. M., Veth, C., and Dehairs, F.

(1997). The distribution of Fe in the Antarctic Circumpolar Current. *Deep-Sea Research Part II: Topical Studies in Oceanography*, **44,** 143-187.

Maldonado, M. T., Allen, A. E., Chong, J.S., Lin, K., Leus, D., Karpenko, N., and Harris, S. L., (2006), Copper-dependent iron transport in coastal and oceanic diatoms, *Limnology and Oceanography*, **51**, 1729-1743.

Martin, J. H., Gordon, R. M., and Fitzwater, S. E. (1990*a*). Iron in the Antarctic waters. *Nature* **345**, 156-158.

Martin, J. H., Fitzwater, S. E., and Gordon, R. M. (1990*b*). Iron deficiency limits phytoplankton growth in Antarctic waters. *Global Biogeochemical Cycles,* **4,** 5-12.

Matear, R. J., Mitchell, R. M., Qin, Y., and Mongin, M. (2012) Decadal increase in clorophyll-A over the Tasman Sea driven by enhanced dust supply from Central Australia, in press.

Marx, S. K., Kamber, B. S., and McGowan, H. A. (2008). Scavenging of atmospheric trace metal pollutants by mineral dusts: Inter-regional transport of Australian trace metal pollution to New Zealand. *Atmospheric Environment*, **42,** 2460-2478.

McGowan, H., and Clark, A. (2008). Identification of dust transport pathways from Lake Eyre, Australia using Hysplit. *Atmospheric Environment,* **42,** 6915-6925.

Mongin, M., Matear, R., and Chamberlain, M. (2011). Simulation of chlorophyll and iron supplies in the Sub Antarctic Zone South of Australia. *Deep-Sea Research Part II: Topical Studies in Oceanography*, **58,** 2126-2134.

Morel, F. M. M. (2008). The co-evolution of phytoplankton and trace element cycles in the oceans. *Geobiology*, **6,** 318-324.

Morel, F. M. M. (2008). The co-evolution of Trace Metals in the Oceans. *Science,*

300, 944-947.

Morel, F. M. M., and Price, N. M. (2003). The biogeochemical cycles of trace metals in the oceans. *Science* **300**, 944-947.

Morel, F. M. M., Hudson, R. J. M., and Price, N. M. (1991). Limitation of Productivity by Trace Metals in the Sea. *Limnology and Oceanography,* 36**,** 1742-1755.

Morel, F. M. M., Reinfelder, J. R., Roberts, S. B., Chamberlain, C. P., Lee, J. G., and Yee, D. (1994). Zinc and carbon co-limitation of marine phytoplankton. *Nature,* **369,** 740-742.

Muller, F. L. L., Jacquet, S., and Wilson, W. H. (2003). Biological Factors Regulating the Chemical Speciation of Cu, Zn, and Mn under Different Nutrient Regimes in a Marine Mesocosm Experiment, *Limnology and Oceanography*, **4**8, 2289-2302.

Pasquer, B. , Laruelle, G. , Becquevort, S. , Schoemann, V. , Goosse, H., and Lancelot, C. (2005). Linking ocean biogeochemical cycles and ecosystem structure and function: results of the complex SWAMCO-4 model, *Journal of Sea Research*, **53**, 93-108.

Peers, G., Quesnel, S. A., and Price, N. M. (2005). Copper requirement for iron acquisition and growth of coastal and oceanic diatoms, *Limnology and Oceanography*, **50**, 1149-1158.

Rost, B., Zondervan, I., and Wolf-Gladrow, D. (2008). Sensitivity of phytoplankton to future changes in ocean carbonate chemistry: current knowledge, contradictions and research directions, *Marine Ecology Progress Series,* **373**, 227-237.

Saito, M. A., Bertrand, E. M., Dutkiewicz, S., Bulygin, V. V., Moran, D. M., Monteiro, F. M., Follows, M. J., Valois, F. W., and Waterbury, J. B.

(2011). Iron conservation by reduction of metalloenzyme inventories in the marine diazotroph Crocosphaera watsonii. *Proceedings of the National Academy of Sciences,* **108,** 2184-2189.

Saito, M. A., Goepfert, T. J., and Ritt, J. T. (2008). Some thoughts on the concept of colimitation: Three definitions and the importance of bioavailability. *Limnology and Oceanography,* **53,** 276-290.

Sarthou, G., Baker, A., Kramer, J., Laan, P., Laës, A., Ussher, S., Achterberg, E., de Baar, H. J. W., Timmermans, K. R., and Blain, S. 2007, Influence of atmospheric inputs on the rion distribution in the subtropical North-East Atlantic Ocean, *Marine Chemistry*, **104**, 186-202.

Sarthou, G., Baker, A. R., Blain, S., Achterberg, E. P., Boye, M., Bowie, A. R., Croot, P. L., Laan, P., de Baar, H. J. W., Jickells, T. D. *et al.* 2003, Atmospheric iron deposition and sea-surface dissolved iron concentrations in the eastern Atlantic ocean, *Deep Sea Research I*, **50**, 1339-1352.

Schlosser, C., de la ROCHA, C. L., Streu, P., and Croot, P. L. (2012). Solubility of iron in the Southern Ocean. *Limnology and Oceanography,* **58,** 684-697.

Shaked, Y., Xu, Y., Leblanc K., and Morel, F. M. M. (2006). Zinc availability and alkaline phosphatase activity in *Emiliania huxleyi*: Implications for Zn-P co-limitation in the ocean *Limnology and Oceanography,* **51,** 299-309.

Sinoir, M., Butler, E. C. V., Bowie, A. R., Mongin, M., Nesterenko, P. N., Hassler, C. S. (2012). Zinc marine biogeochemistry in seawater: a review. *Marine and Freshwater Research,* **63,** 644-657.

Strzepek, R. F., and Harrison, P. J. (2004). Photosynthetic architecture differs in coastal and oceanic diatoms. *Nature,* **431,** 689-692.

Sunda, W. G. (2012). Feedback Interactions between Trace Metal Nutrients and

Phytoplankton in the Ocean. *Frontiers in microbiology,* **3,** 204.

Sunda, W. G., and Huntsman, S. A. (2005). Effect of CO_2 Supply and Demand on Zinc Uptake and Growth Limitation in a Coastal Diatom, *Limnology and Oceanography*, **50**, 1181-1192.

Sunda, W. G., and Huntsman, S. A. (1998). Processes regulating cellular metal accumulation and physiological effects: Phytoplankton as model systems, *Science of The Total Environment*, **219**, 165-181.

Sunda, W. G., and Huntsman, S. A. (1995). Cobalt and zinc interreplacement in marine phytoplankton: biological and geochemical implications. *Limnology and Oceanography*, **40,** 1404-1417.

Sunda, W. G. and Huntsman, S. A. (1992). Feedback interactions between zinc and phytoplankton in seawater. *Limnology and Oceanography*, **37,** 25-40.

Tagliabue, A., and Arrigo, K. R. (2006). Processes governing the supply of iron to phytoplankton in stratified seas. *Journal of Geophysical Research C: Oceans*, **111,** C06019, doi:10.1029/2005JC003363.

Tagliabue, A., and Völker, C. (2011). Towards accounting for dissolved iron speciation in global ocean models. *Biogeosciences,* **8,** 3025-3039.

Tagliabue, A., Mtshali, T., Aumont, O., Bowie, A. R., Klunder, M. B., Roychoudoury, A. N., and Swart, S. (2012). A global compilation of dissolved iron measurements: Focus on distributions and processes in the Southern Ocean. *Biogeosciences,* **9,** 2333-2349.

van den Berg, C. M. G. (1985). Determination of the zinc complexing capacity in seawater by cathodic stripping voltammetry of zinc—APDC complex ions. *Marine chemistry* **16**, 121-130.

Vraspir, J. M., and Butler, A. (2009). Chemistry of marine ligands and siderophores. *Annual Review of Marine Science,* **1,** 43-63.

Whitfield M. (2001). Interactions between Phytoplankton and Trace Metals in the Ocean. *Advances in marine biology,* **41,** 1-128.

Wisniewski-Jakuba, R., Moffett, J. W., and Dyhrman, S. T. (2008). Evidence for the linked biogeochemical cycling of zinc, cobalt, and phosphorus in the western North Atlantic Ocean. *Global biogeochemical cycles,* **22,** 13.

CHAPTER TWO

Zinc marine biogeochemistry in seawater: a review

Sinoir, Marie [(1), (2)], Butler, Edward C.V. [(1)*], Bowie, Andrew R. [(2), (3)], Mongin, Mathieu [(1)], Nesterenko, Pavel N. [(3)], Hassler, Christel S. [(4)]

(1) CSIRO Marine and Atmospheric Research, Hobart Laboratories, Castray Esplanade, Hobart TAS 7000, Australia

(2) Institute for Marine and Antarctic Studies, University of Tasmania, Sandy Bay 7006, Australia

(3) Antarctic Climate and Ecosystem Cooperative Research Centre (ACE CRC), University of Tasmania, Hobart, TAS 7001, Australia

(4) Australian Centre for Research on Separation Science (ACROSS) School of Chemistry, University of Tasmania, TAS 7001, Australia

(5) Plant Functional Biology and Climate Change Cluster, University of Technology Sydney, Broadway, NSW 2007 Australia

* Current address: Ultramarine Concepts, PO Box 476, Sandy Bay TAS 7006

Published in Marine and Freshwater Research, 63, 644-657

2.1 Introduction:

Trace metals in seawater (typically first-row transition metals, e.g. iron —Fe—, zinc —Zn—, cobalt —Co—) are present at concentrations several orders of magnitude lower than macronutrients. Since the early recommendations by Patterson and Settle (1976) and Bruland *et al.* (1979) for contamination-free sampling and analysis for trace elements, which have recently been expanded through protocols recommended for voyages undertaken in the GEOTRACES (www.geotraces.org) program (Bowie and Lohan 2009; Cutter *et al.* 2010), it has become possible to obtain 'oceanographically consistent' distributions for trace metals in the ocean. The priority of this international program is to investigate and understand the distribution and role of trace elements in seawater. The use of isotopes and proxies provides new data information on their sources and important processes in order to characterise their biogeochemical cycle and relation to other nutrient's cycles in a similar way that was established for iron. Indeed, two decades ago, Martin *et al.* (1990) described the relation between supply of Fe, oceanic marine productivity and Earth climate cycles. This led to the famous 'iron hypothesis', illustrating the importance of Fe in nutrient assimilation by phytoplankton, and thus, in the global carbon cycle. New observations linking low concentrations (due to highly organic complexation and low solubility in seawater), a nutrient-like distribution and an essential biological role in many cell functions and reactions brought the notion of Fe acting as a limiting nutrient. As a consequence, Fe has been intensively studied, including both natural and artificial fertilisation experiments (e.g. SOIREE 1999, FeCycle 2003, KEOPS 2005), to describe its cycle and budget (e.g. Bowie *et al.* 2001; McKay *et al.* 2005; Frew *et al.*, 2006).

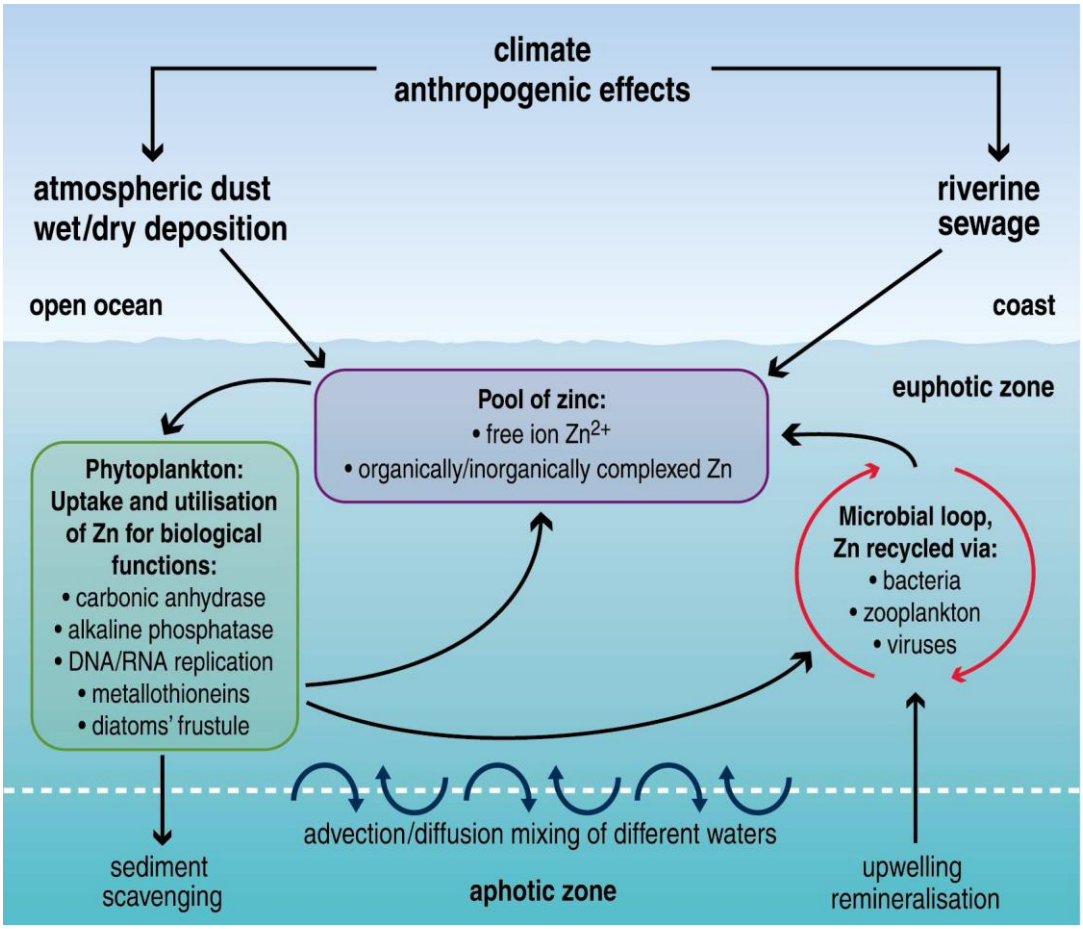

Figure 1: The global biogeochemical cycling of zinc between ocean and atmosphere, placed in a climate context.

The introduction of trace metal clean sampling and analytical methods also allowed vertical distributions of Zn to become more accurate and meaningful. They revealed a nutrient-like distribution with a nanomolar range of concentrations (Bruland *et al.* 2003; Morel *et al.* 2003; Bermin *et al*. 2006). The major roles of Zn as co-factor in two important enzymes for phytoplankton growth (Table 1) combined with its nanomolar concentrations raised the

possibility of the limitation or co-limitation concept to be extended to Zn (Morel *et al.* 1994; Arrigo 2005; Saito *et al.* 2008). Like Fe, Zn oceanic cycle is balanced by its inputs, the reaction with the biota and particles in the surface waters and its outputs (Fig.1.). The Zn associated with the biota and particles can either be recycled in surface waters, or exported and remineralised at depth.

Table 1: Examples of functions of selected trace metals in marine microorganisms (adapted from Morel *et al.* (2003) pp. 122)

Metal	Function
Fe	FeS centers (e.g. aconitase, ferredoxin)
	Cytochromes
	Superoxide dismutase
	Nitrate reductase
	Nitrite reductase
Zn	Carbonic anhydrase
	Alkaline phosphatase
	DNA/RNA replication
	Metallothioneins
Co	Carbonic anhydrase
Cd	Carbonic anhydrase
	Alkaline phosphatase

2.2 Measuring Zn in seawater — a challenge:

The challenge encountered when working with seawater and trace elements is that analytical methods need to be sensitive and selective, possessing low detection limits that enable accurate determination of trace element speciation and their oceanic distributions (e.g. Table 2 for Zn). The various techniques available for Zn provide different chemical information and require time and experienced operators to obtain accurate results. Inductively coupled plasma mass spectrometry (ICP-MS) and Atomic Absorption Spectroscopy (AAS) are multi-element techniques that routinely measure Zn. ICP-MS is a high speed method that gathers precise and sensitive data at a lower limit of detection than AAS, and using only a small volume (microlitres to millilitres) of sample. Trace metal measurements in seawater face challenges not only due to low concentrations but also high contamination risks or interferences (e.g. matrix effects from high salinity or the presence of organic ligands). Although Zn concentrations are usually marginally higher than Fe in ocean waters, Zn measurements are highly prone to contamination due to its ubiquity in the environment. Both AAS and ICP-MS instruments are exposed to contaminants present in the laboratory environment and this exposure must be minimised when working at trace-level concentrations.

For chemical oceanographic studies of Zn, shipboard methods with the required analytical performance (e.g., based on voltammetry, flow injection analysis: FIA, sequential injection analysis: SIA) may be preferred and offer the option of near real-time data. These methods allow for rapid measurement during a voyage, while at the same time avoiding sample contamination or storage concerns by using an effective non-contaminating work environment (e.g. clean laboratory container). They are also usually tailored for Zn.

Table 2: Examples of analytical methods to determine the chemical species of zinc in natural waters; CSV: Cathodic Stripping Voltammetry; ASV: Anodic Stripping Voltammetry; ICP-MS: Inductively Coupled Plasma–Mass Spectrometry; AAS: Atomic Absorption Spectroscopy; FIA-FL: Flow Injection Analysis (coupled with fluorescence detection); SIA-LOV: Sequential Injection Analysis (coupled with lab-on-valve)

The detection limits have been converted in the same unit using a seawater density of $\rho = 1.03$ kg L^{-1} and $M_{Zn} = 65.39$ g mol^{-1}

Analytical method	Chemical forms measured	Study region	Detection limit (nM)	References
AAS	Dissolved Zn	Scheldt Estuary	3.00	Chaudry and Zwolsman 2008
	Zn total	Galician coast	0.31	Yebra-Biurrun and Cespón-Romero 2006
	Dissolved and particulate Zn	Ross Sea/ACC	0.031-0.052	Coale *et al.* 2005
	Total dissolved Zn	Southern Ocean	10-70 x 10^3	Löscher 1999
	Dissolved zinc Particulate zinc	South Australia, Estuary	153 0.76	Ferguson, 1983

ICP-MS Voltammetry techniques:	Dissolved Zn Zn speciation (comparison ASV and CSV)	Subantarctic Zone North Atlantic Ocean	0.062 0.03-0.04 [ASV] 0.08 [CSV]	Ellwood 2008 Wiesniewski Jakuba *et al.* 2008
CSV/ASV	Total dissolved Zn (ASV)	New-Zealand/Tasman Sea	6.20×10^{-3}	Ellwood 2004
	Total dissolved Zn (CSV)	North East Pacific	0.02	Lohan *et al.* 2002
	Zn speciation (CSV)	Northeastern Atlantic		Ellwood and van den Berg 2000
	Total dissolved zinc (CSV)	Irish Sea	0.30	Achterberg and van den Berg 1996
FIA-FL	Total dissolved Zn	Equator, Pacific	< 0.1	Nolting *et al.* 2000
		North Atlantic		Nowicki *et al.* 1994
SIA-LOV	Dissolved Zn	Pacific	0.3	Grand *et al*. 2011

FIA has many advantages; instruments are robust, simple and relatively inexpensive and offer high throughput. The system used for Zn measurements (Nowicki *et al.* 1994; Nolting *et al.* 2000) combines flow-injection with detection by fluorescence (FL) of a Zn complex with the ligand p-tosyl-8-aminoquinoline (pTAQ). Gosnell *et al.* (2012) successfully used the FIA-FL for the first time on a large scale. The resulting profiles that they obtained for total dissolved Zn in the southern Indian Ocean were encouraging and oceanographically consistent. The Sequential Injection Analysis lab-on-valve technique (SIA-LOV) recently developed by Grand *et al* (2011) requires even smaller sample volume, but currently at its early stage of development for Zn determination, it is not sensitive enough for the open ocean. Moreover, both techniques do not provide direct information on the speciation of Zn, which is paramount to define its reactivity and bioavailability. Pretreatment of samples (e.g. by ultraviolet radiation, acidification, or extraction on resin columns) is required for FIA and SIA systems.

Voltammetry gives direct determination of Zn speciation in seawater; cathodic stripping voltammetry with adsorptive preconcentration (AdCSV: van den Berg, C. M. G. 1985; Donat and Bruland 1990; Ellwood and van den Berg 2000) uses a competitive equilibrium between natural Zn ligands and an added chelator, while anodic stripping voltammetry (ASV: Bruland 1989) allows direct measurement of labile Zn (Zn'). The latter has been used reliably at sea during research voyages (Ellwood 2004; Wisniewski-Jakuba *et al.* 2008; Baars and Croot 2011). As first reported by Donat and Bruland (1990), a higher conditional stability constant is obtained with CSV (11.0 –11.5 M^{-1}) than ASV (10.1 –10.5 M^{-1}).

The analytical methods used to determine dissolved Zn concentration in seawater and discussed above require a preconcentration step to improve the limit of detection and separate the Zn analyte from the seawater matrix; solid-phase sorbents, often ion-exchange resins, are usually considered. They allow removal of interfering species from a sample (e.g. matrix elimination – according to their specificity and properties) and, at the same time, concentrating the target analyte. There are different possibilities for the preconcentration step and a careful choice needs to be made with regards to the chemistry of the trace metals analyte, resin properties (selectivity and capacity) and sample characteristics. Different types of resin have been studied for Zn determination under several conditions. Landing *et al.* (1986) introduced the use of the 8-hydroxyquinoline (oxine) functional group and through this study settled on its efficiency to preconcentrate Mn, Fe, Co, Cu, Zn and Cd in freshwater and seawater matrices (recovery of 96% for Zn). Willie *et al.* (2001) used a Toyopearl AF-Chelate-650M iminodiacetate poly(vinyl alcohol)-resin (IDA). The IDA ligand contains negatively charged carboxylic groups, and is a less-selective resin adsorbing a range of trace metals. Recovery of 80 % to 100 % for zinc was obtained when the sample was loaded at pH 5.3. This IDA resin is now a common choice in preconcentration steps used to determine various trace elements in marine waters.

Pretreatment of samples required for some techniques provides an operational definition of the Zn fraction measured (e.g. lability). How Zn lability relates to Zn^{2+} or Zn' is not yet well characterised. As a consequence, comparison of results obtained with different methods need to be done with caution.

Table 3: Examples of typical values for zinc concentrations in the different oceanic basins. Unit have been converted, where necessary, into the uniform nmol L^{-1} using an average seawater density of $\rho = 1.03$ kg L^{-1}

Region	Concentrations (nmol L^{-1})	Depth (m)	References
Northeast Atlantic	0.3	Surface	Ellwood and van den
	1.5 – 2	> 250	Berg 2000
	0.5 – 2	Surface	Nolting *et al.* 1999
Antarctic waters:			
Ross Sea	3.45 – 5.69	Surface	
	4.64 – 5.15	Lower mixed layer	Coale *et al.* 2005
ACC	1.03-3.09	Surface	
	2.17-5.15	Lower mixed layer	
Southern Ocean	1.1 - 8.0	10	Löscher 1999
	0.8 - 3.7	40	
Pacific waters:			
Tasman Sea	0.0062 – 0.062	0 – 20	Ellwood 2004
	0.0062 – 0.0175	45 – 50	
North Pacific	0.23	Surface	Bruland *et al.* 1994
	8	> 1000	
Northeast Pacific	0.04 – 0.64	Surface	Lohan *et al.* 2002
	1.85 – 2.16	> 100	

2.3 Zinc distribution and speciation in seawater

Zn concentrations in the global ocean are in the range 0.1 to 10 nM (Bruland and Lohan 2003; Bermin *et al.* 2006); data gathered in recent studies are shown in Table 3. The vertical distribution of total dissolved Zn is nutrient-like, depleted at the surface by biological activity with concentrations increasing with depth (Fig. 2). In deep waters, Zn reaches a constant concentration that can be up to 1400 times greater than that observed at the surface. Bruland *et al.* (1991) showed such an increase in the Pacific water column where the concentration of free ion — $[Zn^{2+}]$ — stepped from $10^{-11.8}$ M at 200 m to $10^{-8.6}$ M at 600 m. In comparison, the dissolved Zn in this same water column showed only a 50-fold difference between the surface and deeper waters. Such a difference between the free ion and total dissolved forms is linked to the presence of higher concentrations of organic ligands than Zn in surface waters.

Zn concentrations also possess an inter-ocean gradient, with lower concentrations in the Atlantic Ocean and greater in the Pacific Ocean (Bruland and Lohan 2003). In the North Atlantic, at the beginning of the global themohaline circulation known as the 'conveyor belt', surface waters depleted in nutrients are carried into ocean depths. As they follow the main path of circulation, their Zn content gradually accumulates in deep waters to reach a maximum at depth in the Northern Pacific. Returning to the surface exposes Zn to biological uptake, and this is manifested in strong depletion of Zn in the high latitude surface waters often characterised as high-nutrient, low-chlorophyll (HNLC) regions (e.g. Southern Ocean). Vertical and horizontal gradients within water bodies reflect the physico-biogeochemical processes occurring in the water column, for instance, remineralisation of Zn bound to organic particulate matter

sinking to depth, re-supply by advection, or at the smaller scale, mixing and diffusion.

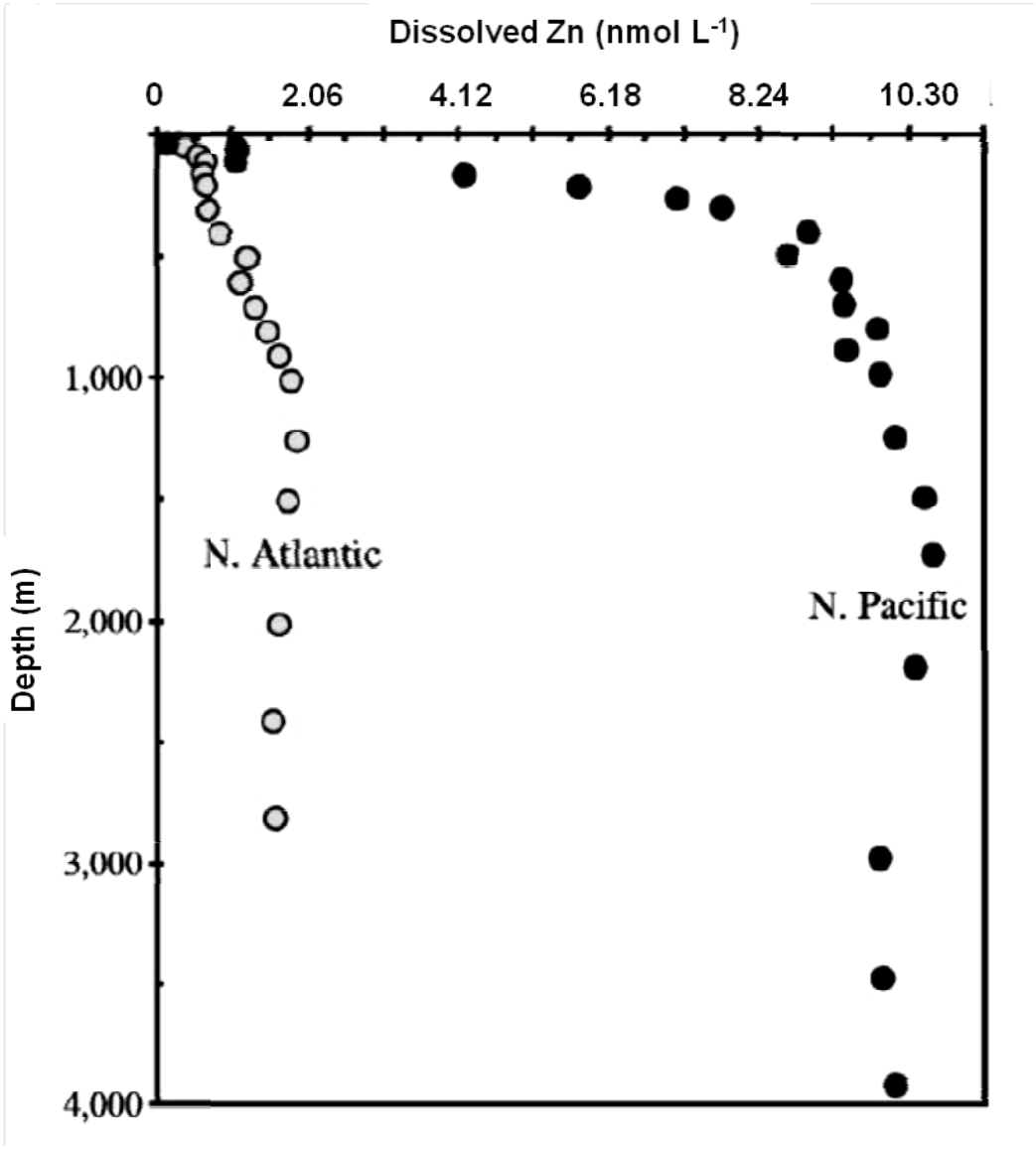

Figure 2: Comparison between North Atlantic and North Pacific zinc distributions, reflecting the influence of global oceanic circulation ('conveyor belt') on deep- water zinc concentrations. The North Atlantic Ocean is early in the circulation, with the North Pacific Ocean toward the end, and therefore, having the oldest deep waters (Adapted from Bruland et Lohan (2003). pp. 28).

Trace elements are supplied to (e.g., riverine discharge, atmospheric deposition, hydrothermal sources) and removed from (e.g., biological activity, scavenging) the ocean via different pathways, which determines their observed distributions in the ocean. The open ocean is sensitive to atmospheric dust deposition, which can be a source of Zn, and varies from one basin to another (Bruland and Lohan 2003; Witt *et al.* 2006). Being surrounded by continents and relatively narrow, the Atlantic Ocean is more subject to anthropogenic influences. Aeolian dusts influencing this ocean are enriched in Zn compared to terrestrial values for the crust (Spokes *et al.* 2001). The Pacific Ocean, because of its vastness, is less influenced by continental dusts. However, the transport pathway from the Gobi and Taklamakan Deserts over the industrial areas of China, Korea and Japan is likely to deliver particulate Zn to the Northern Pacific. Oceans of the Southern Hemisphere are less subjected to inputs of trace elements from aeolian dusts, but localised effects exist. For example, the air masses over the Tasman Sea are influenced by pollutants coming from industrial (coal combustion: Marx *et al.* 2008) or natural (Lake Eyre: McGowan and Clark 2008) Australian sources. These air masses transport Zn in aerosol dusts and enrich waters between Australia and New Zealand (e.g., Tasman Sea), particularly affecting coastal regions of pristine waters and sediments near New Zealand. In polar waters, for instance in the Ross Sea, sea-ice melting can also be relevant to the enrichment of marine systems by macro- and micronutrients. These processes have been shown to supply surface seawater with Fe (Lannuzel *et al.* 2011), although a significant transfer of Zn from the sea-ice to seawater has not been observed, and thus, this source might be inconsequential for Zn.

Turner (1995) described chemical speciation as the 'chemist's nightmare' because of its complexity. Speciation determines the different physico-chemical forms in solution, and whether they are bioavailable or not. Several physico-chemical factors need to be considered when determining the speciation of a trace metal in solution, and at the organism's surface when related to biological uptake. Amongst the most important are: (1) the complexation of the trace metals by inorganic ligands (Cl^-, CO_2^{3-}, SO^{2-}_4, etc) or organic ones, such as humic substances (Campbell et al. 2002); (2) the presence of other cations, such as Ca^{2+} and Mg^{2+}; (3) the variation in pH which can provoke important changes in metal toxicity and accumulation (Heijerick et al. 2002); (4) the temperature of the solution; and (5) the role of UV radiation which can also break down complexes in surface waters. Two different types of speciation can be considered in seawater, both posing challenges for analysis and our understanding of such systems. The first characterisation is a physical one and operationally defined using filtration at various common pore sizes (Fig. 3). Chemical speciation takes into account the different chemical species present in seawater — either free ions or complexes (from simple ligands, such as amino acids, up to complex macromolecular chelates).

Smith *et al.* (2002) have reviewed different properties of metal complexation with their preferred natural ligands, such as Natural Organic Matter (NOM) or amino and sulphide groups present in natural waters. They classified metals as 'hard' (Group A) or 'soft' (Group B) cations; a definition coming from 'the number of electrons in the outer shell of the metal cation and the polarizibility'. Zn is intermediate between a soft and hard metal, and thus, it will form strong bonds with a range of ligand types in aqueous systems. Therefore, a

high percentage of Zn is complexed (between 95 and 98 %: Bruland 1989), but little is known about the ligands that specifically bind it. This natural complexation is important to define and understand chemical speciation in seawater.

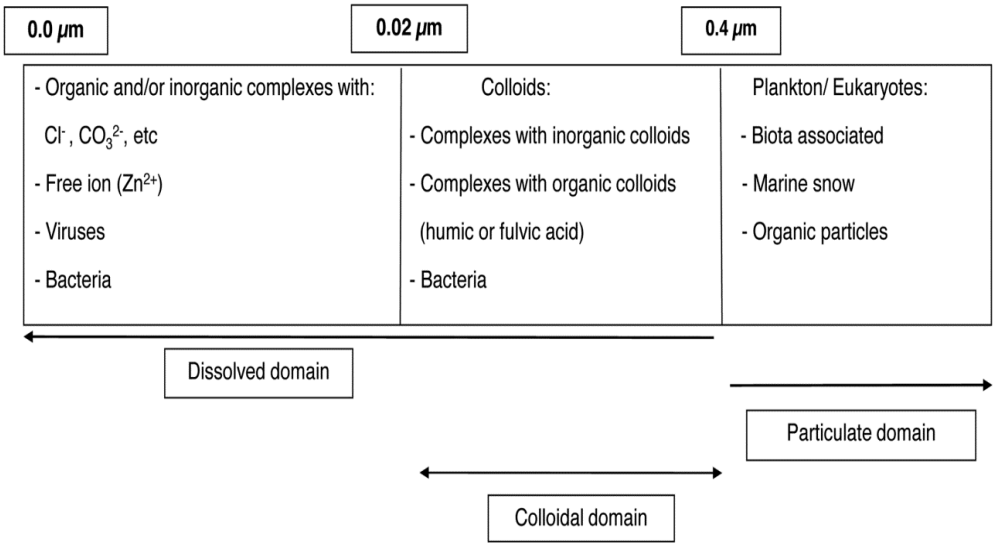

Figure 3: Operational distribution and classification of the different species of the zinc pool in seawater.

Laboratory studies of zinc-complexing NOM, such as humic (HA) or fulvic acids (FA), show that Zn is strongly complexed by these organic ligands, leading to a strong decrease in its bioavailability as a free ion (Oste *et al.* 2002; Yang and van den Berg 2009). The study by Yang and van den Berg (2009) compared different values for metal complexes —Zn, Co and Fe— with FA and HA, especially relevant to coastal waters (Table 4). With a ratio of log K'_{Fe+FA}/ log K'_{Zn+FA} of 2.2 and 2.4 for HA, Fe formed the most stable complexes whereas Zn and Co had very similar and slightly weaker stability constants. Zn complexes

with HA (log K'_{Zn+HA} = 9.9-10.2) were more stable than those with FA (log K'_{Zn+FA} = 9.1).

As an alternative approach to define Zn bioavailability, speciation can be determined by mathematical means using reported chemical thermodynamic data. Zirino and Yamamoto (1972) have determined Zn speciation with a thermodynamic model as a function of pH. According to this model, Zn would be less complexed than other trace metals studied (e.g. copper), with as much as 17% predicted to be free ions. However, the authors specified that this model is quite simple for seawater, which could explain the discrepancy between the model results and the observed values (just 2-5 % of Zn being free ions; Bruland 1989).

Table 4: Conditional stability constants for metal complexes with humic substances in seawater. Adapted from Yang and van den Berg (2009)

a. Complexes with fulvic acids (FA):

Species	Log $K'_{M'FA}$ Based on [M'][a]	Log K'_{Mn+FA} Based on $[M^{n+}]$[b]
Zn	8.79	9.1
Co	8.41	8.6
Fe	10.6	21.9

b. Complexes with humic acids (HA):

Species	Log $K'_{M'HA}$ Based on [M'][a]	Log K'_{Mn+HA} Based on $[M^{n+}]$[b]
Zn	9.59-9.88	9.9-10.2
Co	8.73	8.9
Fe	11.1	22.4

[a] [M'] is the free, inorganic metal concentration, uncorrected for the influence of major anions present in seawater

[b] $[M^{n+}]$ is the corrected concentration. This concentration is obtained by converting the first ones using α-coefficient for inorganic complexation. In this paper, values of 2.0, 1.6 and 2.0×10^{11} were used for Zn, Co and Fe respectively.

2.4 Biological importance of zinc in seawater:

Zn is needed as a metal centre in two important enzymes; carbonic anhydrase (CA), first discovered in 1940, and alkaline phosphatase (AP). CA catalyses the chemical reaction responsible for the hydration/dehydration of CO_2:

$$CO_2 + H_2O \leftrightarrow HCO_3^- + H^+$$

Badger (2003) and Kupriyanova and Pronina (2011) reviewed the differences in CA between organisms and concluded they would have evolved quite independently. These various types of CA have the same catalytic function, but their spatial structure allows them to be classified. Three main classes are well identified: α- for animals, β- for plants and eubacteria, γ- for archae-bacteria. A fourth class, δ-, has recently been defined and attributed to the CAs found in marine diatoms (Roberts *et al.* 1997; McGinn and Morel 2008). Yee *et al.* (1996) studied Zn substitution by Co in the enzyme CA for the marine diatom *Thalassiosira weissflogii*. They concluded Zn and Co were associated with the same CA but this enzyme possessed higher affinity for Zn. The study also led to the discovery of a fifth class, ζ- CA, using Cd to satisfy diatom requirements. It has the same structure than a β-CA (Morel *et al*. 2002; Park *et al.* 2007) but contains Cd as metal centre to overcome Zn limitation.

Badger (2003) and Kupriyanova and Pronina (2011) also reviewed differences in Carbon Concentrating Mechanisms (CCMs) present in several phytoplankton species. These mechanisms, involve CA at different levels, such as in active and passive carbon uptake. CA also supplies RubisCO, the enzyme that catalyses carbon fixation, with bicarbonate ions from an internal pool of carbon and prevents loss of CO_2 by the cells. Therefore, CCMs help RubisCO to make a more efficient capture of carbon.

In order to get a better picture of carbon uptake by marine phytoplankton, increasing research effort has focused on CA and CCMs. Lane and Morel (2000), followed by Morel *et al*. (2002), studied the carbon uptake by the diatom *T. weissflogii* and concluded they possess two different CA enzymes, an external one and an internal one. The first one is regulated by carbon dioxide ―CO_2― concentration in the growth media by negative feedback, and the second one by CO_2 and trace metal concentrations in the intracellular medium. The activity is greater for low CO_2 partial pressure (100 ppm) and the presence of 15 pM of inorganic zinc ―Zn'―, i.e. free Zn ions or associated with simple labile ligands such as Cl^- or CO_3^{2-}. It was also concluded that the activity of this latter CA could be restored by addition of Cd or Co.

The second enzyme, alkaline phosphatase (AP) was discovered in 1912 and confirmed to be a zinc metalloenzyme by Plocke *et al.* (1962). This enzyme is responsible for phosphorus uptake by marine organisms, but also allows recycling of organic phosphate as a means to avoid phosphorus limitation in seawater. Early studies on AP were done by Csopak (1969) with *Escherichia coli* and concluded it contained two Zn ions in its structure. Coleman (1992) confirmed that for enzymatic activity, AP needs two Zn ions and one Mg ion. A change in configuration, such as two Mg ions and one Zn ion for instance, does not imply inactivity but reduces its activity. As underlined by Hoppe (2003), studies concerning AP activity, in relation to Zn in seawater, are still scarce. Marine eukaryotic organisms seem to be important AP producers but their growth can still be limited by inorganic phosphate availability.

Zn is also known to have an important biological function in RNA polymerase (Coleman 1998), where it facilitates interactions between the different subunits of the enzyme. It has also a central role in DNA duplication and gene

transcription. Indeed, Zn is responsible for a structure known as ‘zinc finger’ that stabilises a DNA-binding region (Cotton *et al.* 1999). When the finger binds to the DNA, it activates gene transcription encoding for proteins such as metallothioneins. Their role and function are still not well understood but a detoxifying one has been proposed by several authors (Gaither and Eide 2001; Perales-Vela *et al.* 2006). Blindauer (2008) also mentioned an important role for the metallothioneins in Zn homeostasis, as well as the intracellular distribution of Zn to the different organelles in cyanobacteria. In eukaryotes, the number of proteins required to drive this intracellular transport is of great importance and their synthesis is an appreciable expense of energy for the cell (Eide 2006).

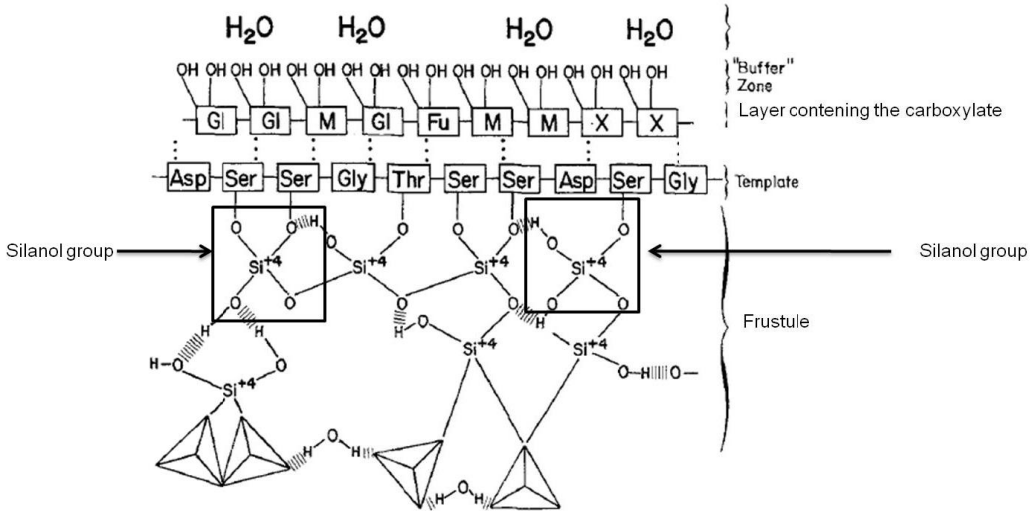

Figure 4: Arrangement of biochemical layers in diatom cell walls showing the potential groups binding Zn. Adapted from Hecky *et al.* (1973).

Zinc's vertical distribution is significantly correlated to that of silicic acid. It is known that diatoms are using most of the assimilated silicic acid for frustule formation, so assessment can be done on the relationship between frustule formation and Zn uptake by diatoms. To determine whether Zn was involved in frustule formation or simply in its chemical structure, Gélabert *et al*. (2006) studied Zn isotope fractionation during frustule formation and determined a generic model for Zn inclusion in frustule structure. Zn could be complexed to silanol and carboxylate groups (Fig. 4) and its adsorption on the surface varied among diatom species. This last result is in good agreement with a previous chemical study by Gélabert *et al.* (2004) on chemical structure and properties of diatom frustules. In this 2004 paper, they compared different analytical methods to build a chemical structure for four different diatoms species (marine and freshwater diatoms). Both studies revealed difficulties in determining properly the role of Zn in diatom frustules and its binding. Indeed, several environmental factors need to be taken account: pH, Zn and biomass concentration, ionic strength and temperature. Nevertheless, this study provides a 'basis for the quantitative physico-chemical description of Zn interaction with planktonic and periphytic diatoms ' (Gélabert 2006).

Ellwood and Hunter (2000) studied the incorporation of Zn and Fe in biogenic opal and found a relation between Zn taken up by diatoms and $[Zn^{2+}]$ in the media. Based on this leading work for seawater, Jaccard *et al.* (2009) studied Zn uptake and its role for a freshwater diatom, *Stephanodiscus hantzschii*. Although the diatom species in freshwaters and seawaters differ, they both have an affinity for silicic acid because they both possess silica frustules. The relationship between Zn/Si ratio and $[Zn^{2+}]$ in the medium obtained for the

freshwater diatom agreed with the one found for marine species, implying similar Zn incorporation in cells. The trends obtained in both studies showed that Zn/Si ratio could possibly be used as a proxy to predict Zn bioavailability in surface waters where diatoms dominate the phytoplankton community. Along this line, GEOTRACES encourages a focus on isotopes. The latter bring new insights and tools to study past and present chemistry of this essential element and its cycling (Hendry and Rickaby 2008; Andersen *et al.* 2011), but also, its interactions with the phytoplankton community including its uptake system (John *et al.* 2008).

2.5 Zinc, a limiting or co-limiting nutrient in seawater?

Interactions between phytoplankton and trace element are often discussed in terms of the limitation or co-limitation concept. Limitation relates to an element diminishing to concentrations where it is insufficient for phytoplankton growth and limits the abundance and diversity of different phytoplankton communities (e.g., Arrigo 2005; Saito *et al.* 2008). Co-limitation is the joint action of two or more environmental factors — biotic or abiotic. Saito *et al.* (2008) described four cases of limitation: 'Type I. Independent nutrient co-limitation', 'Type II. Biochemical substitution co-limitation', 'Type III. Biochemically dependent co-limitation' and a Type 0. If only one nutrient is a limiting factor in Type 0, the difference between the three others is more subtle. In each type, two elements are involved; either both of them are potentially limiting due to their low concentrations but play a role in different biological function (Type I), or they can substitute in the same biological function (Type II) or adequate supply of one of the elements is needed to acquire the other (Type III) (Table 5).

Table 5: Examples of potential Zn co-limitation in seawater. Adapted from Saito *et al.*, 2008. CA: carbonic anhydrase. AP: alkaline phosphatase

Nutrient couple	Co-limitation type (targeted enzyme)		References
Zinc and cobalt	0 or I	Only one nutrient/independent	Saito *et al.* 2002 Sunda and Huntsman 1995*a* Franck *et al.* 2003
Iron and zinc	I	Independent	Wiesniewski *et al.* 2008
Zinc and cobalt	II	Biochemical substitution (CA)	Morel *et al.* 1994 Yee *et al.* 1996
Zinc and cadmium	II	Biochemical substitution (CA)	Price and Morel 1990
Zinc and cobalt (hypothesized)	II	Biochemical substitution (AP)	Shaked *et al.* 2006 Sunda and Huntsman 1995*a*
Zinc on phosphorus	III	Dependent (AP)	Shaked *et al*. 2006
Zinc on carbon	III	Dependent (CA)	Price and Morel 1990

These feedback effects between trace elements and phytoplankton have been studied and described in numerous papers (Sunda and Huntsman 1992; Gonzàlez-Dàvila 1995; Whitfield 2001; Morel 2008). On one hand, trace metals influence the structure of the different phytoplankton communities (Leblanc *et al.* 2005), whilst on the other, microorganisms strongly influence the speciation of the trace elements by producing ligands, such as siderophores for Fe, and thereby regulating their uptake. These reciprocal interactions influence 'trace-element bioavailability', defined as the chemical form that can possibly be assimilated by phytoplankton. These chemical forms vary from one microelement to another and can be organic or inorganic complexes or the free ion present in seawater (Saito *et al.* 2008). However, the concept of bioavailability has recently been demonstrated to be complex, with different sources and biological processes influencing the uptake of chemical species by phytoplankton (Hassler *et al.* in press).There are two forms of Zn in seawater that can be regarded as available and assimilated by phytoplankton; the free ion Zn^{2+} and the inorganically bound Zn (Sunda and Huntsman 1992, 1995a, 2000; Saito *et al.* 2008). These two forms might be preferentially taken up owing to less physiological cost for marine organisms. Genetic and genomic studies have helped to determine the type and role of six main families of inducible Zn transporters identified across a wide range of biological species (Table 6). These proteins may be responsible for Zn internalisation, compartmentalisation or efflux by using driving forces based on electrochemical or proton gradients or adenosine triphosphate (ATP) hydrolysis. They allow the delicate balance between Zn deficiency and intracellular overload through their different roles.

Table 6: Representation of transport families and examples of Zn transporters mostly from Blencowe and Morby, 2003; Eide, 2006; Bildauer, 2008. '?' represents uncertainty of metal transport.

Type of transport	Family	Energy	Main metal ions transported	Example of transport system for Zn
Uptake system	ABC (High affinity system)	ATP	Mn, Zn, Ni, Fe(II)	ZnuABC
	Nramp	Proton gradient	Mn > Cu > Co > Fe > Zn	MntH
	ZIP	Not clearly defined	Fe, Mn, Zn Cd ?, Cu ?	Zrt1, Zrt2 ZupT
	MIT	Chemiosmotic	Most cations Mg, Zn ?	CorA MgtA
	P-type	ATP	Cu/Ag Zn/Cd/Pb	CopAB ZntA, CadA
Efflux systems	RND	Chemiosmotic	Co/Ni Co/Zn/Cd	CzcABC
	CDF	Chemiosmotic	Zn, Cd, Co, Fe	Zrc1, Znt1, ZitB

ZNT, IRT-like Proteins (ZIP) are exclusively involved in Zn transport (Guerinot 2000; Gaither and Eide 2001). They have been identified in a number of marine phytoplankton species, such as the diatom *T. pseudonana* and the coccolithophorid *Emiliania huxleyi* (Sunda and Hunstman 1992, 1998), and are induced to overcome low Zn concentrations. ATP- Binding Cassette (ABC) proteins transport a large variety of substrates and are involved in biological processes such as the excretion of potentially toxic compounds (Schmitt and Tampe 2002; Martinoia *et al.* 2002; Moussatova *et al.* 2008). The subgroup CPx-ATPase of P-type ATPases (Gatti *et al.* 2000; Williams *et al.* 2000) is responsible for heavy metal transport; they are found in a wide variety of organisms and have an early evolution. Cation Diffusion Facilitator (CDF) exclusively transports heavy metals outside organisms or inside the organelles (Gustin *et al.* 2011). These three families of proteins are present in cyanobacteria such as *Synechococcus* and *Prochlorococcus* (Blindauer 2008).

Since Morel *et al.* (1994) discussed the possibility of the 'zinc hypothesis', some studies have confirmed that Zn limits phytoplankton growth rate, for example, by limiting silicic acid uptake (de La Rocha *et al.* 2000), or both nitrate and silicic acid uptake (Franck *et al.* 2003; Varela *et al.* 2011). However, Shaked *et al.* (2006) followed by Wisniewski *et al.* (2008) showed that zinc-phosphorus (Zn-P) co-limitation for *E. huxleyi* occurred in certain parts of the ocean, or under certain conditions, but it does not seem to be a widespread phenomenon. It likely occurs in oligotrophic waters, where phosphate concentrations are very low, with organic P almost unavailable and Zn strongly bound to organic ligands. As a result, Zn limitation could affect phytoplankton communities from regions such as the Tasman Sea (Hassler *et al.*, accepted) or the Sargasso Sea (Wisniewski Jakuba

et al. 2008). The impact of this limitation requires comparison to contrasting regions where P and Zn are replete (e.g. upwelling zones). Indeed, AP from *E. huxleyi* present in Zn-P limited regions is highly efficient, which might give it an advantage over other phytoplankton species under these circumstances. In similar conditions, but in different water masses, the entire phytoplankton community could be limited for want of an efficient AP to acclimate the scarce Zn and P resources.

Zn is also relevant to climate change and ocean acidification studies because of its role in carbon uptake and the relation to carbon species availability. Particular attention is being given to CA that requires Zn as a co-factor. Zn co-limitation can be related to ineffective biological drawdown of CO_2 in surface seawaters; and as a corollary, to climate-induced increases of atmospheric carbon dioxide concentrations (pCO_2), and reduced pH in seawater, i.e., ocean acidification (Ardelan *et al.* 2009; Doney *et al.* 2009). Small changes are predicted for Zn speciation with increasing ocean acidification scenarios; Zn^{2+} concentrations will increase slightly while the fraction of inorganically complexed Zn will tend to decrease (Millero *et al.* 2009). These changes, even if small, will affect the phytoplankton community, because different phytoplankton taxa possess different requirements for Zn, and different preferences for forms of Zn.

Currently, knowledge of Zn and its influence on phytoplankton come from experiments done in the laboratory with species of diatoms, coccolithophorids and cyanobacteria cultured separately. Conflicting results from deck-top incubations studies of Zn impact on regional community (Coale *et al.* 2003 did not find any impact; Crawford *et al.* 2003 and Cullen and Sherrell 2005 observed changes in Chl or Cd:P ratios, respectively) prevent the establishment of a defined limiting

role for Zn. Moreover, such studies ought to reveal the mechanism by which species can alleviate Zn depletion by taking up cadmium (Cd) or cobalt (Co). Because of their chemical similarities, Zn may be replaced by Co and Cd (Sunda and Huntsman 1995*a;* Saito and Goepfert 2008) with no or only partial loss of enzymatic activity, leading to complex interactions for metal mixtures. However, this replacement mechanism can be inefficient or impossible (*Chaetoceros calcitrans* vs. *E. huxleyi*: Timmermans *et al.* 2001) for some phytoplankton species.

2.6 Models for zinc in seawater:

Several simplified steady-state models of trace metal bioavailability have been proposed to consider speciation and metals reacting with the biological binding sites. These include the Windermere Humic Aqueous Model (WHAM: Tipping 1993; 1998), the Free Ion Activity Model (FIAM: Morel 1983) and the Biotic Ligand Model (BLM: Pagenkopf 1983; Playle 1998). The BLM and the FIAM are commonly used because they link the chemistry of trace metals with their bioavailability (or reactivity). This link is important: it is the scarcity of the bioavailable fraction that affects biology, a requisite to underpin the effect of Zn co-limitation or limitation in marine systems. The BLM can take implicitly competitive effects into account through direct correlation of metal binding to sensitive sites of the cell's surface with bioavailability (Di Toro *et al.* 2001; Heijerick *et al.* 2002). Unlike the BLM, in the FIAM, competition must be taken into account explicitly by using equilibrium constants for each of the competition ions, including the proton.

The FIAM and BLM models consider the chemical speciation in solution, surface complexation with transport sites and uptake of the metal inside the organism (Fig. 5). This approach is valid if transport across the biological membrane is rate-limiting (Sunda and Huntsman 1998; Hassler *et al.* 2004). In that case, and below saturation of the uptake sites, biological uptake fluxes will be directly proportional to any of the metal species in equilibrium. Anderson and Morel (1978) have found that Zn uptake was proportional to $[Zn^{2+}]$ in the bulk solution and in qualitative accordance with the FIAM. They also noted that specific growth rate of the diatom *T. weissflogii* was dependent on log $[Zn^{2+}]$ in the bulk solution. Therefore, several authors have observed Zn uptake saturation and plotted their data with a Michaelis-Menten saturation equation. In the case where biological internalisation is rapid (compared to either the physical transport or chemical reactivity of the metal; Hudson 1998), biological uptake fluxes will be better related to some other fraction of the metal species in solution (i.e., mobile or labile species; Hudson and Morel 1993). Two papers have reviewed and analysed assumptions lying behind the application of the FIAM and the BLM (Hassler and Wilkinson 2003; Hassler *et al.* 2004). Both showed that these assumptions, although sometimes reasonable, clearly demonstrate the potential problems in applying models such as BLM or FIAM to Zn internalisation fluxes by phytoplankton. These arise from physiological effects on binding sites, multiple transport routes and varying acclimation conditions. Sunda and Huntsman (1992) showed that the cellular Zn content appeared to be regulated for $[Zn^{2+}]$ in the bulk solution ranging from $10^{-8.5}$ to $10^{-10.5}$ M. At these concentrations, transport kinetics approached the physical limits permitted by diffusion, as was observed for Fe. This implies that kinetics becomes important as

labile complexes could dissociate and contribute to the bioavailable pool. As a consequence, the definition of the bioavailability of trace elements needs to be rigorously established (Hassler *et al.* in press).

Although biological impacts are important, they are not the only reason for these models to improperly portray metal uptake by phytoplankton. Indeed, dynamics of chemical reactions have been shown to play an important role (van Leeuween *et al.* 2005) in the speciation and bioavailability of those metal species. The interplay of biological and chemical conditions imply predicting speciation and uptake of different species in order to better understand the behaviour of trace elements in marine systems.

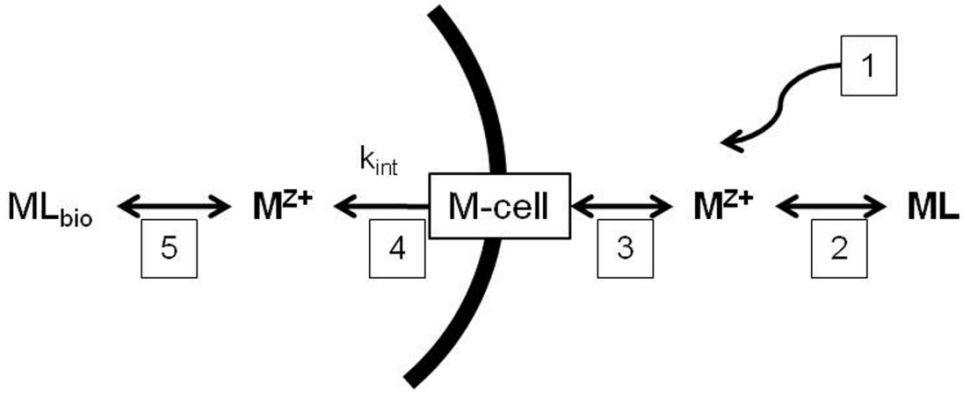

Figure 5: Conceptual interactions taken into account in the FIAM and the BLM models including: (1) mass transport of the free metal and complex in solution; (2) dissociation and complexation with a ligand in solution; (3) rapid and irreversible adsorption to membrane binding sites, specific or not; (4) irreversible and rate-limiting internalisation of metal-carrier complex, characterised by an internalisation constant (k_{int}); and (5) consequent internal biological effect. (Adapted from Hassler *et al.* 2004).

2.7 Conclusions and perspectives:

To get a better comprehension of marine ecosystems, interactions between Fe and microorganisms have been studied in detail. However, with recent advances in oceanographic research leading to an improved understanding of marine biogeochemistry, other trace elements, such as Zn, Co and Cd, also appear to mediate primary productivity or phytoplankton community structure. Laboratory studies have shown the importance of Fe for phytoplankton growth and the mechanisms they develop to maintain their optimal requirements. In a same way, the importance of Zn for marine microorganisms is well established through its different biological roles.

The obvious complexity of zinc's potential role as a limiting, or co-limiting, trace element in seawater is complicated by the fact that (i) Cd and Co can contribute to the biological requirement for Zn and (ii) that Fe is limiting, too, in most regions where low Zn concentrations are found (Croot *et al.* 2011). The uncertainties lying behind the proposal of limitation or co-limitation show our understanding of the role and importance of Zn in seawater needs further study. This must encompass the different responses Zn species can elicit in a phytoplankton community. Emerging results are suggesting that Zn affects oceanic productivity when its concentrations are extremely low, but in association with other biotic or abiotic factors, such as light, carbon or other nutrients (Muller *et al.* 2003; Sunda and Hunstman 2005). For a general understanding of zinc and its role in biological marine processes further research can be foreseen. For instance, synchrotron techniques (e.g. synchrotron-based microfocussed X-ray absorption fine structure) could be used to determine zinc location within cells or organelles, as it has been demonstrated in related work by Twining *et al.* (2008).

A second avenue of investigation would use molecular techniques, such as proteomics and transcriptomics, to reveal the physiology of Zn within the cell along the line of the selenium example (Zhang *et al.* 2005).

The diversity of zinc's roles in phytoplankton growth, and possible oceanic co-limitations, emphasises the need to bring together chemistry and biology in order to include this important trace metal in considerations of ocean surface fertility and the community structure of micro-organisms (phytoplankton, microbes, etc.). Owing to zinc's high susceptibility to contamination during sampling and analysis, determination of accurate Zn concentrations and speciation in seawater remains an open field of research: with the aim of arriving at the best technique to accomplish the task under clean conditions and for a wide range of marine systems. As a result, there is still little detailed information on its distribution, speciation and biological requirements, but thanks to the GEOTRACES research program (www.geotraces.org), new results are already emerging for its speciation in regions such as the Atlantic sector of the Southern Ocean (Baars and Croot 2011, Croot *et al.* 2011). High and low latitudes exhibit differences in bioavailable inorganic Zn in surface waters. Even if the nature of ligands that bind Zn is yet to be determined, these new findings are providing a new research base for Zn biogeochemistry cycling in the oceans. GEOTRACES places a high priority on isotope studies to track zinc sources and isotopic signature in biological processes in which zinc is involved.

The comprehensive picture of its cycle is yet to be completed, but recent studies, new techniques, combined with more intensive application of traditional oceanographic and laboratory studies, and new approaches from the scientific community are greatly enhancing knowledge on the role of Zn in marine systems

and provide exciting research outcomes. They have the potential to finally resolve the ‘zinc hypothesis’ and reveal the potency of zinc as a micronutrient regulating communities of phytoplankton and associated micro-organisms.

2.8 Acknowledgments:

The authors would like to thank the CSIRO-University of Tasmania Quantitative Marine Science Joint program and the scholarship they support through the Institute for Marine and Antarctic Studies. This research was also partly supported by the Australian Government Cooperative Research Centres Programme through the Antarctic Climate and Ecosystems CRC (ACE CRC). We would also like to thank internal reviewers, Dr Richard Matear (CSIRO-CMAR) and Dr. Delphine Lannuzel (UTAS, ACE-CRC), the referees and associate editor for their time and constructive comments, which helped to improve this manuscript.

2.9 References:

Achterberg, E. P., and van den Berg, C. M. G. (1996). Automated monitoring of Ni, Cu and Zn in the Irish Sea. *Marine Pollution Bulletin* **32**, 471-479.

Andersen, M. B., Vance, D. Archer, C., Anderson, R. F., Ellwood, M. J., and Allen, C. (2011). The Zn abundance and isotopic composition of diatom frustules, a proxy for Zn availability in ocean surface water. *Earth and Planetary Science Letters* **301**, 137-145.

Anderson, M. A., Morel, F. M. M., and Guillard, R. R. L. (1978). Growth limitation of a coastal diatom by low zinc ion activity. *Nature* **276**, 70-71.

Ardelan, M. V., Steinnes, E., Lierhagen, S., and Linde, S. O. (2009). Effects of experimental CO_2 leakage on solubility and transport of seven trace metals in seawater and sediment. *Science of the Total Environment* **407**, 6255-6266.

Arrigo, K. R. (2005). Marine microorganisms and global nutrient cycles. *Nature* **437**, 349-355.

Baars, O., and Croot, P. L. (2011). The speciation of dissolved zinc in the Atlantic sector of the Southern Ocean. *Deep-Sea Research II* **58**, 2720-2732.

Badger, M. (2003). The roles of carbonic anhydrases in photosynthetic CO_2 concentrating mechanisms. *Photosynthesis Research* **77**, 83-94.

Bermin, J., Vance, D., Archer, C., and Statham, P. J. (2006). The determination of the isotopic composition of Cu and Zn in seawater, *Chemical Geology* **226**, 280-297.

Blindauer, C. A. (2008). Zinc-handling in cyanobacteria: An update. *Chemistry & Biodiversity* **5,** 1990-2013.

Blencowe, D. K., and Morby, A. P. (2003). Zn(II) metabolism in prokaryotes. *FEMS Microbiology Reviews,* **27,** 291-311.

Bowie, A. R., Maldonado, M. T., Frew, R. D., Croot, P. L., Achterberg, E. P., Mantoura, R. F. C., Worsfold, P. J., Law, C. S., and Boyd, P. W. (2001). The fate of added iron during a mesoscale fertilisation experiment in the Southern Ocean. *Deep Sea Research Part II: Topical Studies in Oceanography,* **48,** 2703-2743.

Bowie, A. R., and Lohan, M. C. (2009). Analysis of Iron in Seawater. In 'Practical guidelines for the analysis of seawater'. pp. 235-257. (O. Wurl, Institute of Ocean Sciences, Syiney, British Columbia, Canada).

Bruland, K. W. (1989). Complexation of zinc by natural organic ligands in the central north pacific. *Limnology and Oceanography* **34**, 269-285.

Bruland, K. W., Franks, R. P., Knauer, G. A., and Martin, J. H. (1979) Sampling and analytical methods for the determination of copper, cadmium, zinc, and nickel at the nanogram per liter level in sea water. *Analytica Chimica Acta* **105**, 233-245.

Bruland, K. W., Donat, J. R., and Hutchins, D. A. (1991). Interactive influences of bioactive trace metals on biological production in oceanic waters. *Limnology and Oceanography* **36**, 1555-1577.

Bruland, K. W., Orians, K. J., and Cowen, J. P. (1994). Reactive trace metals in the stratified central North Pacific. *Geochimica et Cosmochimica Acta* **58**, 3171-3182.

Bruland, K. W., and Lohan, M. C. (2003). Controls of trace metals in seawater. In 'Treatise on geochemistry'. pp. 23-47 (Pergamon, Oxford).

Campbell, P. G. C., Errécalde, O., Fortin, C., Hiriart-Baer, V. P., and Vigneault, B. (2002). Metal bioavailability to phytoplankton--applicability of the biotic ligand model. *Comparative Biochemistry and Physiology Part C: Toxicology & Pharmacology*, **133** 189-206.

Chaudry, M. A., and Zwolsman, J. J. G. (2008). Seasonal Dynamics of Dissolved Trace Metals in the Scheldt Estuary: Relationship with Redox Conditions and Phytoplankton Activity. *Estuaries and Coasts* **31**, 430-443.

Coale, K. H., Michael Gordon, R., and Wang, X. (2005). The distribution and behaviour of dissolved and particulate iron and zinc in the Ross Sea and Antarctic circumpolar current along 170°W. *Deep Sea Research Part I: Oceanographic Research Papers* **52**, 295-318.

Coleman, J. E. (1992). Structure and Mechanism of Alkaline Phosphatase, *Annual Review of Biophysics and Biomolecular Structure* **21**, 441-483.

Coleman, J. E. (1998). Zinc enzymes, *Current Opinion in Chemical Biology* **2**, 222-234.

Cotton, F. A., Wilkinson, K. J., Murillo, C. A., and Bochmann, M. (1999). The group 12 elements: Zn, Cd, Hg. In 'Advanced inorganic chemistry, 6th Edition', pp. 598-629. (Wiley, New York.).

Crawford, D. W., Lipsen, M. S., Purdie, D. A. , Lohan, M. C., Statham, P. J., Whitney, F. A., Putland, J. N., Johnson, W. K., Sutherland, N., Peterson, T. D., Harrison, P. J., and Wong, C. S. (2003). Influence of Zinc and Iron Enrichments on Phytoplankton Growth in the Northeastern Subarctic Pacific. *Limnology and Oceanography* **4,** 1583-1600.

Croot, P. L., Baars, O., and Streu, P. (2010). The distribution of dissolved zinc in the Atlantic sector of the Southern Ocean. *Deep-Sea Research II* 58, 2707-

2719 Csopak, H. (1969). The Specific Binding of Zinc (II) to Alkaline Phosphatase of *Escherichia coli*. *European Journal of Biochemistry* **7**, 186-192.

Cullen, J. T. and Sherrell, R. M. (2005). Effects of dissolved carbon dioxide, zinc, manganese on the cadmium to phosphorus ratio in natural phytoplankton assemblages. *Limnology and Oceanography* **50**, 1193-1204.

Cutter, G., Andersson, P., Codispoti, L., Croot, P., François, R., Lohan, M. C., Obata, H., and Rutgers, M. (2010). 'Sampling and sample-handling protocols for GEOTRACES cruises' (Ed GEOTRACES Standards and intercalibration committee).

de la Rocha, C. L., David, A. H., Mark, A. B., and Yaohong, Z. (2000). Effects of iron and zinc deficiency on elemental composition and silica production by diatoms. *Marine Ecology Progress Series* **195**, 71-79.

Di Toro, D. M., Allen, H. E., Bergman, H. L., Meyer, J. S., Paquin, P. R., and Santore, R.C. (2001). Biotic ligand model of the acute toxicity of metals. 1. Technical Basis. *Environmental Toxicology and Chemistry* **20**, 2383-2396.

Donat, J. R., and Bruland, K. W. (1990). A comparison of two voltammetric techniques for determining zinc speciation in Northeast Pacific Ocean waters. *Marine Chemistry* **28**, 301-323.

Doney, S. C., Fabry, V. J., Feely, R. A., and Kleypas, J. A. (2009). Ocean acidification: the other CO2 problem. *Annual Review of Marine Science* **1**, 169-192.

Eide, D. J. (2006). Zinc transporters and the cellular trafficking of zinc. *Biochimica et Biophysica Acta (BBA) - Molecular Cell Research* **1763,** 711-722.

Ellwood, M. J. (2004). Zinc and cadmium speciation in subantarctic waters east of New Zealand. *Marine Chemistry* **87**, 37-58.

Ellwood, M. J., and Hunter, K. A. (2000). Variations in the Zn/Si record over the last interglacial glacial transition. *Paleoceanography* **15**, 506-514.

Ellwood, M. J., and van den Berg, C. M. G. (2000). Zinc speciation in the Northeastern Atlantic Ocean. *Marine Chemistry* **68**, 295-306.

Ellwood, M. J. (2008). Wintertime trace metal (Zn, Cu, Ni, Cd, Pb and Co) and nutrient distributions in the Subantarctic Zone between 40-52°S; 155-160°E. *Marine Chemistry* **112**, 107-117.

Ferguson, J. (1983). Concentrations and speciation of lead, zinc and cadmium in seawater-like smelter effluent and adjacent marine environments, Port Pirie, South Australia. *Marine and Freshwater Research* **34**, 375-385.

Franck, V. M., Bruland, K. W., Hutchins, D. A., and Brzezinski, M. A. (2003). Iron and zinc effects on silicic acid and nitrate uptake kinetics in three high-nutrient, low-chlorophyll (HNLC) regions. *Marine Ecology Progress Series* **252**, 15-33.

Frew, R. D., Hutchins, D. A., Nodder, S., Sanudo-Wilhelmy, S., Tovar-Sanchez, A., Leblanc, K., Hare, C. E., and Boyd, P. W. (2006). Particulate iron dynamics during FeCycle in subantarctic waters southeast of New Zealand, *Global Biogeochemical Cycles*, **20**, GB1S93, doi:10.1029/2005GB002558.

Gaither, L. A., and Eide, D. J. (2001). Eukaryotic zinc transporters and their regulation. *BioMetals* **14**, 251-270.

Gatti, D., Mitra, B., and Rosen, B. P. (2000). *Escherichia coli* soft metal ion-translocating ATPases. *Journal of Biological Chemistry* **275**, 34009-34012.

Gélabert, A., Pokrovsky, O. S., Schott, J., Boudou, A., Feurtet-Mazel, A., Mielczarski, J., Mielczarski, E., Mesmer-Dudons, N., and Spalla, O. (2004). Study of diatoms/aqueous solution interface. I. Acid-base equilibria and spectroscopic observation of freshwater and marine species. *Geochimica et Cosmochimica Acta* **68**, 4039-4058.

Gélabert, A., Pokrovsky, O. S., Viers, J. , Schott, J., Boudou, A., and Feurtet-Mazel, A. (2006). Interaction between zinc and freshwater and marine diatom species: Surface complexation and Zn isotope fractionation. *Geochimica et Cosmochimica Acta* **70**, 839-857.

González-Dávila, M. (1995). The role of phytoplankton cells on the control of heavy metal concentration in seawater. *Marine Chemistry* **48**, 215-236.

Gosnell, K. J., Landing, W. M., and Milne, A. (2012). Fluorometric detection of total dissolved zinc in the southern Indian Ocean. *Marine Chemistry* doi: 10.1016/j.marchem.2012.01.004.

Grand, M., Oliveira, H. M., Ruzicka, J., and Measures, C. (2011). Determination of dissolved zinc in seawater using micro-Sequential Injection lab-on-valve with fluorescence detection. *Analyst* **136,** 2747-2755.

Guerinot, M. L. (2000). The ZIP family of metal transporters. *Biochimica et Biophysica Acta (BBA) - Biomembranes* **1465**, 190-198.

Gustin, J. L., Zanis, M. J., and Salt, D. E. (2011). Structure and evolution of the plant cation diffusion facilitator family of ion transporters. *BMC Evolutionary Biology* **11,** 76 doi:10.1186/1471-2148-11-76.

Hassler, C. S., and Wilkinson, K. J. (2003). Failure of the biotic ligand and free-ion activity models to explain zinc bioaccumulation by *Chlorella kesslerii*. *Environmental Toxicology and Chemistry* **22**, 620-626.

Hassler, C. S., Slaveykova, V. I., and Wilkinson, K. J. (2004). Some fundamental (and often overlooked) considerations underlying the free ion activity and biotic ligand models. *Environmental Toxicology and Chemistry* **23**, 283-291.

Hassler C.S., Sinoir, M., Clementson, L. A., and Butler, E. C. V. Exploring the link between micro-nutrients and phytoplankton in the Southern Ocean during the 2007 austral summer. *Frontiers of microbiology.* (Accepted).

Hassler C.S., Schoemann, V., Boye, M., Tagliabue, A., Rozmarynowycz, M., and McKay, R. M. L. Iron Bioavailability in the Southern Ocean. *Oceanography and Marine Biology: An annual review* **50, 1-64** (In press).

Hecky, R. E., Mopper, K., Kilham, P., and Degens, E. T. (1973). The amino acid and sugar composition of diatom cell-walls. *Marine Biology* **19**, 323-331.

Heijerick, D. G., de Schamphelaere, K. A C., and Janssen, C. R (2002). Biotic ligand model development predicting Zn toxicity to the alga *Pseudokirchneriella subcapitata*: possibilities and limitations. *Comparative Biochemistry and Physiology Part C: Toxicology & Pharmacology* **133**, 207-218.

Hendry, K. R., and Rickaby, R. E. M. (2008). Opal (Zn/Si) ratios as a nearshore geochemical proxy in coastal Antarctica. *Paleoceanography* **23**, doi: 10.1029/2007PA001576.

Hoppe, H. G. (2003). Phosphatase activity in the sea. *Hydrobiologia* **493**, 187-200.

Hudson, R. J. M. (1998). Which aqueous species control the rates of trace metal uptake by aquatic biota? Observations and predictions of non-equilibrium effects. *Science of the Total Environment* **219**, 95-115.

Hudson, R. J. M., and Morel, F. M. M. (1993). Trace metal transport by marine microorganisms: implications of metal coordination kinetics. *Deep Sea Research Part I: Oceanographic Research Papers* **40**, 129-150.

Jaccard, T., Ariztegui, D., and Wilkinson, K. J. (2009). Incorporation of zinc into the frustule of the freshwater diatom *Stephanodiscus hantzschii*. *Chemical Geology* **265**, 381-386.

John, S. G., Geis, R. W., Saito, M. A., and Boyle, E. A. (2007). Zinc isotope fractionation during high-affinity and low-affinity zinc transport by the marine diatom *Thalassiosira oceanic*. *Limnology and Oceanography* **52**, 2710-2714.

Kupriyanova, E. V., and Pronina, N. A. (2011). Carbonic anhydrase: Enzyme that has transformed the biosphere. *Russian Journal of Plant Physiology* **58**, 197-209.

Landing, W. M., Haraldsson, C., and Paxeus, N. (1986). Vinyl polymer agglomerate based transition metal cation-chelating ion-exchange resin containing the 8-hydroxyquinoline functional group. *Analytical Chemistry* **58**, 3031-3035.

Lane, T. W., and Morel, F. M. M. (2000). Regulation of Carbonic Anhydrase Expression by Zinc, Cobalt, and Carbon Dioxide in the Marine Diatom Thalassiosira weissflogii. *Plant Physiol.* **123,** 345-352.

Lannuzel, D., Bowie, A. R., van der Merwe, P. C., Townsend, A. T., and Schoemann, V. (2011). Distribution of dissolved and particulate metals in Antarctic sea ice. *Marine Chemistry* **124,** 134-146.

Leblanc, K., Hare, C. E., Boyd, P. W., Bruland, K. W., Sohst, B., Pickmere, S., Lohan, M. C., Buck, K., Ellwood, M., and Hutchins, D. A. (2005). Fe and Zn effects on the Si cycle and diatom community structure in two contrasting high and low-silicate HNLC areas. *Deep Sea Research Part I: Oceanographic Research Papers* **52**, 1842-1864.

Lohan, M. C., Statham, P. J., and Crawford, D. W. (2002). Total dissolved zinc in the upper water column of the subarctic North East Pacific. *Deep Sea Research Part II: Topical Studies in Oceanography* **49**, 5793-5808.

Löscher, B. M. (1999). Relationships among Ni, Cu, Zn, and major nutrients in the Southern Ocean. *Marine Chemistry* **67**, 67-102.

Martin, J. H., Gordon, R. M., and Fitzwater, S. E. (1990). Iron in the Antarctic waters. *Nature* **345**, 156-158.

Martinoia, E., Klein, M., Geisler, M., Bovet, L., Forestier, C., Kolukisaoglu, Ü., Müller-Röber, B., and Schultz, B. (2002). Multifunctionality of plant ABC transporters - more than just detoxifiers. *Planta* **214**, 345-355

Marx, S. K., Kamber, B. S., and McGowan, H. A. (2008). Scavenging of atmospheric trace metal pollutants by mineral dusts: Inter-regional transport of Australian trace metal pollution to New Zealand. *Atmospheric Environment* **42**, 2460-2478.

McGinn, P. J., and Morel, F. M. M. (2008). Expression and regulation of carbonic anhydrases in the marine diatom *Thalassiosira pseudonana* and in natural phytoplankton assemblages from Great Bay, New Jersey. *Physiologia Plantarum* **133,** 78-91.

McGowan, H., and Clark, A. (2008). Identification of dust transport pathways from Lake Eyre, Australia using Hysplit. *Atmospheric Environment* **42**, 6915-6925.

McKay, R. M. L., Wilhem, S. W., Hall, J., Hutchins, D. A., Al-Rshaidat, M. M. D., Mioni, C. E., Pickmere, S., Porta, D., and Boyd, P. W. (2005). Impact of phytoplankton on the biogeochemical cycling of iron in subantarctic waters southeast of New Zealand during FeCycle. *Global Biogeochemical Cycle*,**19**, GB4S24, 10.1029/2005GB002482.

Millero, F.J., Woosley R., DiTrolio, B. and Waters, J. (2009) Effect of ocean acidification on the speciation of metals in seawater. *Oceanography* **22**, 72–85.

Morel, F. M. M. (1983). 'Principles of aquatic chemistry'. pp. 300-309. (Wiley, New York).

Morel, F. M. M. (2008). The co-evolution of phytoplankton and trace element cycles in the oceans. *Geobiology* **6**, 318-324.

Morel, F. M. M., Reinfelder, J. R., Roberts, S. B., Chamberlain, C. P., Lee, J. G., and Yee, D. (1994). Zinc and carbon co-limitation of marine phytoplankton. *Nature* **369**, 740-742.

Morel, F. M. M., Cox, E. H., Kraepiel, A M. L., Lane, T. W., Milligan, A J., Schaperdoth, I., Reinfelder, J. R., and Tortell, P. D. (2002). Acquisition of

inorganic carbon by the marine diatom *Thalassiosira weissflogii*. *Functional Plant Biology* **29**, 301-308.

Morel, F. M. M., Milligan, A. J., Saito, M. A., Heinrich, D. H. and Karl, K. T. (2003). Marine bioinorganic chemistry: The role of trace metals in the oceanic cycles of major nutrients. In 'Treatise on geochemistry'. pp. 113-143. (Pergamon, Oxford).

Morel, F. M. M., and Price, N. M. (2003). The biogeochemical cycles of trace metals in the oceans. *Science* **300**, 944-947.

Moussatova, A., Kandt, C., O'Mara, M. L., and Tieleman, D. P. (2008). ATP-binding cassette transporters in Escherichia coli. *Biochimica et Biophysica Acta (BBA) - Biomembranes* **1778,** 1757-1771.

Muller, F. L. L., Jacquet, S., and Wilson, W. H. (2003). Biological Factors Regulating the Chemical Speciation of Cu, Zn, and Mn under Different Nutrient Regimes in a Marine Mesocosm Experiment. *Limnology and Oceanography* **48**, 2289-2302.

Nolting, R. F., Heijne, M., de Jong, J. T. M., Timmermans, K. R., and de Baar, H. J. W. (2000). The determination and distribution of Zn in surface water samples collected in the northeast Atlantic Ocean. *Journal of Environmental Monitoring* **2**, 534-538.

Nowicki, J. L., Johnson, K. S., Coale, K. H., Elrod, V. A., and Lieberman, S. H. (1994). Determination of Zinc in Seawater Using Flow Injection Analysis with Fluorometric Detection. *Analytical Chemistry* **66**, 2732-2738.

Oste, L. A., Temminghoff, E. J. M., Lexmond, T. M., and van Riemsdijk, W. H. (2002) Measuring and Modeling Zinc and Cadmium Binding by Humic Acid. *Analytical Chemistry* **74**, 856-862.

Pagenkopf, G. (1983). Gill surface interaction model for trace-metal toxicity to fishes: role of complexation, pH, and water hardness. *Environmental Science and technology* **17**, 342-347.

Patterson, C. C., and Settle, D. M. (1976). The reduction of orders of magnitude errors in lead analysisof biological materials and natural waters by controlling external sources of industrial Pb contaminationintroduced during sample collection and handling. In 'Reliability in Trace Analysis'. (Ed.D. M. La Fleur, National Bureau of Standards, Washington, Special Publication 422) pp. 321-351.

Park, H., Song, B., and Morel, F. M. M. (2007). Diversity of the cadmium-containing carbonic anhydrase in marine diatoms and natural waters. *Environmental Microbiology* **9**, 403-413.

Perales-Vela, H. V., Peña-Castro, J. M., and Cañizares-Villanueva, R. O. (2006) Heavy metal detoxification in eukaryotic microalgae. *Chemosphere* **64,** 1-10.

Playle, R. C. (1998). Modelling metal interactions at fish gills. *Science of the Total Environment* **219**, 147-163.

Plocke, D. J., Levinthal, C., and Vallee, B. L. (1962) Alkaline Phosphatase of *Escherichia coli*: A Zinc Metalloenzyme. *Biochemistry* **1,** 373-378.

Price, N. M., and Morel, F. M. M. (1990). Cadmium and cobalt substitution for zinc in a marine diatom. *Nature* **344**, 658-660.

Roberts S. B., Lane T. W., and Morel, F. M. M. (1997) Carbonic Anhydrase in the Marine Diatom *Thalassiosira weissflogii* (Bacillariophyceae). *Journal of Phycology* **33,** 845-850.

Saito, M. A., Moffett, J. W., Chisholm, S. W., and Waterbury, J. B. (2002) Cobalt Limitation and Uptake in *Prochlorococcus. Limnology and Oceanography* **47**, 1629-1636.

Saito, M. A., and Goepfert, T. J. (2008) Zinc-cobalt colimitation of *Phaeocystis Antarctica*. *Limnology and Oceanography* **53**, 266-275.

Saito, M. A., Goepfert, T. J., and Ritt, J. T. (2008). Some thoughts on the concept of co-limitation: Three definitions and the importance of bioavailability. *Limnology and Oceanography* **53**, 276-290.

Schmitt, L., and Tampé, R. (2002). Structure and mechanism of ABC transporters. *Current Opinion in Structural Biology* **12**, 754-760.

Shaked, Y., Xu, Y., Leblanc, K., and Morel, F. M. M. (2006). Zinc availability and alkaline phosphatase activity in Emiliania huxleyi: Implications for Zn-P co-limitation in the ocean. *Limnology and Oceanography* **51**, 299-309.

Smith, D. S., Bell, R. A., and Kramer, J. R. (2002). Metal speciation in natural waters with emphasis on reduced sulfur groups as strong metal binding sites. *Comparative Biochemistry and Physiology Part C: Toxicology & Pharmacology* **133**, 65-74.

Spokes, L., Jickells, T., and Jarvis, K. (2001). Atmospheric inputs of trace metals to the northeast Atlantic Ocean: the importance of southeasterly flow. *Marine Chemistry* **76**, 319-330.

Sunda, W. G., and Huntsman, S. A. (1992). Feedback interactions between zinc and phytoplankton in seawater. *Limnology and Oceanography* **37**, 25-40.

Sunda, W. G., and Huntsman, S. A. (1995*a)*. Cobalt and Zinc Interreplacement in Marine Phytoplankton: Biological and Geochemical Implications. *Limnology and Oceanography* **40**, 1404-1417.

Sunda, W. G., and Huntsman, S. A. (1996). Antagonisms between Cadmium and Zinc Toxicity and Manganese Limitation in a Coastal Diatom. *Limnology and Oceanography* **41**, 373-387.

Sunda, W. G., and Huntsman, S. A. (1998). Processes regulating cellular metal accumulation and physiological effects: Phytoplankton as model systems. *Science of The Total Environment* **219**, 165-181.

Sunda, W. G., and Huntsman, S. A. (2000). Effect of Zn, Mn, and Fe on Cd Accumulation in Phytoplankton: Implications for Oceanic Cd Cycling. *Limnology and Oceanography* **45**, 1501-1516.

Sunda, W. G., and Huntsman, S. A. (2005). Effect of CO_2 Supply and Demand on Zinc Uptake and Growth Limitation in a Coastal Diatom. *Limnology and Oceanography*, **50,** 1181-1192.

Timmermans, K. R., Snoek, J., Gerringa, L. J. A., Zondervan, I., and de Baar, H. J. W. (2001). Not All Eukaryotic Algae Can Replace Zinc with Cobalt: *Chaetoceros calcitrans* (Bacillariophyceae) versus Emiliania huxleyi (Prymnesiophyceae). *Limnology and Oceanography* **46**, 699-703.

Tipping, E. (1993). WHAM- A computed equilibrium model and computer code for waters, sediments, and soils incorporating a discrete site/electrostatic model of ion-binding by humic substances. *Computers & Geosciences* **20**, 973-1023.

Tipping, E. (1998). Humic Ion-Binding Model VI: An Improved Description of the Interactions of Protons and Metal Ions with Humic Substances. *Aquatic Geochemistry* **4**, 3-48.

Turner, D. R. (1995). Problems in Trace Metal Speciation Modeling. In 'Metal speciation and bioavailability in aquatic systems'. (Eds: A. Tessier and D.R. Turner.) pp. 149-203.

Twining, B. S., Baines, S. B., Vogt, S., and de Jonge, M. D. (2008). Exploring Ocean Biogeochemistry by Single-Cell Microprobe Analysis of Protist Elemental Composition. *Journal of Eukaryotic Microbiology* **55**, 151-162.

van den Berg, C. M. G. (1985). Determination of the zinc complexing capacity in seawater by cathodic stripping voltammetry of zinc—APDC complex ions. *Marine chemistry* **16**, 121-130.

van Leeuwen, H. P., Town, R. M., Buffle, J., Cleven, R. F. M., Davison, W. Puy, J., van riemsdijk, W. H., and Sigg, L. (2005) Dynamic speciation analysis and bioavailability of metals in aquatic systems. *Environmental Science & Technology* **39**, 8545-8556.

Varela, D. E., Willers, V., and Craawford, D. W. (2011). Effect of zinc availability on growth, morphology, and nutrient incorporation in a coastal and an oceanic diatom. *Journal of Phycology* **47,** 302-312.

Whitfield M. (2001). Interactions between Phytoplankton and Trace Metals in the Ocean. *Advances in marine biology* **41**, 1-128.

Williams, L. E., Pittman, J. K., and Hall, J. L. (2000). Emerging mechanisms for heavy metal transport in plants. *Biochimica et Biophysica Acta (BBA) - Biomembranes* **1465**, 104-126.

Willie, S. N., Lam, J. W. H., Yang, L., and Tao, G. (2001). On-line removal of Ca, Na and Mg from iminodiacetate resin for the determination of trace elements in seawater and fish otoliths by flow injection ICP-MS. *Analytica Chimica Acta* **447**, 143-152.

Wisniewski Jakuba, R., Moffet, J. W., and Dyhrman, S. T. (2008). Evidence for the linked biogeochemical cycling of zinc, cobalt, and phosphorus in the western North Atlantic Ocean. *Global Biogeochemical Cycles* **22,** doi:10.1029/2007gb003119.

Wisniewski Jakuba, R., Moffett, J. W., and Saito, M. A. (2008). Use of a modified, high-sensitivity, anodic stripping voltammetry method for determination of zinc speciation in the North Atlantic Ocean. *Analytica Chimica Acta* **614**, 143-152.

Witt, M., Baker, A. R., and Jickells, T. D. (2006). Atmospheric trace metals over the Atlantic and South Indian Oceans: Investigation of metal concentrations and lead isotope ratios in coastal and remote marine aerosols. *Atmospheric Environment* **40**, 5435-5451.

Yang, R. J., and van den Berg, C. M. G. (2009). Metal complexation by humic substances in seawater. *Environmental Science & Technology* **43**, 7192-7197.

Yebra-Biurrun, M. C., and Cespón-Romero, R. M. (2006). Minicolumn field sampling-preconcentration of trace zinc from seawater and its laboratory detection by flow injection flame atomic absorption spectrometry. *Analytical Sciences* **22**, 51-55.

Yee, D., and Morel, F. M. M. (1996). In Vivo Substitution of Zinc by Cobalt in Carbonic Anhydrase of a Marine Diatom. *Limnology and Oceanography* **41**, 573-577.

Zhang, Y., Fomenko, D. E., and Gladyshev, V. N. (2005) The microbial selenoproteome of the Sargasso Sea. *Genome Biology*. **6** (4), R37

Zirino, A., and Yamamoto, S. (1972). A pH-Dependent Model for the Chemical Speciation of Copper, Zinc, Cadmium, and Lead in Seawater. *Limnology and Oceanography*, **17**, 661-671.

CHAPTER THREE

Uptake response of two phytoplankton species from the Tasman Sea to low Zn media

Marie Sinoir[(1), (2)], Christel S. Hassler[(3)#], Andrew R. Bowie[(2), (4)], Mathieu Mongin [(1)], Edward C.V.Butler[(5)]

[(1)] CSIRO Marine Laboratories, Castray Esplanade, GPO Box 1538, Hobart TAS 7000

[(2)] Institute for Marine and Antarctic Studies (IMAS), Sandy Bay campus, University of Tasmania, Hobart TAS 7001, Australia

[(3)] Plant Functional Biology and Climate Change Cluster, University of Technology Sydney, Broadway, NSW 2007, Australia

[(4)] Antarctic Climate and Ecosystem Cooperative Research Centre (ACE CRC), University of Tasmania, Hobart, TAS 7001, Australia

[(5)]Australian Institute of Marine Science, Arafura Timor Research Facility, Brinkin, NT 8010, Australia.

#current address: University of Geneva, Institute FA Forel, 10 Route de Suisse, 1290 Versoix, Switzerland

In prep. for submission

3.1 Introduction

Since the iron hypothesis (Martin et al. 1990), many studies have focused on the limiting role that trace elements impose on the oceanic biological carbon pump. Improvement of technical and theoretical advances in chemical oceanography (Patterson and Settle 1976, Bruland *et al.* 1979, Bowie and Lohan 2009, Cutter *et al.* 2010) have increased our understanding of the roles and distributions of important trace metals, other than iron (Bruland and Lohan 2003; Morel *et al.* 2003). Amongst them, zinc (Zn) can play an important role for the phytoplankton community, and interest for this element is currently rising. The key Zn-dependent enzymes for phytoplankton growth are carbonic anhydrase (CA) and alkaline phosphatase (AP). These enzymes are responsible for carbon uptake and internal conversion of inorganic carbon (CA) and phosphate uptake (AP). Biological carbon uptake is obviously of critical interest, because of CO_2 drawdown in the ocean mitigating the rise of atmospheric CO_2, ocean acidification and the ability for organisms to calcify (Sunda and Hunstman 2002; Schultz *et al.* 2004). Phosphate can be a limiting macronutrient and P-Zn co- limitation has been postulated in particular marine environments (Shaked *et al.* 2006, Wisniewski *et al.* 2008). Deck incubations are still scarce for Zn studies, however, they highlighted important interactions between Zn and phytoplankton communities possibly inducing species shifts or reduced chlorophyll *a* (Chl) concentrations or Cd:P ratio (Coale *et al.* 2003; Cullen and Sherrell 2005; Leblanc *et al.* 2005, Wisniewski-Jakuba *et al.* 2012, Hassler *et al*. 2012*b*, Sinoir *et al.* 2012).

As known for other elements, such as iron (Fe) or silicic acid (Sarthou *et al.*, 2005), cellular requirements for Zn differ from one species to another and

phytoplankton can adapt their requirements according to replete/deplete concentrations (Sunda and Huntsman 1992). Previous studies have also shown that diatoms cannot grow without Zn (Sunda and Huntsman 1995, Varela *et al.* 2011), while the coccolithophorid *E. huxleyi* or the marine phytoplankter *Phaeocystis antartica* can replace it with cobalt (Co, Timmermans *et al.* 2001, Saito and Goepfert 2008). On the other hand, cyanobacteria need Co but not Zn (Saito *et al.* 2002). *E. huxleyi* and the diatom *Thalassiosira weissflogii* can also partially replace Zn with cadmium (Cd, Lane *et al.* 2000, Xu *et al.* 2007). It is to be noted that the Co, Zn, and Cd inter-replacement and requirement measured in laboratory phytoplankton isolates is not as obvious for complex natural phytoplankton communities as noted in Hassler *et al* (2012*a*).

Recent studies have brought new data and observations for Zn chemistry and revealed its very low total dissolved and free ion concentrations in certain parts of the ocean, including the Tasman Sea (Ellwood and van den Berg 2000, Lohan *et al.* 2002, Ellwood 2004, Wisniewski–Jakuba *et al.* 2008; Baars and Croot, 2011; Croot *et al.* 2011). These low levels reflect a high degree of complexation with organic ligands present in seawater, which potentially decreases Zn bioavailability. However, recent work has presented the possibility for phytoplankton to access Zn complexed with a weaker organic ligand (e.g. Cysteine associated complex: Aristilde *et al.* 2012). The presence of these ligands increases the importance of better understanding how organisms cope with matching their Zn requirements given its low concentrations and high degree of complexation. Few studies have focused on the Tasman Sea region. Ellwood (2008) revealed low dissolved Zn concentrations in these waters and Hassler *et al.* (2012*b*) showed that Zn in this region could potentially limit the phytoplankton.

Here, we studied two phytoplankton species relevant for the phytoplanktonic assemblages from the Tasman Sea, the pennate diatom *Nitzschia closterium* (Furuya *et al.* 1986) and the coccolithophorid *Emiliania huxleyi* (Calvo *et al.* 2004). These two species were exposed to low free zinc concentration regimes, comparable to concentrations previously reported in the literature for two different regimes—a productive one and a depleted one. Short-term uptake experiments (4–24 h) in presence of radiolabelled zinc and carbon (^{65}Zn and ^{14}C) were performed to explore the effect of growth conditions on zinc uptake rate, and the zinc biological transport pathway in action. The bioavailability of variable free zinc concentrations was determined using a strong ligand (NTA) at different concentrations. Monitoring the biological uptake of zinc in the presence of five different inhibitors helped to interpret the role of cellular metabolism, as well as the uptake pathways involved in Zn uptake.

3.2 Materials and methods

3.2.1 Phytoplankton species:

The coccolithophorid *Emiliania huxleyi* (CS-812; Prymnesiophyceae) was isolated from the Mercury Passage (TAS, Australia) in November 2004 (Ian Jameson). The pennate diatom *Nitzschia closterium* (CS-1; Baccillariophyceae) was isolated from Port Hacking (NSW, Australia) in January 1962 (G.F. Humphrey). Both strains (Fig. 1) were taken and grown at the Australian National Algal Culture Collection (ANACC).

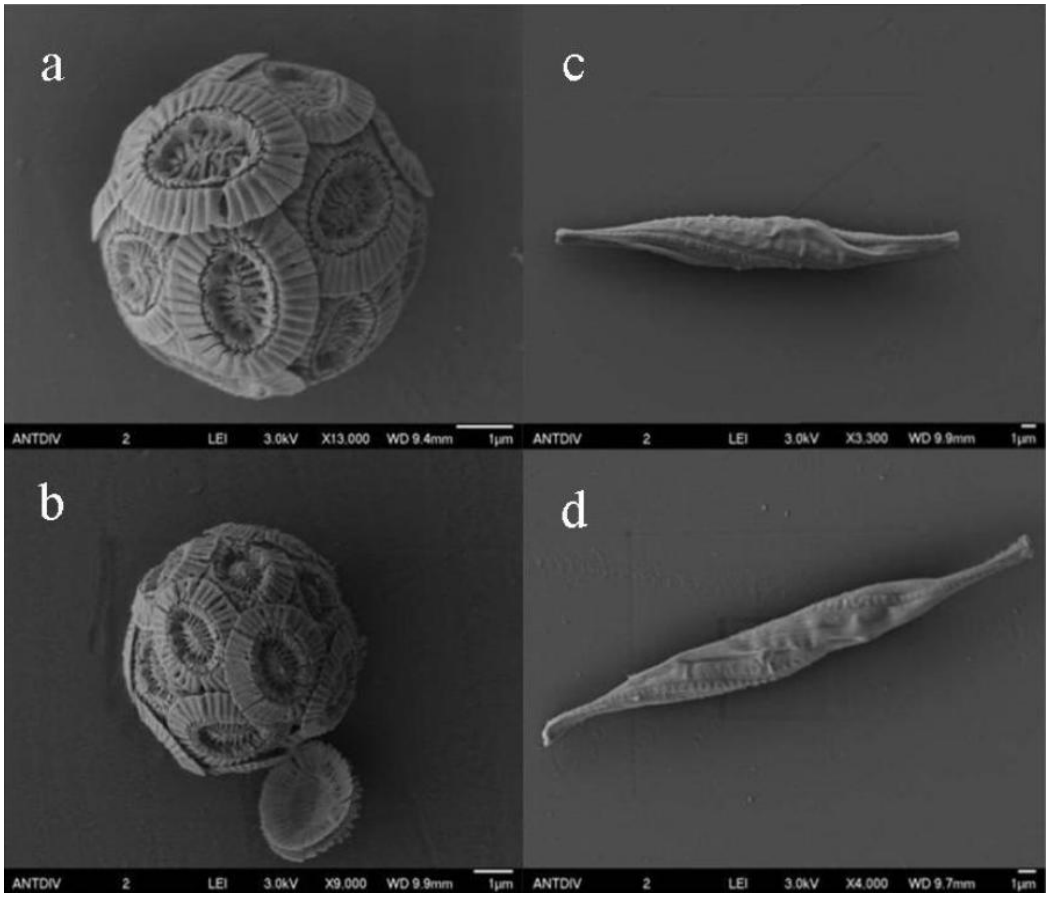

Figure 1: Electronic micrograph of both species cultured in laboratory: *E. huxleyi* in high (a, x 13000) and low zinc concentrations(b, x 9000), and *N. closterium* in high (c, x 3300) and low concentrations, (d, x 4000). Photo credit, Rick van den Enden and Marie Sinoir.

3.2.2 Culture media:

Both strains were grown in natural, low-nutrient Northern Tasmanian seawater (< 0.2 µm; Zn = 0.02 nmol L^{-1}, 30.00ºS; 165.00ºW, 15 m depth) sampled using trace-metal clean techniques during the Productivity Induced by Nitrogen in the Tasman Sea cruise (PINTS, http://www.marine.csiro.au/nationalfacility/voyagedocs/2010/MNF_SS01-2010_summary.pdf, Hassler *et al.*2012, in prep.). The seawater was enriched in trace elements and vitamins as per Wake *et al.* (2011). Two different Zn additions

(0.13nmol L^{-1} and 13 nmol L^{-1}) were done to achieve a low (LZn) and high (HZn) regime, respectively, for which the free zinc concentrations ($[Zn^{2+}]$) were calculated as 1.5 pmol L^{-1} (LZn) and 1.5 nmol L^{-1} (HZn), respectively (MINEQL+, ver. 4.5, Table 1). Since background Zn dissolved concentrations present in the Tasman Sea water used were at least an order of magnitude lower than the ones we added, the calculations did not take the background zinc into account. All micronutrients and trace metal solutions were prepared and passed through chelating resin (BioRad, Chelex-100) in a clean room (ISO Class 5) following trace-metal-clean techniques (Price et al 1988/89; Bowie and Lohan, 2009). Culture media were sterilised using a low-heat microwave cycle and equilibrated for at least 24 h at room temperature before enrichment and transfer of the different strains.

Table 1: Trace metal mix and vitamin concentrations used to enrich the culture media during the acclimation process. The seawater used was sampled in the Tasman Sea and filtered (0.2 µm).

Trace metal mix	[M] in media (mol L^{-1})
Fe-EDTA:	
$FeCl_3$	$2.00 * 10^{-6}$
Na_2EDTA	$3.55 * 10^{-5}$
Trace metals:	
$CoCl_2$	$1.00 * 10^{-7}$
$MnCl_2$	$1.35 * 10^{-7}$
Na_2MoO_4	$1.00 * 10^{-8}$
$NiCl_2$	$6.00 * 10^{-8}$
Na_2EDTA	$6.00 * 10^{-5}$
$CuCl_2$	$1.20 * 10^{-8}$
Selenium:	
Na_2SeO_3	$1.00 * 10^{-9}$
Vitamins	Stock present in f/2 media

3.2.3 Experimental culture conditions:

Algae were grown in 10 % acid-washed vials (HCl, Li-em-supply) and double-bagged in plastic bags in an incubation chamber (ThermoLine Scientific Equipment) at 20 °C, with a 12-h light:dark cycle (130 µmol photons m^{-2} s^{-1}). Cells were acclimated for at least 10 generations in the culture media prior to experiments. Culture transfers and cell handling were conducted under a clean laminar flow work station (Clyde-Apac HWS Series). Cell numbers (N, cells mL^{-1}) were determined daily with a particle size counter (Coulter, Multisizer II) from lag to stationary phases (14 days for both species) and used to calculate specific growth rates (µ, d^{-1}, Eq. (1)) for each Zn regime:

$$\mu = (\ln N_{t2} - \ln N_{t1})/(t_2 - t_1) \quad (1)$$

where t_1 and t_2 are incubation times taken at the beginning and end of the exponential growth phase.

Volume (V) and surface area (SA) were calculated from the Coulter measurements considering the cells were spherical for *E. huxleyi* (Eq. 2 and 3). For *N. closterium*, we compared two different ways to obtain volume and surface areas. Volumes and surface areas were deduced from Coulter counter measurements assuming cells were spheroids (Eq. 2 and 3). Alternatively, the prolate spheroid formula was used to calculate SA and V (Eq. 4 and 5) using the length (L) and width (l) measured with a field emission scanning electron microscopy (JEOL JSM-6701F, FESEM) with samples (n = 10) prepared as per Marchant and Thomas (1983).

$$SA = 4 \times \pi \times R^2 \quad (2)$$

$$V = (4/3) \times \pi \times R^3 \quad (3)$$

$$SA = 2 \times \pi \times l^2 (1 + (L/ l \times e) \times \sin^{-1}(e)) \text{ with } e = 1-(l/L)^2 \quad (4)$$

$$V = (4/3) \times \pi \times l^2 \times L \quad (5)$$

The ratio SA/V was calculated and used as indicator for adaption to the different concentrations of Zn. The photosynthetic health of the cells during the experimental process was measured with a Water-PAM (Heinz Walz GmbH) on aliquots of samples kept in the dark for 5 min prior to determination of their maximum quantum yield (Fv/Fm).

3.2.4 Experimental design:

Table 2: Concentrations of macronutrients used to make up the AQUIL medium (inorganic seawater). Only macronutrients were added for the bioaccumulation experiments. All reagents used were ultrapure Sigma-Aldrich or BDH.

Salt anhydrous solution	[M] in media (mol L^{-1})	Salt hydrated solution	[M] in media (mol L^{-1})	Enrichment macronutrients	[M] in media (mol L^{-1})
NaCl	$4.20*10^{-1}$	$MgCl_2*6H_2O$	$5.46*10^{-2}$	$NaNO_3$	$3.00*10^{-4}$
Na_2SO_4	$2.88*10^{-2}$	$CaCl_2*6H_2O$	$1.05*10^{-2}$	$NaH_2PO_4*2H_2O$	$2.00*10^{-5}$
KCl	$9.39*10^{-3}$	$SrCl_2*6H_2O$	$6.38*10^{-5}$	$NaSiO_3*5H_2O$	$1.00*10^{-4}$
$NaHCO_3$	$7.14*10^{-3}$				
KBr	$8.40*10^{-4}$				
H_3BO_3	$1.46*10^{-3}$				
NaF	$7.14*10^{-5}$				

The three experiments conducted in this study were carried out in AQUIL, a synthetic media in which chemical speciation was modelled (Price *et al.*1988, Wake *et al*. 2011, Table 2). For each bioaccumulation experiment, only macronutrients were added. Each experiment was performed in duplicate for Zn, but in triplicate for the carbon uptake. To avoid contamination, only polymer containers (polycarbonate or polypropylene) were used. All labware was washed in HCl (10%); rinsed seven times in Milli-Q water (R > 18 MΩ

cm) prior to use.

For each experiment, cells were grown until the mid-exponential growth phase to work with a total biomass over 100,000 cells mL^{-1}. They were then collected by gentle filtration (2 µm, polycarbonate, Millipore) and washed with 10 mM EDTA (for 2 min, 3 rinses of 5mL) then 3 rinsed with Chelex-stripped NaCl (0.6 M) + $NaCOH_3$ (2.38 mM) at pH 8 before further manipulations (Hassler *et al.*, 2004; Tang and Morel 2006). Cells were then resuspended into 10 mL of Zn-free experimental media at pH 8.1 (AQUIL major salts and macronutrients only, Chelex-stripped, Table 2). Ten mL of concentrated cells were redistributed equally in the different media to start the experiments, with the same biomass in the different incubation bottles.

Bioaccumulation experiments were made under the hypothesis that dissolved Zn was essentially constant over the time of each experiment. For each of the three experiment, 50 nmol L^{-1} Zn enrichment from a ^{65}Zn source (as $^{65}ZnCl_2$: Perkin Elmer, 12.36 mCi mL^{-1}) was done resulting in a 1.84 nCi mL^{-1}activity in the experimental solution. The enrichment was done 24 h prior the addition of microorganisms to let the experimental solution equilibrate at room temperature in the dark. For each bioaccumulation experiment, the Zn enrichment associated with the ^{65}Zn source was used to calculate the total Zn concentration in the experimental solution. Measurements of sample radioactivity were done with a scintillation counter (Tri- Carb 2810 TR). Radioactivity was measured in a 10-mL scintillation counter (Ultima Gold, Perkin Elmer) prior to the equilibration phase to obtain the initial radioactivity, as well as on filters and solution collected at the end of the short-term uptake experiment.

Table 3: Preparation of the quenching curves used to convert cpm in dpm. Two quenching curves were established for both the seawater correction and filters (nitrocellulose) corrections.

a. In filtered seawater (Fsw):

Label	Fsw (mL)	^{65}Zn (µL)	Quenching agent (µL)
1	2.00	20	0
2	1.99	20	15
3	1.97	20	30
4	1.96	20	45
5	1.94	20	60
6	1.93	20	75
7	1.91	20	90
8	1.90	20	105
9	1.88	20	120
10	1.87	20	135

b. For the filters:

Label	Fsw (mL)	^{65}Zn (µL)	Quenching agent (µL)
1	135	20	0
2	120	20	15
3	105	20	30
4	90	20	45
5	75	20	60
6	60	20	75
7	45	20	90
8	30	20	105
9	15	20	120
10	0	20	135

All results, obtained in counts per minute (cpm), were converted into

disintegrations per minutes (dpm) with two homemade quenching curves (Table 3) using Nitromethane (HPLC grade, Sigma Aldrich®) as quenching agent. The quenching curves obtained (Fig. 2) allowed us to obtain the correlation between the transformed Spectral Index of External Standard (t-SIE) and the efficiency of counting for liquid samples (0.086 ± 0.004, R^2 = 0.98) and filters (0.078 ± 0.003, R^2 = 0.98). The dpm were then converted to intracellular ($[Zn]_{int}$: nmol Zn L^{-1} h^{-1} μm^{-2}) and adsorbed Zn concentration ($[Zn]_{ads}$: nmol Zn L^{-1} h^{-1} μm^{-2}, concentration of zinc extractible with EDTA), taking into account the Zn isotopic ratios for the experiment (dpm from $^{65}Zn/[Zn]$). To consider differences in cell abundance, as well as size, biological Zn concentrations were normalised with cell numbers and cellular average surface area. The following equations were used for the different calculations:

$[Zn]_{int}$ = (dpm * cell number) / (volume filtered * ($^{65}Zn/[Zn]$) * SA) (6)

$[Zn]_{ads}$ = (dpm * cell number) / (dilution by EDTA wash * volume filtered * SA) (7)

Linearity of the Zn uptake was verified over a 24-h period in the presence of 50 nM inorganic Zn. The slope of the correlation between the internalised Zn ($[Zn]_{intra}$) over time provided the Zn internalisation flux for both species and Zn growth conditions. Uptake values (nmol L^{-1} $cells^{-1}$) were calculated by averaging the values of Zn uptake (nmol L^{-1} $cells^{-1}$) obtained during the course of the experiment (24h).

The impact of varying free Zn concentration on biological uptake was identified by adding excess of NTA to different experimental treatments (Table 4).

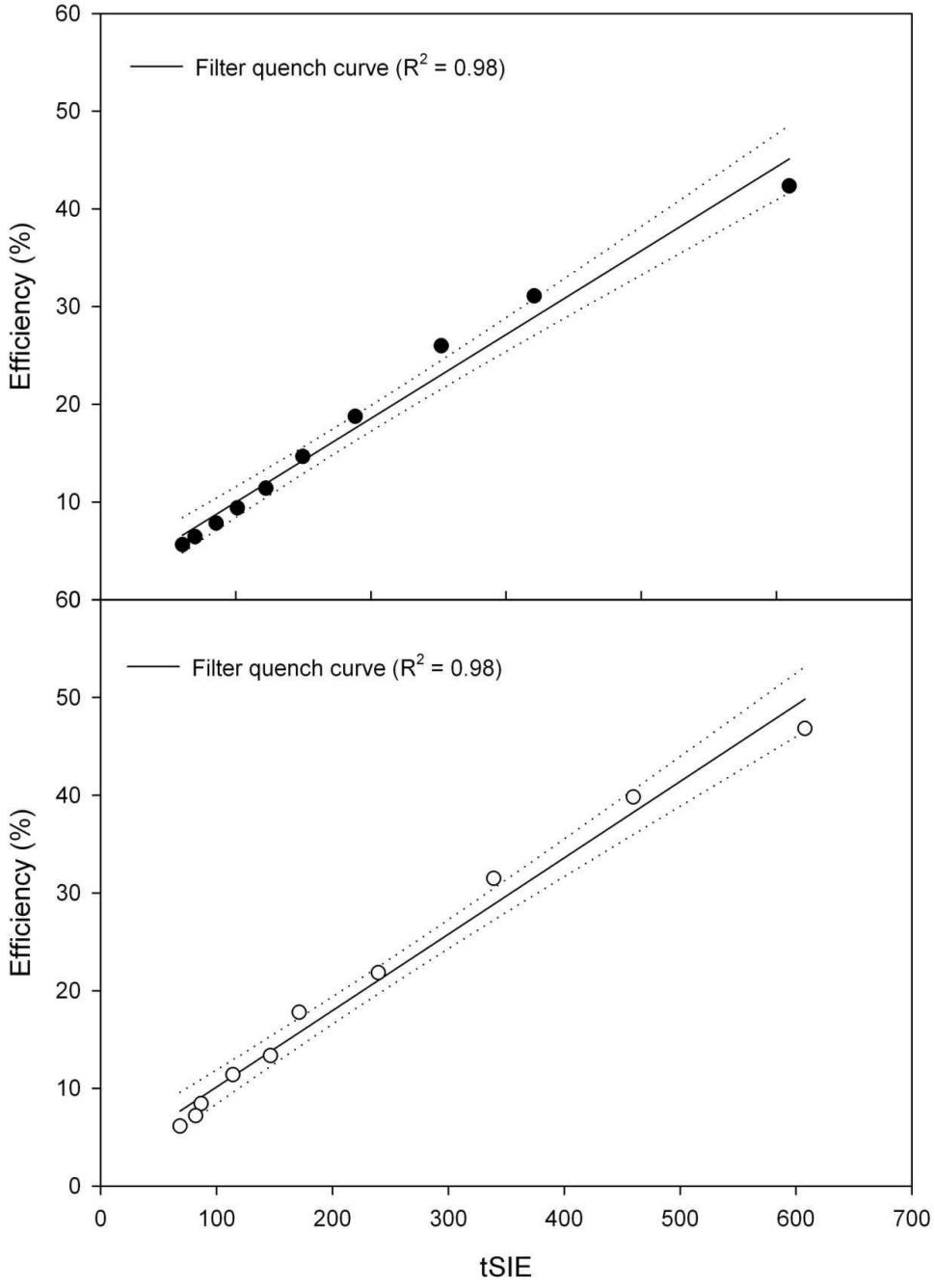

Fig. 2: Quench curves obtained for the calculation of dpm from the cpm measured during the bioaccumulation experiments. The top panel corresponds to the liquid correction and the bottom one to the filter.

According to Sunda and Huntsman (1998), Hudson (1998), and Hassler and Wilkinson (2003), internalisation flux were compared to the calculated maximum diffusive flux (J_{diff}) to identify the rate-limiting processes controlling Zn bioavailability. The maximum radial diffusion was calculated as per:

$$J_{diff} = (D_{Zn}/R) \times [Zn^{2+}] \quad (8)$$

where, $D_{Zn} = 2.28 \times 10^{-6}$ m^2 h^{-1} (Kariuki and Dewald 1996) and R was the radius of each cell in meters measured with the particle-size counter (Multisizer®). $[Zn^{2+}]$ were calculated with MINEQL+ ver. 4.5 (Table 4).

Table 4: Concentration of NTA added in the media and Zn^{2+} concentration calculated with MINEQL, ver. 4.5.

Label	$[Zn^{2+}]$ (nM)	[Zn]tot (nM)	[NTA]tot (mM)	AQUIL (L)	Spike NTA (µL)	^{65}Zn spike (µL)
1	$1.67*10^{-3}$	25	2.5	1000	1000	50
2	$3.34*10^{-3}$	50	2.5	1000	1000	100
3	$9.83*10^{-3}$	50	1	750	300	75
4	$3.01*10^{-2}$	50	0.35	650	910	65
5	0.11	50	0.1	500	200	50
6	0.96	50	0.01	400	16	40
7	2.85	50	0.0025	300	3	30

Identification of the different pathways for Zn and carbon (C) uptake was done in the presence of five metabolic inhibitors added to the media. The five inhibitors were chosen for their different role on phytoplankton metabolism. Vanadate (20 µM, BDH®) was prepared according to Furla *et al.* (2000). It is a specific inhibitor purportedly acting on the P-type ATPase transport system and related to high affinity transporters (Balnokin *et al.* 1997; Hassler and Wilkinson 2003). Carbonyl cyanide m-chlorophenyl hydrazone (CCCP: 20 µM, Sigma®) was prepared by diluting a stock solution in ethanol. CCCP acts on the oxidative photophosphorylation, disrupts transmembrane pH and decreases the ability of H^+-ATP synthetase to function optimally (Heytler 1980). Dichlorophenyldimethylurea (DCMU Sigma®: 0.5 µM) was also prepared by diluting a stock solution in a stoichiometric solution of ethanol and MilliQ water. DCMU is a very specific and acts on the photosynthesis system II by blocking the flow of electrons and thus production of NADPH (Gnassia-Barelli and Roméo 1987). As a consequence, it prevents the algae from turning light into chemical energy. Ethoxyzolamide (EZA Sigma®: 500 µM) and acetazolamide (AZA Sigma®: 100 µM) were both prepared by diluting a stock solution in DMSO. While EZA action concerns both CA, internal and external (Moroney *et al.* 1985), AZA acts only on the external CA, located in the periplasmic space (Williams and Turpin 1987, Badger and Price 1994). Cells were exposed for 4 h to the different inhibitors, to avoid high levels of mortality, to the different inhibitors in parallel to a control experiment without inhibitor.

Because ethanol and DMSO could alter the permeability of the biological membrane (DMSO: Murata *et al.* 2003) with a cascading effect on bioaccumulation, blank experiments in the presence of identical concentrations of

these solvents used for the inhibitor experiment were carried out. In these experiments, impacts were calculated on the basis they represented a certain percentage of the different uptakes. We, thus, obtained that CCCP impact represented 3.3 times the uptake for *E. huxleyi*, AZA, 3.4 times, EZA, 18.4 times and DCMU 1.7 times. In the same manner, CCCP represented 12.7 times the uptake for *N. closterium*, EZA, 2.9 times, AZA, 20.3 times and DCMU, 6.35 times. As a result, values of Zn and C uptake obtained during the inhibitors experiments have been corrected from the influence of ethanol and DMSO solutions in which they were prepared.

3.2.5 Statistical data treatment:

Statistical validations of significant differences between each set of experiments and species were performed using t-test or one-way ANOVA between each group with a confidence interval of 95% and using Sigma plot statistical tools (version 11). All values were expressed as average of duplicates or triplicates with the precision of the standard error.

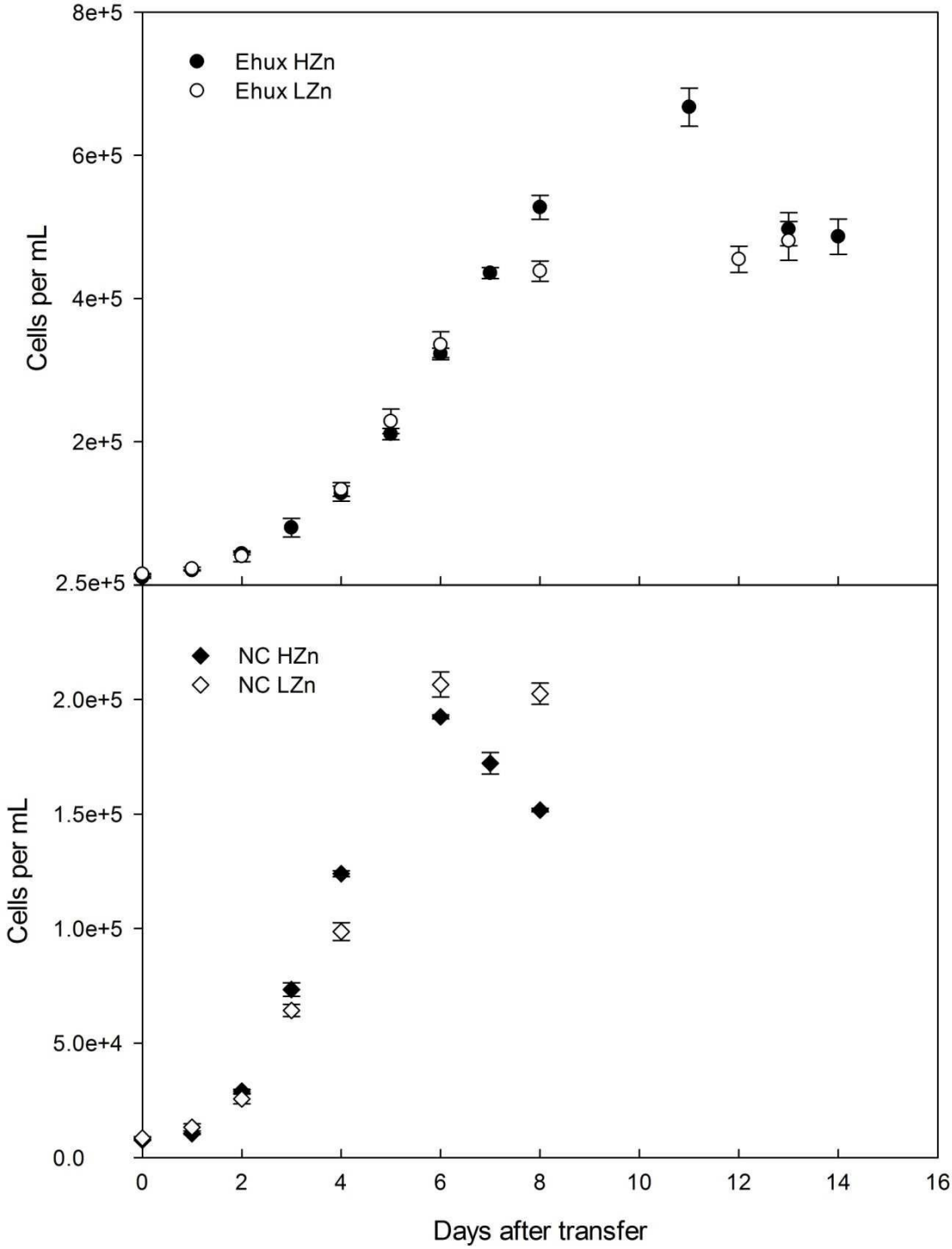

Figure 3: Examples of growth curves obtained for both species to establish the mid exponential phase of the growth. The top panel relates to *E. huxleyi* (●, ○) and the bottom one, to *N. closterium* (♦, ◊). For all values, the error bar represented the standard error.

3.3 Results:

3.3.1 Impact on physical parameters:

The mid-exponential phase for both species was quite similar, 5 days for *E. huxleyi* and 4 days for *N. closterium* (Fig. 3, HZn and LZn treatments). Growth rate for *E. huxleyi* was not significantly affected by Zn concentrations in the growth media ($p = 0.605$), whereas *N. closterium* grew significantly faster with increasing Zn concentrations ($p = 0.014$). The growth phase of *E. huxleyi* lasted longer in HZn than in LZn media (Fig. 3). Higher values of growth rates were observed for the diatom than for *E. huxleyi.* The ratios Fv/Fm measured during those experiments are all above 0.8 for both species and treatments (Table 5).

Table 5: Parameters measured throughout the culturing process for both species and exposed to the two media. Radius and volumes are both from the Coulter counter and were used to calculate the surface area.

Species	$[Zn^{2+}]$ (mol L^{-1})	Radius (µm)	Volume (μm^3)	Surface (μm^2)	SA/V ratios	Growth rate	Fv/Fm ratios
EHux HZn	2.70e-12	2.07 (±0.05)	37.43 (± 1.30)	53.84 (±1.25)	1.46 (± 0.01)	0.42 (± 0.02)	0.85 (± 0.02)
EHux LZn	1.50e-14	2.17 (±0.05)	43.00 (± 1.37)	59.13 (±1.28)	1.39 (± 0.02)	0.35 (± 0.01)	0.84 (± 0.03)
NClost HZn	2.70e-12	7.08 (±0.18)	1580 (± 101)	644 (±28.6)	0.41 (± 0.02)	0.47 (± 0.01)	0.83 (± 0.02)
NClost LZn	1.50e-14	6.86 (±0.04)	1355 (± 25.2)	591 (±7.46)	0.44 (± 0.01)	0.31 (± 0.02)	0.84 (± 0.03)

Volumes and surface areas were calculated using measurements from the SEM samples and the Coulter counter for *N. closterium.* To be consistent in our measurements and process, we used the Coulter measurements for all calculations in this study. However, the limitation in doing so is that both species have been considered as spheres for the calculation of diameter and surface area from the measured cellular volume. *E. huxleyi* had significantly different radius ($p = 0.02$, t-test), size ($p = 0.02$, t-test) and volume ($p = 0.03$, t-test) between both media (Table 5). *N. closterium* showed a slight decrease in length and a significant decrease in volume and surface areas ($p \leq 0.001$) in the LZn media (Table 5). Changes in size and volume implied a change in the SA/V ratio for both species (Table 5). *E. huxleyi* ratio varied between 0.66 ± 0.01 μm^{-1} and 0.70 ± 0.03 μm^{-1} for the HZn and LZn, respectively; while *N. closterium* varied from 0.41 ± 0.02 μm^{-1} for HZn to 0.44 ± 0.01 μm^{-1} for LZn.

3.3.2 Bioaccumulation experiments:

3.3.2.a Uptake characterisation and bioavailability:

The dissolved Zn data were in the 10% confident interval for both phytoplankton species and media (Fig. 4). The concentration of dissolved Zn was in the range 3 to 6 nmol L^{-1} for *E. Huxleyi* and 4 to 5 nmol L^{-1} for *N. closterium*. The adsorbed and internalised Zn concentrations considered were small compared to the initial dissolved Zn.

When plotted against time, both species exhibited a linear Zn uptake over a period of 24 h (Fig. 5). For *E. huxleyi*, the Zn internalisation flux obtained from linear regression, was not statistically different for both growth media ($p = 0.910$), with $0.7 \pm 1.0 \times 10^{-3}$ pmol Zn L^{-1} μm^{-2} ($R^2 = 0.97$) and $0.8 \pm 5.3 \times 10^{-5}$ pmol Zn L^{-}

^{1} μm^{-2} (R^2 = 0.99) for cells grown in HZn and LZn, respectively. The Zn internalisation rate was significantly greater for *N. closterium* grown in HZn media ($p = 0.001$), with values of $1.2 \pm 1.3 \times 10^{-4}$ pmol Zn L^{-1} μm^{-2} for HZn (R^2 = 0.96) and $0.14 \pm 1.5 \times 10^{-5}$ pmol Zn L^{-1} μm^{-2} for LZn ($R^2 = 0.98$). The difference observed for the internalisation rates between both species and between both media was, as expected, also found in their uptake rates (6.16 ± 1.99 nmol $cells^{-1}$ and 0.70 ± 0.21 nmol $cells^{-1}$ for the HZn and LZn, respectively). The internalisation process was significantly quicker for *N. closterium* than for *E.huxleyi* in the presence of 50 nmol L^{-1} inorganic Zn ($p \leq 0.001$).

The results from the bioaccumulation experiment in presence of NTA showed the internalisation ($[Zn]_{intra}$) rate and adsorbed Zn ($[Zn]_{ads}$) after 24 h as a function of $[Zn^{2+}]$ (Fig. 6.1 and 6.2). No linear relations were observed between $[Zn^{2+}]$ and $[Zn]_{intra}$ or $[Zn]_{ads}$ for either species (Fig. 6.1), and only a logarithmic one was observed with a slope lower than one between $[Zn^{2+}]$ and $[Zn]_{ads}$ for both species (Fig. 6.2). This means the relationship was not linear but logarithmic with a tendency to a plateau. In fact, the slope of the relationship between $[Zn^{2+}]$ and $[Zn]_{ads}$ for both species was similar; 0.68 ± 0.04 μm^{-2} ($R^2 = 0.98$) for *E. huxleyi* (Fig. 6.2 A) and 0.70 ± 0.03 μm^{-2} ($R^2 = 0.99$) for *N. closterium* (Fig 6.2 B). For both species, no significant differences in $[Zn]_{ads}$ was observed between HZn and LZn treatments ($p = 0.783$ for *E. huxleyi* and $p = 0.581$ for *N. closterium*), suggesting that Zn adsorption sites are not affected by the free Zn levels used in the growth media.

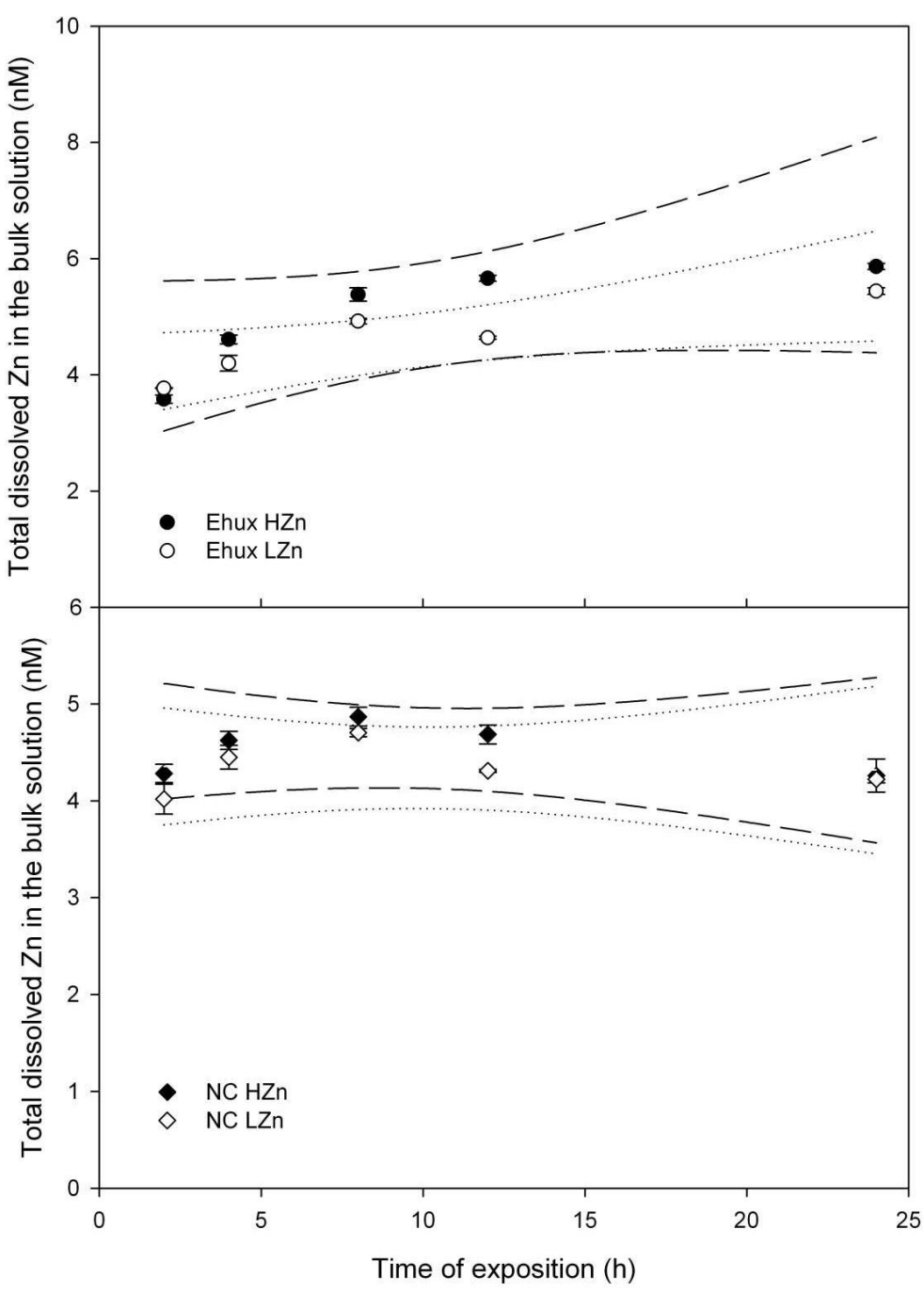

Figure 4: 10% confidence interval of confidence of the dissolved zinc contained in the bulk solution. The long dash interval corresponds to cells exposed to HZn and the dotted one, to cells exposed to LZn. For all values, the error bar represented the standard error.

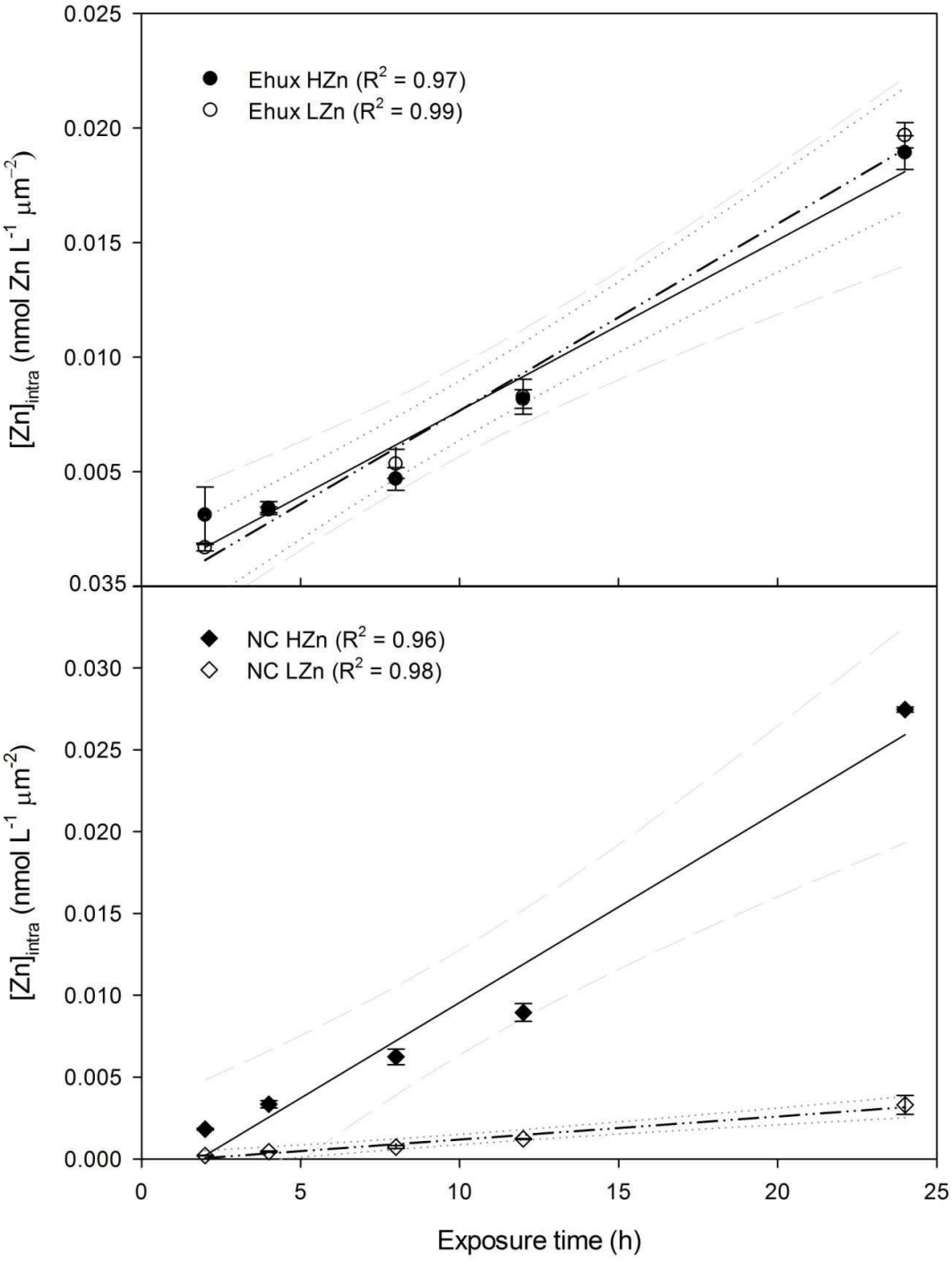

Figure 5: Internalisation of Zn by both species as a function of time. The top panel relates to *E. huxleyi* and the bottom one relates to *N. closterium*. In each panel, the long dash interval corresponds to cells exposed to HZn, and the dotted, to cells exposed to LZn. For all values, the error bar represented the standard error.

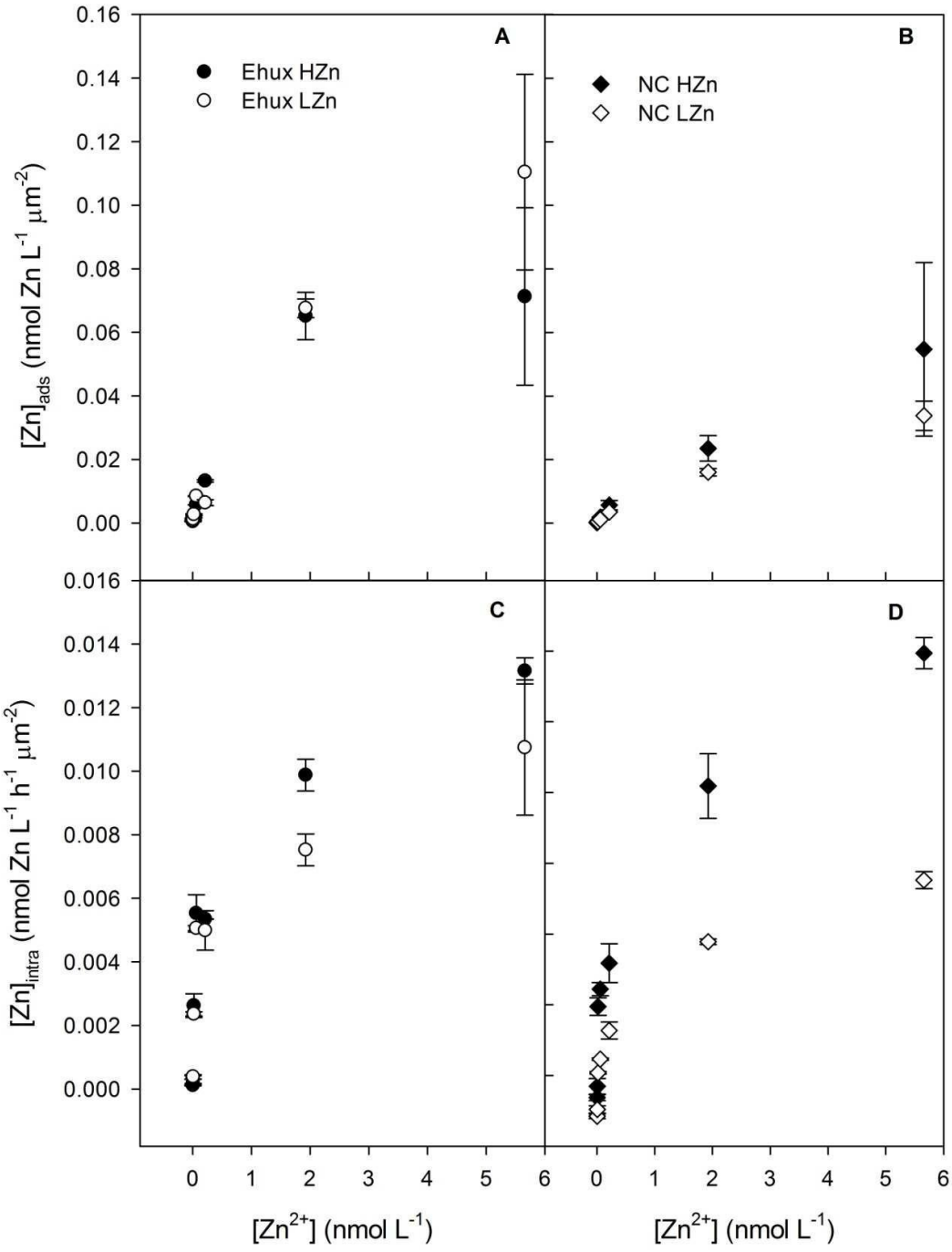

Figure 6.1: Results obtained in the window of bioavailability experiments for both species. In this figure, the results are expressed in linear concentration scales. Error bars have been added for each series: Ehux LZn and Ehux HZn correspond to *E. huxleyi* exposed to low and high Zn concentrations respectively (A and C), in the same manner, NC LZn and NC HZn correspond to *N. closterium* (B and D). For all values, the error bar represented the standard error.

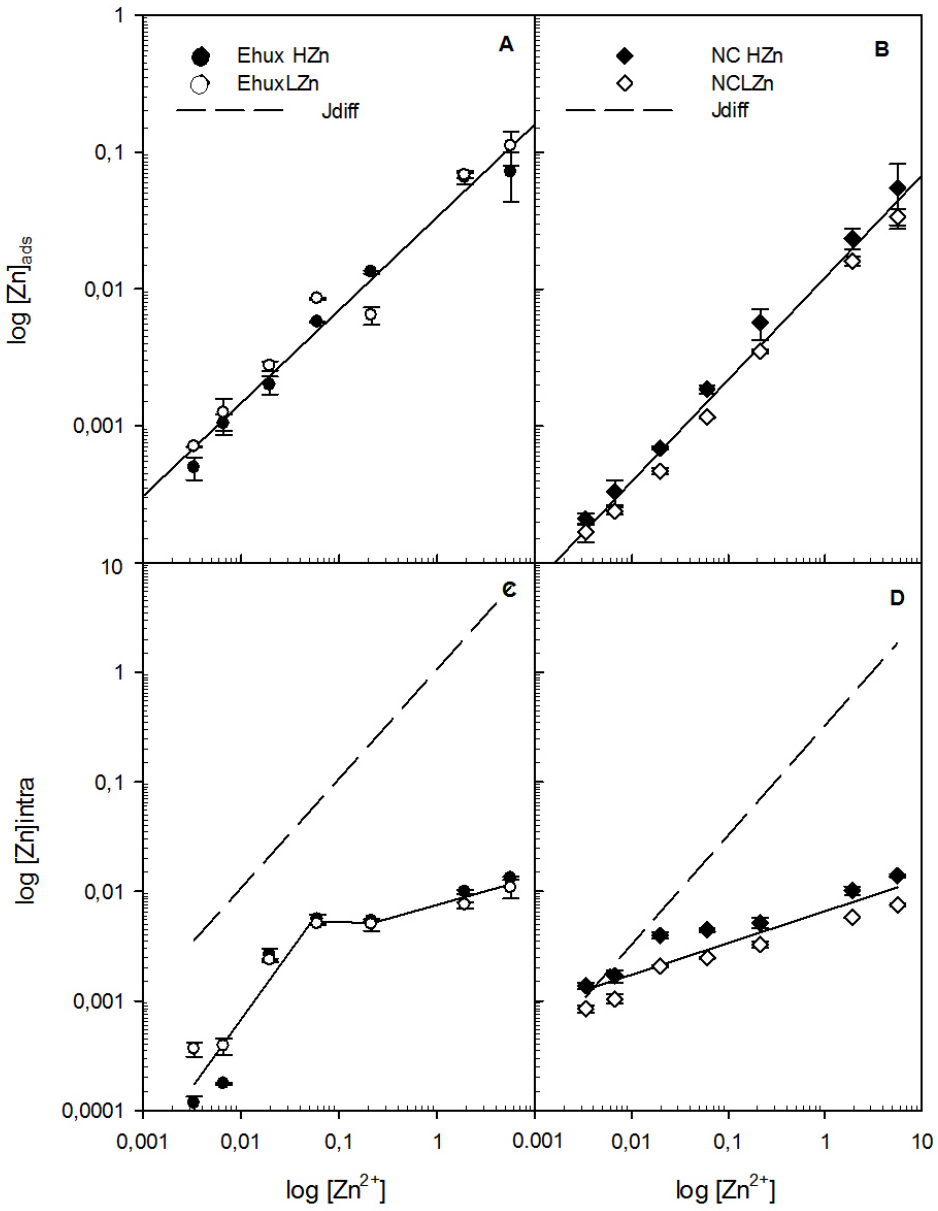

Figure 6.2: Results obtained in the window of bioavailability experiments for both species. In this figure, the results are expressed in logarithmic concentration scales. Error bars have been added for each series: Ehux LZn and Ehux HZn correspond to *E. huxleyi* exposed to low and high Zn concentrations respectively (A and C), in the same manner, NC LZn and NC HZn correspond to *N. closterium* exposed to the different Zn concentrations (B and D). For all values, the error bar represented the standard error.

The internalised Zn obtained for *E. huxleyi* showed two clear increases separated by a plateau but no significant difference between the two media ($p = 0.982$, Fig 6.2 C). For $[Zn^{2+}]$ higher than 10^{-9} M, the slope between the log of the concentrations of Zn^{2+} in the media and Zn_{intra} is 0.25 ± 0.01 h^{-1} μm^{-2} ($R^2 = 0.99$), whereas for Zn^{2+} between 10^{-10} and 10^{-12} M, the slope between $[Zn^{2+}]$ and $[Zn]_{intra}$ is of 1.24 ± 0.22 h^{-1} μm^{-2} ($R^2 = 0.99$). $[Zn]_{intra}$ was higher for cells exposed to LZn for the two lowest free Zn concentrations tested. The relation between $[Zn^{2+}]$ in experimental media and $[Zn]_{intra}$ for *N. closterium* showed no differences between both media ($p = 0.108$). Over the four orders of magnitude of $[Zn^{2+}]$ tested, $[Zn]_{intra}$ varied by only two orders of magnitude, leading to slope between log $[Zn^{2+}]$ in media and log $[Zn]_{intra}$ of 0.51 ± 0.009 h^{-1} μm^{-2} ($R^2 = 0.99$). Therefore, Zn uptake is homogeneously and strongly regulated by *N. closterium* over the range of $[Zn^{2+}]$ tested. For both species, the internalisation rate was lower than the maximum diffusive flux (dotted line in Fig. 6.2 C and D). However, for the lowest concentrations tested ($Zn^{2+} = 3.34$ pmol L^{-1}), *N. closterium* takes up Zn at a rate similar to its maximum diffusive supply.

3.3.2.b Action of inhibitors:

The presence of inhibitors in the treatments helped characterise the different Zn and C uptake pathways. The results obtained during this experiment have been expressed as percentage relative to the control for both uptakes and species (Fig. 7 A and B). A detailed statistical study (t-test on one group) was run to determine whether we observed differences between species for each media and inhibitor (Table 6). The interspecies comparison was significantly different for all inhibitors except for one group. The CCCP concentration for the LZn media did not significantly affect the species.

Table 6: Detailed results of interspecies statistical test for the inhibitors experiment. Each t-test has been run between the two media for both species to show whether the difference between species was significant. CCCP: Carbonyl cyanide m-chlorophenyl hydrazone, DCMU: Dichlorophenyldimethylurea, EZA: Ethoxyzolamide, AZA: Acetazolamide

a. Zn uptake:

Media	Vanadate	CCCP	DCMU	EZA	AZA
HZn	0.021	0.006	0.039	0.001	0.011
LZn	0.019	0.005	0.0.020	≤0.001	0.029

b. C uptake:

Species/Inhibitors	Vanadate	CCCP	DCMU	EZA	AZA
E. huxleyi	0.019	0.014	0.030	0.010	0.003
N. closterium	0.019	0.0131	0.007	0.014	0.012

When exposed to vanadate, we observed a 49 % average decrease of Zn uptake for *E. huxleyi* grown in HZn and LZn, as well as a 40 % decrease for *N. closterium*. Both species exposed to CCCP showed extremely high decrease of Zn uptake (86 % for *E. huxleyi* for both media and 97 % for *N. closterium*). DCMU decreased by 69 % Zn uptake for *E. huxleyi* and by 77 and 83 % the uptake for *N. closterium* (Fig. 8A). Vanadate decreased by 56 and 70 % the C uptake for *E. huxleyi* grown in HZn and LZn, respectively, while it decreased it by 49 % for *N. closterium*. CCCP and DCMU both decreased C uptake by 95 to 99 %, respectively, for both species and both media (Fig. 7B).

Both species showed strong decrease in Zn and C uptakes when exposed

to CA inhibitors. EZA is an inhibitor of both internal and external CA and AZA acts on the external one (Moroney *et al.* 1985; Mercado *et al.* 1998; Satoh *et al.* 2001). EZA decreased Zn uptake by 80 and 87 % for *E. huxleyi* exposed to HZn and LZn, respectively; while AZA decreased it by 76 and 81 %. The same trend was observed for *N. closterium* exposed to EZA as a reduction of 75 and 83 % was observed with HZn and LZn, respectively. We observed a 95 % reduction of Zn uptake due to AZA for both media (Fig 8B). The presence of EZA (Fig. 7B) had a stronger influence on *E. huxleyi* C uptake (96 %) than *N. closterium* (77 and 69 % decrease for HZn and LZn, respectively). AZA also had a stronger effect on *N. closterium* for C uptake (93 %) than *E. huxleyi* (60 and 76 % for HZn and LZn respectively).

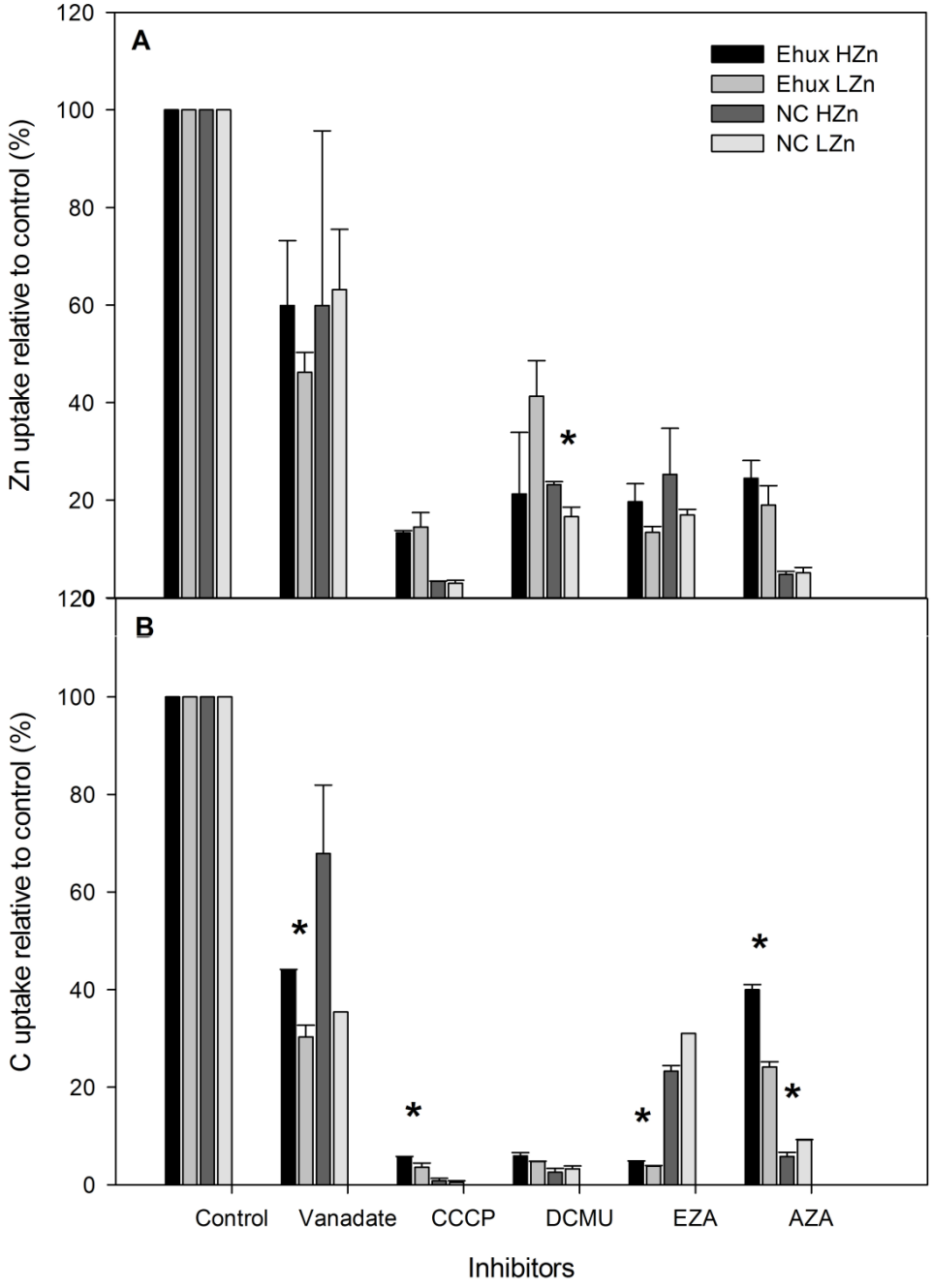

Figure 7: Inhibition of Zn (top panel) and C (bottom panel) uptakes for both species exposed to both media. The action of the different inhibitors has been expressed as percentage relative to control. When an intraspecies statistical difference was observed for each inhibitor, results have been marked with an asterix above the corresponding species. For all values, the error bar represented the standard error.

3.4 Discussion:

3.4.1 Choice and culture of the species:

Our two test species were chosen for their presence in the Tasman Sea and the importance to compare strains and evaluate their response to the different experimental conditions. The advantage of working with species such as *E. huxleyi* is that comparisons with various regions can be established due to the numerous publications concerning this species. However, we could not establish similar comparisons for *N. closterium* as studies on this species are scarce and do not concern Zn depletion, but Zn toxicity at high concentrations. Both phytoplankton species were grown in f/2 media made with natural seawater and nutrient concentrations. The use of the strong ligand EDTA to obtain the free concentration desired in our experimental media resulted in 98% of Zn being complexed and potentially less available for the phytoplankton during our experiment. Indeed, it has been suggested recently that species could access Zn bound by ligands weaker than EDTA in natural assemblages (Aristilde *et al.* 2012; Xu *et al.* 2012). The use of EDTA as buffer displaces Zn-complexes. As a result, the use of EDTA does likely not reflect the binding of Zn by natural ligands present in seawater as previously observed for Fe (Gerringa *et al.* 2000; Aristilde *et al.* 2012).

3.4.2 Physical and uptake response to exposure to the low Zn concentrations:

The decrease in size and volume obtained for *N. closterium* exposed to low nutrient concentrations agreed with previous observations in laboratory studies (Hassler and Schoemann 2009; Varela *et al.* 2011). This decrease in size

and volume is a natural adaptation to maximise diffusive transport of Zn to the cell's surface (Litchman *et al.* 2007). The greater size and volume obtained here for *E. huxleyi* exposed to LZn were unexpected. Pahlow *et al.* (1997) first showed quantitatively the relation between shape and nutrient acquisition. Hassler and Shoemann (2009) showed qualitatively the relation between the SA/V ratio and the Fe bioaccumulation for four phytoplankton species of the Southern Ocean. An SA/V ratio > 1.0, such as for our *E. huxleyi*, would indicate an adaptation to low concentrations. The pennate diatom *N. closterium* had a SA/V < 0.5 and a fast Zn internalisation, suggesting that this diatom possesses strategies to survive under low Zn nutrient concentrations. In our study, *E. huxleyi* showed growth rates lower than previously reported in a study for the open ocean (Xu *et al.* 2007) but they were in the range obtained by Schultz *et al.* (2004). The interspecies difference previously reported in studies on Zn limitation for different phytoplankton species (Sunda and Hunstmann 1992, 1995; Timmermans *et al.* 2001; Aristilde *et al.* 2012) was observed here as *E. huxleyi* possessed lower growth rates, and lower Zn requirement, than the diatom. However, there was no obvious physical indication of limitation despite these very low Zn^{2+} concentrations in the growth media. Despite the low $[Zn^{2+}]$ present in the media and the reduced uptake, the Fv/Fm showed the cells' aptitude to grow properly during our experiments and maintain their photosynthetic activity.

For the two species, similar $[Zn]_{ads}$ but different $[Zn]_{intra}$ were measured for the same $[Zn^{2+}]$ in experimental solution, suggesting differences in the strategy to growth in LZn between the two species did not arise from the adsorption process but from the Zn transporters' efficiency. Both species were able to efficiently maintain an important Zn uptake as $[Zn]_{intra}$ varied much less

than the [Zn^{2+}], except for *E. huxleyi* grown in LZn for [Zn^{2+}] < 10^{-10} mol L^{-1}. Previous studies demonstrated that Zn transporters consist of one high affinity system induced at low free Zn concentrations and an ever present one or low affinity transporter (Sunda and Hunstman 1992, 1995, 2002; Hassler and Wilkinson 2003; Seth *et al.* 2007). The presence of several transporters is typically identified by the combination of a sigmoidal relation between [Zn^{2+}] tested and $[Zn]_{intra}$ or different slopes for $[Zn]_{intra}$ at different [Zn^{2+}], as observed here for *E. huxleyi*..Greater $[Zn]_{intra}$ at low [Zn^{2+}], with stronger vanadate inhibition for *E. huxleyi* grown at low Zn, suggests that *E. huxleyi* induced the high affinity transporter when grown in LZn media, as previously observed for other phytoplankton (Sunda and Huntsman, 1992; Hassler and Wilkinson, 2003). Our observations indicate two different Zn uptake pathways for *E. huxleyi. N. closterium* also responded with a sigmoidal relationship between $[Zn]_{intra}$ and [Zn^{2+}], suggesting that more than one transporter were involved. The homogeneous slope of 0.5 for $[Zn]_{intra}$: [Zn^{2+}] meant we could not distinguish transporter with different affinity for Zn as opposed as for *E. huxleyi*. The internalisation rate for *E. huxleyi* was always smaller than the maximum diffusion, meaning in our case, its uptake was not limited by the diffusion of Zn towards the cell. This result was consistent with the previous study by Sunda and Hunstman (1995) for a similar range of Zn^{2+} concentration. However, the linearity of the slope obtained at the lowest Zn concentrations for *E. huxleyi* suggests that diffusion could potentially control the internalisation rate. The presence of external shells is likely to play a role in slowing down the Zn^{2+} diffusive supply. The internalisation rate was also found smaller than the maximum diffusive supply for *N. closterium*, except for the lowest free Zn concentration tested (1.67

x 10^{-13} nmol L^{-1}), where the diffusion rate equaled the internalisation rate. In this case, Zn was taken up at the same rate at which it was diffusing towards the cell and, the dissociation kinetics of the complexes need to be taken into account when evaluating the relation between the uptake and the internalised Zn. Hassler and Wilkinson (2003) found similar results for the freshwater phytoplankton C*hlorella kesslerii*. From our data and the observations of similar results in other study, we can suggest that Zn-NTA complexes were potentially contributing to the kinetically labile pool of Zn for the diatom. However, the supposition relies on the results obtained for the lowest concentrations and the range of concentrations tested here was not low enough to definitively argue this for *N. Closterium*. Thus, further experiments at lower free zinc concentrations are needed to investigate whether the uptake depends on free ion concentration present in the media or both kinetics of the complexes and concentrations together for both species.

The evaluation of this full set of results suggests that the studied species, even if exposed to low bioavailable Zn concentrations, have the capacity to maintain their photosynthetic activity and growth. A possibility behind this lack of Zn limitation is the metal inter-replacement occurring between Zn, Co and Cd for some phytoplankton species, including coccoliths and diatoms. However, E. *huxleyi* has a Zn requirement that cannot be met by Cd (Timmermans *et al.* 2001; Xu *et al.* 2007). In our case, free Co concentration was not reduced in the media (18 pmol L^{-1}), meaning Co could possibly be available and fulfil some of the biological requirements and allow *E. huxleyi* to grow. However, Cd was not added and its concentrations in the Tasman Sea was lower than Zn (2 pmol L^{-1} at 15m depth for P1, Ellwood pers. comm.), suggesting there was little chance for Cd to fulfill this biological requirement. The results obtained for *N. closterium*

suggest that this species might be able to replace Zn by Co but probably not by Cd; however, previous similar studies with *N. closterium* could not be found to confirm this hypothesis.

3.4.3 Differences of transporters and mechanisms of Zn and C uptakes:

The deduction of two transporters for both species was also supported by the action of inhibitors on Zn and C uptake. The action of vanadate, CCCP and DCMU on both species suggested that Zn and C uptakes were strongly energy dependent. The effect of vanadate was more pronounced at lower concentrations for *E. huxleyi*, suggesting the transport of Zn and C via P-ATPases might be induced in these conditions, as observed for intracellular Zn concentration at low free Zn concentration. This result is consistent with a previous study done on C. *kesslerii* (Hassler and Wilkinson 2003) and identifies that this transporter is associated with a primary transport system, directly requiring ATP to transport Zn. Zn transport was also associated with the energy produced by light (photosynthesis; effect of DCMU) and dark (phosphorylation oxidative; effect of CCCP) reactions. However, the DCMU effect was lower than that of CCCP for both species and media, which suggests that Zn transport is influenced more by the dark reactions and the generation of ATP. C uptake is also affected by both light and dark reactions for the two species and media, which is, for *E. huxleyi* in agreement to a similar conclusion of Sekino and Shiraiwa (1994). The dependence on light and dark reaction for Zn and C transport and fixation has been previously reported (Sunda and Huntsman 2004). *N. closterium* showed a higher dependence on photosynthesis processes for both Zn and C uptakes as the inhibitor effects were stronger than for *E. huxleyi*.

As previously mentioned, EZA and AZA are both related to the carbonic

anhydrase (CA) present in the cell. Both inhibitors had a strong effect on Zn and C uptakes. While EZA and AZA had a similar effect on Zn uptake for *E. huxleyi*, *N. closterium* exhibited a stronger inhibition when the external CA only was inhibited. As a result, Zn uptake seemed to be more related to the external CA in the diatom. This corresponds well with the results obtained for C uptake. The stronger inhibition of Zn uptake for the lowest concentrations revealed Zn requirement for the proper functioning of CA (Sunda and Hunstman 2002).

E. huxleyi showed a stronger repression of both C and Zn uptake when both CA were inhibited compared to the external CA alone, revealing its dependence on the internal CA for C metabolism (e.g. RubisCO). Previous studies on *E. huxleyi* (Sekino and Shiraiwa 1994; Buitenhuis *et al.* 2003; Rost *et al.* 2003) suggested a minor role of external CA for carbon acquisition. In our study, AZA inhibits C uptake less than EZA does, suggesting that the external CA helps in C acquisition but is not required. This also suggests that *E. huxleyi* is more likely to be a CO_2 user (Buitenhuis *et al.* 2003). As stated by previous studies, there is still a need for a better understanding on C acquisition and underlying processes that cannot be addressed with our study. Soto *et al.* (2006) suggested the presence of two different CA for *E. huxleyi* that could partially explain the repression of C uptake with both AZA and EZA here.

Different species have been shown to exhibit a variability of carbon species acquisition (Elzenga *et al.* 2000), which also suggest the discrepancies observed between our study and previous ones. In this study, *N. closterium* showed a higher inhibition of the external CA only, contrary to *E. huxleyi*. Although, there might be a suppression of the internal one, we suggest that this diatom builds up an internal pool of C (luxury uptake) and still process to the

functioning of the internal one to acquire C. The existence of both CA and the functioning of the CCMs for diatoms have been shown in previous studies (Morel *et al.* 2002; Hopkinson *et al.* 2011) and have been recently reviewed (Kupriyanova and Pronina 2011). Although *N. closterium* has not been studied to the same extent, it is reasonable to assume the existence of such CCMs for this diatom. Our findings do not concord with the minor role of external CA on inorganic C acquisition established by Mitchell and Beardall (1996) and Trimborn *et al.* (2008) for the different strains of *Nitzschia*. Our findings for the species *N. closterium* need careful interpretation as there are strong variations and diversity in this genus, as underlined by Trimborn *et al.* (2008).

3.5 Conclusion:

Recent studies increased the knowledge of Zn biogeochemistry in seawater and its influence on phytoplankton. Studies of its impact on the phytoplankton community come principally from experiments conducted in laboratory and existing conflicting results between laboratory studies and deck-top incubations prevent the establishment of a defined limiting role for Zn (Sinoir *et al*. 2012).

Here, we showed even if species are exposed to low Zn concentrations, they are able to adapt to the low bioavailability of Zn. This suggests that if the Tasman Sea exhibits such low concentrations, we could expect species to possess strategies to still access the impoverished resource, either by accelerating their uptake with specific and efficient transporters, access complexed Zn (*N. closterium*) or replace it by Co (*E. huxleyi*). Further experiments with natural communities are required to definitively conclude on the impact of zinc bioavailability on the phytoplankton community, and increase our understanding

of interactions of trace metal micronutrients (and their mechanisms) in the Tasman Sea and similar temperate oligotrophic regions.

3.6 Acknowledgments:

Thanks go to the Microalgae team from the CSIRO Marine Laboratories, particularly Ian Jameson and Cathy Johnston for providing strains, help in culture techniques and use of instruments; Sue Blackbird for the use of her *E. huxleyi* strain from the Tasman Sea; and Rick van den Eden for his help with the SEM technique and preparation of the sample.

3.7 References:

Aristilde, L., Xu, Y., and Morel, F. M. M. (2012). Weak organic ligands enhance zinc uptake in marine phytoplankton. *Environmental Science and Technology*, **46,** 5438-5445.

Baars, O., and Croot P. L. (2011) the speciation of dissolved zinc in the Atlantic sector of the Southern Ocean. *Deep Sea Research Part II: Tropical Studies in Oceanography*, **58**, 2720–2732.

Badger, M. R., and Price, G.D. (1994) The Role of Carbonic Anhydrase in photosynthesis, *Annual Review of Plant Physiology and Plant Molecular Biology*, **45,** 369-392, doi: 10.1146/annurev.pp.45.060194.002101

Balnokin, Y., Popova, L., and Gimmler, H. (1997). Further evidence for an ATP-driven sodium pump in the marine alga Tetraselmis (Platymonas) viridis. *Journal of Plant Physiology*, **150,** 264-270.

Bowie, A. R., and Lohan, M. C. (2009). Determination of iron in seawater. In 'Practical Guidelines for the Analysis of Seawater'. (Ed. O. Wurl.) pp. 235–258.

Bruland, K. W., and Lohan, M. C. (2003). Controls of trace metals in seawater. In 'Treatise on geochemistry'. pp. 23-47 (Pergamon, Oxford).

Bruland, K. W., Franks, R. P., Knauer, G. A., and Martin, J. H. (1979). Sampling and analytical methods for the determination of copper, cadmium, zinc, and nickel at the nanogram per liter level in sea water. *Analytica Chimica Acta***105**, 233–245.

Buitenhuis, E. T., Timmermans, K. R., and de Baar, H. J. W. (2003). Zinc-bicarbonate colimitation of *Emiliania huxleyi Limnology and Oceanography*, **48,** 1575-11582.

Calvo, E., Pelejero, C., Logan, G. A., and De Deckker, P. (2004). Dust-induced changes in phytoplankton composition in the Tasman Sea during the last four glacial cycles. *Paleoceanography,* **19**, PA2020, doi: 10.1029/2003PA000992

Coale, K. H., Wang, X., Tanner, S. J., and Jonhson, K. S. (2003). Phytoplankton growth and biological response to iron and zinc addition in the Ross Sea and Antarctic Circumpolar Current along 170°W. *Deep Sea Research Part II: Topical Studies in Oceanography,* **50,** 635-653.

Croot, P. L., de Baars, O. *et al*. (2011). The distribution of dissolved zinc in the Atlantic sector of the Southern Ocean. *Deep Sea Research Part II: Tropical Studies in Oceanography*, **58**, 2707–2719.

Cullen, J. T. and Sherrell, R. M. (2005). Effects of dissolved carbon dioxide, zinc, manganese on the cadmium to phosphorus ratio in natural phytoplankton assemblages. *Limnology and Oceanography* **50**, 1193-1204.

Cutter, G., Andersson, P., Codispoti, L., Croot, P., François, R., Lohan, M. C., Obata, H., and Rutgers, M. (2010). Sampling and sample-handling protocols for GEOTRACES cruises. (Ed. GEOTRACES Standards and Intercalibration Committee.) GEOTRACES Library, available at http://www.geotraces.org/libraries/documents/Intercalibration/Cookbook.pdf [accessed 4 January 2010]

Ellwood, M. J. (2008). Wintertime trace metal (Zn, Cu, Ni, Cd, Pb and Co) and nutrient distributions in the Subantarctic Zone between 40-52°S; 155-160°E. *Marine Chemistry,* **112,** 107-117.

Ellwood, M. J. (2004). Zinc and cadmium speciation in subantarctic waters east of New Zealand. *Marine Chemistry* **87**, 37-58.

Ellwood, M. J., and van den Berg, C. M. G. (2000). Zinc speciation in the Northeastern Atlantic Ocean. *Marine Chemistry* **68**, 295-306.

Elzenga, J. T. M., Prins, H. B. A., and Stefels, J. (2000). The Role of Extracellular Carbonic Anhydrase Activity in Inorganic Carbon Utilization of *Phaeocystis globosa* (Prymnesiophyceae): A Comparison with other Marine Algae Using the Isotopic Disequilibrium Technique. *Limnology and Oceanography,* **45,** 372-380.

Furla, P. and Allemand, D. (2000). Involvement of H^+-ATPases in carbon concentrating mechanism for endosymbiont photosynthesis in *Anemonia viridis*. *Comparative Biochemistry and Physiology-Part A: Molecular & Integrative Physiology* **126** Supplement 1, 53.

Furuya, K., Hasumoto, H., Nakai, T., and Nemoto, T. (1986). Phytoplankton in the subtropical convergence during the austral summer: community structure and growth activity. *Deep Sea Research Part A. Oceanographic Research Papers,* **33,** 621-630.

Gerringa, L. J. A., De Baar, H. J. W., and Timmermans, K. R. 2000. A comparison of iron limitation of phytoplankton in natural oceanic waters and laboratory media conditioned with EDTA. *Marine Chemistry,* **68,** 335-346.

Gnassia-Barelli, M., and Romeo, M. (1987) Uptake of zinc by cultured phytoplankters *Hymenomonas elongate, Disease of aquatic organisms*, **3**, 45-49.

Hassler, C. S., and Shoemann, V. (2009). Bioavailability of organically bound Fe to model phytoplankton of the Southern Ocean. *Biogeosciences,* **6,** 2281-2296.

Hassler, C. S. and Wilkinson, K. J. (2003). Failure of biotic ligand and free-ion activity models to explain zinc bioaccumulation by *Chlorella kesslerii*. *Environmental Toxicology and Chemistry* **22**, 620-626.

Hassler, C. S., Slaveykova, V. I., and Wilkinson (2004). Discriminating between intra- and extracellular metals using chemical extractions. *Limnology and Oceanography: Methods* **2**, 237-247.

Hassler, C. S., Behra, R., Wilkinson, K. J. (2005) Impact of zinc acclimation on bioaccumulation and homeostasis in *Chlorella kesslerii*. *Aquatic Toxicology*, **74**, 139-149.

Hassler C.S., Schoemann, V., Boye, M., Tagliabue, A., Rozmarynowycz, M., and McKay, R. M. L. (2012*a*) Iron Bioavailability in the Southern Ocean. *Oceanography and Marine Biology: An annual review* **50,** 1-64.

Hassler C. S, Sinoir M, Clementson L.A., and Butler E. C. V. (2012*b*) Exploring the link between micronutrients and phytoplankton in the Southern Ocean during the 2007 austral summer. *Frontiers in. Microbiology*. **3**:202. doi: 10.3389/fmicb.2012.00202.

Heytler P. G. (1980). Uncouplers of oxidative phosphorylation. *Pharmacology and Therapeutics*, 10, 461–472.

Hobday, A. J., Poloczanska, E. S., and Matear R .J. (eds) (2008), *Implications of climate change for Australian fisheries and aquaculture: a preliminary assessment*, Report to the Department of Climate Change, Canberra

Hopkinson, B. M., Dupont, C. L., Allen, A. E., and Morel, F. M. M. 2011. Efficiency of the CO2-concentrating mechanism of diatoms. *Proceedings of the National Academy of Sciences*. **108,** 3830-3837.

Hudson, R. J. M. (1998) Which aqueous species control the rate of trace metal uptake by aquatic biota? Observations and predictions of non-equilibrium effects. *Science of the total environment,* **219**, 95-115.

John, S. G., Geis, R. W., Saito, M. A., and Boyle, E. A. (2007). Zinc isotope fractionation during high-affinity and low-affinity zinc transport by the marine diatom *Thalassiosira oceanic. Limnology and Oceanography* **52**, 2710-2714.

Kariuki, S., and Dewald, H. D. 1996. Evaluation of diffusion coefficients of metallic ions in aqueous solutions. *Electroanalysis,* **8,** 307-313.

Kupriyanova, E. V., and Pronina, N. A. (2011). Carbonic anhydrase: Enzyme that has transformed the biosphere. *Russian Journal of Plant Physiology* **58**, 197-209.

Lane, T. W., and Morel, F. M. M. (2000). Regulation of Carbonic Anhydrase Expression by Zinc, Cobalt, and Carbon Dioxide in the Marine Diatom *Thalassiosira weissflogii*. *Plant Physiol.,* **123,** 345-352.

Leblanc, K., Hare, C. E., Boyd, P. W., Bruland, K. W., Sohst, B., Pickmere, S., Lohan, M. C., Buck, K., Ellwood, M., and Hutchins, D. A. (2005). Fe and Zn effects on the Si cycle and diatom community structure in two contrasting high and low-silicate HNLC areas. *Deep Sea Research Part I: Oceanographic Research Papers* **52**, 1842-1864.

Litchman, E., Klausmeier, C. A., Schofield, O. M., and Falkowski, P. G. (2007). The role of functional traits and trade-offs in structuring phytoplankton communities: scaling from cellular to ecosystem level. *Ecology Letters,* **10,** 1170-1181.

Lohan, M. C., Statham, P. J., and Crawford, D. W. (2002). Total dissolved zinc in

the upper water column of the subarctic North East Pacific. *Deep Sea Research Part II: Topical Studies in Oceanography* **49**, 5793-5808.

Lohan, M. C., Crawford, D. W., Purdie, D. A., and Statham, P. J. (2005). Iron and zinc enrichments in the northeastern subarctic Pacific: Ligand production and zinc availability in response to phytoplankton growth. *Limnology and Oceanography*, **50,** 1427-1437.

Marchant, H. J. And Thomas, D. P. (1983). Polylysine as an adhesive for the attachment of nanoplankton to substrates for electron microscopy. *Journal of Microscopy*, **131,** 127-129.

Martin, J. H., Gordon, R. M., and Fitzwater, S. E. (1990). Iron in the Antarctic waters. *Nature* **345**, 156-158.

Mercado, J. M., Gordillo, F. J. L., Figueroa, F. L., and Niell, F. X. (1998). External carbonic anhydrase and affinity for inorganic carbon in intertidal macroalgae. *Journal of Experimental Marine Biology and Ecology*, **221,** 209-220.

Mercado, J. M., Ramírez, T., Cortés, D., and Liger, E. (2009). Effect of carbonic anhydrase inhibitors on the inorganic carbon uptake by phytoplankton natural assemblages. *Journal of Phycology*, **45,** 8-15.

Mitchell, C., and Beardall, J. (1996). Inorganic carbon uptake by an Antarctic sea-ice diatom, *Nitzschia frigid, Polar Biology*, **16,** 95-99.

Morel, F. M. M., Milligan, A. J., Saito, M. A., Heinrich, D. H. and Karl, K. T. (2003). Marine bioinorganic chemistry: The role of trace metals in the oceanic cycles of major nutrients. In 'Treatise on geochemistry'. pp. 113-143. (Pergamon, Oxford).

Morel, F. M. M., Cox, E. H., Kraepeil, A. M. L., Lane, T. W., Milligan, A. J., Schaperdoth, I., Reinfelder, J. R., and Tortell, P. D. (2002). Acquisition of

inorganic carbon by the marine diatom Thalassiosira weissflogii. *Functional Plant Biology,* **29,** 301-308.

Moroney, J. V., Husic, H. D., and Tolbert, N. E. (1985). Effect of Carbonic Anhydrase Inhibitors on Inorganic Carbon Accumulation by *Chlamydomonas reinhardtii*. *Plant Physiol,* **79,** 177-83.

Murata, Y., Watanabe, T., Sato, M., Momose, Y., Nakahara, T., Oka, S.-I., and Iwahashi, H. 2003. Dimethyl Sulfoxide Exposure Facilitates Phospholipid Biosynthesis and Cellular Membrane Proliferation in Yeast Cells. *Journal of Biological Chemistry,* **278,** 33185-33193.

Pahlow, M., Riebesell, U., and Wolf-Gladrow, D. A. (1997). Impact of Cell Shape and Chain Formation on Nutrient Acquisition by Marine Diatoms. *Limnology and Oceanography,* **42,** 1660-1672.

Patterson, C. C., and Settle, D. M. (1976). The reduction of orders of magnitude errors in lead analysis of biological materials and natural waters by controlling external sources of industrial Pb contamination introduced during sample collection and handling. In 'Reliability in Trace Analysis'. (Ed. D. M. La Fleur.) pp. 321–351. Special Publication 422, National Bureau of Standards, Washington.

Price, N.M., Harrison, G.I., Hering, J.G., Hudson, R.J., Nirel, P.M.V., Palenik, B., Morel, F.M.M., 1988/1989. Preparation and chemistry of the artificial algal culture medium Aquil. *Biological Oceanography* **6**, 443–461.

Rost, B., Riebesell, U., Burkhardt, S., and Sültemeyer, D. (2003). Carbon acquisition of bloom-forming marine phytoplankton. *Limnology and Oceanography,* **48,** 55-67.

Satoh, D., Hiraoka, Y., Colman, B., and Matsuda, Y. (2001). Physiological and Molecular Biological Characterization of Intracellular Carbonic

Anhydrase from the Marine Diatom *Phaeodactylum tricornutum*. *Plant Physiology*, **126,** 1459-1470.

Schulz, K. G., Zondervan, I., Gerringa, L. J. A., Timmermans, K. R., Veldhuis, M. J. W. and Riebesell, U. (2004). Effect of trace metal availability on coccolithophorid calcification. *Nature*, **430,** 673-676.

Saito, M. A., Moffett, J. W., Chisholm, S. W., and Waterbury, J. B. (2002) Cobalt Limitation and Uptake in *Prochlorococcus*. *Limnology and Oceanography* **47**, 1629-1636.

Saito, M. A., and Goepfert, T. J. (2008) Zinc-cobalt colimitation of *Phaeocystis Antarctica*. *Limnology and Oceanography* **53**, 266-275.

Sarthou, G., Timmermans, K. R., Blain, S., and & Treguer, P. 2005. Growth physiology and fate of diatoms in the ocean: a review. *Journal of Sea Research*, **53,** 25-42.

Sekino, K., and Shiraiwa, Y. (1994). Accumulation and utilization of dissolved inorganic carbon by a Marine Unicellular Coccolithophorid, *Emiliania huxleyi*. *Plant and Cell Physiology*, **35,** 353-361.

Seth, J. G., Geis, R. W., Saito, M. A., and Boyle, E. A. (2007). Zinc isotope fractionation during high-affinity and low-affinity zinc transport by the marine diatom *Thalassiosira oceanica*. *Limnology and Oceanography*, **52,** 2710-2714.

Shaked, Y., Xu, Y., Leblanc, K., and Morel, F. M. M. (2006). Zinc availability and alkaline phosphatase activity in Emiliania huxleyi: Implications for Zn-P co-limitation in the ocean. *Limnology and Oceanography* **51**, 299-309.

Soto, A. R., Zheng, H., Shoemaker, D., Rodriguez, J., Read, B. A., and Wahlund, T. M. (2006). Identification and Preliminary Characterization of Two

cDNAs Encoding Unique Carbonic Anhydrases from the Marine Alga *Emiliania huxleyi*. *Applied and Environmental Microbiology*, **72,** 5500-5511.

Sinoir, M., Butler, E. C. V., Bowie, A. R., Mongin, M., Nesterenko, P., and Hassler, C. S. (2012) Zinc marine biogeochemistry in seawater: a review. *Marine and Freshwater Research*, **63**, 644-657.

Sunda, W. G., and Huntsman, S. A. (1992). Feedback interactions between zinc and phytoplankton in seawater. *Limnology and Oceanography*, **37,** 25-40.

Sunda, W. G. and Huntsman, S. A. (1995). Cobalt and zinc interreplacement in marine phytoplankton: Biological and Geochemical Implications. *Limnology and Oceanography*, **40,** 1404-1417.

Sunda, W. G. and Huntsman, S. A. (1998). Processes regulating cellular metal accumulation and physiological effects: Phytoplankton as model systems. *Science of the total environment* **219**, 165-181.

Sunda, W. G., and Huntsman, S. A. (2004). Relationships among Photoperiod, Carbon Fixation, Growth, Chlorophyll a, and Cellular Iron and Zinc in a Coastal Diatom. *Limnology and Oceanography*, **49,** 1742-1753.

Sunda, W. G., and Hunstman, S. A. (2005). Effect of CO_2 Supply and Demand on Zinc Uptake and Growth Limitation in a Coastal Diatom. *Limnology and Oceanography*, **50,** 1181-1192.

Tang, D., and Morel, F. M. M. (2006). Distinguishing between cellular and Fe-oxide-associated trace elements in phytoplankton. *Marine Chemistry*, **98,** 18-30.

Timmermans, K. R., Snoek, J., Gerringa, L. J. A., Zondervan, I., and de Baar, H. J. W. (2001). Not all eukaryotic algae can replace zinc with cobalt: *Chaetoceros calcitrans* (Bacillariophyceae) versus *Emiliania huxleyi*

(Prymnesiophyceae). *Limnology and Oceanography* **46**, 699-703.

Trimborn, S., Lundholm, N., Thoms, S., Richter, K.-U., Krock, B., Hansen, P. J., and Rost, B. (2008). Inorganic carbon acquisition in potentially toxic and non-toxic diatoms: the effect of pH-induced changes in seawater carbonate chemistry. *Physiologia Plantarum,* **133,** 92-105.

Varela, D. E., Willers, V., and Craawford, D. W. (2011). Effect of zinc availability on growth, morphology, and nutrient incorporation in a coastal and an oceanic diatom. *Journal of Phycology* **47,** 302-312.

Wake, B. D., Hassler, C. S., Bowie, A. R., Haddad, P. R., and Butler, E. C. V. 2012. Phytoplankton selenium requirements: The case for species isolated from temperate and polar regions of the southern hemisphere. *Journal of Phycology,* **48,** 585-594.

Williams, T. G., and Turpin, D. H. (1987). The Role of External Carbonic Anhydrase in Inorganic Carbon Acquisition by Chlamydomonas reinhardii at Alkaline pH. *Plant Physiology,* **83,** 92-96.

Wisniewski-Jakuba, R., Moffet, J. W., and Dyhrman, S. T. (2008). Evidence for the linked biogeochemical cycling of zinc, cobalt, and phosphorus in the western North Atlantic Ocean. *Global Biogeochemical Cycles* **22,** doi:10.1029/2007gb003119.

Wisniewski Jakuba, R., Moffett, J. W., and Saito, M. A. (2008). Use of a modified, high-sensitivity, anodic stripping voltammetry method for determination of zinc speciation in the North Atlantic Ocean. *Analytica Chimica Acta* **614**, 143-152.

Wisniewski-Jakuba, R., Saito, M. A., Moffett, J. W. and Xu, Y. (2012). Dissolved zinc in the subarctic North Pacific and Bering Sea: Its distribution, speciation, and importance to primary producers. *Global*

Biogeochemical Cycles, **26**.

Xu, Y., Tang D., Shaked, Y., and Morel, F. M. M. (2007). Zinc, cadmium, and cobalt interreplacement and relative use efficiencies in the coccolithophore *Emiliania huxleyi Limnology and Oceanography,* **52,** 2294-2305.

Xu, Y., Shi, D., Aristilde, L., and Morel, F. M. M. (2012). The effect of pH on the uptake of zinc and cadmium in marine phytoplankton: Possible role of weak complexes. *Limnology and Oceanography,* **57,** 293-304.

CHAPTER FOUR

Total dissolved zinc in the Tasman Sea: its distribution, speciation and relation to phytoplankton community.

Marie Sinoir [(1), (2)], Michael Ellwood [(3)], Edward Butler [(1), (4)], Andrew Bowie [(2), (5)], Mathieu Mongin [(1)], Christel S. Hassler [(6), (7)]

[(1)] CSIRO Marine and Atmospheric Research Laboratories, Castray Esplanade, GPO Box 1538, Hobart TAS 7000, Australia

[(2)] Institute for Marine and Antarctic Studies, Sandy Bay Campus, University of Tasmania, Hobart TAS 7001, Australia

[(3)] Research School of Earth Sciences, Australian National University, Building 8, 61 Mills Road, Canberra ACT 2000, Australia

[(4)] Australian Institute of Marine Science, Arafura Timor Research Facility, PO Box 41775, Casuarina MC, NT 0811, Australia

[(5)] Antarctic Climate and Ecosystem Cooperative Research Centre (ACE CRC), University of Tasmania, Hobart TAS 7001, Australia

[(6)] Plant Functional Biology and Climate Change Cluster, University of Technology of Sydney, Broadway NSW 2007, Australia

[(7)] Present address: University of Geneva, Institute FA Forel, 10 Route de Suisse, 1290 Versoix, Switzerland

Subm. in Marine Chemistry

4.1 Introduction:

4.1.1. Zinc speciation in seawater:

Zinc is now well known to be involved in multiple biological and structural functions, especially in relation to carbon and phosphate uptake (Badger 2003, Hoppe 2003, Kupriyanova and Pronina 2011, Sinoir *et al.* 2012). It is also known that phytoplankton species possess different responses to zinc depletion due to their own biological requirement (Sunda and Huntsman 1992). In the previous chapter, it has also been suggested that the different species of a phytoplankton community do not seem to access the same chemical zinc species. Recent studies also suggested a relationship between zinc concentrations and phytoplankton community structure (Leblanc *et al.* 2005; Hassler *et al.*2012; Wisniewski-Jakuba 2012).

Chemical speciation is undoubtedly required to assess and define a metal's reactivity but also to understand the bioavailability of a chemical element to phytoplankton. Indeed, the chemical speciation can decrease the bioavailability by two or three orders of magnitude (Saito *et al.* 2008). Although, the concept of bioavailability is often difficult to define (Saito *et al*. 2008; Hassler *et al.* 2012), in the bioavailability of an element is critical to assess micronutrient limitation and its influence on the phytoplankton community. Thus it is essential to know the speciation of zinc in seawater in different ocean regions and throughout the water column in order to understand its biogeochemistry and cycling in the sea.

Nonetheless, and in contrast to iron, there is little information for zinc, especially concerning ligand complexation. For these many reasons, studies on chemical speciation are one of the priorities from the GEOTRACES research program (Trace Elements and Isotopes, SCOR group, 2007). New data on zinc speciation are recently emerging for different regions of the open ocean (Baars

and Croot 2011; Croot *et al.* 2011; Wisniewski-Jakuba 2012; this study), revealing and specifying the biogeochemistry of this trace element.

In open ocean waters, dissolved concentrations of Zn are in the nanomolar range (Bruland and Lohan 2003; Bermin *et al.* 2006) with a nutrient-like behaviour including depletion in surface waters and higher concentrations at depth. A high percentage of dissolved Zn (98%) that is complexed by natural strong organic ligands (Hirose *et al.* 2011). This strongly reduces the concentration of biologically available forms, usually addressed as labile Zn (Zn'). Zn' falls in the picomolar range in most regions studied (Ellwood and van den Berg 2004; Baar and Croot 2011; Croot *et al.* 2011). Ellwood *et al.* (2004) previously reported nanomolar dissolved zinc concentrations in the south eastern Tasman Sea in winter. Moreover, the difference observed between winter and summer concentrations were of 0.2 – 0.3 nmol kg^{-1} (Ellwood *et al.* 2004; Butler, personal communication), suggesting picomolar range of free ion concentration and low bioavailability for the phytoplankton due to high complexation.

The following results in this chapter represent the first set of data for Zn speciation along a north south transect of the Tasman Sea, a sensitive region to climate change (Hobday *et al.* 2008). Zinc concentration (labile, total dissolved and free) were measured using a voltammetry ASV technique for four different stations. The comparison with biological data for the same region revealed an important correlation between zinc chemistry and phytoplankton species, especially zinc importance for the local phytoplankton community assemblages.

4.1.2. Background on voltammetry technique:

Voltammetry is the analytical technique that allows determining the speciation of trace element speciation in seawater. Two main types of voltammetry are available to measure indirectly zinc speciation. The cathodic stripping voltammetry (CSV) and anodic stripping voltammetric (ASV) techniques are commonly used and compared to determine Zn speciation in seawater (Donat and Bruland, 1990; Jakuba-Wiesniewski *et al* 2008). Although both techniques are quite similar, they possess their own specificity. Both techniques concentrate the Zn present in a sample on a mercury surface (drop or film) to allow low ranges of detection limit. The CSV (van den Berg 1985) used a competitive equilibrium between natural zinc-ligand and an added chelator. Complexes are then collected as a film onto a mercury drop. The CSV measures the current produced by reduction of free Zn present in the film as a function of the negative potential applied in the sample. The final Zn^{2+} concentration is obtained by solving a quadratic equation involving the concentration of complex, stability constants and inorganic side-reaction coefficient. The ASV technique (Bruland, 1989; Donat and Bruland, 1990; Ellwood, 2004; Wisniewski-Jakuba *et al*., 2008) titrates a sample containing zinc and directly measures the oxidation current of inorganic zinc species deposited on a mercury film. The current (i_P) is measured as a function of the zinc added in the sample and, then, Zn labile (Zn′) in the sample is related to the concentration adsorbed onto the mercury film with the following relationship:

$$i_p = (S\alpha_{Zn}) \times [Zn^{2+}] = SZn' \quad (1)$$

The slope of the titration (current/concentration added) defines the sensitivity of the method (S). A value of α_{Zn} = 2.1 (Turner *et al*. 1981) was chosen for the side reaction coefficient for Zn complexes in seawater. The calculation

behind ASV determination takes into account the different chemical equations lying behind metal complexation. In natural seawater, complexes (ZnL) are formed between labile zinc (Zn′ = free ion + inorganically complexed Zn) and natural organic ligand (L′) present in seawater as follow:

$$Zn' + L' \leftrightarrow ZnL$$

In this case, at equilibrium, the relationship between the complexes and the ligand is given by the conditional stability constant for inorganic complexation (K'_{ZnL}) expressed as follow:

$$K'_{ZnL} = [ZnL]/([Zn^{2+}][L']) \quad (2)$$

The concentration of natural complexes ([ZnL] is calculated as the difference between the total dissolved concentration in the sample and the Zn′ measured. The mass balance equation for total ligand (C_L) is described as follow:

$$C_L = [ZnL] + [L^t] \quad (3)$$

The concentration of ligand present in the sample is, then, easily obtained from the previous equation. The combination and rearrangement of equations (2) and (3) gives the following Langmuir relationship (Ruzic 1982; van den Berg, 1982):

$$([Zn^{2+}]/[ZnL]) = ([Zn^{2+}]/C_L + 1/(K'_{ZnL}\, C_L) \quad (4)$$

Values of C_L and K'_{ZnL} are the slope and the intercept, respectively, of the plot of experimental data [Zn′]/[ZnL] versus [Zn′]. As previously mentioned, free zinc concentrations ($[Zn^{2+}]$) can be obtained by solving the following quadratic equation:

$$a[Zn^{2+}]^2 + b[Zn^{2+}] - c = 0 \quad (5)$$

in which $a = \alpha_{Zn} K^t_{ZnL}$; $b = K^t_{ZnL} C_L - K^t_{ZnL} C_{Zn} + \alpha_{Zn}$ and $c = C_{Zn}$

4.1.3: Non Linear Langmuir fit calculations:

The van den Berg calculation has been previously described and is the usually applied for the open-ocean measurements. It is based on the hypothesis of only one ligand class present in seawater to complex trace elements. A non linear fit also exists and was established by Wilkinson (Wilkinson *et al.* 1992) in SYSTAT. Several studies have been using both to compare the outputs and relevance of both in marine ecosystems (Gerringa *et al* 1995; Capodaglio *et al.* 1995; Durán and Nieto 2011). This calculation is mainly used in estuarine environments as they exhibit higher concentrations of zinc, as well as particulate matter. It takes into account two classes of ligand (L_1 and L_2) with respective condition stability constants (K'_1 and K'_2). Therefore the calculation of zinc speciation follows the equation below:

$$[Zn']/([Zn]_{tot} - [Zn']) = 1/(C_{L1}/([Zn'] + 1/K'_1) + C_{L2}/([Zn'] + 1/K'_2)) \quad (6)$$

4.2 Materials and methods:

4.2.1 Study site and sampling:

Samples chosen to work with during this experiment were sampled and collected during the PINTS (Primary productivity Induced by Iron and Nitrogen in the Tasman Sea, January and February 2010, RV *Southern Surveyor*, Hassler *et al.* 2013 (In prep)). Three process stations were visited during this voyage to collect profiles using trace metal protocols for GEOTRACES voyage from surface to deep waters (Table 1; Fig.2). A fourth station, a revisit from the SAZ-Sense voyage (2007, Bowie et *al*. 2011) was also studied. Sampling bottles and all labware used for sampling and measuring were soaked in

detergent (Decon) overnight and then soaked in acid (10% HCl) for a month. They were then rinsed seven times with Milli-Q water (18 MΩ) in a clean room (ISO Class 5) according to the trace metal protocols recommended for GEOTRACES cruises and trace metal analysis (GEOTRACES cookbook, Cutter *et al.* 2010). Samples were collected using Teflon-coated Niskin X-1010 bottles (General Oceanics, USA) mounted on an autonomous rosette (Model 1018, General Oceanics, USA) and deployed using a Kevlar hydroline (Strongrope, AU). Water samples for trace metal analyses were filtered (Pall, Acropack 200) and then transferred into polypropylene bottles (125–150 mL) in a clean container under a HEPA filter (ISO Class 5 conditions) on board the *Southern Surveyor*. Samples were stored in triple plastic bags and directly frozen without acidification after water collection to preserve the speciation. Bottles were not filled entirely to prevent cracking.

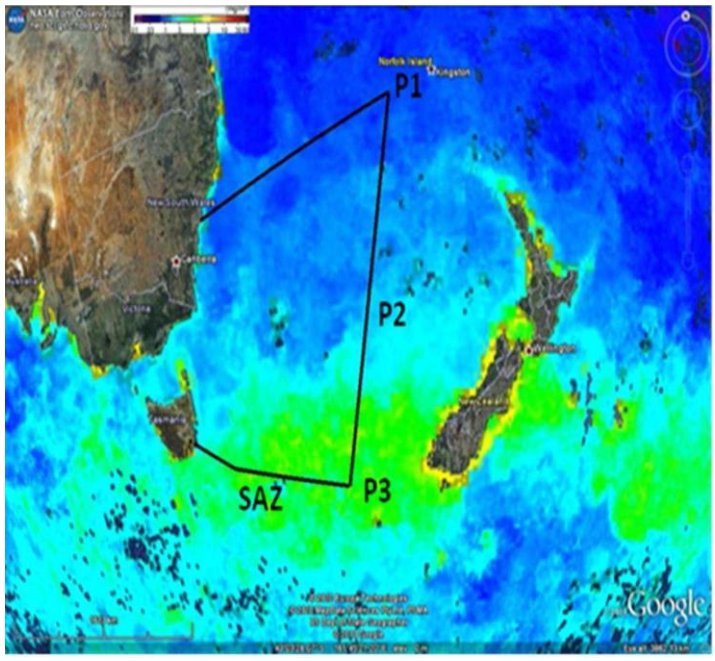

Fig. 1**:** Google Earth NASA Modis image, colour composite of Chlorophyll Concentration and location of the stations analysed in this work.

Table 1: Location of the four stations studied. The depths indicated are the depths analysed with voltammetry in this study and in brackets are the depths sampled for each station.

Station name	Longitude	Latitude	Depth (m)
P1	165 E	30 S	15–300 m (15–3500 m)
P2	162.1 E	39.6 S	15–750 m (15–4500 m)
P3	159.5 E	46.2 S	15–1000 m (15–3500 m)
SAZ-SENSE Station 14	153.2 E	45.6 S	15–1000 m (15–3750 m)

4.2.2. Instrumentation and mercury film formation:

Zn speciation was determined using a 663 VA stand (Metrohm, Herisau, Switzerland) with a glassy carbon rotating electrode, a glassy carbon rod counter electrode and a reference electrode Ag/AgCl equilibrate with a 3M KCl solution (Fig. 2). The system was connected to a µAutolab II and a current amplifier (PGSTAT 12). The software GPES version 4.9 (EcoChimie, The Netherlands) was connected to the system and automatically drove the measurements and routine operated on samples (Table 2).

Fig. 2: Set-up and instruments used to determine zinc speciation in a clean environment in the ANU laboratory.

The mercury film required to perform the analysis was plated onto the working electrode. The plating was done as per Ellwood (2004). The working Teflon cup was filled with a solution containing 10 mg L^{-1} of Hg^{2+} (BDH) and 30 mmol L^{-1} for KCl (Suprapur, Merk) and after a 5-min purge with nitrogen gas, the mercury was plated at a potential of –1.0 V for 15 min. The film was replaced before each full titration to avoid its loss. A cycle of five quick scans without accumulation was performed before any titration to certify no zinc was detected in the blank signal.

Table 2: Parameters defined for the voltammetry measurements with the Autolab interface.

Parameters	Time or voltage required
Pretreatment:	
Purge time	240 s
Conditioning potential	–0.2 V
Duration	120 s
Deposition potential	–1.2 V
Duration	300 s
Equilibration time	15 s
Measurement:	
Modulation time	0.3 s
Interval time	0.2 s
Potentials:	
Initial potential	–1.3 V
End potential	–0.2 V
Step potential	4.95m V
Modulation amplitude	25.05 V
Standby potential	0 V

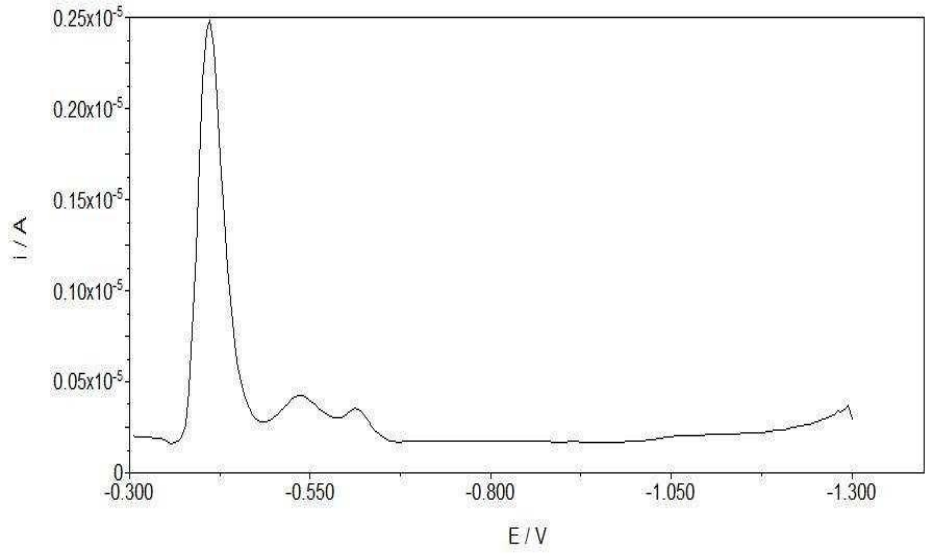

Fig. 3: A typical scan obtained during the mercury film plating.

4.2.3: Zinc determination:

In this study, Zn speciation was determined as per Ellwood (2004). Briefly, ten 23-mL teflon vials (Savillex, USA) used for titration were conditioned for 24 h with the appropriate spike of zinc from a low zinc concentration (background seawater) to a higher concentration ($10\ nmol\ L^{-1}$) water. This step is required to saturate the vial walls in Zn, avoiding the loss of zinc by adsorption onto the vial walls during the experiment and prevent experimental artefacts. The zinc standard (34.5 ppm) was prepared by adding 100 µL of zinc stock solution (ICP-MS std) and 0.560 µL of HCl ultrapure (AR grade) in 100 mL of NANOpure water. The standard was prepared once and stored at room temperature for the entire experiment. Each sample (125 mL) was defrosted overnight at room temperature before measurements and 10-mL aliquots were prepared daily by pipetting 10 mL of sample and an accurate volume of Zn standard. Each aliquot was equilibrated for 10 min before analysis. After a 5-min purge, sample was accumulated onto the mercury film during 300 s at a potential

of –1.2 V, this step was followed by an equilibration time of 15 s. The current peak linked to Zn detection was typically observed at –1.04 V, which was in good agreement with previous studies.

The accumulation time plays a role in the sensitivity of the method, used to calculate Zn speciation. Therefore, the linearity of the relationship between the accumulation time of the sample and the current peak height was checked between 3 and 300 seconds (Fig. 4). The linearity of the peak height was verified and the relationship gave a regression of $R^2 = 0.98$. All data tested were in the 5 % confidence interval of the relationship. In order to achieve greater sensitivity and lower detection limit, a 300s deposition time was used (Wiesniewski-Jakuba *et al.* 2008). The peaks also increased with the addition of Zn in the samples (Fig. 5). Each titration was preceded by two scans with no zinc additions to ensure that the working electrode was properly conditioned and duplicates of scans were done for each spike. All manipulations in this work were done under a laminar flow hood and in a clean area.

Total dissolved concentrations required to calculate zinc speciation were determined using isotopic dilution after solvent extraction (Danielsson *et al.* 1978, Ellwood 2008) for the three process stations visited during the PINTS cruise. Total dissolved zinc concentrations for the last station measured in this study (Stn 14 or SAZ-SENSE), concentrations were determined using an ICP-MS coupled with flow injection as per O'Sullivan *et al.* (2013).

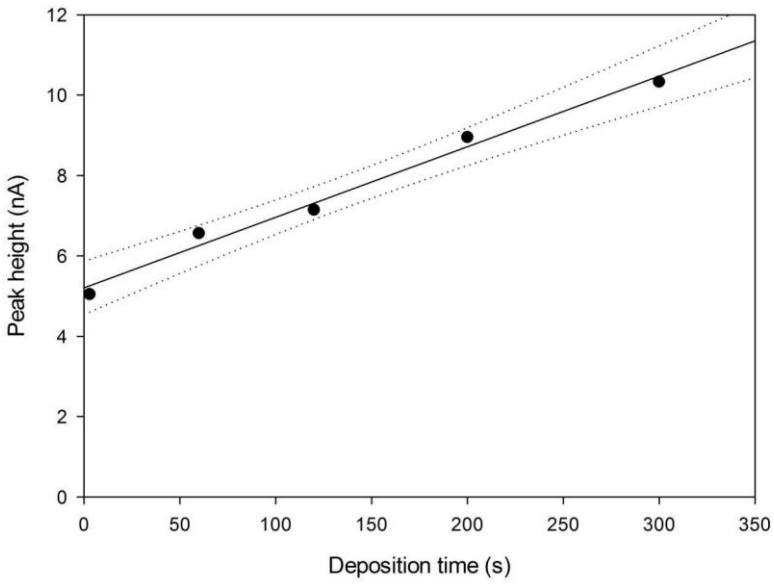

Fig. 4: Influence of the deposition time on the peak height for zinc oxidation during the ASV measurement.

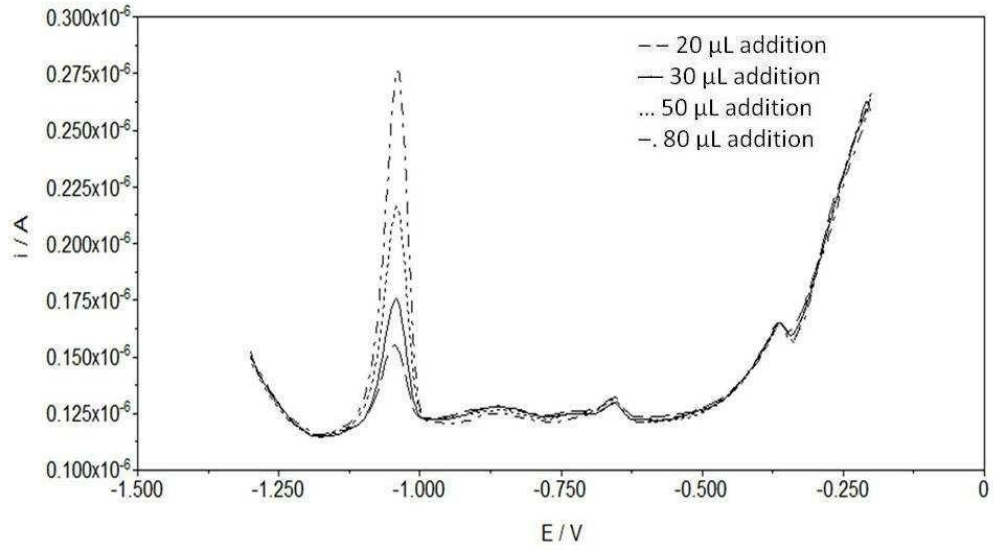

Fig. 5: A typical stripping voltammogram obtained for the same sample with increasing zinc concentrations added to the sample. It represents the entire range of the scan.

4.2.4. Biological data:

Table 3: Correspondence of biomarkers pigments and species from phytoplankton assemblages.

Biomarker pigment	Phytoplankton Class
Hex-Fucoxanthin	Haptophytes
But-Fucoxanthin	Diatoms
Fucoxanthin	
Zeaxanthin	Cyanobacteria
Chl *b*	Chlorophytes
DV Chl *b*	Tropical series

For each station analysed, we collected biological, chemical and physical data (Hassler, personal communication). Profiles of temperature, salinity and major nutrients were taken using a CTD-rosette system as per Hassler *et al.* (2013, in prep). Different biomarker pigments were measured to relate dominating species forming the phytoplanktonic assemblage (Jeffrey and Vesk 1997; Jeffrey and Wright 2006: Table 3). To obtain an approximation of the local assemblages, concentrations of pigments were integrated from 0-125 m depth. The fraction of species was then established in relation to integrated Tot Chl *a*. Physical, biological and chemical data were compared qualitatively to establish the different correlations between phytoplankton and Zn chemistry in the region. All statistical tests (t-tests, ANOVA and Pearson's correlations) were run using

Sigma Plot 11 to establish significant difference between samples or correlations between parameters.

4.3 Results:

4.3.1 Total dissolved zinc concentrations (Zn_{tot}):

For this study, Zn_{tot} measurements were taken from surface to deep waters samples for the process stations (15–3000 m P1, and 15-3500 m for P2 and P3). The profile from the reoccupation of the site from SAZ-Sense was less extended with concentrations measured down to 1000 m. Total dissolved Zn concentrations were generally low (~ 0.1 nM) in surface waters and increased with depth in a nutrient-like fashion to about 6–7 nM at 3000 m (Fig. 6).

In the first 1000 m, Zn concentrations slightly increased along to the north-south transect with P1 exhibiting the lowest range of concentration (0.011 to 1.75 nM) and Stn 14 the highest (0.10 to 2.91 nM). P2 (0.11 to 2.61 nM) and P3 (0.18 to 2.44 nM) exhibited a similar range of dissolved Zn concentrations to station 14 except in the first 70 m of the water column where P2 showed lower concentrations than P3. Total dissolved Zn concentrations for P1 and P2 were the first to be established for this region. The ones obtained for P3 and Stn 14 are in the same range as the ones obtained by Ellwood (2008) in winter for a southern transect in the Tasman Sea.

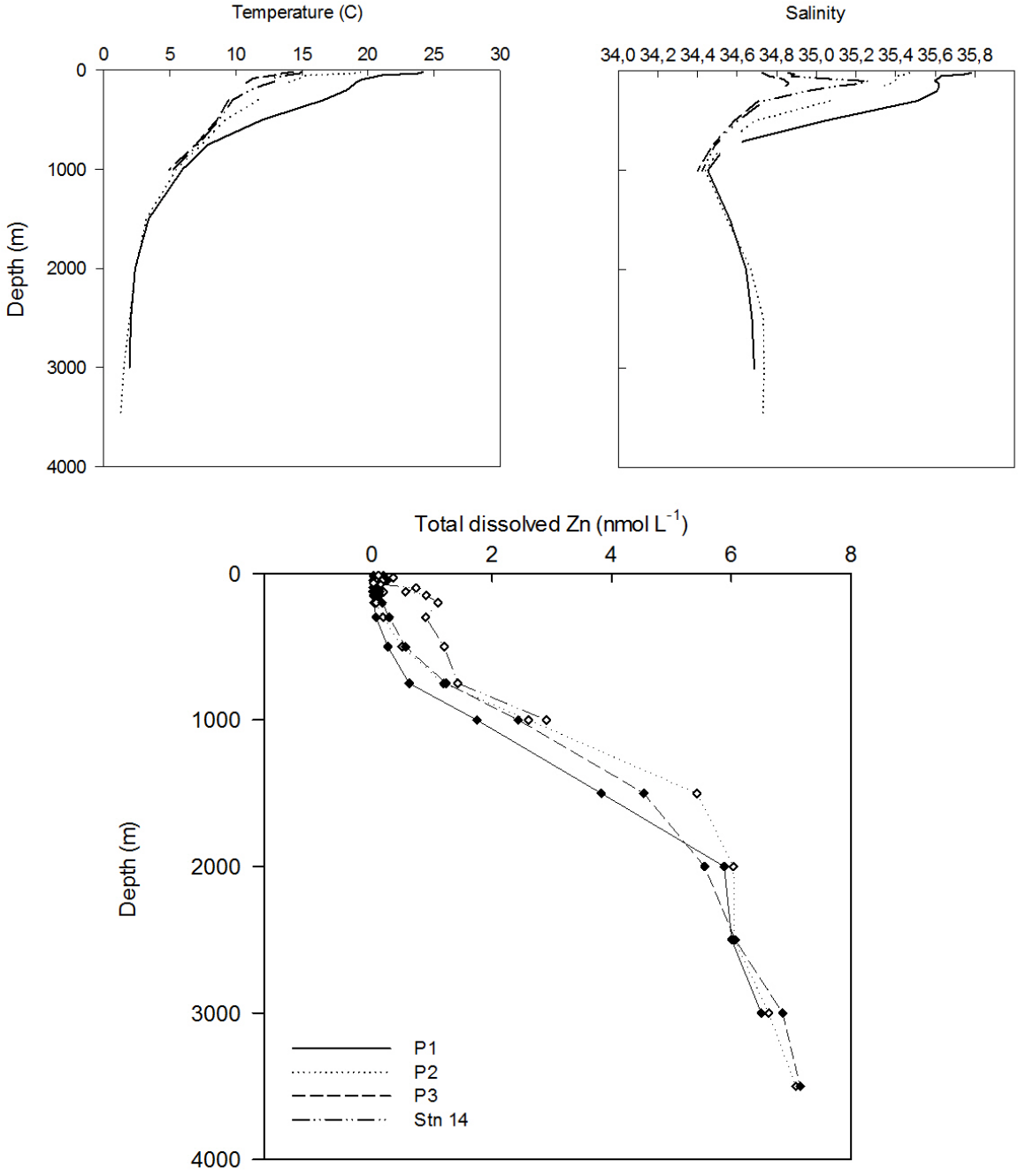

Fig. 6: Profiles of temperature, salinity and total dissolved zinc for the four stations studied here.

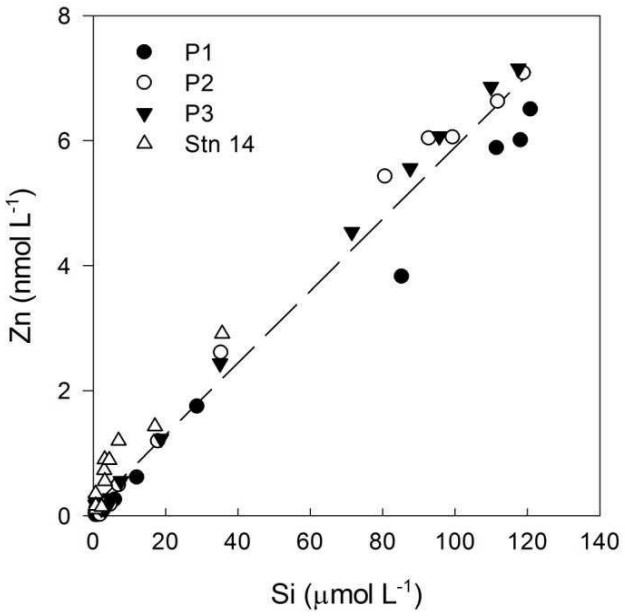

Fig. 7: Relation between silicic acid and total dissolved Zn for the four stations analysed in this study.

Temperature and salinity were significantly inversely correlated to total dissolved Zn with all *p* values falling below 0.05, meaning there was significant inverse relationship between each variable with Zn. As previously observed (Ellwood *et al.* 2008; Gosnell *et al.* 2012; Jakuba *et al.* 2012), there was a tight correlation (R^2 = 0.98) between silicic acid concentrations and total dissolved Zn for the four stations (Fig. 7). The disappearance ratio yielded a value of 0.059 ± 0.001 (n = 57, p≤ 0.001). This result was in concordance with previous results obtained for different regions and compiled in Croot *et al.* (2011).

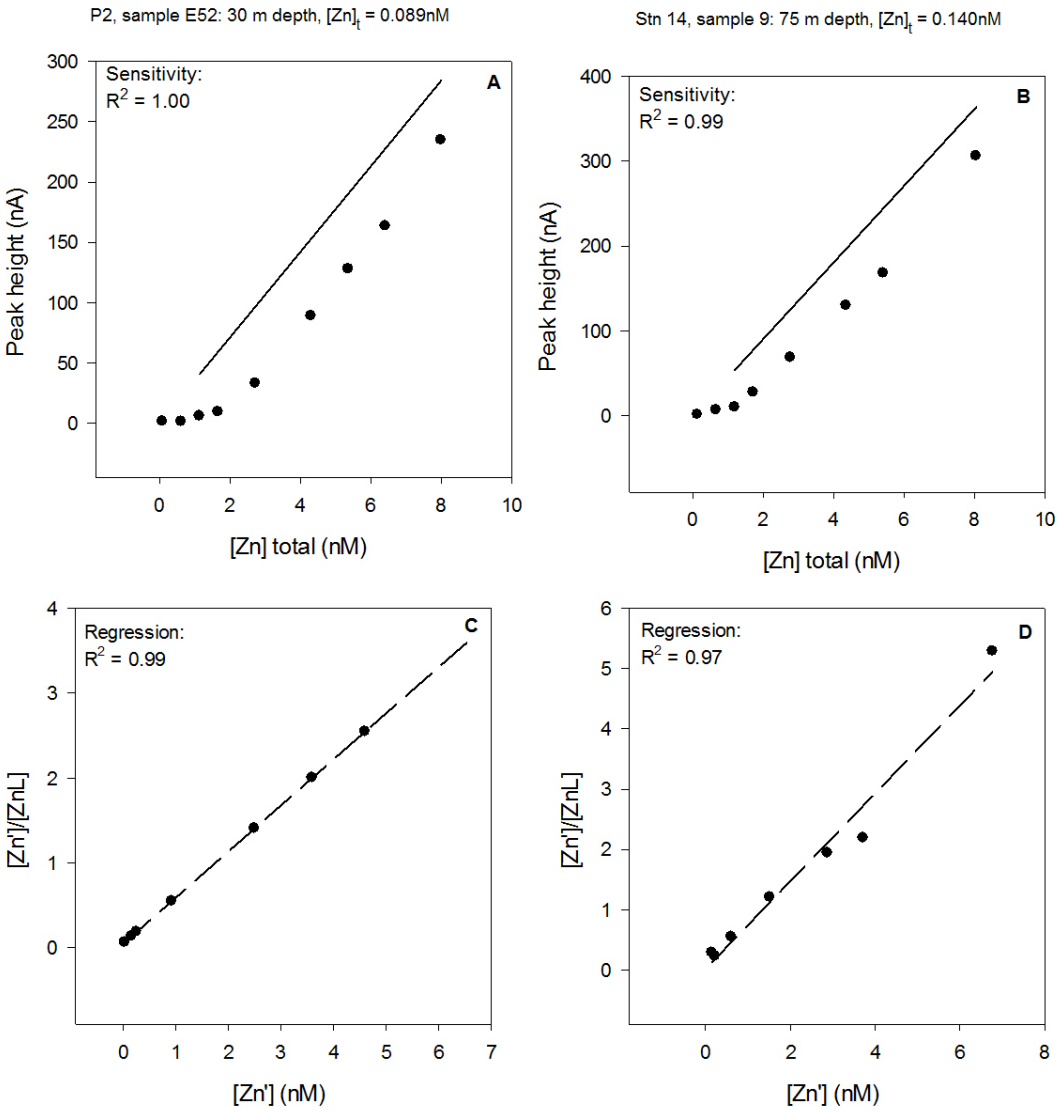

Fig. 8: Examples of titration curves obtained for titration of two different samples of P2 and Stn 14.

4.3.2. Zinc speciation:

To determine whether to use a single (Ruzic) or double ligand (Wilkinson) model to calculate Zn speciation in this region, plots of titration curves and [Zn′]/[ZnL] versus [Zn′] are presented (Fig. 8) for two stations. Titration curves (Fig. 7 A and B) exhibited a curvature at the lowest Zn concentrations, suggesting the presence of ligand binding this metal. As we increase the Zn concentration with standard additions, the electrode response became linear, meaning that all the Zn-binding ligand(s) was titrated in the sample. [Zn′]/[ZnL] versus [Zn′] curves

were linear (Fig. 8 C and D), meaning the simple one ligand model could be used for the determination of Zn speciation in our study.

Dissolved ligand concentrations ranged between 0.23 and 4.19 nM (Table 4) and always exceeded the dissolved Zn (Fig. 9). P3 and Stn 14 exhibited fairly constant distributions of the ligand through the water column, while P2 exhibited a distribution reflecting the biological activity in the first 200 m was observed. Unfortunately, we were not able to measure the entire profile for P1, which limit the comparison of deep water concentrations with the other stations. A distinct increase in ligand concentration (4.19 nM) was seen at station P2 at 70 m, where phytoplankton numbers peaked. Stability constant values ranged from log K'_{ZnL} = 9.3 to 11.4 (Table 4) and were consistent with previous ones found in the similar studies.

Labile Zn (Zn′) concentrations also increased in a North to South gradient with P1 having concentrations ranging from 0.6 to 16.8 pM. Concentrations at P2 ranged from 1 to 401 pM while P3 and Stn 14 had similar ranges with minimum values of 3 pM and maximum values between 430 and 500 pM. The strong complexation with organic ligands implied that labile Zn concentrations were close to the concentrations that can limit phytoplankton growth in surface waters (Sunda and Hunstman 1992).

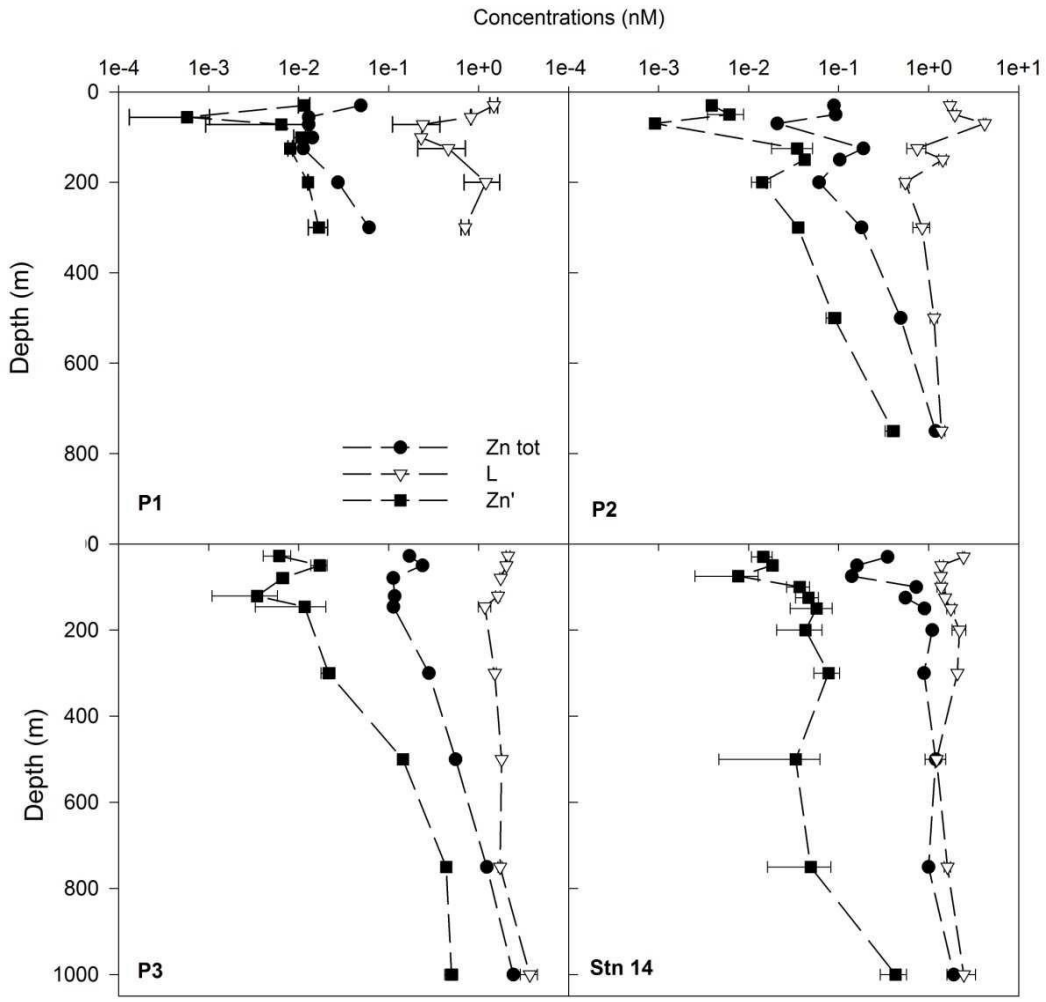

Fig.9: Profile of total dissolved zinc, labile zinc and ligands concentrations for the four stations analysed in this study. The error bars present for the ligand and labile concentrations are the standard errors based on duplicate of scans.

Table 4: Comparison of Zn speciation results obtained in this study and in previous studies. Adapted from Baars and Croot (2011).

Region	Sample	$[L_T]$ (nmol L^{-1})	log K'_{ZnL}	References	Method
North Pacific	Profile	1.0 – 1.5	10.7– 11.3	Bruland (1989)	ASV
North Pacific	60 and 150m	1.7–2.3	11.0 – 11.5	Donat and Bruland (1990)	ASV
	60 and 150m	1.6 – 2.3	10.1 – 10.5	Donat and Bruland (1990)	CSV
North Pacific	15 m	0.7	10.5	Lohan *et al.* (2005)	CSV
North Atlantic	Surface	0.4 – 2.5	10.0 – 10.5	Ellwood and van den Berg (2000)	CSV
North Atlantic	Profile	0.9 – 1.5	9.8 – 10.5	Wisniewski-Jakuba *et al.* (2008)	FF - ASV
	Profile	0.6 – 1.3	9.8 – 11.3	Wisniewski-Jakuba et al. (2008)	FF- ASV
South Pacific	20 m	1.3	10.6	Ellwood (2004)	ASV
	20 m	1.2	10.2	Ellwood (2004)	CSV
Southern Ocean	10–200 m	1.4 – 5.3	9.1 – 10.4	Baars and Croot (2011)	ASV
Drake Passage	25–100 m	1.4 – 2.5	9.7 – 9.8	Baars and Croot (2011)	ASV
Zero Meridian	10–200 m	2.5 – 5.3	9.1 – 10.4	Baars and Croot (2011)	ASV
Tasman Sea					
P1	15–300m	0.23 – 1.48	9.3 – 11.0	This study	ASV
P2	Profile	0.55 – 4.19	9.3 – 11.1	This study	ASV
P3	Profile	1.18 – 3.71	9.4 – 10.8	This study	ASV
Stn 14	Profile	1.23 – 2.65	9.6 – 11.4	This study	ASV

There was no significant difference in Zn speciation between the four stations (t- test, p = 0.124). However, the concentrations of ligands increased from North to South along transect, as per the total dissolved Zn, and showing interactions with the biology, especially in the first 200 of the water column. This is discussed in more detail in the next section.

4.3.3: Biological data:

For clarity, the pigments hex-fucozanthin, But- fucoxanthin, fucoxanthin and zeaxanthin have been defined as Hex-Fuco, But-Fuco, Fuco and Zea, respectively, in the following analyses. An approximation of the phytoplankton community was established from the pigments data and revealed differences between stations (Fig. 10). P1 was dominated by haptophytes (23.5 %) and cyanobacteries (22.2 %). The diatoms were present at low levels (11.8 and 5.11 %). P1 was the only station with presence of tropical phytoplankton (22.6 %), due to its location. P2 was also dominated by the same species, haptophytes (27.3%) and cyanobacteria (15.2 %) while chlorophytes represented 10.5 %. The amount of diatoms was still low (9.87 and 5.27 %). Diatoms increased at P3 (10.7 and 8.98 %) while haptophytes were still dominant (44.1 %). Cyanobacteria were not significant with 4.59 % of the assemblages, while the chlorophytes represented 13.7 %. Stn 14 was dominated by haptophytes, cyanobacteria and chlorophytes (32.1, 12.5 and 14.6 %) while the diatoms represented 9.5 and 7.78 % of the phytoplankton assemblages.

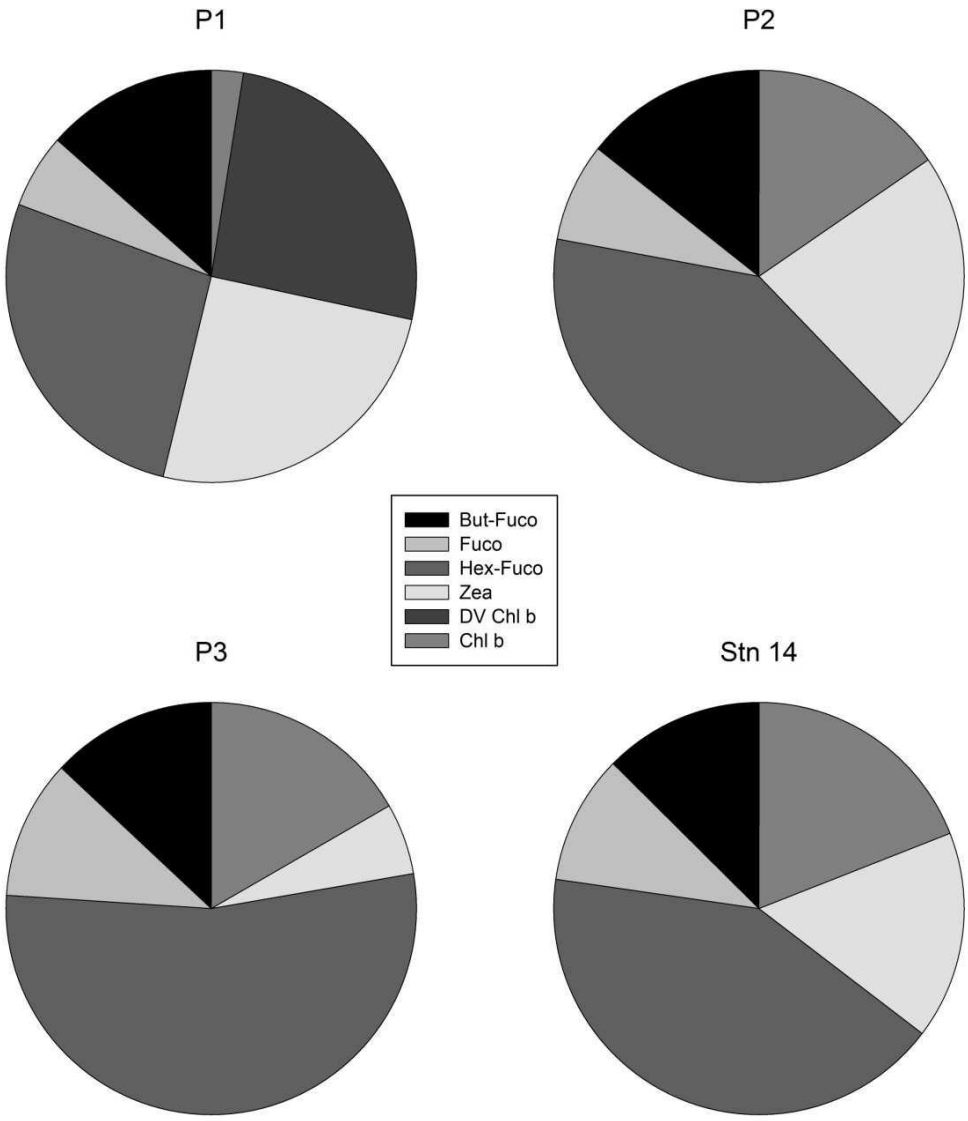

Fig. 10: Composition of phytoplankton community for each station in the first 100 m of the water column. Fractions were calculated from Tot Chl *a* and pigments data.

Table 5: Biological data selected from the PINTS cruise to establish comparison and correlations in the surface waters. The zinc data have been added, taken from the analyses done in this work, to complete the biochemical picture of the region visited.

Station	Days of occupation	Depth (m)	Zn_T (pM)	Zn' (pM)	Zn^{2+} (pM)	L_T (nM)	But-Fuco ($\mu g\ L^{-1}$)	Fuco ($\mu g\ L^{-1}$)	Hex-Fuco ($\mu g\ L^{-1}$)	Zea ($\mu g\ L^{-1}$)	DV Chlb ($\mu g\ L^{-1}$)	Chl b ($\mu g\ L^{-1}$)	Tot Chl a ($\mu g\ L^{-1}$)
P1	28 Jan – 31 Jan 2010	30	49	11.6	5.5	1.48	0.008	0.008	0.027	0.069	0	0	0.116
		50	13	0.6	0.3	0.82	0.014	0.016	0.047	0.072	0	0.017	0.192
		75	13	6.4	3.1	0.24	0.028	0.018	0.084	0.074	0.002	0.004	0.327
		101	14	10.7	5.1	0.23	0.049	0.009	0.084	0.035	0.071	0.010	0.320
		125	11	8.1	3.8	0.46	0.067	0.015	0.072	0.038	0.214	0	0.360
P2	3 Feb– 4 Feb 2010	15	110	2	1	1.26	0.011	0.011	0.035	0.066	0	0	0.164
		31.8	90	4	2	1.73	0.014	0.016	0.048	0.067	0	0.019	0.214
		50	90	6	3	1.96	0.067	0.029	0.196	0.094	0	0.140	0.693
		70.2	20	1	0	4.20	0.057	0.027	0.120	0.002	0	0.106	0.408
P3	7 Feb– 9 Feb 2010	15	180	10	5	1.58	0.098	0.049	0.418	0.057	0	0.077	0.916
		28	170	6	3	2.13	0.063	0.057	0.270	0.036	0	0.0905	0.573
		50	240	17	8	2.04	0.037	0.047	0.145	0.011	0	0.061	0.350
		79	110	7	3	1.76	0.025	0.029	0.071	0	0	0.030	0.182
Stn 14	12 Feb– 14 Feb 2010	15	100	4	2	2.65	0.05	0.033	0.163	0.122	0	0.068	0.565
		30	350	15	7	2.44	0.047	0.039	0.169	0.056	0	0.080	0.492
		50	160	18	9	1.39	0.015	0.018	0.052	0.003	0	0.027	0.158
		75	140	8	4	1.37	0.012	0.015	0.040	0	0	0.020	0.121

The pigments data were taken from 30 to 125 m for P1, 15 to 70.2 m P2, 15 to 79 m for P3 and 15 to 75 m for Stn 14 during the cruise. In that regard, Zn data were considered in accordance with the measured pigments concentrations for each station, giving a dataset of 17observations (Table 5) for which different correlations were established between Zn speciation and the biology (via pigments). Values obtained for Tot Chl *a* for the four different stations revealed four different distribution of biomass in the water column. As previously mentioned, P1 had the lowest range of Tot Chl *a* concentrations (0.116 to 0.36 µg L^{-1}). The lowest values were found in surface waters and increased with depth. P3 (0.182 to 0.920 µg L^{-1}) and Stn 14 (0.121 to 0.565 µg L^{-1}) had higher concentrations in the surface and decreased with depth. P2 exhibited an intermediate range, between P3 and Stn 14, with values from 0.164 to 0.693 µg L^{-1}. This is confirmed with the surface satellite data for Chl *a* (Fig. 1), in which we clearly observed that the biomass at P1 and P2 is less abundant than P3 and Stn 14, in the surface waters. However, the distribution of Chl *a* in the water column revealed that for P2, an increase of biomass was observed in a deep chlorophyll maximum between 40 and 80 m. This productive zone extended to 80 to 100 m at P1. Following this, stations were separated into two groups according to their Chl *a* concentration to evaluate the different correlations between zinc and biology.

The correlation between $[Zn]_{tot}$ and Tot Chl *a* confirmed the two regimes, since two correlations were identified (Fig. 11). The first regression corresponded to the deep waters for P3 and Stn 14 and near surface waters for P1 and P2. The opposite, shallow waters of P3 and Stn 14 with deep waters of P1 and P2, corresponded to the second correlation. Except the regression with the But-Fuco, all regressions with total dissolved Zn were significant.

The free ion Zn^{2+} and inorganic form of Zn are assumed to be the form assimilated by the phytoplankton (Sunda and Hunstman 1995), therefore, it was important to also study it. For Zn^{2+}, we obtained two significant correlations with the Tot Chl a and Hex-Fuco ($p = 0.013$ and $p = 0.028$, respectively) for the highest biomasses. Following the same separation of stations, the comparison between total dissolved Zn or [Zn^{2+}] and Fuco revealed a significant correlation ($p < 0.01$) between the total dissolved but no regression with Zn^{2+} (Fig. 12). Total dissolved Zn and Fuco was a stronger correlation than with Hex-Fuco, which related to higher Zn requirements for the diatoms already mentioned in previous studies (Sunda and Hunstman, 1992, 1995). However, no significant correlation was observed between Si and Fuco ($R^2 = - 0.166$, $p = 0.525$) or Si and But-Fuco ($R^2 = 0.005$, $p = 0.843$).

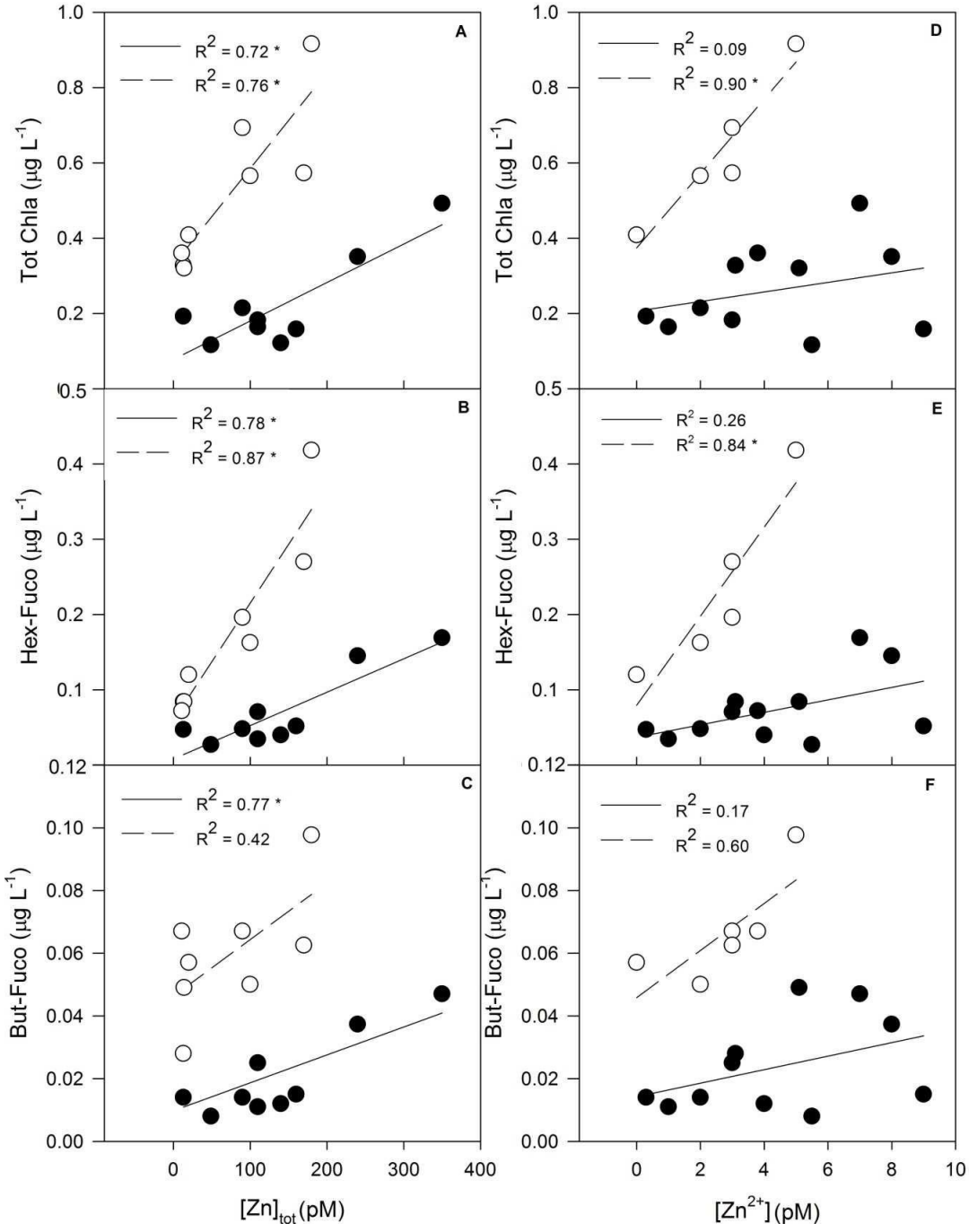

Fig. 11: Relationship between two biomarkers for haptophytes and Zn chemical species. The black dots (●) correspond to depth where the Tot Chl *a* was the lowest for each station and the white dots (○) corresponded to the depth where the Tot Chl *a* was the highest in the water column for each station. Regression coefficients have been added to the corresponding curve and the significant regressions have been notified with a little asterix.

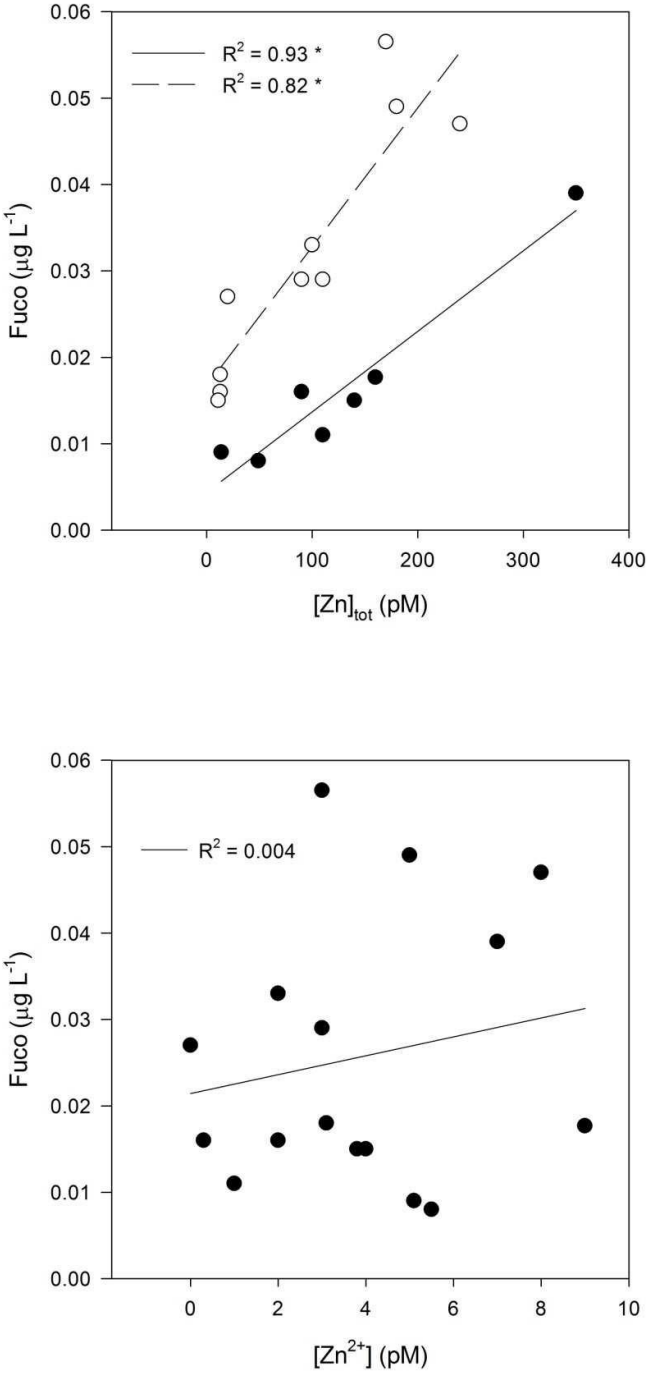

Fig. 12: Relationship between the different chemical forms of Zn and the biomarker Fuco, biomarker for diatom. In the top panel, the black dots (●) correspond to depth where the Tot Chl *a* was the lowest for each station and the white dots (○) corresponded to the depth where the Tot Chl *a* was the highest in the water column for each station. The significant correlations have been specified with an asterix.

Chlorophytes and cyanobacteria were also important species for all stations. There was no correlation between the biomarkers Zea and Chl *b* and the concentrations of total dissolved Zn or Zn^{2+} (data not shown). This is in good agreement with the fact that chlorophytes such as *Prochlorococcus* and *Synechoccocus* do not require Zn to grow but do have a requirement for Co or Cd.

To go further in the analysis of our results, we studied the correlation and regressions between Zn ligands and the different pigments (Table 6, Fig. 13). The ligand concentration was significantly correlated to all pigments in the following order: Chl *b* ~ Hex-Fuco > But-Fuco ~ Fuco, which can be seen as Chlorophytes ~ Haptophytes > Diatoms. Although they represented an important part in the composition of the different assemblages, no significant correlation was obtain for the cyanobacteria,

Table 6: Results of statistical correlation and regression between the Zn ligand concentration and the different biomarkers used in this study.

Pigments	Coefficient of regression	St error	R^2	p value regression	Correlation
Chl b	0.05	0.01	0.66	0.008	0.76 *
Hex-Fuco	0.09	0.02	0.69	0.006	0.75 *
But-fuco	0.02	0.01	0.70	0.005	0.71 *
Fuco	0.02	0.01	0.58	0.02	0.70 *

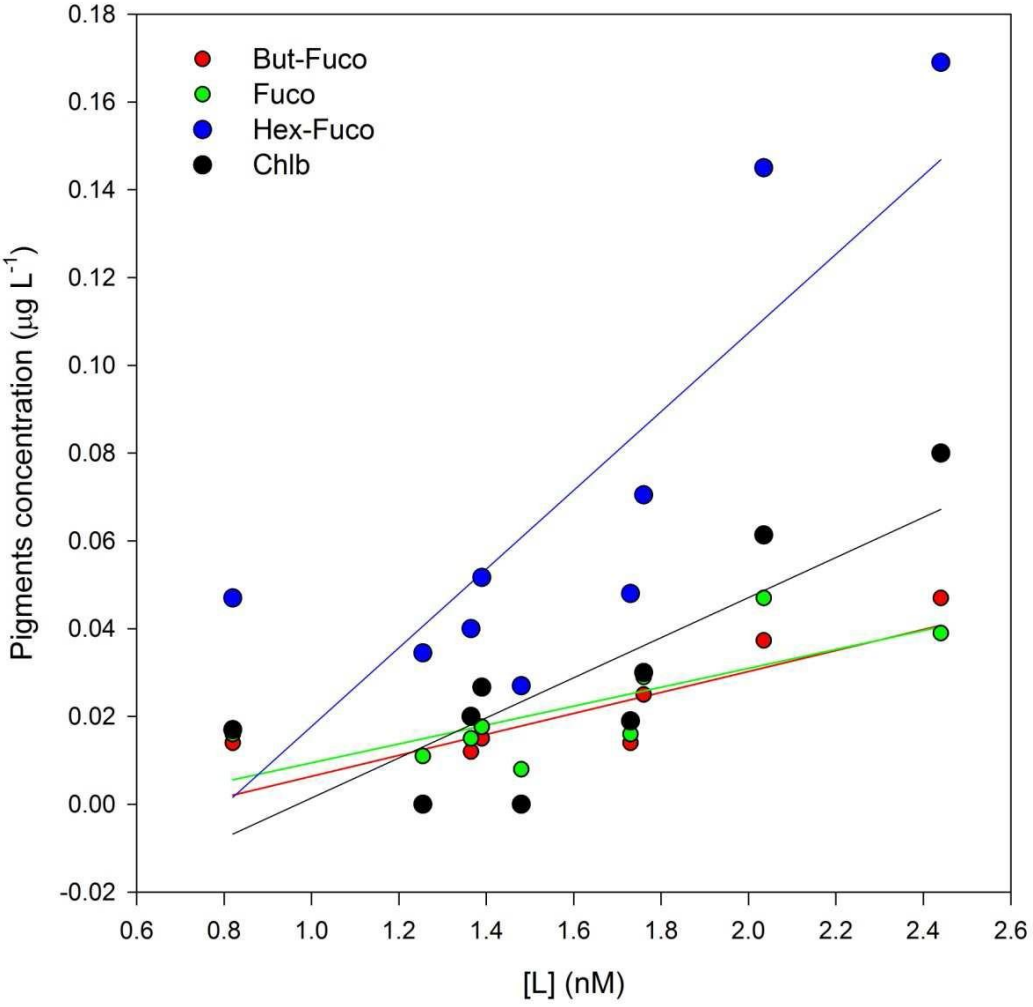

Fig. 13: Existing relationships and correlations between Zn ligands concentrations and pigments from the different phytoplankton groups.

4.4 Discussion:

A first finding of this work is that Zn speciation did not change along the north-south transect studied as Baars and Croot (2012) showed for the southern Atlantic and for lower latitudes. However, a gradient of concentration along the north-south transect was observed. Increasing concentrations of total dissolved zinc matched the increasing ligand concentrations, therefore the fraction of Zn associated with the strong ligand (ZnL) also increased, leaving concentrations of labile Zn (Zn′) close to limiting levels. This was especially true for P2, P3 and Stn

14 (59 to 98%). It has been shown in laboratory studies that the threshold for limiting the growth of the coastal and open ocean diatoms (*Thalassiosira weissflogii* and *Thalassiosira* oceanica) was a concentration of Zn' lower than 10 pM and 2 pM, respectively (Sunda and Huntsman 1992, 1995; Morel et al., 1994). Surface concentrations at P2 (1 to 6 pM) were close to limit growth of phytoplankton. However, P3 (6 to 17 pM) and Stn 14 (4 to 18 pM) manifested Zn´ concentrations that were able to sustain phytoplankton growth and a bloom. P1 exhibited a lower rate of complexation, which agreed with the lower concentrations of ligands observed. Those high rates of complexation, suggesting low bioavailability, were in good agreement with previous studies for different regions (Bruland 1989, Donat and Bruland 1990, Ellwood 2004, Baars and Croot 2011). The north-to-south gradient observed for the different concentrations was also observed for the biological activity with a Tot Chl *a* increasing from P1 to Stn 14. Studies trying to understand the link between Zn and the local biology are increasing (e.g. Ellwood 2004, Lohan *et al.* 2005, Shaked *et al.* 2006, Wisniewski-Jakuba *et al.* 2008, Jakuba *et al.* 2012) with results differing from one region to another. From all studies, Zn seems to be influencing the local community by favoring or inhibiting phytoplankton (and possibly other microbial) species, acting subtlety on the productivity or the composition of the assemblages (Crawford *et al.* 2003, Cullen and Sherrell 2005) The study in the Tasman Sea seems to also demonstrate the influence of Zn on the biology.

In surface waters (0–100 m), Zn was more related to the biology than the physical parameters in this region. This has been previously indicated in the study by Hassler *et al.* (2012) for the SAZ region. A finding from this work

was the possibility of two different 'regimes' for the four stations not only as a function of phytoplankton biomass but also depth, location, Zn concentrations and biological species present. This allowed us to evaluate the picture of relationship between Zn and biology for the first 100 m.

The community of the four stations was dominated by the haptophytes (e.g. *E. huxleyi* as picked up from the MODIS calcite composite map from the study region during the cruise, Mark Baird, pers. comm.). Aside from this group, chlorophytes and cyanobacteria dominated the phytoplankton communities in the South and the North, respectively. Although diatoms increased in the composition of the assemblages from P1 to P3 and are usually a dominant type in phytoplankton communities, they never exceeded the haptophytes. Contrary to Wisniewski-Jakuba *et al.* (2012) who found no significant relationship between Zn and the biomass, our data showed a significant relationship between the total dissolved Zn and the biomass inferred by Tot Chl *a*, which is also consistent with Hassler *et al.* (2012). However, the fact that total dissolved Zn was more correlated than Zn^{2+} to Tot Chl *a* was consistent with Wisniewski-Jakuba *et al.* (2012). This agrees with the fact that although Zn^{2+} is considered as the chemical species available for the phytoplankton (Sunda and Huntsman 1992, 1995), some species have the possibility to access organically complexed Zn to fulfill their requirements (Saito *et al.* 2002; Aristilde *et al.* 2012; Xu *et al.*2012). Our data showed that the correlation between total dissolved Zn and Fuco was also more significant than the one for Zn^{2+}. As previously stated, Fuco is a biomarker for diatoms. In this regard, we can suggest that diatoms could rely more on weakly organically complexed Zn rather than solely on Zn^{2+}.

The correlations between total dissolved zinc and free zinc with two pigments found in the haptophytes (e.g. *E. huxleyi*) was consistent with the finding in Hassler *et al.* (2012) study where Zn was found to be only positively correlated with the Hex-Fuco related to the small phytoplankton (<10 μm). Haptophytes might rely on Zn^{2+} to fulfill their requirements, even under low Zn concentrations. It is also known that species such as *E. huxleyi* can alleviate zinc depletion by replacing Zn by cobalt (Co: Timmermans *et al.* 2001; Xu *et al.* 2007), which could explain their ability to grow under all conditions encountered for all stations. The constant domination of haptophytes can also be related to the high ligand concentrations. Indeed, the concentrations of ligands at P2 and P3 found in this study were higher than other studies done with ASV (Table 3). Although higher ligand concentrations have been previously reported in incubation after Zn additions (Lohan *et al.* 2005), we can also suggest that other species from the community had the possibility to exudates organic ligand (Vasconcelos *et al*. 2002). The study by Vasconcelos *et al.* (2002) suggested that *E. huxleyi* growth could be promoted due to the nature of exudates, especially green algae exudates. If *E. huxleyi* is indeed promoted by exudates and because of its lower requirements for Zn, this could also explain the dominance of small species in the phytoplankton community of the Tasman Sea.

The small species were also species such as cyanobacteria which can grow without Zn but do have a requirement for Co (Saito *et al.* 2002; Saito and Goepfert 2008*a*). In that regard, the lack of correlation with Zn concentrations observed was expected. However, the different relationships obtained between Zn complexing ligands and pigments revealed the further possibility of a link between that biology and speciation. The chlorophyte were, indeed, found to be the most correlated to the ligand concentrations, and, thus, likely to influence

the community by producing exudates to promote the haptophytes. This is confirmed by Vasconcelos *et al.* (2002); Vasconcelos and Leal (2008) who showed that chlorophytes were able to promote the growth of other species by releasing exudates which increase uptake of low micronutrients. Where they are present, cyanobacteria could overcome species like diatoms in assemblages due to their low requirements for Zn and the impossibility for large diatoms to substitute efficiently Zn by Co or cadmium (Cd: Timmermans *et al.* 2001). Moreover, it has been shown that smaller diatoms can grow even under lower Zn^{2+} concentrations than larger ones (Sunda and Hunstman 1992, 1995). A size partitioning has not been taken into account in this study. The possibility of a phytoplankton community with small diatoms could explain their presence at low concentration while the large diatoms could be limited (Ellwood 2004, Lohan *et al.* 2005). No obvious relationship between Si and the diatoms (Fuco) was observed. This lack of relationship is surprising as both usually go together and this relationship has previously been demonstrated in other regions (Wiesniewski-Jakuba *et al.* 2012). However, the time of the bloom at which the different stations were sampled was different, explaining the absence of clear relationship between Si and diatoms.

The factor that has not been taken into account here to discuss the influence of Zn on the assemblages is the limitation by Fe. Indeed, several studies have previously shown the link between Zn and Fe limitation in deck incubations and cultures. De la Rocha *et al.* (2000) showed the influence of Zn-Fe limitation on Si uptake by phytoplankton while Franck *et al.* (2003) showed it on NO_3 uptake. The metal-metal interactions and their influence on macronutrient uptake have not been explored in this study and further study need to relate speciation of micronutrients, availability and composition of phytoplankton in this region.

Indeed, this study showed the importance of differentiate chemical species and phytoplankton community to understand the role of complexation in bioavailability of Zn for the different species present.

4.5 Acknowledgements:

I would like to thank the Australian National University, Research School for Environmental Science in Canberra for hosting this work. Particular thanks is addressed to Claire Thompson for her time, help and providing PINTS samples.

4.6 References:

Aristilde, L., Xu, Y., and Morel, F. M. M. (2012). Weak organic ligands enhance zinc uptake in marine phytoplankton. *Environmental Science and Technology,* **46,** 5438-5445.

Baars, O., and Croot, P. L. (2011). The speciation of dissolved zinc in the Atlantic sector of the Southern Ocean. *Deep-Sea Research II* **58**, 2720-2732.

Badger, M. (2003). The roles of carbonic anhydrases in photosynthetic CO_2 concentrating mechanisms. *Photosynthesis Research* **77**, 83-94.

Bermin, J., Vance, D., Archer, C., and Statham, P. J. (2006). The determination of the isotopic composition of Cu and Zn in seawater, *Chemical Geology* **226**, 280-297.

Bowie, A. R., Griffiths, F. B., Dehairs, F., and Trull, T. W. (2011). Oceanography of the subantarctic and Polar Frontal Zones south of Australia during summer: Setting for the SAZ-Sense study. *Deep Sea Research Part II: Topical Studies in Oceanography,* **58,** 2059-2070.

Bruland, K. W. (1989). Complexation of Zinc by Natural Organic Ligands in the Central North Pacific. *Limnology and Oceanography,* **34,** 269-285.

Bruland, K. W., and Lohan, M. C. (2003). Controls of trace metals in seawater. In 'Treatise on geochemistry'. pp. 23-47 (Pergamon, Oxford).

Capodaglio, G., Scarponi, G., Toscano, G., Barbante, C., and Cescon, P. (1995). Speciation of trace metals in seawater by anodic stripping voltammetry: Critical analytical steps. *Fresenius' Journal of Analytical Chemistry,* **351,** 386-392.

Crawford, D. W., Lipsen, M. S., Purdie, D. A., Lohan, M. C., Statham, P. J., Whitney, F. A., Putland, J. N., Johnson, W. K., Sutherland, N., Peterson,

T. D., Harrison, P. J., and Wong, C. S. (2003). Influence of zinc and iron enrichments on phytoplankton growth in the northeastern subarctic Pacific. *Limnology and Oceanography* **48**, 1583–1600.

Croot, P. L., Baars, O., and Streu, P. (2011). The distribution of dissolved zinc in the Atlantic sector of the Southern Ocean. *Deep-Sea Research II* **58**, 2707-2719.

Cullen, J. T., and Sherrell, R. M. (2005). Effects of dissolved carbon dioxide, zinc, manganese on the cadmium to phosphorus ratio in natural phytoplankton assemblages. *Limnology and Oceanography* **50**, 1193–1204.

Cutter, G., Andersson, P., Codispoti, L., Croot, P., François, R., Lohan, M. C., Obata, H., and Rutgers, M. (2010). Sampling and sample-handling protocols for GEOTRACES cruises. (Ed. GEOTRACES Standards and Intercalibration Committee.) GEOTRACES Library, Available at http://www.geotraces.org/libraries/documents/Intercalibration/Cookbook.pdf [accessed 4 January 2010]

Danielsson, L-G., Magnusson, B., Westerlund, S. (1978) An improved metal extraction procedure for the determination of trace metals in sea water by atomic absorption spectrometry with electrothermal atomization, *Analytica Chimica Acta,* **98**, 47-57.

De la Rocha C. L., Hutchins, D. A., Brzezinski M. A., and Zhang Y. (2000). Effects of iron and zinc deficiency on elemental composition and silica production by diatoms. *Marine Ecology Progress Series,* **195,** 71-79.

Donat, J. R. and Bruland, K. W. (1990). A comparison of two voltammetric techniques for determining zinc speciation in Northeast Pacific Ocean waters. *Marine Chemistry*, **28,** 301-323.

Durán, I., and Nieto, Ó. (2011). Electrochemical speciation of dissolved Cu, Pb and Zn in an estuarine ecosystem (Ria de Vigo, NW Spain): Comparison between data treatment methods. *Talanta,* **85,** 1888-1896.

Ellwood, M. J. (2008). Wintertime trace metal (Zn, Cu, Ni, Cd, Pb and Co) and nutrient distributions in the Subantarctic Zone between 40-52°S; 155-160°E. *Marine Chemistry,* **112,** 107-117.

Ellwood, M. J. (2004). Zinc and cadmium speciation in subantarctic waters east of New Zealand. *Marine Chemistry,* **87,** 37-58.

Ellwood, M. J. and van den Berg, C. M. G. (2000). Zinc speciation in the Northeastern Atlantic Ocean. *Marine Chemistry,* **68,** 295-306.

Franck V., M., Bruland, K. W., Hutchins, D. A., and Brzezinski M. A. (2003). Iron and zinc effects on silicic acid and nitrate uptake kinetics in three high-nutrient, low-chlorophyll (HNLC) regions. *Marine Ecology Progress Series,* **252,** 15-33.

Gerringa, L. J. A., Herman, P. M. J. and Poortvliet, T. C. W. (1995) Comparison of the linear Van den Berg/Ružić transformation and a non-linear fit of the Langmuir isotherm applied to Cu speciation data in the estuarine environment. *Marine Chemistry,* **48,** 131-142.

Hassler, C. S., Ridgway, K., Bowie, A. R., Butler, E. C. V., Clementson, L., Doblin, M. A., Ralph, P., Davies, D. M., van der Merwe, P., Watson, R., Ellwood, M. E. (2013) Primary Productivity induced by iron and nitrogen in the Tasman Sea – an overview of the PINTS expedition (In prep).

Hassler C.S., Schoemann, V., Boye, M., Tagliabue, A., Rozmarynowycz, M., and McKay, R. M. L. (2012) Iron Bioavailability in the Southern Ocean. *Oceanography and Marine Biology: An annual review* **50,** 1-6.

Hirose, K., Saito, T., Lee, S. H., and Gastaud, J. (2011). Vertical distributions of the strong organic ligand in the twilight zone of Southern Hemisphere Ocean particulate matter. *Progress In Oceanography,* **89,** 108-119.

Hobday, A. J., Poloczanska, E. S., and Matear R .J. (eds) (2008), *Implications of climate change for Australian fisheries and aquaculture: a preliminary assessment*, Report to the Department of Climate Change, Canberra.

Hoppe, H. G. (2003). Phosphatase activity in the sea. *Hydrobiologia* **493**, 187-200.

Jeffrey S. W., and Wright S. W. (2006). Photosynthetic pigments in marine microalgae: insights from cultures and the sea, in Algal Cultures, Analogues of Blooms and Applications, ed. Subba Rao D. V., editor. (Enfield, NH: Science Publishers;), 33–90.

Jeffrey S. W., and Vesk M. (1997). Introduction to marine phytoplankton and their pigment signatures, in Phytoplankton Pigments in Oceanography: Guidelines to Modern Methods, eds Jeffrey S. W., Mantoura R. F. C., Wright S. W., editors. (Paris: UNESCO Publishing), 37–84.

Kupriyanova, E. V., and Pronina, N. A. (2011). Carbonic anhydrase: Enzyme that has transformed the biosphere. *Russian Journal of Plant Physiology* **58**, 197-209.

Leblanc, K., Hare, C. E., Boyd, P. W., Bruland, K. W., Sohst, B., Pickmere, S., Lohan, M. C., Buck, K., Ellwood, M., and Hutchins, D. A. (2005). Fe and Zn effects on the Si cycle and diatom community structure in two contrasting high and low-silicate HNLC areas. *Deep Sea Research Part I: Oceanographic Research Papers,* **52,** 1842-1864.

Lohan, M. C., Crawford, D. W., Purdie, D. A., and Statham, P. J. (2005). Iron and zinc enrichments in the northeastern subarctic Pacific: Ligand production

and zinc availability in response to phytoplankton growth. *Limnology and Oceanography,* **50,** 1427-1437.

Morel, F. M. M., Reinfelder, J. R., Roberts, S. B., Chamberlain, C. P., Lee, J. G., and Yee, D. (1994). Zinc and carbon co-limitation of marine phytoplankton. *Nature,* **369,** 740-742.

O'Sullivan, J. E., Watson, R. J. and Butler, E. C. V. (2013). An ICP-MS procedure to determine Cd, Co, Cu, Ni, Pb and Zn in oceanic waters using in-line flow-injection with solid-phase extraction for preconcentration. *Talanta,* submitted

Ružić, I. (1982). Theoretical aspects of the direct titration of natural waters and its information yield for trace metal speciation. *Analytica Chimica Acta,* **140,** 99-113.

Saito, M. A., and Goepfert, T. J. (2008). Zinc-Cobalt Colimitation of *Phaeocystis Antarctica*. *Limnology and Oceanography,* **53,** 266-275.

Saito, M. A., Goepfert, T. J., and Ritt, J. T (2008) Some thoughts on the concept of co-limitation: Three definitions and the importance of bioavailability, *Limnology and Oceanography*, **53** (1), 276-290.

Saito, M. A., Moffett, J. W., Chisholm, S. W., and Waterbury, J. B. (2002). Cobalt Limitation and Uptake in *Prochlorococcus*. *Limnology and Oceanography*, **47,** 1629-1636.

SCOR, Working group 2007, 'GEOTRACES - An international study of the global marine biogeochemical cycles of trace elements and their isotopes', *Chemie der Erde - Geochemistry,* **67** (2), 85-131

Shaked, Y., XU, Y., Leblanc, K., and Morel, F. M. M. (2006). Zinc availability and alkaline phosphatase activity in *Emiliania huxleyi*: Implications for Zn-P co-limitation in the ocean *Limnology and Oceanography,* **51,** 299-

309.

Sinoir, M., Butler, E. C. V., Bowie, A. R., Mongin M., Nesterenko, P. N., and Hassler, C. S. 2012. Zinc marine biogeochemistry in seawater: a review. *Marine and Freshwater Research*, **63,** 644-657.

Sunda, W. G. and Huntsman, S. A. (1992). Feedback interactions between zinc and phytoplankton in seawater. *Limnology and Oceanography*, **37,** 25-40.

Sunda, W. G., and Huntsman, S. A. (1995). Cobalt and Zinc Interreplacement in Marine Phytoplankton: Biological and Geochemical Implications. *Limnology and Oceanography*, **40,** 1404-1417.

Timmermans, K. R., Snoek, J., Gerringa, L. J. A., Zondervan, I., and de Baar, H. J. W. (2001). Not all eukaryotic algae can replace zinc with cobalt: *Chaetoceros calcitrans* (Bacillariophyceae) versus *Emiliania huxleyi* (Prymnesiophyceae). *Limnology and Oceanography* **46**, 699-703.

Turner, D.R., Whitfield, M., and Dickson, A.G. (1981). The equilibrium speciation of dissolved components in freshwater and seawater at 25°C and 1atm pressure. *Geochimica and Cosmochimica Acta*, **45,** 855-881.

Van den Berg, C. M. G. (1982). Determination of copper complexation with natural organic ligands in seawater by equilibration with MnO2 I. Theory. *Marine Chemistry*, **11,** 307-322.

Van den Berg, C. M.G. (1985). Determination of the zinc complexing capacity in seawater by cathodic stripping voltammetry of zinc—APDC complex ions. *Marine Chemistry*, **16,** 121-130.

Vasconcelos, M. Teresa. S. D., and Leal, M. Fernando. C. (2008). Exudates of different marine algae promote growth and mediate trace metal binding in *Phaeodactylum tricornutum*. *Marine Environmental Research*, **66,** 499-507.

Vasconcelos, M. Teresa. S. D., Leal, M. Fernando. C., and van den Berg, C. M. G. (2002). Influence of the nature of the exudates released by different marine algae on the growth, trace metal uptake and exudation of *Emiliania huxleyi* in natural seawater. *Marine Chemistry*, **77,** 187-210.

Wilkinson, L., Hill, M.,Welna, J. P., and Birkenbeuel, G. K. (1992) SYSTAT for Windows: Statistics, Version 5 Edition. SYSTAT, Evanston, IL, 750 pp.

Wisniewski-Jakuba., R., Moffett, J. W., and Saito, M. A. (2008*a*). Use of a modified, high-sensitivity, anodic stripping voltammetry method for determination of zinc speciation in the North Atlantic Ocean. *Analytica Chimica Acta,* **614,** 143-152, doi:10.1016/j.aca.2008.03.006.

Wisniewski-Jakuba., R., Moffett, J. W., and Dyhrman, S. T. (2008*b*). Evidence for the linked biogeochemical cycling of zinc, cobalt, and phosphorus in the western North Atlantic Ocean. *Global Biogeochemical Cycles,* **22,** 13.

Wisniewski-Jakuba., R., Saito, M. A., Moffett, J. W., and Xu, Y. 2012. Dissolved zinc in the subarctic North Pacific and Bering Sea: Its distribution, speciation, and importance to primary producers. *Global biogeochemical Cycle*, **26**, doi: 10.1029/2010GB004004

Xu, Y., Tang D., Shaked, Y., and Morel, F. M. M. (2007). Zinc, cadmium, and cobalt interreplacement and relative use efficiencies in the coccolithophore *Emiliania huxleyi Limnology and Oceanography,* **52,** 2294-2305.

Xu, Y., Shi, D., Aristilde, L., and Morel, F. M. M. (2012). The effect of pH on the uptake of zinc and cadmium in marine phytoplankton: Possible role of weak complexes. *Limnology and Oceanography,* **57,** 293-304

CHAPTER FIVE

Analysing the influence of zinc speciation on ecosystem dynamics using a conceptual model

5.1 Introduction:

As previously shown (Chapter II, III and IV), zinc is likely to exert a subtle influence on the phytoplankton community structure. In order to account for zinc chemical species in solution (and as an indirect approach to measurement), its speciation has been determined by mathematical means, knowing important chemical parameters. Several studies of speciation models have been already explored (Zirino and Yamamoto 1972). Mackey and Zirino (1994) developed the 'onion model' to explain interaction between trace metals and organic compounds present in seawater. However, none of these models integrate the impact of biological processes on the zinc chemistry. So far, only models like the Free Ion Activity Model (FIAM; Morel, 1983) and the Biotic Ligand Model (BLM: Pagenkopf 1983, Playle 1998, Paquin *et al.* 2002) were used to relate trace metal chemistry, bioavailability and reactivity with the biota. To do so, the FIAM and BLM models consider the chemical speciation in solution, surface complexation with transport sites and uptake of the metal inside the organism. However, both models still present several drawbacks (*e.g.* Campbell, 1995; Campbell *et al.*, 2002; Heijerick *et al.*, 2002) due to over-simplified chemistry or lack of complex biological interactions between aquatic organisms.

To predict and understand the behavior of an ecosystem, it is important to trace the flow of material between its various components. Based on this idea, several models have been developed, with different degrees of complexity. Several authors have introduced the one-dimensional models including phytoplankton, zooplankton, nutrients and detritus (NPZD type models: Steel and

Frost 1977, Evans and Parslow 1985, Fasham *et al*. 1990, Frost *et al.* 1987). Such models exist for nutrients, such as nitrogen (N: Fasham *et al*. 1990) or iron (Fe: Mongin *et al*. 2006). The complexity could then be extended to global ocean circulation models (Aumont *et al.* 2008), which investigate the complex dynamics of local ecosystems by integrating physics, chemistry and biology. Such models also exist for region like the Southern Ocean (Lancelot *et al*. 2000, Bopp *et al.* 2008).

The biogeochemistry model created by Oschlies and Garcon (1998) describes the seasonal dynamics of the open-ocean. Several improvements have been made since the original model was created, which led to the OG99 version being chosen as a reference NPZD model. The aim of this work was to adapt the existing model by Oschlies and Garcon (1998) to simulate the impact of Zn speciation on an ecosystem structure. To do so, we integrated Zn speciation, two phytoplankton groups (P) and two zooplankton groups (Z) to the original OG99 model to obtain a ZnPPZZD model. This arrangement permitted a study of the response of a small community to change in Zn speciation.

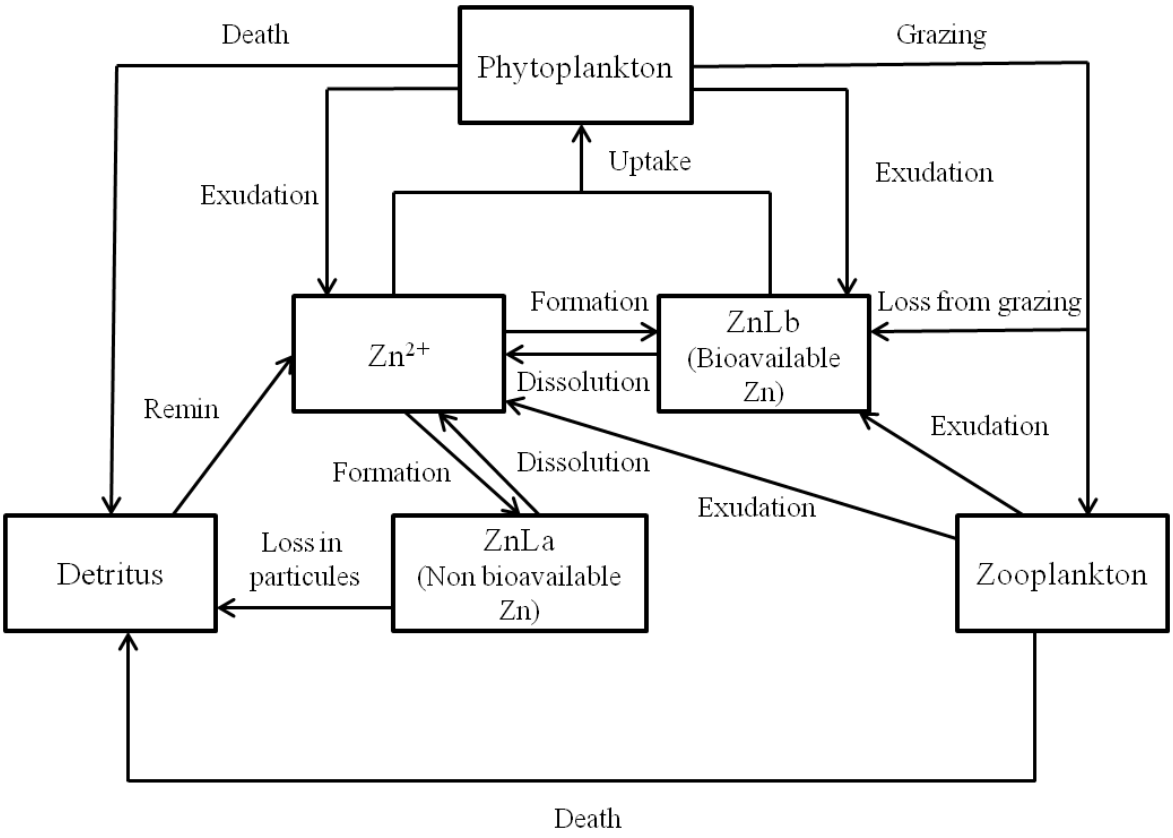

Figure 1: Conceptual model developed for this work, including, variables and processes.

5.2 Model description and simulations:

5.2.1. Structure of the model:

The structure of the conceptual model developed in this work is based on the work by Evans and Parslow (1985) optimised later by Oschlies and Schartau (2005), or OG99 model. However, to include Zn cycling, the nutrient box has been replaced by Zn and divided in three to correspond to a speciation of zinc (Fig 1.), as did Tagliabue and Arrigo (2005) in their model for iron cycling in the sea ice. The different stability constants for dissociation and formation of the various complexes formed with labile Zn and non labile Zn have been obtained from speciation analysis done using voltammetry technique as previously described (Chapter IV) for the three stations studied. Initial parameters for zinc

concentrations have been calculated from observations obtained in studies detailed in the previous chapter. Three concentrations were needed, the free ion concentration ($[Zn^{2+}]$), the inorganic or labile zinc (ZnLb) and the non-bioavailable zinc (ZnLa). In our case, an average of free Zn concentration (Zn^{2+}) and labile Zn concentrations (Zn') concentrations for the top 100 m of the water column was

taken as initial concentration for each of the three stations studied (Chapter IV). The non- labile zinc was established from the difference between an average total Zn in the upper 100 m of the water column and the difference of the two previous concentrations.

The model is forced with light (sra = constant, no seasonality) and constant mixed layer depth (MLD = 50m). The aim was to quantify and establish the different processes that would trigger an ecosystem response. The model simulates the evolution of a phytoplankton community in response to zinc speciation; the system operates in a zero dimension sense (simulate water column with no water circulation or change in vertical mixing). As a result, this model represents an instantaneous picture of a phytoplankton bloom for three different locations and the response of the phytoplankton community to the change of zinc speciation.

The equations to describe the different fluxes entering and leaving the different variables for Zn speciation are inspired from the work by Tagliabue and Arrigo (2006), Tagliabue *et al.* (2009) and Fan and Dunn (2010). All parameters used in the different equations composing the model are defined in table 1 (for their values, *cf* appendix at the end of this chapter).

Table 1*:* List of parameters used in the conceptual model to describe fluxes between the different compartments considered in the model.

Parameters	**Name**
k_{fZnLb}	Rate of formation for labile complexes
k_{dZnLb}	Rate of dissociation for labile complexes
k_{fZnLa}	Rate of formation for non labile complexes
k_{fZnLa}	Rate of dissociation for non labile complexes
Lb	Concentration of 'weak' ligand
La	Concentration of 'strong' ligand
alpha	Initial slope of P-I curve
par	Photosynthetically active radiation
kw	Light attenuation due to water
kc	Light attenuation due to phyto
a_s a_l	Growth rate parameter
b	Growth rate parameter
c	Growth rate parameter
Jmax	Specific light saturated growth
Ks K1l K2l	Half saturation constant for Zn uptake
mup1	Fraction Uptake value for Zn^{2+} for L phyto
morp morpL	Specific mortality rate for s and L phyto

Table 1(following)*:* List of parameters used in the conceptual model to describe fluxes between the different compartments considered in the model.

Parameters	**Name**
exup	Excretion rate into Zn total pool
gam	Assimilation efficiency
g_s g_l	Maximum grazing rate
eps	Prey capture rate
morz morzL	Mortality rate
exuz	Exudation term to Zn pool
rem	Remineralisation
exuzn	Exudation rate of Zn non labile to detritus
w_sink	Sinking rate

The following equations describe the fluxes and a list of parameters of the final model used can be found in appendix of this chapter. The variation of free Zn (Zn, pmol Zn $m^{-3}s^{-1}$) with time is:

$$\frac{dZn^{2+}}{dt} = rem \times D + \alpha_1 \times exup \times Ph1 + \beta_1 \times exuz \times Z1 + k_{dZnLb} \times ZnLb + k_{dZnLa} \times ZnLa - mup \times Ph1 - \delta 1 \times mupL \times Ph2 - k_{fZnLa} \times La \times Zn^{2+} - k_{fZnLb} \times Lb \times Zn^{2+}$$

Where the free ion can be complexed either by La, a strong chelator, or Lb, a weaker chelator. Both complexes are formed at a rate of k_{fZnLa} and k_{fZnLb}, respectively, or dissociate at a rate k_{dZnLa} and k_{dZnLb}, respectively. The

dissociation of those complexes is linked to the ligands present in the media ([La] and [Lb]). While the rates of dissociation and formation have been taken from ranges defined in Fe and Zn studies (Bruland 1989, Witter and Luther III 1998, Witter *et al.* 2000, Tagliabue 2006, Fan and Dunn 2011), the initial ligand concentration was defined by the range measured in the previous chapter.

The variation of bioavailable and non-bioavailable Zn (ZnLb, pmol Zn m^{-3} s^{-1}) are defined as follow:

$$\frac{dZnLb}{dt} = \alpha_2 \times exup \times Ph1 + (1-\gamma) \times G \times Z1 + \beta_2 \times exuz \times Z1 + k_{fZnLb} \times Lb \times Zn^{2+} - (1-\delta 1) \times mupL \times Ph2 - k_{dZnLb} \times ZnLb$$

$$\frac{dZnLa}{dt} = k_{fZnLa} \times La \times Zn^{2+} - k_{dZnLa} \times ZnLa - exuzn \times ZnLa$$

To match results found in our biological experiments as much as possible, we decided to have 2 contrasting phytoplankton groups in the model. Both communities do not take up nutrients in the same way (illustrated in the model by having different uptake kinetics). We assumed that the small phytoplankton only takes up the free ion according to Michaelis-Menten uptake kinetics and the large phytoplankton can access the labile zinc and free zinc ion using the Hill uptake kinetics (Fig 2.). Both communities growth is also driven by temperature and light as per Oschlies and Schartau (2003). The following growth limitation terms have been used:

$$L_{light} = (-1 \div MLD) \times cobeta \times kw \times (fu1 - fu2 - fx3 + fx4)$$

In this equation, the terms are related to the angle of the sun with cobeta being the cosines of the incidence angle of solar radiation at noon, the attenuation of light

by water (kw), the mixed layer depth (MLD). The other functions depend on light and MLD, which are constant.

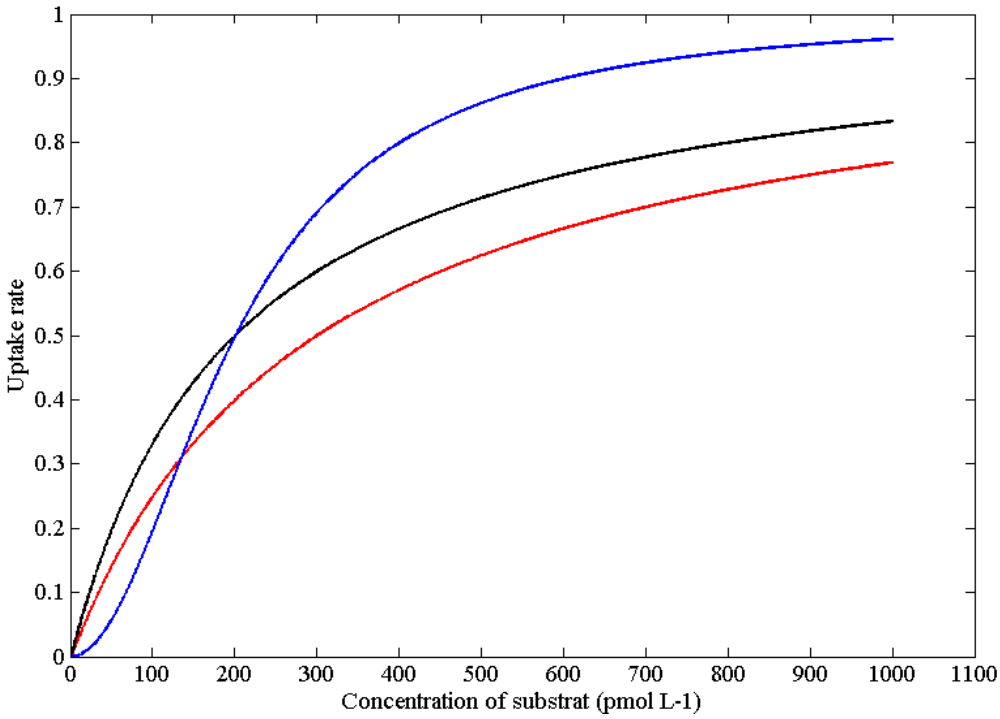

Fig. 2: Uptake kinetics used for phytoplankton nutrient uptake. In black and red are two classic Michaelis-Menten plots with two different Ks chosen for the uptake of free Zn (Zn^{2+}). In blue, the representation of the two transporters system with a Hill equation for the uptake of labile Zn (ZnLb).

The Zn growth term is defined as classically Michaelis-Menten with half saturation constant (Ks, K1l and K2l) adapted for both species according to values found in literature for iron (Mongin *et al.* 2006, Tagliabue *et al.* 2006) and using a Zn/Fe ratio of 0.1 (Ho *et al.* 2003). We also defined these constants using sensitivity analyses.

The uptake of the different forms of Zn is defined using the following equations.

$$LZn_s = Zn \div (Ks + Zn)$$

$$LZn_l = Zn \div (K_{1l} + Zn)$$

$$LZnLb = ZnLb^2 \div ({K_{2l}}^2 + ZnLb^2)$$

The limitation term for labile Zn was defined by the Hill equation to match the sigmoid relationship of induction of multiple transporters that can be found in biological uptakes studied in laboratory cultures (Sunda and Hunstman 1992, Seth *et al.* 2007, chapter three in this work). The limitation term was, then, expressed as a function of the growth rate and the light:

$$mups = Jmax * \ minimum(L_{light}, LZn_s)$$

$$mupl = Jmax * \ minimum(L_{light}, \times LZn_l, \times LZnLb)$$

In both equations, J_{max} is defined as the specific maximum growth rate. It followed an Eppley curve (Eppley 1972) , J_{max} = a x b^{cT}, with a, b and c being maximum growth rates parameters depending on the species. The difference between both species is that the larger phytoplankton community access both resources.

In that regard, the rates of change of the small phytoplankton (Ph1, pmol Zn m^{-3} s^{-1}) and the larger one (Ph2, pmol Zn m^{-3} s^{-1}) are defined as:

$$\frac{dPh1}{dt} = mups \times Ph1 - morp \ \times Ph1 - \ G \times Z1 - exup \times Ph1$$

$$\frac{dPh2}{dt} = mupl \times Ph2 - morpL \ \times Ph2 - \ G2 \times Z2$$

As our conceptual model incorporates two different phytoplanktons, the balance was made by adding two groups of zooplankton (Z1 and Z2) that are able to graze on Ph1 and Ph2, respectively. The rate of change of both zooplankton (Z1 and Z2, pmol Zn m^{-3} s^{-1}) are defined as:

$$\frac{dZ1}{dt} = \gamma \times G \times Z1 - exuz \times Z1 - \ morz \times Z1^2$$

$$\frac{dZ2}{dt} = \gamma \times G2 \times Z2 \; - \; morzL \times Z2^2$$

The grazing term, g, has been kept from the original model by Oschlies and Schartau (2003) and is related to an efficiency of capturing the prey (eps) and a maximum grazing rate (g_s and g_l). The structure of the grazing equation has been kept the same:

$$G\_s = g\_s \; \times eps \times Ph1^2 \div (g\_s + eps \times Ph1^2)$$

$$G_l = 1.5 \times (g\_l \; \times eps \times Ph2^2 \div (g\_l + eps \times Ph2^2))$$

The large zooplankton have a grazing rate 1.5 times larger than the small one (Aumont *et al.* 2008)

The rate of change of detritus (D, pmol Zn m^{-3} s^{-1}) regroups all the loss from the plankton. We also assume that detritus sink out of the mixed layer depth.

$$\frac{dD}{dt} = morp \times Ph1 + \; morz \times Z1^2 + exuzn \times ZnLa - rem \times D + morzL$$

$$\times Z2^2 + morpL \times Ph2 - \left(\frac{W_{sink}}{MLD}\right) * D$$

The model currency is in pmol Zn m^{-3}, but in order to better assess the model against observations, concentrations of phytoplankton, zooplankton and detritus have been expressed in mg Chl *a* m^{-3} using a Zn : C ratio of 0.37 mol : mol for the phytoplankton (Sunda 2012) and a C:Chl ratio of 50 mmol : mg. By taking into account the C mass and a C: Chl *a* ratio of 50, a conversion factor of $74 * 10^3$ was obtained. As our model was defined according to the single nutrient Zn, we also converted the fluxes present in the original model, depending on nitrate (N), in pmol Zn m^{-3} s^{-1} using a conversion factor of 529. This factor was calculated recognising the previously defined Zn : C ratio and a C : N ratio of 7.

Table 2: Chemical and biological conditions found at P3.

Parameters measured	Concentrations
Ligands	1.9 nmol, L^{-1}
total dissolved Zn	175 pmol L^{-1}
labile Zn	10 pmol L^{-1}
Free Zn	4.75 pmol L^{-1}
Tot Chl *a*	0.505 μg L^{-1}

5.2.2. Scenarios simulations:

To understand the model behavior, three sensitivity analyses were performed. Because this model was built to establish the response of phytoplankton to Zn speciation, the model was highly sensitive to the concentration of the different zinc species, the half-saturation constant for the phytoplankton and the concentrations of ligands found in the solution. Forty sensitivity tests (40 set of parameters) were used with initial conditions remaining constant.

Conditions of Zn speciation and biomass of Station P3, visited during the PINTS research voyage, were chosen to establish the response of this conceptual model (Table 2). This station exhibited a higher productivity than the other three, as stated in the previous chapter, and a diversity of phytoplankton species blooming. Initials conditions of the diverse Zn concentrations were not changed during each test run and the total concentration of chlorophyll *a* (Tot Chl *a*) measured during the cruise was chosen as a reference.

5.3 Results:

5.3.1 Response of the model without any inputs:

In this test, the model test without any light (sra = 0 W m^{-2}) or Zn (Zn = 0, ZnLb = 0 and ZnLb = 0). This simulation does not bring information on the behaviour of the ecosystem. However, it allowed checking the stability and having an idea on the functioning of the model (Fig. 3). We observed a rapid increase of the different Zn species, especially Zn (0 to 6.5 * 10^{-10} pmol m^{-3} in 30 days) and ZnLb (0 to 1.8 * 10-7 pmol m^{-3} in 30 days). This reflected the no consumption and recycling through detritus and the kinetics of exchange between the different pools of Zn chosen. None of the phytoplankton grew as light and zinc were set to zero at the start. We also observed the non-development of both zooplankton as the biomass on which they graze was not present. We also observed that the model quickly became unstable with these missing inputs.

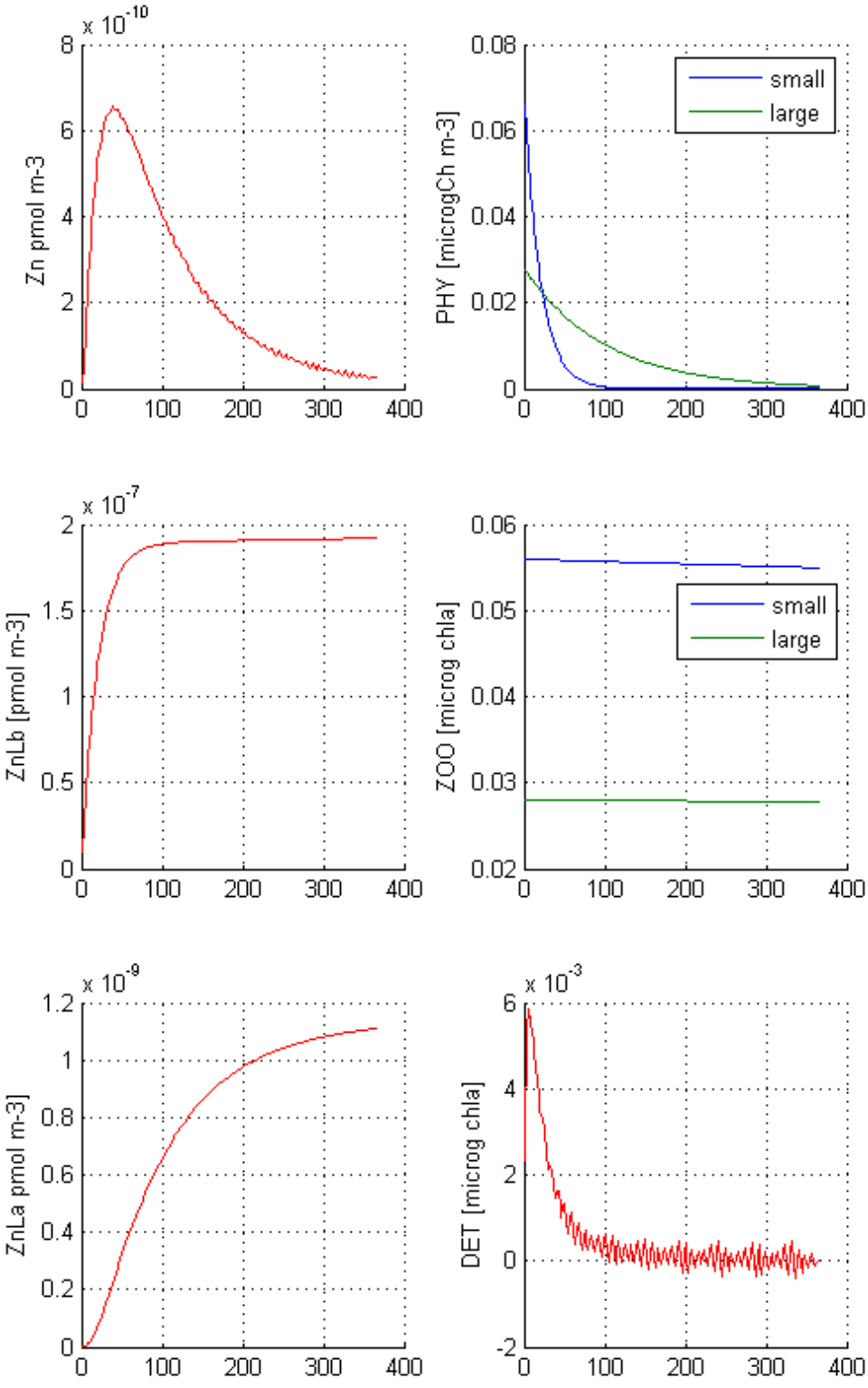

Fig. 3: Response of the model without Zn (Zn = ZnLa = ZnLb = 0 pmol L^{-1}) and light (sra = 0).

5.3.2: Sensitivity analyses on Ks:

The different Ks tested (Ks for Ph1, K1l and K2l for Ph2) were adapted according to values found in literature, usually related to models having iron limitation effect on different groups of phytoplankton (Arrigo *et al.* 2003, Gregg *et al.* 2003, Mongin *et al.* 2006, Tagliabue and Arrigo 2006, Gregg and Casey 2007). Ks were also chosen in relation to the range of Zn concentrations simulated in the model. Thus, half-saturation constants chosen ranged from 0.01 to 350 pmol Zn L^{-1} for both phytoplankton. The idea behind these tests was to simulate the impact on phytoplankton uptake with possible Zn limitation.

5.3.2.1 Scenario A: Three low half saturation constants, non-limited species:

In this scenario (Fig. 4 A), the simulated P1 reached a value of 6 µg Chl *a* m^{-3} and P2 followed with a biomass increasing to a value of 4 µg Chl *a* m^{-3}. The simulation of Z1 and Z2 followed the increase of both phytoplankton biomasses and reached a value of 10 µg Chl *a* m^{-3}. The simulation implies that in this scenario, none of the species were limited. After 200 days of simulations, the system reached a steady state for phytoplankton, zooplankton and detritus.

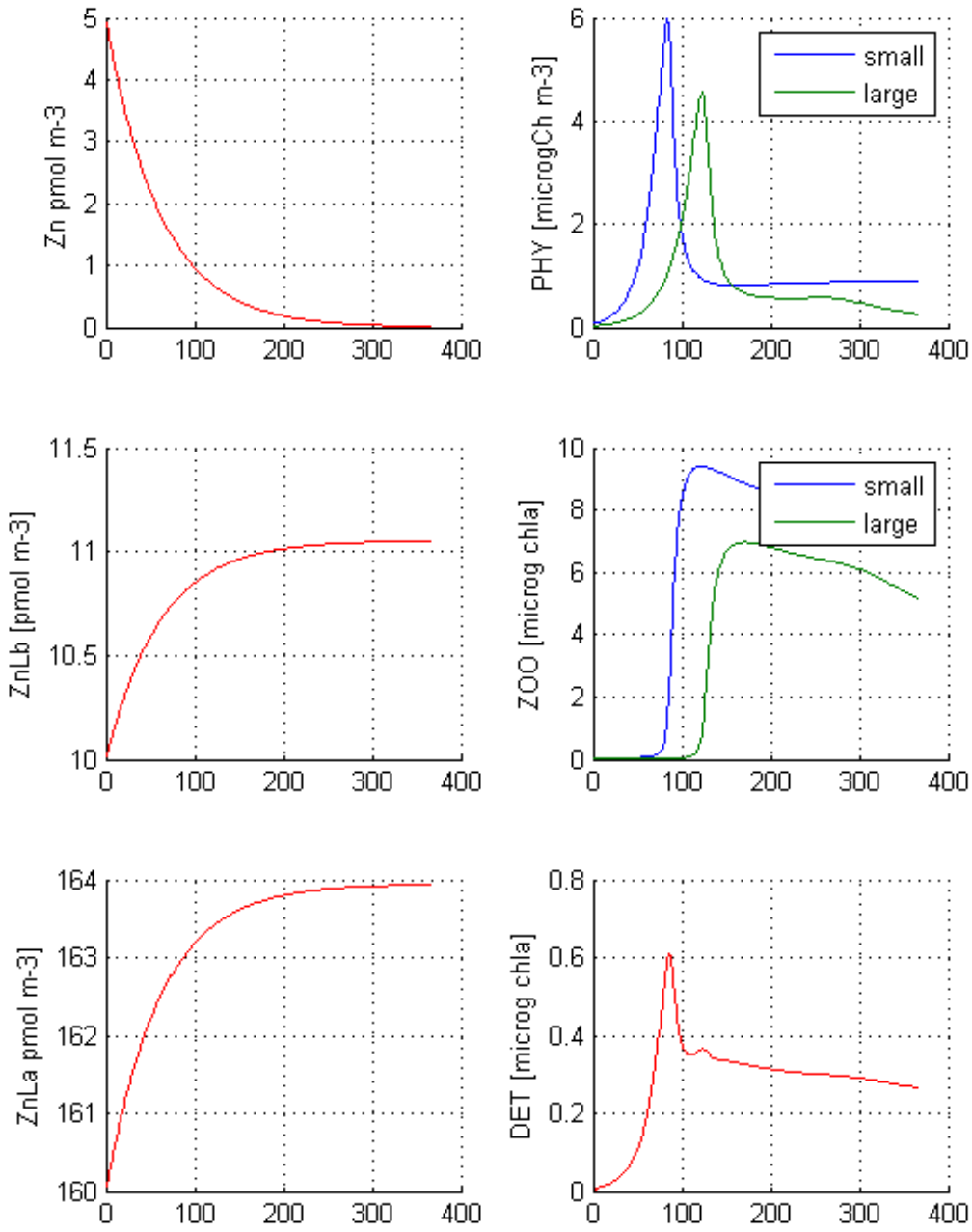

Fig. 4A: Examples of the influence of changing Ks for both species. Values of Ks = 0.01, K1l = 0.1 and K2l = 0.5 were attributed. Initial conditions of Zn used were PINTS concentrations (Zn = 5 pmol L^{-1}; ZnLa = 160 pmol L^{-1}; ZnLb = 10 pmol L^{-1}) and light was constant (sra = 300 W m^{-2}).

5.3.2.2 Scenario B: Non limited P1 and limited P2:

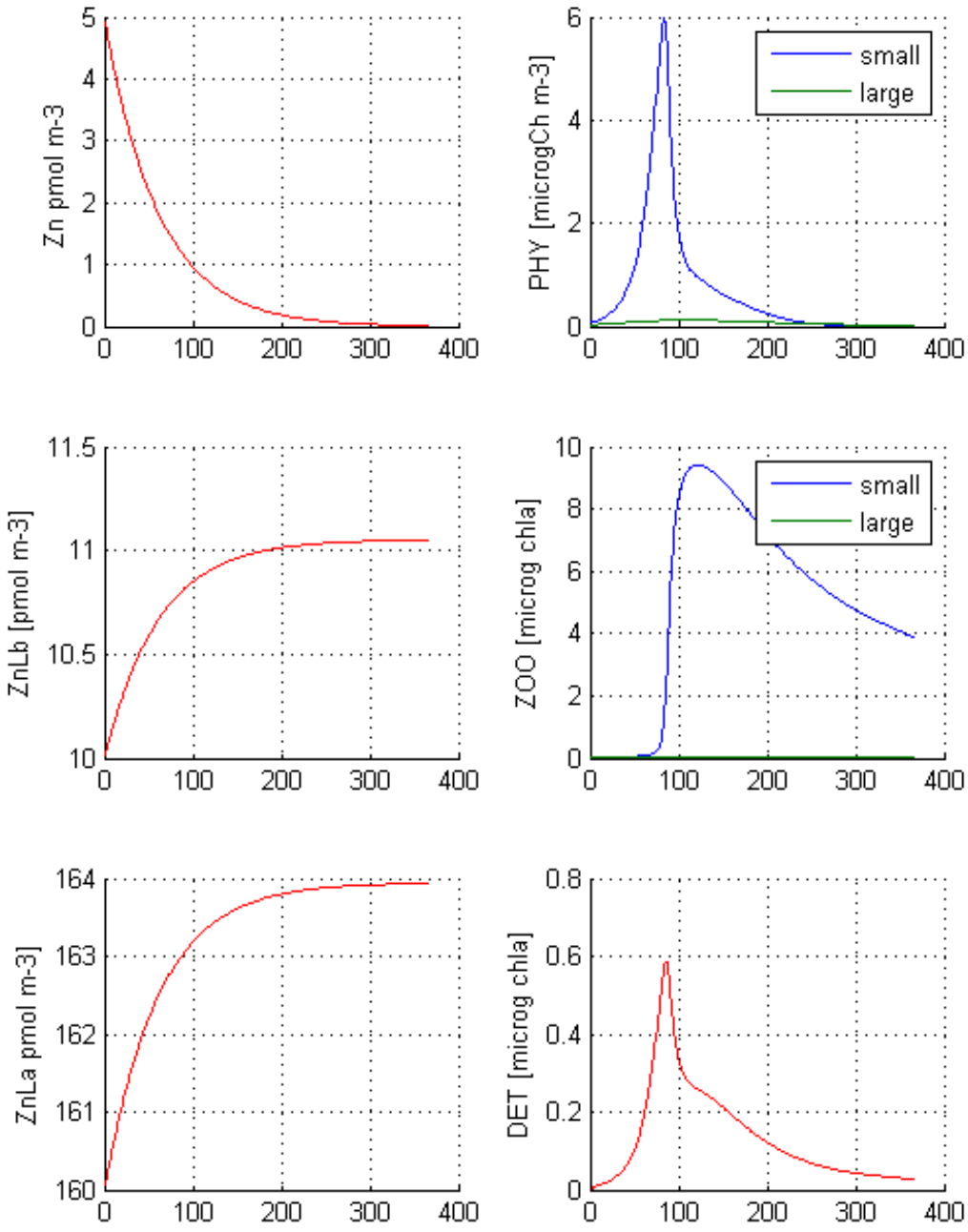

Fig. 4B: Examples of the influence of changing the Ks for both species. Values of Ks = 1, K1l = 10 and K2l = 10. Initial conditions of Zn used were PINTS concentrations (Zn = 5 pmol L^{-1}; ZnLa = 160 pmol L^{-1}; ZnLb = 10 pmol L^{-1}) and light was constant (sra = 300 W m^{-2}).

In this scenario (Fig. 4 B), only the simulated Ph1 was able to grow and increase its biomass (6 µg Chl *a* m^{-3}) while the simulated Ph2 was not able to grow and develop. As a consequence, the simulation of Z1 followed the increase of P1 (8 µg Chl *a* m^{-3}). The simulation implies that in this scenario, only P2 was limited. The system did not reach equilibrium after the full extent of the simulation (365 days).

5.3.2.3 Scenario C: Two limited phytoplankton groups:

In this scenario (Fig. 4 C), none of the phytoplankton was able to grow properly. The slight increase simulated for Ph2 (0.05 µg Chl *a* m^{-3}) is more likely to reflect numerical noise in the model. In this case, none of the zooplankton was able to grow. The range of values in the detritus was very low and revealed the limitation of the model and its working with small concentrations. The simulation implies that in this scenario, only Ph2 was limited.

5.3.2.4 Scenario D: Two near limited phytoplankton groups:

In this scenario (Fig. 4 D), both simulated phytoplankton increase in biomass (Ph1: 0.3 µg Chl *a* m^{-3} and Ph2: 0.1 µg Chl *a* m^{-3}). The simulated biomass of Ph1 was just high enough to induce a reaction by Z1, but it was not the case for Z2. However, we cannot resolve whether it is numerical noise or a simulated response, because the values obtained are really low. The detritus simulated well the transfer of Ph biomasses (0.03 µg Chl *a* m^{-3}) and recycling of Zn, compensated by the sinking of particles. This could explain the low values also obtained in this case.

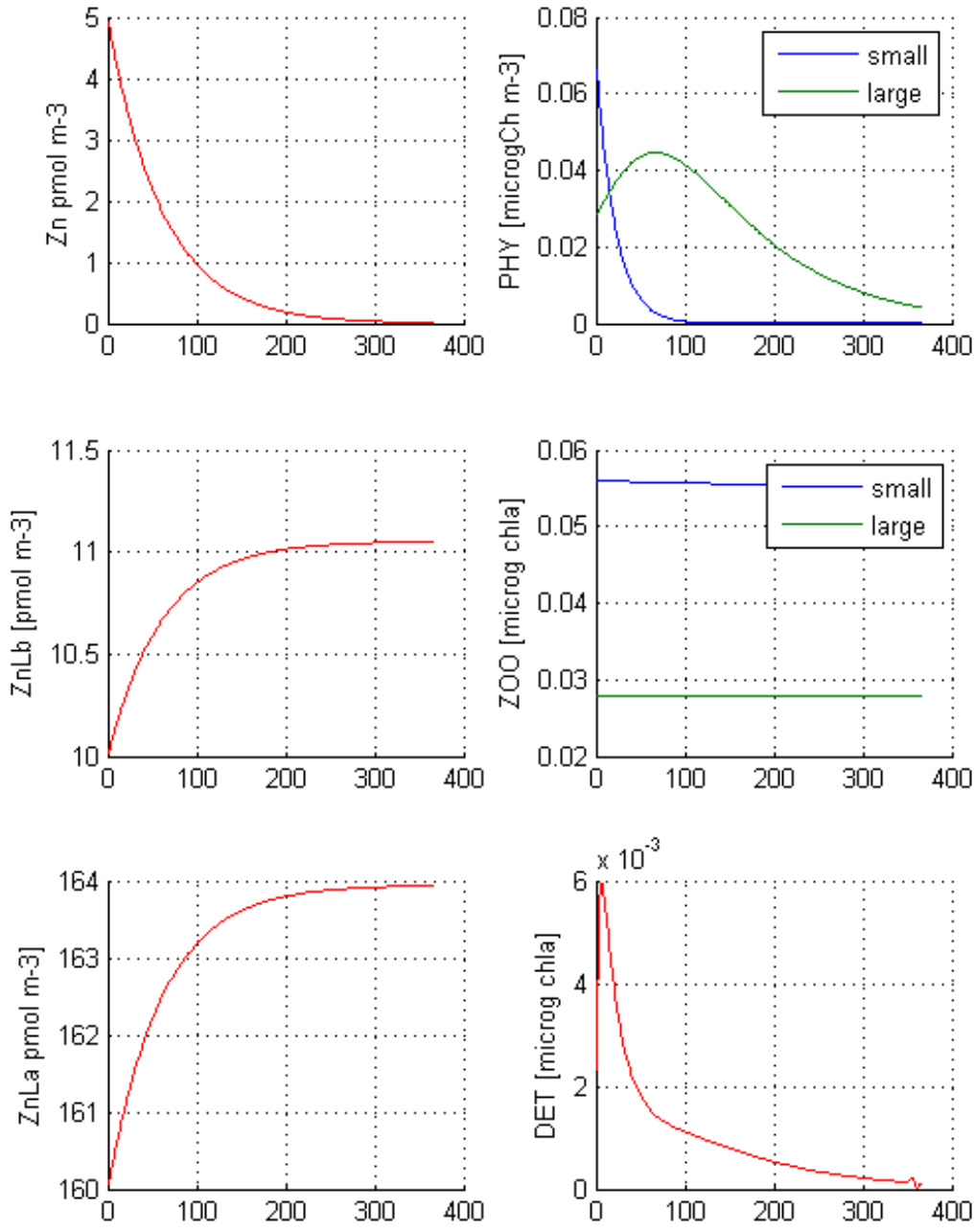

Fig. 4C: Examples of the influence of changing the Ks for both species. Values of Ks = 350, K1l = 20 and K2l = 20. Initial conditions of Zn used were PINTS concentrations (Zn = 5 pmol L^{-1}; ZnLa = 160 pmol L^{-1}; ZnLb = 10 pmol L^{-1}) and light was constant (sra = 300 W m^{-2}).

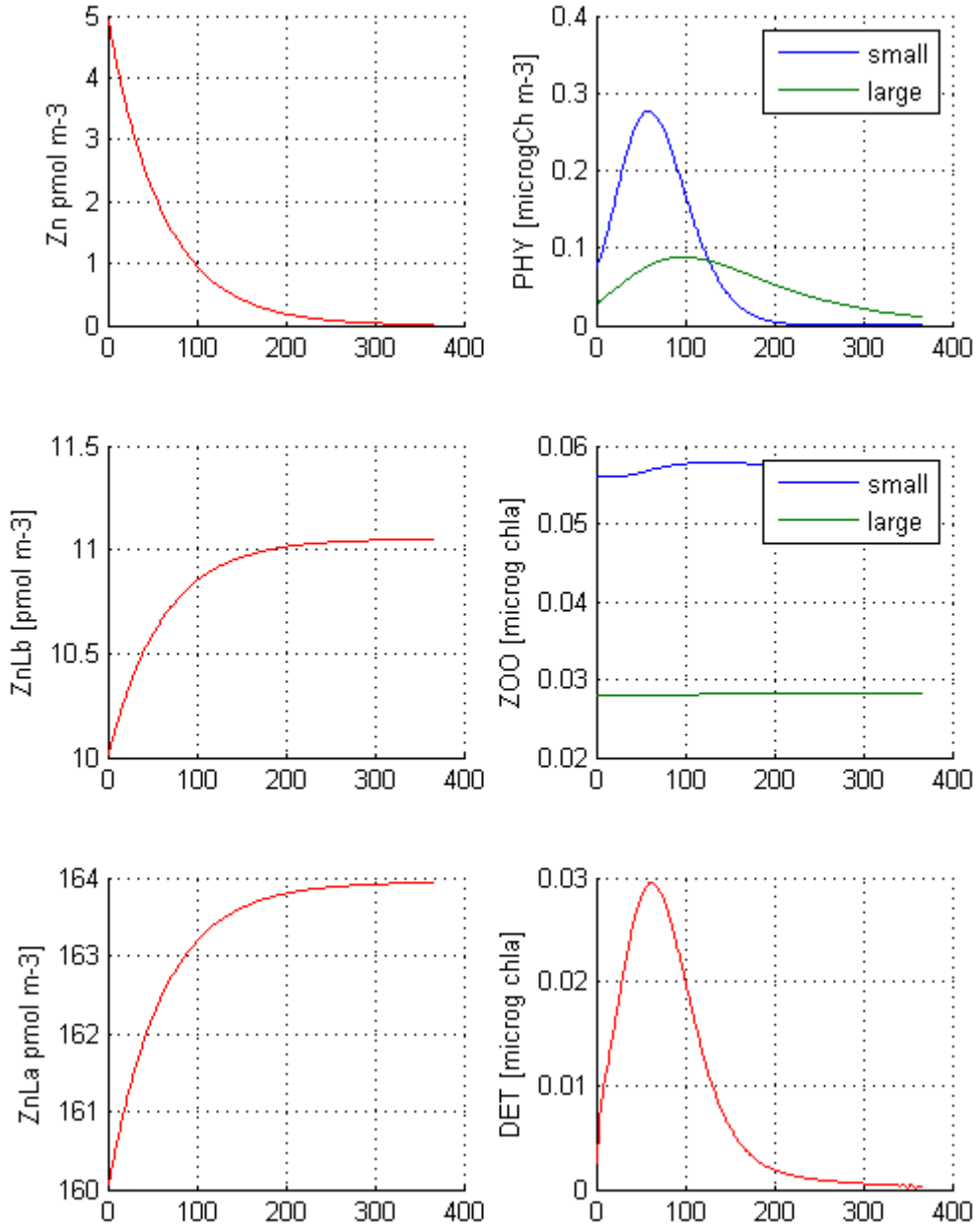

Fig. 4D: Examples of the influence of changing the Ks for both species. Values of Ks = 8, K1l = 12 and K2l = 12. Initial conditions of Zn used were PINTS concentrations (Zn = 5 pmol L^{-1}; ZnLa = 160 pmol L^{-1}; ZnLb = 10 pmol L^{-1}) and light was constant (sra = 300 W m^{-2}).

5.3.3: Sensitivity analyses on Zn chemistry:

The second test included changes in the uptake kinetics occurring between the different pools of Zn. The sensitivity analyses on these parameters were to

obtain a fine balance between decreasing the exchange between Zn chemistry and response of the biology. No similar work on iron cycling could be found for Zn complexation rate. The tested values for the rate of dissociation and formation of Zn complexes were adapted and taken from previous work on iron speciation (Witter and Luther III 1998, Witter *et al.* 2000, Tagliabue 2006, Fan and Dunn 2011) and a Zn complexation study (Bruland 1989). The model is forced by Zn so it was expected that the chemistry of Zn complexes would drive the phytoplankton and zooplankton biomass (Fig. 5 A, B, C and D). Moreover, the calculated values for log K_{ZnLa} and log K_{ZnLb} were to be in the range of the ones obtained in Chapter IV (9.4 – 10.8). For each run, both stability constant were calculated according to Witter *et al.* (2000).

5.3.3.1 Scenario A: Slow kinetics for both complexes, values of log K close to the measured ones:

In this case, log K_{ZnLb} = 7.11 and log K_{ZnLa} = 7.32. In this scenario (Fig. 5A), the simulated exchange between Zn and ZnLb was low enough to affect the biomass of both phytoplankton groups. A balance between kinetic exchanges, uptake and phytoplankton growth was balance enough to allow the simulation of two phytoplankton blooms after 125 and 200 days of simulation for Ph1 and Ph2, respectively. Ph1 reached a value of 1.5 µg Chl *a* m^{-3} while Ph2 reached a value of 0.4 µg Chl *a* m^{-3}. The simulated Ph1 biomass was high enough to induce the zooplankton increase of biomass (Z1: 0.25 µg Chl *a* m^{-3}), but not Ph2. Detritus (0.15 µg Chl *a* m^{-3}) simulated the transfer of loss fluxes from the phytoplankton and zooplankton biomasses.

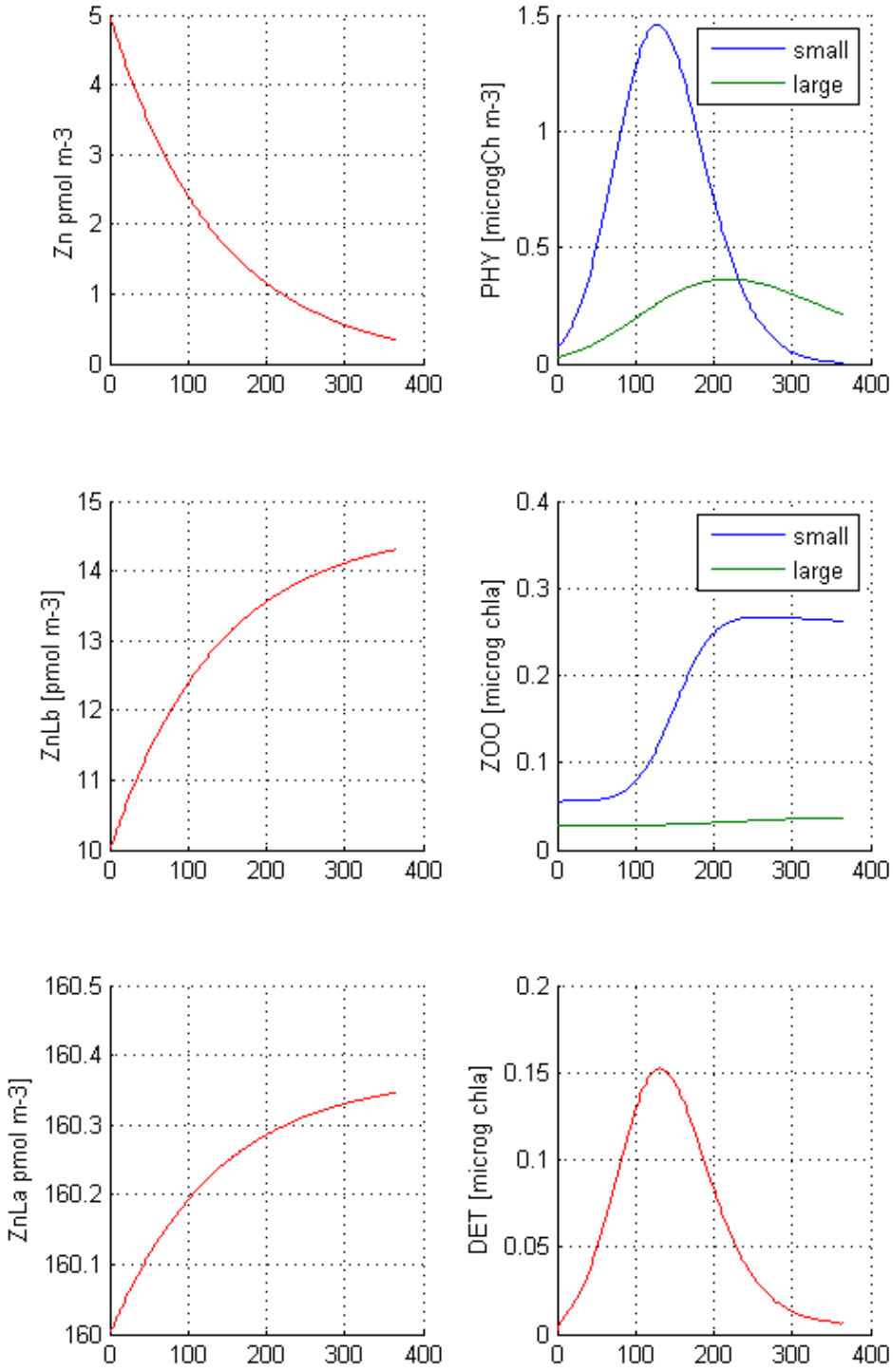

Fig. 5A: Examples of the influence of changing the kinetics exchange of Zn chemistry. Values of k_{fZnLb} = 1.96 x 10^{-10} pmol $L^{-1}s^{-1}$, k_{dZnLb} = 1.50 x 10^{-17} s^{-1} and k_{fZnLa} = 4.2 x 10^{-12} pmol $L^{-1}s^{-1}$, k_{dZnLa} = 2.0 x 10^{-19} s^{-1}. Initial conditions of Zn used were PINTS concentrations (Zn = 5 pmol L^{-1}; ZnLa = 160 pmol L^{-1}; ZnLb = 10 pmol L^{-1}) and light was constant (sra = 300 W m^{-2}).

5.3.3.2 Scenario B: Slower kinetics for labile complexes, same for non-labile, values of log K close to the one measured:

In this case, log K_{ZnLb} = 8.11 and log K_{ZnLa} = 7.32. In this scenario, the simulated exchange between Zn and ZnLb was slower than in the previous one (Fig 5B). The phytoplankton responded after 100 and 200 days of simulation for Ph1 and Ph2, respectively. The simulated biomasses were also more substantial with Ph1 reaching a value of 5 µg Chl *a* m^{-3} and P2, a value of 3 µg Chl *a* m^{-3}. Both simulated phytoplankton allowed a response of the two zooplankton groups (Z1: 8 µg Chl *a* m^{-3} and Z2: 4.5 µg Chl *a* m^{-3}). Detritus (0.5 µg Chl *a* m^{-3}) simulated the transfer of loss fluxes from the phytoplankton and zooplankton biomasses with a delay corresponding to both simulated blooms.

5.3.3.3 Scenario C: Rapid kinetics for labile and non labile complexes:

In this case, log K_{ZnLb} = 1 and log K_{ZnLa} = 1, which cannot correspond to a real situation in our case. In this scenario, the simulated exchange between Zn and ZnLb was a lot quicker than in two previous ones. All exchanges between the different Zn pools were simulated to happen in the first 50 days of the run. This impacted on the response of both phytoplankton. Their growth was not simulated properly as the values obtained here were low (Ph1: 0.08 µg Chl *a* m^{-3} and Ph2: 0.035 µg Chl *a* m^{-3}). The simulated rapid increases of biomasses followed by the large decrease were more likely to reflect numerical noise of the model. This was confirmed by the instability observed in the detritus after 200 days.

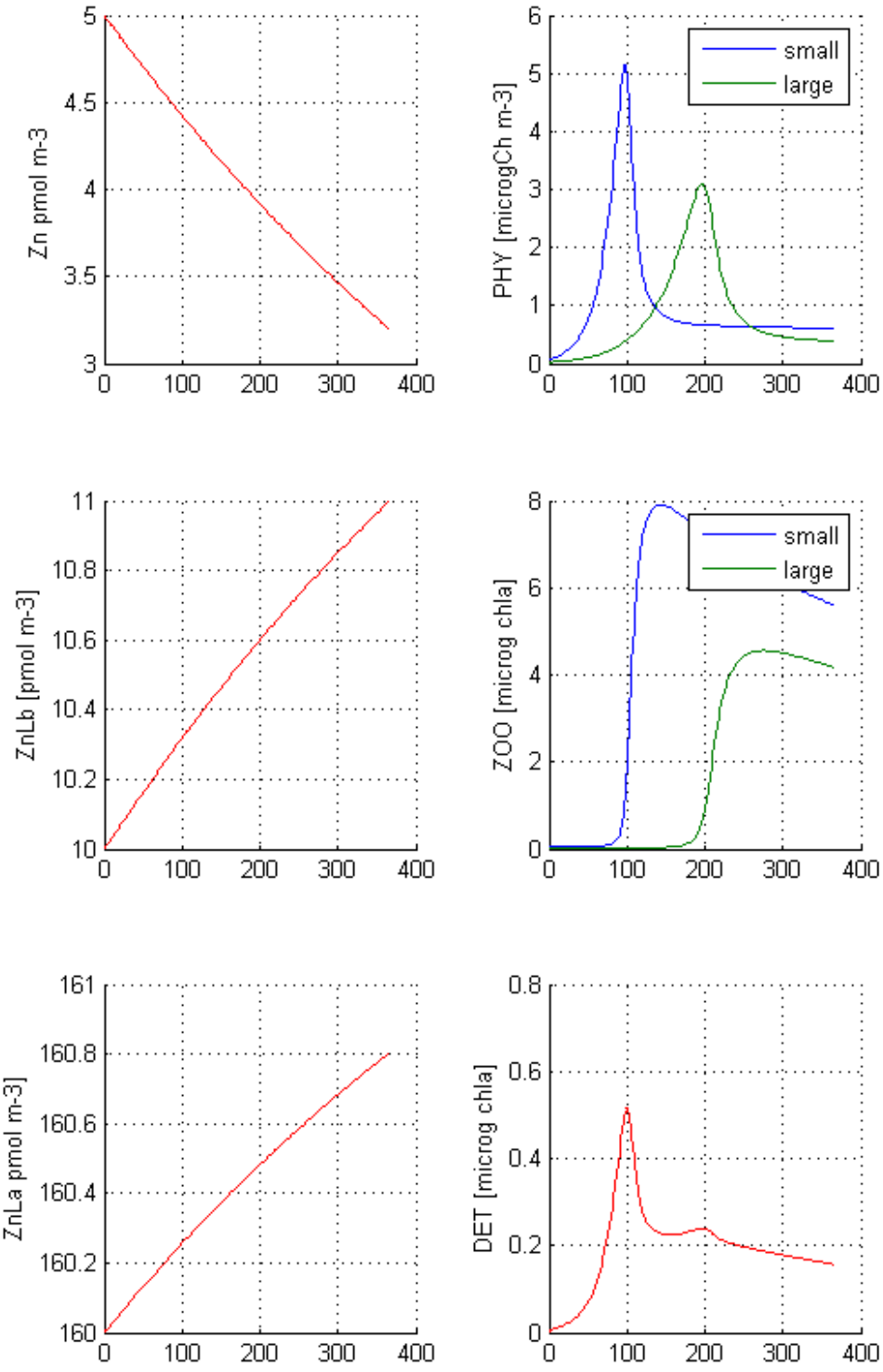

Fig. 5B: Examples of the influence of changing the kinetics exchange of Zn chemistry. Values of k_{fZnLb} = 1.96 x 10^{-11} pmol $L^{-1}s^{-1}$, k_{dZnLb} = 1.50 x 10^{-19} s^{-1} and k_{fZnLa} = 4.2 x 10^{-12} pmol $L^{-1}s^{-1}$, k_{dZnLa} = 2.0 x 10^{-19} s^{-1}. Initial conditions of Zn used were PINTS concentrations (Zn = 5 pmol L^{-1}; ZnLa = 160 pmol L^{-1}; ZnLb = 10 pmol L^{-1}) and light was constant (sra = 300 W m^{-2}).

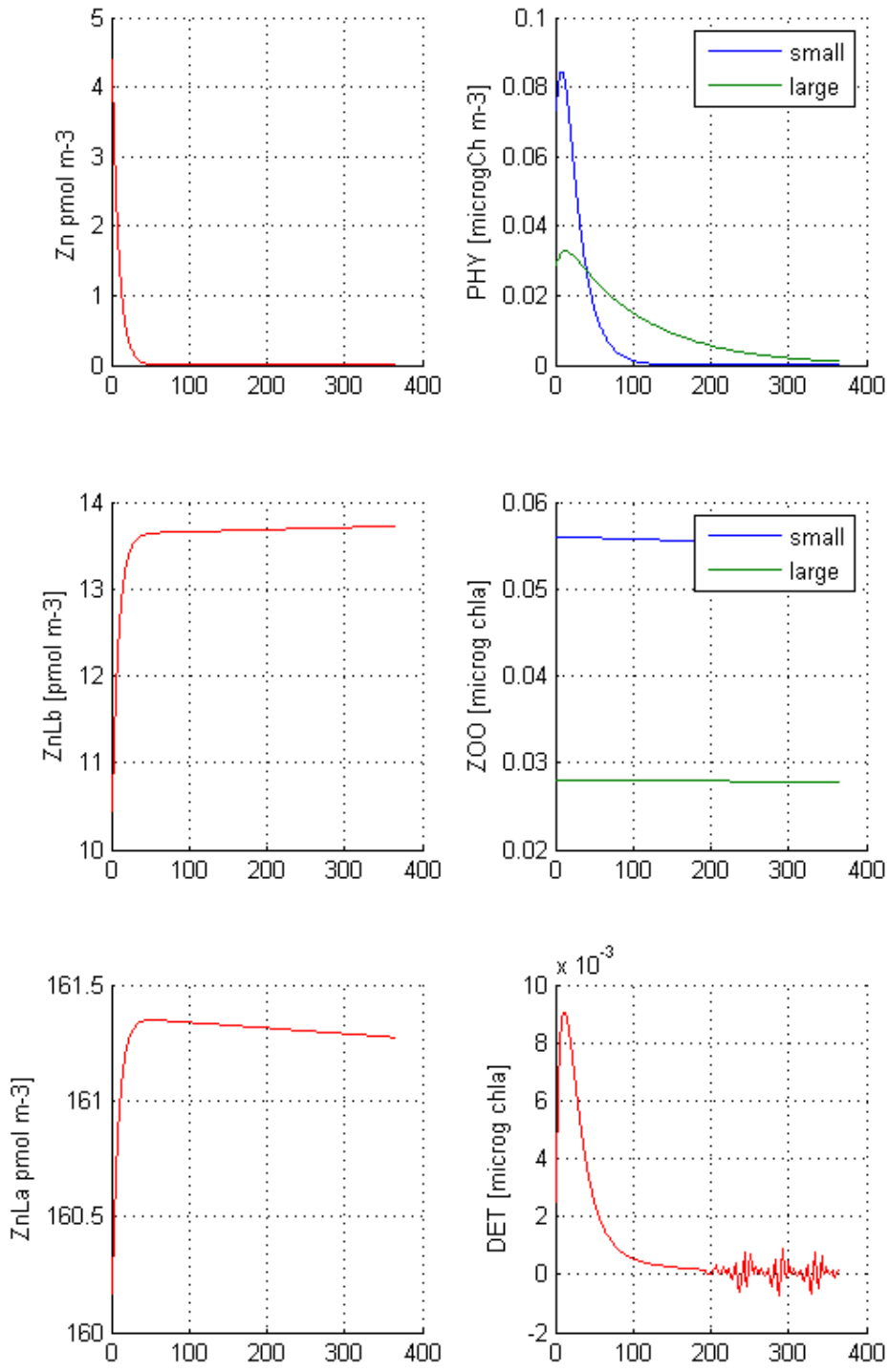

Fig. 5C: Examples of the influence of changing the kinetics exchange of Zn chemistry. Values of k_{fZnLb} = 2.5 x 10^{-10} pmol $L^{-1}s^{-1}$, k_{dZnLb} = 2.50 x 10^{-11} s^{-1} and k_{fZnLa} = 2.5 x 10^{-10} pmol $L^{-1}s^{-1}$, k_{dZnLa} = 2.5 x 10^{-11} s^{-1}. Initial conditions of Zn used were PINTS concentrations (Zn = 5 pmol L^{-1}; ZnLa = 160 pmol L^{-1}; ZnLb = 10 pmol L^{-1}) and light was constant (sra = 300 W m^{-2}).

5.3.3.4 Scenario D: Rapid kinetics, slower than the previous ones:

In this case, log K_{ZnLb} = 2 and log K_{ZnLa} = 2, which is also not in the range of reality. In this scenario, the simulated exchange between Zn and ZnLb was slower than the previous test, but quicker than the first two. All exchanges between the different Zn pools were simulated to happen in 200 days of the run. This simulation lead to an increase of Ph1 biomass (0.3 µg Chl *a* m^{-3}) after 75 days followed by a Ph2 increase after 100 days (0.1 µg Chl *a* m^{-3}). The simulated biomasses were not important enough for the zooplankton to respond.

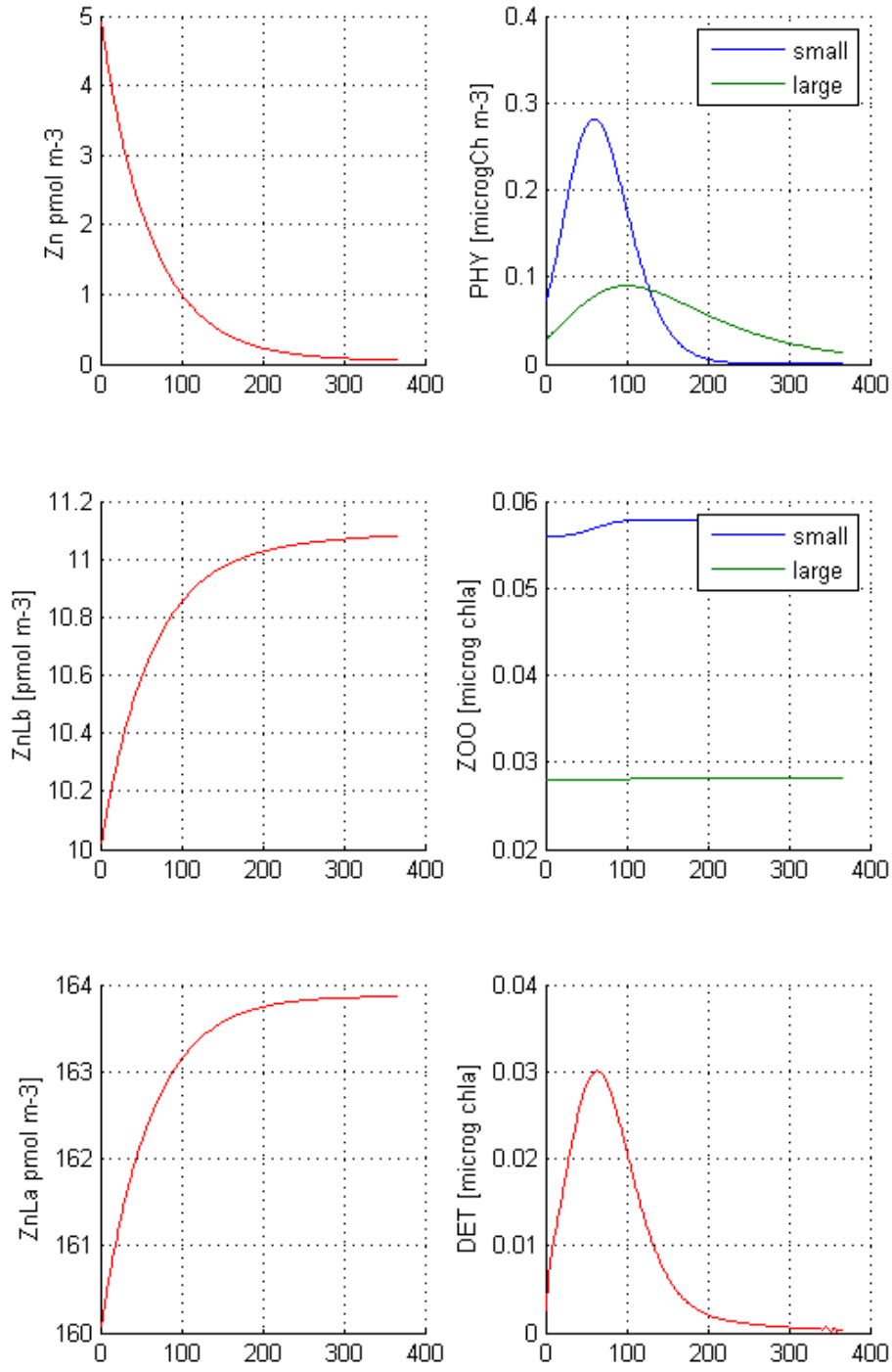

Fig. 5D: Examples of the influence of changing the kinetics exchange of Zn chemistry. Values of k_{fZnLb} = 1.0 x 10^{-10} pmol $L^{-1}s^{-1}$, k_{dZnLb} =1.0 x 10^{-12} s^{-1} and k_{fZnLa} = 1.0 x 10^{-10} pmol $L^{-1}s^{-1}$, k_{dZnLb} = 1.0 x 10^{-12} s^{-1}. Initial conditions of Zn used were PINTS concentrations (Zn = 5 pmol L^{-1}; ZnLa = 160 pmol L^{-1}; ZnLb = 10 pmol L^{-1}) and light was constant (sra = 300 W m^{-2}).

5.3.4: Sensitivity analyses on ligand concentrations:

The last set of scenarios simulation was used to explore the model sensitivity to a change in ligand concentrations. The idea behind such a test is the potential production of ligands by phytoplankton and the presence of more or less organic matter and particles. Those assumptions are likely to depend on the community and the region considered. In all these runs, the total dissolved Zn concentration at the start does not change.

5.3.4.1 Scenario A: Lower strong ligands than P3, constant weak ligands :

In this case, the initial concentrations are close to the ones observed in our reference station. However, the concentration of non-labile ligands decreased, meaning the simulated kinetics of exchange were affected and decreased with time, too (Fig 6A). Our modelled community of Ph1 increases its biomass during the simulated bloom (0.45 µg Chl *a* m^{-3}), followed by Ph2 (0.15 µg Chl *a* m^{-3}). The simulated response of zooplankton was a bit higher than the last test. The transfer of biomass into the detritus compartment was modelled and visible in spite of the low values of µg Chl *a* m^{-3} obtained.

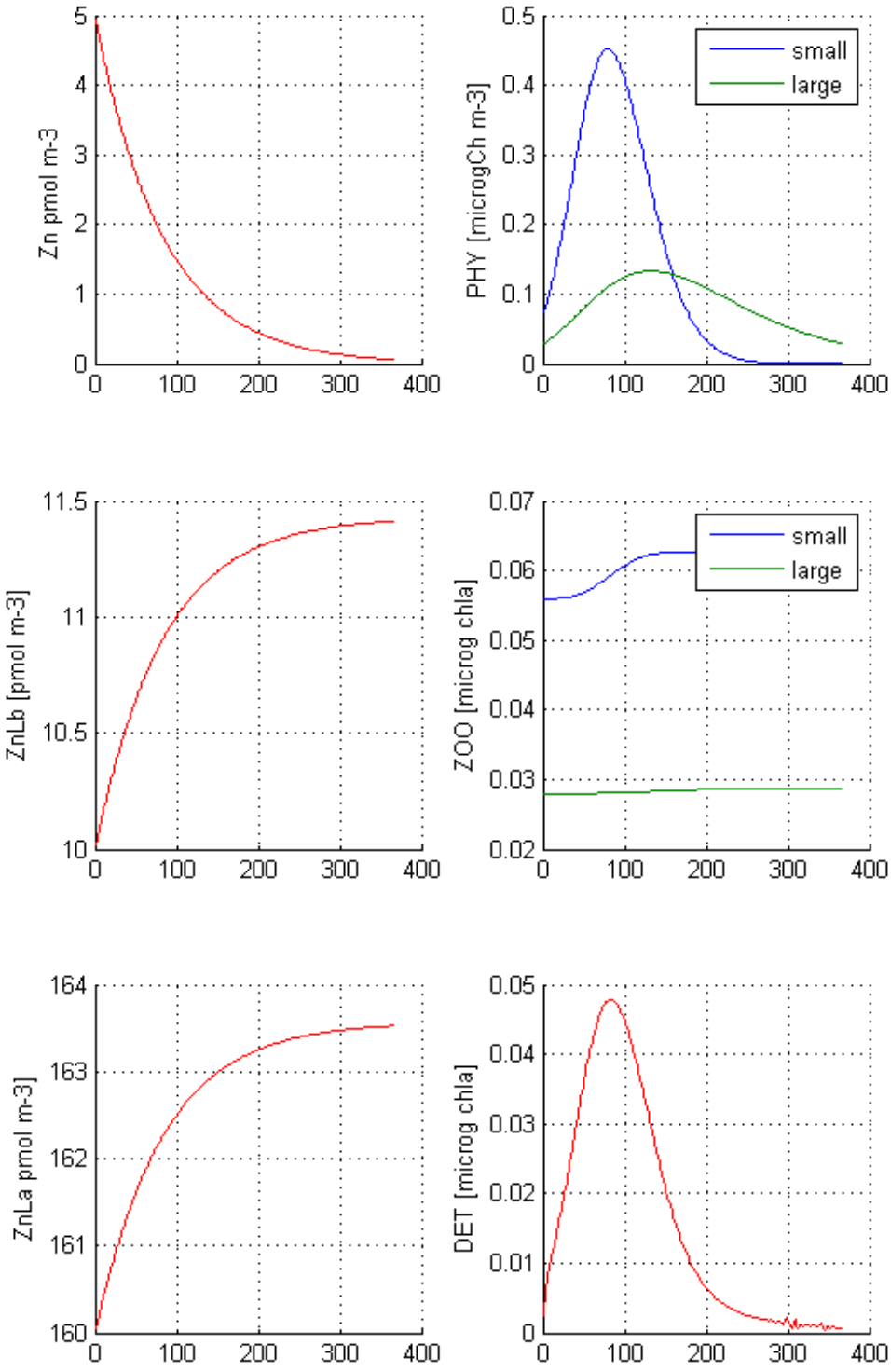

Fig. 6A: Examples of the influence of changing ligand concentrations. Values of La = 1000 pmol m^{-3} and Lb = 400 pmol m^{-3}. Initial conditions of Zn used were PINTS concentrations (Zn = 5 pmol L^{-1}; ZnLa = 160 pmol L^{-1}; ZnLb = 10 pmol L^{-1}) and light was constant (sra = 300 W m^{-2}).

5.3.4.2 Scenario B: Lower strong ligands than P3, higher weak ligands

In this case, the simulation started with fewer non-labile ligands but more labile ligands. The simulated kinetics of exchange were increased, and resulted in lower quantities of Zn between the different pools, because the complexes were more important (Fig 6B). The modelled community of Ph1 decreased its biomass during the simulated bloom (0.2 µg Chl *a* m^{-3}) but was at its maximum, still faster than in the previous test. The Ph2 community responded in the same way, with a smaller biomass (0.07 µg Chl *a* m^{-3}). In this case, the simulated response of zooplankton could be considered as nil and most of the biomass is transferred into the detrital compartment. The low values obtained are consistent with the low biomass conditions circulating in this model.

5.3.4.3 Scenario C: Lower weak ligands than P3, higher weak ones:

In this case, the simulation was similar to the previous one but concentrations of both ligands were lowered. As a result, the simulated kinetics of exchange were decreased. However, the simulated concentrations of complexed species were slightly higher, increasing the response of the biomass (Fig 6C). This simulation and the previous one gave, as expected, similar results for biomass.

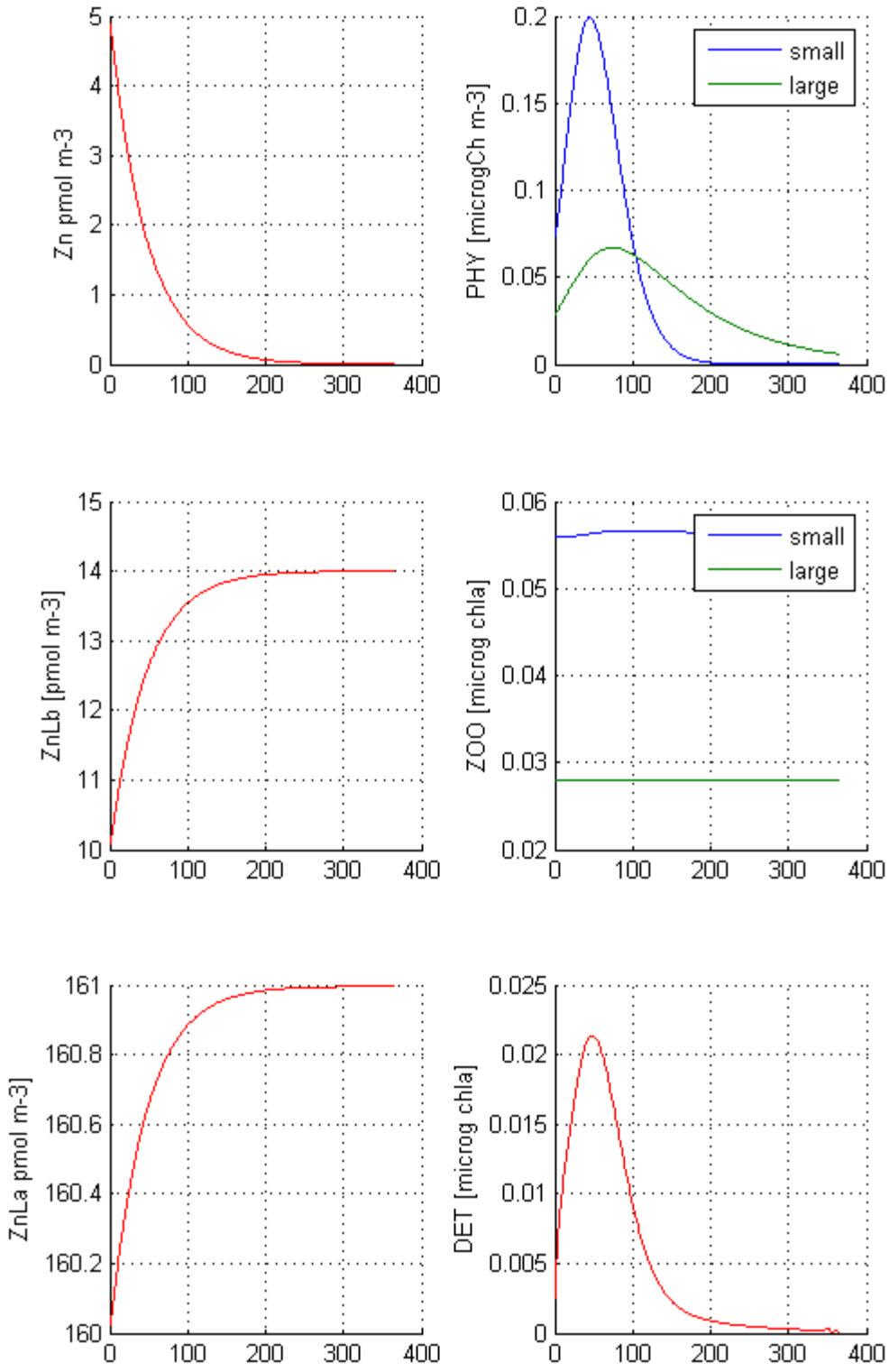

Fig. 6B: Examples of the influence of a change in the ligand concentrations. Values of La = 500 pmol m^{-3} and Lb = 2000 pmol m^{-3}. Initial conditions of Zn used were PINTS concentrations (Zn = 5 pmol L^{-1}; ZnLa = 160 pmol L^{-1}; ZnLb = 10 pmol L^{-1}) and light was constant (sra = 300 W m^{-2}).

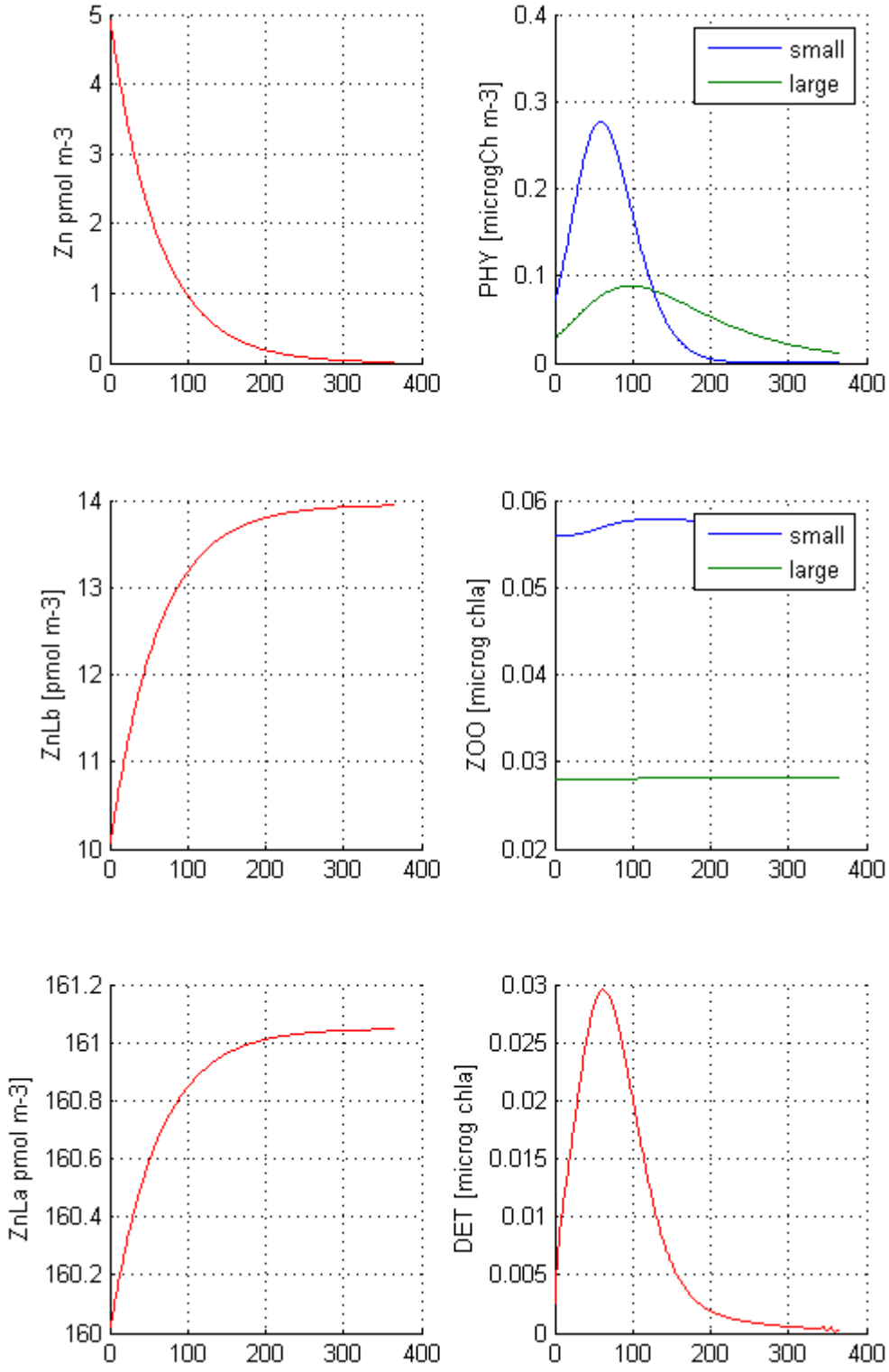

Fig. 6C: Examples of the influence of a change in the ligand concentrations. Values of La = 400 pmol m^{-3} and Lb = 1500 pmol m^{-3}. Initial conditions of Zn used were PINTS concentrations (Zn = 5 pmol L^{-1}; ZnLa = 160 pmol L^{-1}; ZnLb = 10 pmol L^{-1}) and light was constant (sra = 300 W m^{-2}).

5.3.4.4 Scenario D: Doubling of the P3 concentrations:

In this case, the initial concentrations were doubled in comparison to our reference simulation. As expected, kinetics of exchange were faster but as the concentrations of ligands were higher also, the model simulated a smaller growth in phytoplankton (Ph1: 0.15 µg Chl *a* m^{-3} and Ph2: 0.05 µg Chl *a* m^{-3}). The simulated response of zooplankton was considered as nonexistent. For all biomasses, low values were obtained as fluxes of biomass in this test were low.

5.3.5: Other parameters:

The observed response of the zooplankton was small or nonexistent in most cases, in spite of the adaptation of the parameters to decreased mortality and increased grazing. The phytoplankton biomass simulated in most cases does not reach 1 µg Chl *a* m^{-3}, which is a small production and can explain the non-response of the zooplankton. But if the phytoplankton biomass was high enough (> 0.5 µg Chl *a* m^{-3}), the zooplankton could follow slightly and if the phytoplankton was above a biomass of 1 µg Chl *a* m^{-3} (Fig. 5 A and B), the zooplankton were more likely to grow properly.

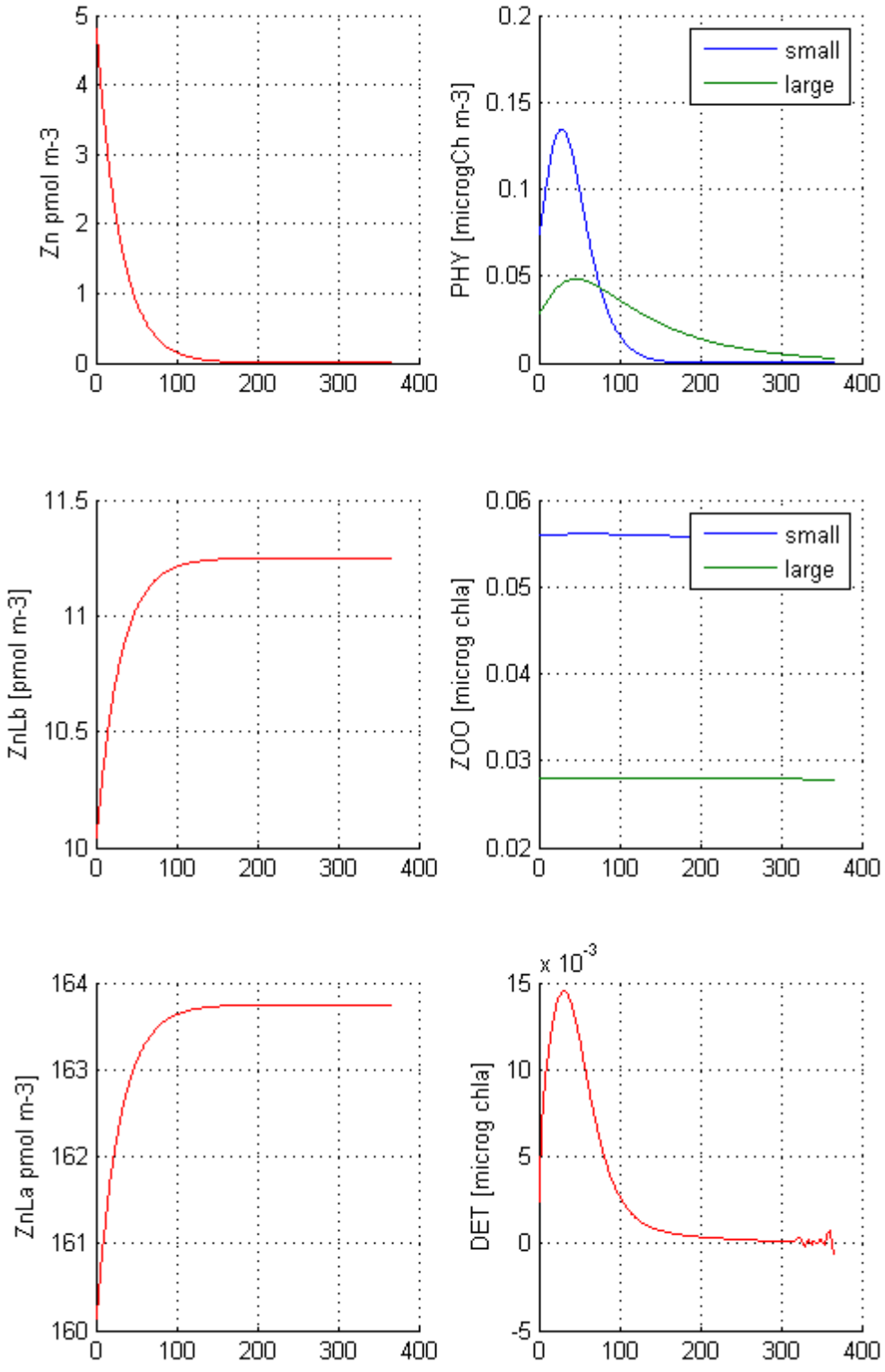

Fig. 6D: Examples of the influence of a change in the ligand concentrations. Values of La = 3000 pmol m^{-3} and Lb = 1000 pmol m^{-3}. Initial conditions of Zn used were PINTS concentrations (Zn = 5 pmol L^{-1}; ZnLa = 160 pmol L^{-1}; ZnLb = 10 pmol L^{-1}) and light was constant (sra = 300 W m^{-2}).

5.4: Discussions and consequences for further model development:

The model used here and the conclusions obtained thanks to the different analyses are to be interpreted carefully as several assumptions lie behind the use of such a simple model. Of course, this work focused only one station of the cruise to settle the parameters and check the validity of their existence. However, this work establishes the different parameters and conditions of speciation and zinc species concentrations for Zn to possess an impact on phytoplankton community.

The high effect of a change of Ks on the model results was expected as this parameter defines the importance with which a nutrient is taken up and the limitation terms depend on it. Both phytoplankton and zooplankton biomass were most affected by the change in the half-saturation constant. Our species were not limited in the biological studies (Chapter III, p. 97), thus, half-saturation constants were chosen to not limit the phytoplankton. The values of Ks = 8 pmol Zn m^{-3} and K1l = K2l = 12 pmol Zn m^{-3} were chosen to match the biomass observed at P3. Moreover, they were reflecting the non-limitation of the phytoplankton species, but a non-optimal growth in the case of low Zn concentrations.

The sensitivity of the model to changes of rates of formation and dissociation of complexes was also expected as the model was forced by Zn speciation. As a result, Zn, ZnLb and ZnLa were more or less available for the phytoplankton and the biomass responded strongly to these changes of chemistry and changes of kinetics. The quicker the release, the smaller the phytoplankton's response was. However, when exchanges were slow, phytoplankton groups were able to develop properly. The most relevant values were a formation rate of 1.0 x 10^{-10} (pmol Zn m^{-3})$^{-1}$ s^{-1} and a dissociation rate of 1.0 x 10^{-12} (pmol Zn m^{-3})$^{-1}$ s^{-1} for labile complexes. The non-labile complexes

were forming and dissolving at the same rate in this model. However, when different log K values were calculated according to Witter *et al.* (2000), using the formation and dissociation rates of complexes, we obtained smaller values than the ones previously measured with voltammetry (Chapter IV, p. 134). The values tested that were in the range of the log K measured (9.3) allowed us to obtain a simulated increase of biomass that was more important than for our reference station.

The last sensitivity test simulated the impact of ligand concentrations on the structure of the community. The values of ligand concentrations were known from analytical measurements done for P3 (Chapter IV), hence, model parameters and concentration could not deviate much from them. This gave similar simulations but the importance of working with close simulations was also to detect any threshold or range of concentrations that could have modelled a different response of the community. This difference was not only in terms of biomass but also in term of structure and species dominance. However, in this study for the reference station conditions, no obvious change of community was simulated. The assumption behind these simulations is that none of the species were limited by Zn, according to our biological results. In this case, none of the phytoplankton groups will take over the other one.

During these analyses, the conditions determined at the end of the different simulations are interesting to discuss. According to the values chosen in the sensitivity analyses, the model arrived at complete death of organisms due to the low nutrient concentrations, low biomass, loss through sinking and no inputs. However, when the biomass is high enough, the model did arrive at a steady state, with final conditions that were different from the initial ones. This meant the solution of the model would be different if it had to run again for a same period of

time. This underlines the fact that this model was not forced by external factors, such as temperature or external inputs of Zn and represented an instantaneous picture of the reaction of a community. To match the real data from P3 station, we had to consider low concentrations of biomass and low concentrations of Zn. In this regard, the model was not stable in some simulations. The study of the fluxes between the different compartments revealed high values of fluxes for Zn remineralisation (data not shown) and the two zooplankton mortality rates in comparison to growth of the phytoplankton. This can promote the instability of the model in addition to missing information.

The approach undertaken here was simple, limiting the model to the influence of Zn speciation on two phytoplankton groups and simulating their behaviour during a specified timeframe and non-disrupted ecosystem. Other parameters and variables need to be taken into account for future work and integration of Zn in biogeochemical models. The Zn limitation term for the large phytoplankton has been separated into two limitation terms. Further work will take uptake preferences into account as per Mongin *et al.* (2006) or Aumont *et al.* (2008) and integrate this preference into the limitation term. The next step would also be to possibly consider variable trace metal quotas, with recent biological data (Twining *et al.* 2011), to represent the regulation of phytoplankton intracellular composition. This work has been introduced in biogeochemical models, such as SWAMCO-4 (Pasquer *et al.* 2005). Two zooplanktons were added to balance the model and as in a natural marine system, our model showed that zooplankton biomass depended a lot on the phytoplankton biomass. The subject of this work was the influence of Zn on the community so the zooplankton compartment has not been considered properly and interpretation of these results have to be done carefully. The lack of qualitative parameters about the natural

behaviour of the zooplankton, especially grazing rate and efficiency of catching a prey, implies that this work still needs further study. Further work and case studies are to be taken into account for the integration of Zn in biogeochemical models. However, we can consider introducing a Zn speciation effect in existing models to introduce its impact on the community in selected regions as it will be discussed in the main discussion of this PhD (next chapter).

5.5 References:

Arrigo, K.R., Worthen, D. L., and Robinson, D. H. (2003). A coupled ocean-ecosytem model of the Ross sea: Iron regulation of phytoplankton taxonomic variability and primary production. *Journal of geophysical research*, **108**, doi: 10.1029/2001JC000856.

Aumont O., Bopp, L.**,** and Schultz, M. (2008) What does temporal variability in aeolian dust deposition contribute to sea-surface iron and chlorophyll distributions?, *Geophys. Res. Lett*, **35**, L07607, doi:10.1029/2007GL031131.

Bopp L., Belviso S., Aumont O., and Blain S. (2008) Modeling the effect of iron fertilisation on dimethylsulfide emissions in the Southern Ocean, *Deep Sea Research II*, **55**, 901-912.

Bruland, K. W. (1989). Complexation of Zinc by Natural Organic Ligands in the Central North Pacific. *Limnology and Oceanography,* **34,** 269-285.

Campbell, P. G. C. (1995). Metal speciation and bioavailability in aquatic systems : Edited by André Tessier and David R. Turner. IUPAC Series on Analytical and Physical Chemistry, John Wiley & Sons. 3**,** 1, 679.

Campbell, P. G. C., Errecalde, O., Fortin, C., Hiriart-Baer, V. P., and Vigneault, B. (2002). Metal bioavailability to phytoplankton--applicability of the biotic ligand model. *Comparative Biochemistry and Physiology Part C: Toxicology & Pharmacology*, **133,** 189-206.

Donat, J. R., and Bruland, K. W. (1990). A comparison of two voltammetric techniques for determining zinc speciation in Northeast Pacific Ocean waters. *Marine Chemistry* **28**, 301-323.

Eppley RW (1972) Temperature and phytoplankton growth in the sea. Fish Bull **70**, 1063–1085.

Evans, G. T., and Parslow, J. S. (1985). A model of annual plankton cycles. *Biological Oceanography* **3**, 327-347.

Fan, S. M., and Dunne J. P. (2011)**.** Models of iron speciation and concentration in the stratified epipelagic ocean. *Geophysical Research Letter* **38,** L15611, doi:10.1029/2011GL048219

Fasham, M. J. R., Ducklow, H. W., and McKelvie, S. M. (1990). A nitrogen-based model of plankton dynamics in the oceanic mixed layer, *Journal of Marine Research,* **48,** 591-639.

Frost, B. (1987). Grazing control of phytoplankton stock in the open subarctic Pacific Ocean: A model assessing the role of mesozooplankton, particularly the large calanoid copepods *Neocalanus* spp., *Marine ecology progress series,* **39**, 49-68.

Gregg, W. W., and Casey, N. W. (2007) Modeling coccolithophores in the global ocean, *Deep sea research II,* **54**, 447-477, doi: 10.1016/j.dsr2.2006.12.007.

Gregg, W. W., Ginoux, P., Schopf, P. S., and Casey, N. W. (2003). Phytoplankton and iron: validation of a global three-dimensional ocean biogeochemical model, *Deep Sea research II,* **50**, 3143-3169, doi: 10.1016/j.dsr2.2003.07.013.

Ho, T. Y., Quigg, A., Finkel, Z. V., Milligan, A. J., Wyman, K., Falkowski, P. G., and Morel, F. M. M. (2003). The Elemental Composition Of Some Marine Phytoplankton. *Journal of Phycology,* **39**, 1145-1159.

Heijerick, D. G., de Schamphelaere, K. A. C., and Janssen, C. R. (2002). Biotic ligand model development predicting Zn toxicity to the alga *Pseudokirchneriella subcapitata*: possibilities and limitations. *Comparative Biochemistry and Physiology Part C: Toxicology & Pharmacology*, **133**, 207-218.

John, S. G., Geis, R. W., Saito, M. A., and Boyle, E. A. (2007). Zinc isotope fractionation during high-affinity and low-affinity zinc transport by the marine diatom *Thalassiosira oceanica*. *Limnology and Oceanography*, **52,** 2710-2714.

Lancelot, C., Hannon E., Becquevort S., Veth C., and De Baar, H.J.W. (2000). Modeling phytoplankton blooms and carbon export production in the Southern Ocean: dominant controls by light and iron in the Atlantic sector in Australia spring 1992, *Deep Sea Research Part I, Oceanographic Research Papers,* **47**, 1621-1662.

Mongin, M. Nelson, D. M., Pondaven, P., and Tréguer, P. (2006). Simulation of upper-ocean biogeochemistry with a flexible-composition phytoplankton model: C, N and Si cycling and Fe limitation in the Southern Ocean, *Deep sea research*, **53**, 601-619, doi: 10.1016/j.dsr2.2006.01.021.

Morel, F. M. M. (1983) In: *Principles of Aquatic Chemistry*, Wiley, New York, 300-309

Oschlies, A., and Schartau, M. (2005). Basin-scale performance of a locally optimized marine ecosystem mode. *Journal of Marine Research* **62**, 335-358.

Pagenkopf, G. (1983), Gill surface interaction model for trace-metal toxicity to fishes: role of complexation, pH, and water hardness, *Environmental Science and technology*, **17**, 342-347.

Pasquer, B., Laruelle, G., Becquevort, S., Schoemann, V., Goosse, H., and Lancelot, C. (2005). Linking ocean biogeochemical cycles and ecosystem structure and function: results of the complex SWAMCO-4 model, *Journal of Sea Research*, 53, 93-108.

Playle, R. C. (1998). Modelling metal interactions at fish gills, *Science of the Total Environment*, **219**, 147-163.

Saito, M. A., and Goepfert, T. J. (2008). Zinc-Cobalt Colimitation of *Phaeocystis Antarctica*. *Limnology and Oceanography*, **53**, 266-275.

Schartau, M., and Oschlies, A. (2003). Simultaneous data-based optimization of a 1D-ecosystem model at three locations in the North Atlantic: Part I-Method and parameter estimates. *Journal of Marine Research*, **61**, 765-793.

Steele, J., and Frost, B. (1977). The structure of plankton communities, *Philosophical transactions of the Royal Society of London. Series B, Biological Sciences*, **280**, 485-534.

Sunda, W. G. (2012). Feedback Interactions between trace metal nutrients and Phytoplankton in the Ocean. *Frontiers in microbiology*, **3**, 204.

Sunda, W. G., and Huntsman, S. A. (1995). Cobalt and Zinc Interreplacement in Marine Phytoplankton: Biological and Geochemical Implications. *Limnology and Oceanography*, **40**, 1404-1417.

Sunda, W. G., and Huntsman, S. A. (1992). Feedback interactions between zinc and phytoplankton in seawater. *Limnology and Oceanography,* **37**, 25-40.

Tagliabue, A., and Arrigo, K. R. (2006). Processes governing the supply of iron to phytoplankton in stratified seas. *Journal of Geophysical Research* 11, C06019

Tagliabue, A., Bopp L., Aumont O., and Arrigo K. R. (2009). Influence of light and temperature on the marine iron cycle: From theoretical to global modelling. *Global Biogeochemical Cycles* **23,** GB2017, doi:10.1029/2008GB003214.

Twining, B. S., Baines, S. B., Bozard, J. B., Vogt, S., Walker, E. A., and Nelson, D. M. (2011) Metal quotas of plankton in the equatorial Pacific Ocean, *Deep-Sea Reasearch II*, **58**, 325-341, doi: 10.1016/j.dsr2.2010.08.018.

Witter, A. E., Hutchins, D. A., Butler, A., and Luther III, G. W. (2000). Determination of conditional stability constants and kinetics constants for strong model Fe-binding ligands in seawater, *Marine Chemistry,* **69**, 1-17.

Witter, A. E., and Luther III, G. W. (1998), Variation in Fe-organic complexation with depth in the Northwestern Atlantic Ocean as determined using a kinetic approach, *Marine Chemistry*, **62**, 241-258.

Zirino, A., and Yamamoto, S. (1972). A pH-Dependent Model for the Chemical Speciation of Copper, Zinc, Cadmium, and Lead in Seawater. *Limnology and Oceanography,* **17,** 661-671.

5.6 Appendix:

Table 1*:* List of parameters used in the conceptual model to describe fluxes between the different compartments considered in the model. sda is the conversion factor for units in seconds and equal to 86400.

a. Chemical Parameters:

Parameters	Name	Value	Units
k_{fZnLb}	Rate of formation for labile complexes	1.0×10^{-10}	$(\text{pmol Zn m}^{-3})^{-1}\ \text{s}^{-1}$
k_{dZnLb}	Rate of dissociation for labile complexes	1.0×10^{-12}	$(\text{pmol Zn m}^{-3})^{-1}\ \text{s}^{-1}$
k_{fZnLa}	Rate of formation for non labile complexes	1.0×10^{-10}	$(\text{pmol Zn m}^{-3})^{-1}\ \text{s}^{-1}$
k_{fZnLa}	Rate of dissociation for non labile complexes	1.0×10^{-12}	$(\text{pmol Zn m}^{-3})^{-1}\ \text{s}^{-1}$
Lb	Concentration of 'weak' ligand	1500	pmol m^{-3}
La	Concentration of 'strong' ligand	400	pmol m^{-3}

b. Phytoplankton parameters:

Parameters	Name	Value	Units
alpha	Initial slope of P-I curve	0.25/sda	$W\ s^{-1}\ m^{-2}$
par	Photosynthetically active radiation	0.43/sda	
kw	Light attenuation due to water	1/0.04/sda	m
kc	Light attenuation due to phyto	1/0.047/529	$m^{-1}\ (pmol\ Zn\ m^{-3})^{-1}$
a_s	Growth rate parameter	0.1/sda	s^{-1}
a_l		0.05/sda	
b	Growth rate parameter	1.066	Dimensionless
c	Growth rate parameter	1.0	$(^oC)^{-1}$
Jmax	Specific light saturated growth	$a \times b^{cT}$	s^{-1}
Ks	Half saturation constant for Zn uptake	8	$pmol\ Zn\ m^{-3}$
K1l		12	
K2l		12	
mup1	Fraction Uptake value for Zn^{2+} for L phyto	0.4	Dimensionless
morp	Specific mortality rate for s and L phyto	0.01/sda	s^{-1}
morpL			
exup	Excretion rate into Zn total pool	0.05/sda	s^{-1}

c. Zooplankton parameters:

Parameters	Name	Value	Units
gam	Assimilation efficiency	0.975	s^{-1}
g_s	Maximum grazing rate	4/sda	s^{-1}
g_l		2/sda	
eps	Prey capture rate	$150*(529^2)/sda$	m^6 pmol Zn^{-2} s^{-1}
morz	Mortality rate	$0.34*529/sda$	m^3 pmol Zn^{-2} s^{-1}
morzL			
exuz	Exudation term to Zn pool	0.00001/sda	s^{-1}

d. Detritus parameters:

Parameters	Name	Value	Units
rem	Remineralisation	0.0005/sda	s^{-1}
exuzn	Exudation rate of Zn non labile to detritus	0.0001/sda	s^{-1}
w_sink	Sinking rate	20/sda	m s^{-1}

CHAPTER SIX

Enlarging the view: Conclusions and perspectives

6.1 Concluding remarks:

The element zinc (Zn) was the focus of this interdisciplinary thesis. The diversity of zinc's roles in phytoplankton growth, and possible oceanic co-limitations, emphasized the need to bring together qualitative and quantitative studies. The research has yielded new data on Zn speciation; insights to phytoplankton response to low Zn concentrations; and a testing of Zn (and its speciation) in a biogeochemical NPZD model as a micronutrient mediating primary production and community composition at the base of the pelagic ecosystem in the Tasman Sea. This work prompts multiple strands for future research and questions to answer about this trace element's oceanic biogeochemistry.

The approach used covered culturing experiments, analytical speciation of Zn, data analysis and interpretation, conceptual modeling of Zn cycling and quantitative modeling of its putative biological role in the Tasman Sea. It underlined the importance of bringing together present knowledge and integrating results from three disciplines to interpret Zn biogeochemistry in one oceanic region. As the debate between limitation and co-limitation for Zn is still not resolved, the focus was set here on the Australasian regional sea to understand Zn's role locally. Indeed, as previously discussed, Zn limitation is not a widespread phenomenon and occurs only in particular regions, such as the Sargasso Sea (Jakuba *et al.* 2008, Shaked *et al.* 2006). However, it also plays an essential role in structuring the phytoplankton community in other regions such as the North Pacific (Jakuba *et al*. 2012).

The qualitative work involved two phytoplankton species, *Nitzschia closterium* and *Emiliania huxleyi*, exposed to low Zn concentration and bioavailability in a culturing process. Zn's role explored through biological

experiments revealed that phytoplankton species were not limited and were able to grow or develop strategies to alleviate the deplete conditions. While *E. huxleyi* had the possibility to access other trace elements such as cobalt (Co) or cadmium (Cd), *N. closterium* was limited by the kinetics of the Zn organic complexes. In that regard, and in spite of the low Zn concentrations detected in the Tasman Sea, the expectations were that planktonic species, such as chlorophytes, cyanobacteria and coccolithophorids, could develop and bloom.

The dominance of haptophytes and small phytoplankton versus large diatoms was confirmed by the combination of our chemical and biological results in the study presented in Chapter IV. The different concentrations measured covered labile Zn, more likely to be associated with 'weak' ligands, free Zn ion concentrations and the ligand concentrations. Both labile and free Zn concentrations were in the picomolar range and the three stations analysed had high concentrations of ligands. This qualitative work linked analytical Zn speciation by voltammetric methods, especially ligand concentrations, with the distribution of species in the community and in the water column.

A quantitative study of the impact of Zn speciation was presented in Chapter V. It helped predict the impact of different factors over a set interval and evaluated the influence that zinc chemistry would have on an ecosystem based around two model phytoplankton groups. This basic work represented a first step in predicting Zn mediation of growth and structure of planktonic assemblages. Briefly, our results showed that in the biological conditions of the P3 station during the 'PINTS' (ss2010v01) voyage, where phytoplankton species were not limited by [micro]nutrients concentrations, the same structural assemblage was

observed in every scenario tested. These results suggest community resilience at this locality.

The model was developed to simulate and explore the impact of ligand production on Zn-limited phytoplankton groups. The Ks tested during the sensitivity analysis simulated no limitation for the phytoplankton P1 and the total ligand concentrations were distributed with the hypothesis that the non-labile complexes were present at higher concentrations than labile ones. If species exhibit a Ks smaller than the Zn concentrations chosen, they are not affected by low Zn concentrations. However, a Ks that is of greater value than the Zn concentration induces a limitation and the induction of a two-transporters-system response (Sunda and Hunstman 1992). We simulated the effect of Zn limiting conditions for one species and considered the labile complexes were more available than the non-labile ones with the hypothesis of a production of organic ligands. In this case, the model simulated a change of abundance and dominance of species. The model simulated the change of abundance between the phytoplankter able to only access the free Zn and the phytoplankter able to access labile Zn and free Zn. The different simulations also matched the difference between P2 and P3 visited during the PINTS voyage, with a bloom dominated by coccolithophorids and chlorophytes at P3 and the inverse at P2. The difference observed with limited species and induced production of ligands confirmed that Zn can potentially mediate the structure of the phytoplankton assemblage in this region. It also demonstrated that the model created could simulate such results. We could not explore further results in the model as several parameters (*e.g.* grazing, Co/Cd interreplacement) and external forcing (*e.g.* light and mixed layer seasonality) are missing in the model. However, further quantitative work is to be

done to predict composition of phytoplankton assemblages and domination of species in a changing ocean (Fig. 1).

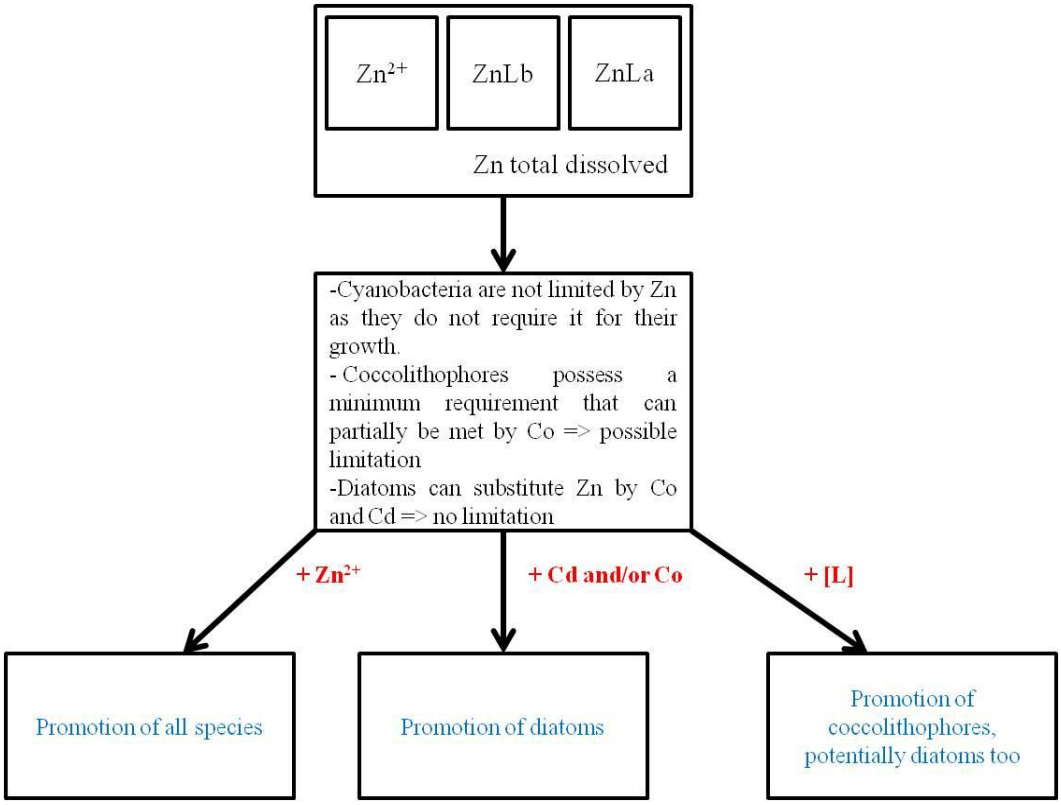

Fig.1: Proposed role of Zn on the phytoplankton community and prediction with eventual changes of speciation with ocean acidification and adaptation of phytoplankton species.

6.2 Future perspectives:

As previously mentioned in the literature (Coale *et al.* 2003, Leblanc *et al.* 2005, Twining *et al.* 2011), is it the phytoplankton that are influencing the speciation of Zn or the low concentrations causing micro-organisms to instigate mechanisms to alleviate those low concentrations? This involves taking into account the particularities of the studied region. In the Tasman Sea, the interaction between Zn, Cd and Co and the different requirements for these species were also likely to influence the community structure. In that regard, we can suggest that in regions where Zn is highly complexed and another nutrient is limiting (*e.g.* N, Fe), Zn speciation is likely to influence the dominance of small phytoplankton. Whereas, in a region where presumably other [micro]nutrients are not limiting, phytoplankton species will develop strategies to access the depleted resource and possibly even mechanisms to enhance their uptake. In that case, the community is likely to exhibit a classic species succession (chlorophytes, coccolithophorids and small then large diatoms) during a bloom. Further experiments with natural communities from the Tasman Sea and deck incubations are required to conclude definitively on the influence of zinc bioavailability on the phytoplankton community. They are also required to increase our understanding of interactions of trace metal micronutrients (and their mechanisms) in the Tasman Sea and similar temperate oligotrophic regions.

Previous laboratory studies showed the limitation or promotion of species in presence of low Zn concentrations, while other stations visited during PINTS showed a correlation between chlorophytes and ligands. Moreover, this entire work concurred with the studies of Wisniewski – Jakuba *et al.* (2012), Xu *et al.*

(2012) and Aristilde *et al.* (2012). Those studies exposed the role of Zn biogeochemistry on the structure of the phytoplankton assemblages. Wisniewski – Jakuba *et al.* (2012) linked Zn speciation and bioavailability to the composition of phytoplankton assemblages in the North Pacific. Xu *et al*. (2012) looked at the influence of the ocean acidification (change of pH) on the Zn and Cd uptake for two species of phytoplankton, *E. huxleyi* and *T. weissflogii*. Aristilde *et al.* (2012) showed the role of ligands, and thus, Zn bioavailability on Zn uptake for the same two species. Further culture experiments with keystone species from different region (*e.g. T. oceanica, E. huxleyi, Synechococcus*) are required to understand Zn speciation and its bioavailability and extract information on its role at low concentrations. Field experiments need to follow to compare the in situ response of phytoplankton assemblages between regions and establish a more precised 'map' of Zn role for the ocean.

It is still unknown whether species are releasing ligands to access the depleted Zn resource. However, few studies suggest this scenario seems a possibility in different laboratory studies (Vasconcelos *et al.* 2002, Vasconcelos *et al.*2008, Aristilde *et al.* 2012, Xu *et al.* 2012). The nature of these ligands is yet to be established. Aristilde *et al.* (2012) started investigating the nature of these weak ligands and suggested the existence of a Zn-Cysteine (Zn-Cys) transporter. These transporters help the acquisition of Zn at low concentrations. Emerging results (McIntyre and Guéguen 2013) indicate the importance of understanding the role of organic ligands in the speciation and bioavailability of Zn for phytoplankton. Whether ligands are related to biological species or derive from the presence of polyvalent humic substances, their identity and activity are likely

to help us predict and understand the interactions between trace elements and phytoplankton. Several techniques are available to directly detect the nature of organic ligands for Fe, such as solid-phase extraction (Macrellis *et al.* 2001), chrome azurol S assay (CAS) (Velasquez *et al.* 2011). They are required to be adapted for Zn and to first characterize the nature of organic ligands released, if they are present, in culture experiments. Their identification will help define what they could be in the field and their influence on the whole community.

We can extend the influence of Zn speciation on the phytoplankton communities to the changing ocean. Millero *et al.* (2009) reviewed the impact of pH change for few trace elements. Fewer changes are predicted for Zn in comparison to Fe or Cu, but an increase of free Zn is predicted in parallel to a decrease of inorganic $ZnOH^+$ and $ZnCO_3$ complexes (Millero *et al.* 2009). It is still unknown whether organic complexation will necessarily respond to ocean acidification as inorganic speciation does. We can suggest that if Zn speciation does play a role in the community, those changes will probably have an impact in regions that are more susceptible to ocean acidification and where free Zn is low such as the Southern Ocean or the Tasman Sea. The evolution of assemblages in such regions would lead towards a dominance of chlorophytes, cyanobacteria and coccolithophores and small diatoms compared to large ones. It has been previously shown that phytoplankton can evolve in a changing ocean (Morel 2008) and develop strategies to adapt to their ambient environment. Recent studies can confirm the adaptation of coccolithophorids to increasing pH (Richier *et al.* 2011) and the study by Xu *et al.* (2012) showed the importance of weak complexes in favoring a diatom and a coccolithophorid in taking up Zn. A possible adaptation to a decrease of labile Zn is the production of organic ligands

by some phytoplankton species (*e.g.* chlorophytes) to enable access to the low resource.

The future incorporation of Zn in biogeochemical models will be useful for the prediction of phytoplankton assemblages in regions, where Zn can be identified as a co-limiting nutrient and regions susceptible to ocean acidification. The limiting role or co-limiting role of Zn for the phytoplankton can be the base of this work and further work along the ones existing for Fe (Gregg *et al.* 2003, Tagliabue *et al.* 2009) is required. The conceptual model will include seasonality of the light and possible co-limitation between Fe and Zn to evaluate the impact of a strong co-limitation on phytoplankton assemblage (Fig 2). Both Fe and Zn speciation are required as the kinetics of complexes and relation to Fe and Zn uptake plays an important role in the bioavailability of the different complexes presents in seawater.

Speciation and ligands origin, which link to Zn bioavailability, are the key points to better understand Zn cycling in the different regions where it is considered as driver for the phytoplankton community. Measurements of Zn speciation and its response to ocean acidification will allow evaluating the impact of ocean acidification and incorporate carbon (C) and Zn co-limitation in further model to predict the impact of ocean acidification on a phytoplankton community.

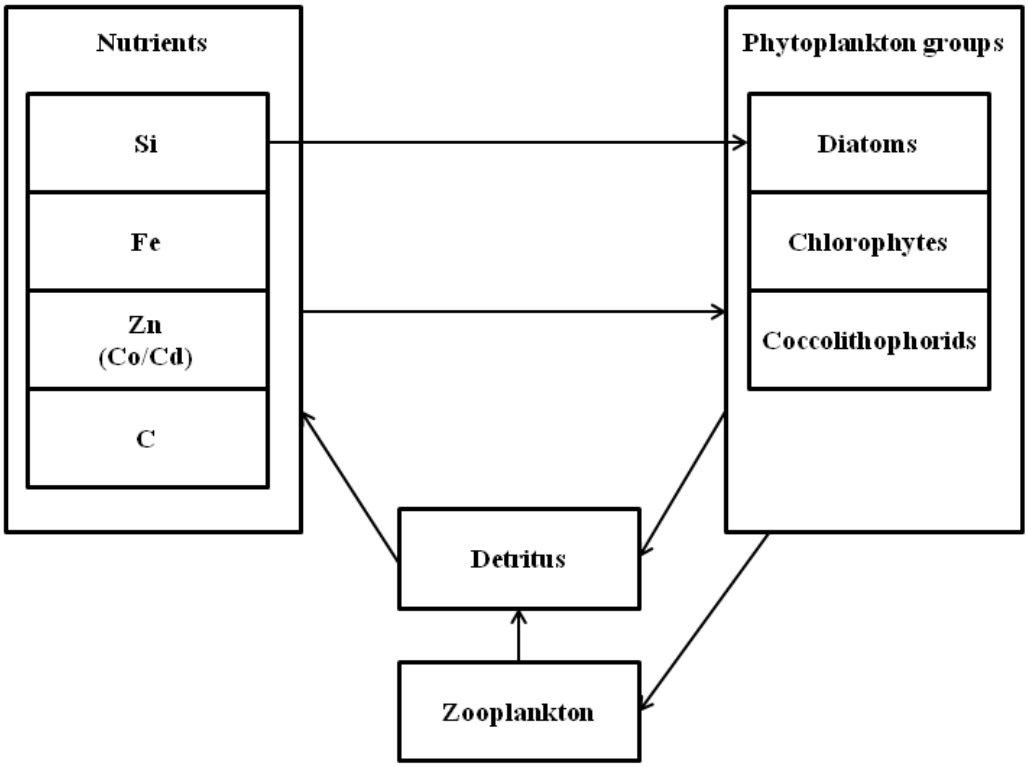

Fig. 2: Conceptual biogeochemical model imagined to predict the influence of Zn speciation and co-limitation with Fe on the phytoplankton assemblages.

6.3 References:

Aristilde, L., Xu, Y., and Morel, F. M. M. (2012). Weak organic ligands enhance zinc uptake in marine phytoplankton. *Environmental Science and Technology*, **46,** 5438-5445.

Arrigo, K. R. (2005). Marine microorganisms and global nutrient cycles. *Nature,* **437,** 349-355.

Coale, K. H., Wang, X., Tanner, S. J., and Johnson, K. S. (2003). Phytoplankton growth and biological response to iron and zinc addition in the Ross Sea and Antarctic Circumpolar Current along 170°W. *Deep Sea Research Part II: Topical Studies in Oceanography*, **50,** 635-653.

Gregg, W. W., and Casey, N. W. (2007) Modeling coccolithophores in the global ocean, *Deep sea research II*, **54**, 447-477, doi: 10.1016/j.dsr2.2006.12.007.

Leblanc, K., Hare, C. E., Boyd, P. W., Bruland, K. W., Sohst, B., Pickmere, S., Lohan, M. C., Buck, K., Ellwood, M., and Hutchins, D. A. (2005). Fe and Zn effects on the Si cycle and diatom community structure in two contrasting high and low-silicate HNLC areas. *Deep Sea Research Part I: Oceanographic Research Papers,* **52,** 1842-1864.

Macrellis, H. M., Trick, C. G., Rue, E. L., Smith, G., and Bruland, K. W. (2001). Collection and detection of natural iron-binding ligands from seawater. *Marine Chemistry*, **76,** 175-187.

McIntyre, A. M., and Guéguen, C. (2013). Binding interactions of algal-derived dissolved organic matter with metal ions. *Chemosphere*, **90,** 620-626.

Millero, F.J., R. Woosley, B. DiTrolio, and J. Waters. (2009). Effect of ocean acidification on the speciation of metals in

seawater. *Oceanography* **22**, 72–85, doi: 10.5670/oceanog.2009.98.

Morel, F. M. M. (2008). The co-evolution of phytoplankton and trace element cycles in the oceans. *Geobiology*, **6,** 318-324.

Oschlies, A. and Garcon, V. (1998). Eddy-induced enhancement of primary production in a coupled ecosystem-circulation model of the North Atlantic ocean, *Nature*, **394**, 266-269.

Richier, S., Fiorini, S., Kerros, M.-E., von Dassow, P., and Gattuso, J.-P. (2011). Response of the calcifying coccolithophore *Emiliania huxleyi*; to low pH/high pCO_2: from physiology to molecular level. *Marine Biology,* **158,** 551-560.

Saito, M. A., Goepfert, T. J., and Ritt, J. T. (2008). Some thoughts on the concept of colimitation: Three definitions and the importance of bioavailability. *Limnology and Oceanography*, **53,** 276-290.

Shaked, Y., Xu Y., Leblanc K., and Morel, F. M. M. (2006). Zinc availability and alkaline phosphatase activity in *Emiliania huxleyi*: Implications for Zn-P co-limitation in the ocean *Limnology and Oceanography*, **51,** 299-309.

Sunda, W. G., and Hunstman, S. A. (1992). Feedback interactions between zinc and phytoplankton in seawater. *Limnology and Oceanography*, **37,** 25-40.

Tagliabue, A., Bopp L., Aumont O., and Arrigo K. R. (2009). Influence of light and temperature on the marine iron cycle: From theoretical to global modelling. *Global Biogeochemical Cycles* **23,** GB2017, doi:10.1029/2008GB003214.

Twining, B. S., Baines, S. B., Bozard, J. B., Vogt, S., Walker, E. A., and Nelson, D. M. (2011) Metal quotas of plankton in the equatorial Pacific Ocean,

Deep-Sea Reasearch II, **58**, 325-341, doi: 10.1016/j.dsr2.2010.08.018.

Vasconcelos, M. Teresa. S. D., and Leal, M. Fernando. C. (2008). Exudates of different marine algae promote growth and mediate trace metal binding in *Phaeodactylum tricornutum*. *Marine Environmental Research*, **66,** 499-507.

Vasconcelos, M. Teresa. S. D., Leal, M. Fernando. C., and van den Berg, C. M. G. (2002). Influence of the nature of the exudates released by different marine algae on the growth, trace metal uptake and exudation of *Emiliania huxleyi* in natural seawater. *Marine Chemistry*, **77,** 187-210.

Velasquez, I., Nunn, B. L., Ibisanmi, E., Goodlett, D. R., Hunter, K. A., and Sander, S. G. (2011). Detection of hydroxamate siderophores in coastal and Sub-Antarctic waters off the South Eastern Coast of New Zealand. *Marine Chemistry*, **126,** 97-107.

Wisniewski-.Jakuba, R., Saito, M. A., Moffett, J. W., and Xu, Y. (2012). Dissolved zinc in the subarctic North Pacific and Bering Sea: Its distribution, speciation, and importance to primary producers. *Global Biogeochemical Cycles*, **26**.

Wisniewski-.Jakuba, R., Moffett, J. W., and Dyrhan, S. T. (2008). Evidence for the linked biogeochemical cycling of zinc, cobalt, and phosphorus in the western North Atlantic Ocean. *Global Biogeochemical Cycles*, **22,** 13.

Xu, Y., Shi, D., Aristilde, L., and Morel, F. M. M. (2012). The effect of pH on the uptake of zinc and cadmium in marine phytoplankton: Possible role of weak complexes. *Limnology and Oceanography*, **57,** 293-304.

APPENDIX

Appendix 1: Detailed concentrations for the profiles analysed with voltammetry. In all speciation tables, [Zn^{2+}] is calculated according to the quadratic solution in Chapter IV (p. 149).

Stn 4 (P1) data for total dissolved Zn concentrations and ligands concentrations:

Samples	Depth (m)	[Zn]tot (nM)	[L] (nM)	Average	Standard error	log K_{ZnL}	Average	Standard error
Stn4_11	30	0.049	1.63	1.48	0.15	9.55	9.67	0.12
			1.33			9.79		
Stn4_10	56	0.013	0.83	0.82	0.01	11.4	10.94	0.46
			0.81			10.48		
Stn4_09	72	0.013	0.37	0.24	0.13	10.88	10.03	0.85
			0.11			9.18		
Stn4_08	101	0.014	0.23	0.23	0	9.76	9.385	0.375
			0.23			9.01		
Stn4_07	125	0.011	0.21	0.46	0.25	9.51	9.33	0.18
			0.71			9.15		
Stn4_05	200	0.027	1.71	1.2	0.51	9.16	9.345	0.185
			0.69			9.53		
Stn4_04	300	0.061	0.78	0.71	0.07	10.03	9.905	0.125
			0.64			9.78		

Stn 4 (P1) data from voltammetry titrations using van den Berg solution.

		Solution to quadratic								
Samples	Depth (m)	a	b	c	Zn^{2+} (pM)	Average	Standard error	Zn' (pM)	Average	Standard error
Stn4_11	30	7.45E+09	7.71	-4.9E-11	6.33	5.53	0.80	13.29	11.62	1.67
		1.29E+10	10.30	-4.9E-11	4.74			9.95		
Stn4_10	56	5.27E+11	207	-1.3E-11	0.06	0.27	0.21	0.13	0.58	0.45
		6.34E+10	26.56	-1.3E-11	0.49			1.02		
Stn4_09	72	1.59E+11	29.19	-1.3E-11	0.44	3.06	2.61	0.93	6.42	5.49
		3.18E+09	2.27	-1.3E-11	5.67			11.90		
Stn4_08	101	1.21E+10	3.34	-1.4E-11	4.18	5.11	0.93	8.79	10.74	1.95
		2.15E+09	2.34	-1.4E-11	6.05			12.69		
Stn4_07	125	6.8E+09	2.74	-1.1E-11	4.06	3.84	0.22	8.53	8.06	0.47
		2.97E+09	3.10	-1.1E-11	3.61			7.59		
Stn4_05	200	3.04E+09	4.53	-2.7E-11	6.01	6.06	0.05	12.62	12.72	0.10
		7.12E+09	4.44	-2.7E-11	6.10			12.82		
Stn4_04	300	2.25E+10	9.81	-6.1E-11	6.09	8.02	1.93	12.79	16.85	4.06
		1.27E+10	5.96	-6.1E-11	9.9			20.91		

P2 data for total dissolved Zn concentrations and ligands concentrations:

Samples	Depth (m)	[Zn]tot (nM)	[L] (nM)	Average	Standard error	log KZnL	Average	Standard error
P2a-E128	15	0.11	1.27			10.77		
			1.24	1.255	0.015	11.37	11.07	0.3
P2a-E52	30	0.09	1.84			10.39		
			1.62	1.73	0.11	10.48	10.435	0.045
P2a-E209	50	0.09	2.04			10.44		
			1.87	1.955	0.085	10.03	10.235	0.205
P2a-E83	70	0.02	4.05			10.12		
			4.34	4.195	0.145	9.97	10.045	0.075
P2b-12	125	0.19	0.93			9.85		
			0.57	0.75	0.18	10.53	10.19	0.34
P2b-10	150	0.10	1.57			9.38		
			1.3	1.435	0.135	9.29	9.335	0.045
P2b-8	200	0.06	0.61			10.24		
			0.49	0.55	0.06	10.01	10.125	0.115
P2b-6	300	0.18	0.67			10.18		
			1.03	0.85	0.18	9.93	10.055	0.125
P2b-4	500	0.49	1.26			9.94		
			1.04	1.15	0.11	10.04	9.99	0.05
P2b-2	750	1.19	1.52			9.6		
			1.26	1.39	0.13	9.54	9.57	0.03

P2 data from voltammetry titrations using van den Berg solution.

		Solution to quadratic								
Samples	Depth (m)	a	b	c	Zn^{2+} (pM)	Average	Standard error	Zn' (pM)	Average	Standard error
P2a-E128	15	1.24E+11	70.56	-1.1E-10	1.52			3.19		
		4.92E+11	292	-1.1E-10	0.37	0.94	0.58	0.77	1.98	1.21
P2a-E52	30	5.15E+10	45.08	-8.9E-11	1.97			4.14		
		6.34E+10	51.02	-8.9E-11	1.74	1.86	0.11	3.66	3.90	0.24
P2a-E209	50	5.78E+10	55.73	-9.3E-11	1.66			3.49		
		2.25E+10	22.14	-9.3E-11	4.18	2.92	1.26	8.77	6.13	2.64
P2a-E83	70	2.77E+10	55.21	-2.1E-11	0.38			0.79		
		1.96E+10	42.60	-2.1E-11	0.49	0.43	0.06	1.03	0.91	0.12
P2b-12	125	1.49E+10	7.35	-1.9E-10	24.44			51.33		
		7.12E+10	21.41	-1.9E-10	8.56	16.50	7.94	18.00	34.65	16.68
P2b-10	150	5.04E+09	5.62	-1E-10	18.04			37.88		
		4.09E+09	4.63	-1E-10	21.80	19.92	1.88	45.79	41.83	3.95
P2b-8	200	3.65E+10	11.65	-6.1E-11	5.12			10.76		
		2.15E+10	7.11	-6.1E-11	8.31	6.72	1.60	17.46	14.11	3.35
P2b-6	300	3.18E+10	9.52	-1.8E-10	17.80			37.39		
		1.79E+10	10.87	-1.8E-10	16.10	16.95	0.85	33.81	35.60	1.79
P2b-4	500	1.83E+10	8.80	-4.9E-10	50.52			106.09		
		2.3E+10	13.50	-4.9E-10	34.36	42.44	8.08	72.14	89.18	16.97
P2b-2	750	8.36E+09	3.40	-1.2E-09	225.46			473.46		
		7.28E+09	6.47	-1.2E-09	156.69	191.08	34.38	329.06	401.26	72.20

P3 data for total dissolved Zn concentrations and ligands concentrations:

Samples	Depth (m)	[Zn]tot (nM)	[L] (nM)	Average	Standard error	log KZnL	Average	Standard error
P3c-E71	15	0.18	1.66			10.5		
			1.49	1.58	0.09	10.28	10.39	0.08
P3c-E233	28	0.17	2.02			10.67		
			2.23	2.13	0.11	10.27	10.47	0.14
P3c-E126	50	0.24	2.09			10.07		
			1.98	2.04	0.05	10.24	10.155	0.06
P3c-E26	79	0.11	1.71			10.39		
			1.81	1.76	0.05	10.2	10.295	0.07
P3c-E44	121	0.12	1.74			10.39		
			1.54	1.64	0.10	11.16	10.775	0.27
P3c-E66	146	0.11	0.99			10.9		
			1.36	1.178	0.19	9.85	10.375	0.37
P3c-9	300	0.28	1.45			10.42		
			1.57	1.51	0.06	10.12	10.27	0.11
P3c-7	500	0.55	1.79			9.62		
			1.82	1.81	0.02	9.5	9.56	0.04
P3c-5	750	1.23	1.83			9.48		
			1.64	1.74	0.10	9.35	9.415	0.05
P3c-3	1000	2.44	2.91			9.8		
			4.51	3.71	0.8	9.31	9.555	0.17

P3 data from voltammetry titrations using van den Berg solution:

		Solution to quadratic								
Samples	Depth (m)	a	b	c	Zn^{2+} (pM)	Average	Standard error	Zn' (pM)	Average	Standard error
P3c-E71	15	6.64E+10	48.85	-1.8E-10	3.70			7.78		
		4E+10	30.49	-1.8E-10	5.92	4.81	1.56	12.42	10.10	2.32
P3c-E233	28	9.82E+10	88.60	-1.7E-10	1.92			4.03		
		3.91E+10	43.62	-1.7E-10	3.90	2.91	1.40	8.18	6.11	2.07
P3c-E126	50	2.47E+10	23.85	-2.4E-10	9.90			20.79		
		3.65E+10	36.51	-2.4E-10	6.49	8.20	2.41	13.63	17.21	3.58
P3c-E26	79	5.15E+10	41.30	-1.1E-10	2.72			5.72		
		3.33E+10	30.79	-1.1E-10	3.65	3.19	0.66	7.67	6.70	0.98
P3c-E44	121	5.15E+10	41.94	-1.2E-10	2.78			5.83		
		3.04E+11	224.70	-1.2E-10	0.52	1.65	1.59	1.09	3.46	2.37
P3c-E66	146	1.67E+11	71.74	-1.1E-10	1.57			3.31		
		1.49E+10	11.73	-1.1E-10	9.55	5.56	5.64	20.05	11.68	8.37
P3c-9	300	5.52E+10	32.87	-2.8E-10	8.41			17.66		
		2.77E+10	22.80	-2.8E-10	12.12	10.26	2.62	25.45	21.55	3.89
P3c-7	500	8.75E+09	7.25	-5.5E-10	70.47			147.99		
		6.64E+09	7.86	-5.5E-10	66.81	68.64	2.59	140.30	144.15	3.85
P3c-5	750	6.34E+09	3.90	-1.2E-09	230.17			483.35		
		4.7E+09	5.77	-1.2E-09	185.68	207.92	31.45	389.93	436.64	46.71
P3c-3	1000	1.33E+10	5.08	-2.4E-09	278.16			584.14		
		4.29E+09	11.31	-2.4E-09	200.36	239.26	55.01	420.77	502.45	81.69

SAZ-SENSE (Stn 14) data for total dissolved Zn concentrations and ligands concentrations:

Samples	Depth (m)	[Zn]tot (nM)	[L] (nM)	Average	Standard error	log KZnL	Average	Standard error
16a_12	15	0.1	2.62			10.32		
			2.68	2.65	0.03	10.3	10.31	0.01
16a_11	30	0.35	2.38			10.51		
			2.5	2.44	0.06	10.18	10.345	0.165
16a_10	50	0.16	1.46			10.1		
			1.32	1.39	0.07	10.07	10.085	0.015
16a_9	75	0.14	1.36			10.23		
			1.37	1.365	0.005	10.92	10.575	0.345
16a_8	100	0.73	1.53			10.83		
			1.24	1.385	0.145	10.37	10.6	0.23
16a_7	125	0.554	1.5			10.24		
			1.55	1.525	0.025	10.32	10.28	0.04
16a_6	150	0.9	1.95			10.25		
			1.59	1.77	0.18	10.59	10.42	0.17
16a_5	200	1.1	2.59			10.33		
			1.82	2.205	0.385	10.78	10.555	0.225
16a_4	300	0.89	2.1			10.42		
			2.08	2.09	0.01	9.87	10.145	0.275
16a_3	500	1.2	1.55			10.97		
			0.91	1.23	0.32	11.77	11.37	0.4

16a_2	750	1.00	1.49			11.4		
			1.75	1.62	0.13	10.11	10.755	0.645
16a_1	1000	1.90	3.33			9.39		
			1.6	2.465	0.865	9.79	9.59	0.2

SAZ-Sense (Stn 14) data from voltammetry titrations using van den Berg solution:

		Solution to quadratic								
Samples	Depth (m)	a	b	c	Zn^{2+} (pM)	Average	Standard error	Zn' (pM)	Average	Standard error
16a_12	15	4.39E+10	54.75	-1E-10	1.82			3.83		
		4.19E+10	55.57	-1E-10	1.80	1.81	0.01	3.77	3.80	0.03
16a_11	30	6.8E+10	67.79	-3.5E-10	5.14			10.79		
		3.18E+10	39.94	-3.5E-10	8.70	6.92	1.78	18.28	14.53	3.74
16a_10	50	2.64E+10	18.47	-1.6E-10	8.56			17.98		
		2.47E+10	17.61	-1.6E-10	8.97	8.77	0.21	18.84	18.41	0.43
16a_9	75	3.57E+10	22.82	-1.4E-10	6.08			12.76		
		1.75E+11	116.05	-1.4E-10	1.20	3.64	2.44	2.53	7.65	5.12
16a_8	100	1.42E+11	56.19	-7.3E-10	12.59			26.44		
		4.92E+10	31.17	-7.3E-10	22.61	17.60	5.01	47.49	36.97	10.52
16a_7	125	3.65E+10	18.54	-5.5E-10	28.30			59.44		
		4.39E+10	34.48	-5.5E-10	15.75	22.03	6.28	33.07	46.26	13.18
16a_6	150	3.73E+10	20.77	-9E-10	40.39			84.83		
		8.17E+10	63.96	-9E-10	13.83	27.11	13.28	29.04	56.93	27.90
16a_5	200	4.49E+10	33.96	-1.1E-09	31.12			65.34		
		1.27E+11	111.77	-1.1E-09	9.73	20.42	10.69	20.44	42.89	22.45
16a_4	300	5.52E+10	33.93	-8.9E-10	25.20			52.92		
		1.56E+10	17.52	-8.9E-10	48.69	36.95	11.75	102.26	77.59	24.67
16a_3	500	1.96E+11	34.76	-1.2E-09	29.58			62.13		

		1.24E+12	537.95	-1.2E-09	2.22	15.90	13.68	4.66	33.39	28.73
16a_2	750	5.27E+11	125.18	-1E-09	7.74			16.25		
		2.71E+10	24.64	-1E-09	38.91	23.33	15.59	81.72	48.98	32.74
16a_1	1000	5.15E+09	5.61	-1.9E-09	271.12			569.36		
		1.29E+10	11.97	-1.9E-09	138.14	204.63	66.49	290.09	429.73	139.63

Appendix 2:

Matlab code used in this study. The code was divided into two files, a file to run the model and a function that was integrating data and calculating the set of differential equations.

Appendix 2.1: Main file for running the model

```
%%%%%%%%%%%%%%%%%%%%%%%%%%%%%%%%%%%%%%%%%%%%%%%%%%%%%%%%%%%%%%%%%%%%%%%%%%%%%%%%
%%%%%
%%%%%%%%%%%%%%%%%%%%%%%%%%%%%%%%%%%%%%%%%%%%%%%%%%%%%%%%%%%%%%%%%%%%%%%%%%%%%%%%
%%%%%
% Executable file to run ZnPPZZD biogeochemical
% Uses aos_Znpzd.m, Function model
% Referred to Oschlies & Schartau (2005) for the original model
% and modified for this PhD
%%%%%%%%%%%%%%%%%%%%%%%%%%%%%%%%%%%%%%%%%%%%%%%%%%%%%%%%%%%%%%%%%%%%%%%%%%%%%%%%
%%%%%%
%%%%%%%%%%%%%%%%%%%%%%%%%%%%%%%%%%%%%%%%%%%%%%%%%%%%%%%%%%%%%%%%%%%%%%%%%%%%%%%%
%%%%%
%%%%%%%%%%%%%%%%%%%%%%%%%%%%%%%%%%%%%%%%%%%%%%%%%%%%%%%%%%%%%%%%%%%%%%%%%%%%%%%%
%%%%%

%Set some global variables used by aos_Znpzd_cte_light.m
 global sst sra lat K

%Define integration interval in units [s]:
 iint = 365*60*24*60; %Will solve for 365 days

%Define the forcing:
sst  = 15;       %[°C] Temperature, influencing growth rates
sra = 300;       %[W/m^2] solar radiation shortwave watt m^-2
K = 4;           %[month]time of year; used to calculate angle of
incoming sra
MLD = 50;        %[m] Depth of the mixed layer

% unit in the model is pmol Zn m-3
% equation in nmol Zn/m-3 and have consistency in the model:
% Zn:C ratio: (3.7e3) nmol/mol
% Zn:C ratio:  3.7e6 pmol /mol
% Zn:C ratio:  3.7e3 pmol /mmol
% C/Chla is 50 mmol C / mg Chl => 0.05 mmol C / microg Chl
% and C/N = 6.63
%  Zn:N ratio: 3.7e3/7 =529   pmol Zn / m3 => to convert the
%variables in pmol Zn instead of nmol N m-3
% => 3.7e3/0.05 = 74e3 to convert in Chl a. Biomass converted in
microg Chl a in the plots.

%Initial conditions:
 Zn = 5; % pmol Zn m^-3
 ZnLb= 10; % pmol Zn m^-3
 ZnLa = 160; % pmol Zn m^-3
 PHY = (5e-4)/529;   % picol mo
```

```
 ZOO = (4e-4)/529;
 DET = 0.0/529;
 PHY2= (2e-4)/529;
 ZOO2= (2e-4)/529;


%Set a couple of options for the differential equation solver:

 odeopt=odeset('RelTol',1e-12,'AbsTol',[1e-8 1e-8 1e-8 1e-8 1e-8
1e-8 1e-8 1e-8 1e-8], 'InitialStep',[10]);

%Solve the system by calling the equations set up:
 [t,x]=ode45('aos_Znpzd_cte_light_2zoo'  ,iint,[Zn  ZnLb  ZnLa  PHY
ZOO DET MLD PHY2 ZOO2],odeopt);


 %plot solution:
solution=figure (1);
set(gcf,'position',[163    52   560
                           896]);
 t=t./60./60./24;
 subplot(3,2,1); hold on; grid on;
  plot(t,x(:,1),'r');
  ylabel('Zn pmol m^-3 ')

 subplot(3,2,3); hold on; grid on;
  plot(t,x(:,2),'r');
  ylabel('ZnLb [pmol m^-3]')

subplot(3,2,5); hold on; grid on;
  plot(t,x(:,3),'r');
  ylabel('ZnLa pmol m^-3]')

 subplot(3,2,2); hold on; grid on;
  plot(t,x(:,4).*(74e3),t,x(:,8).*(74e3))
  ; legend('small','large')
  ylabel('PHY [microgCh m^-3]')

 subplot(3,2,4); hold on; grid on;
  plot(t,x(:,5).*(74e3),t,x(:,9).*(74e3))
  ; legend('small', 'large')
  ylabel('ZOO [microg chla]')

 subplot(3,2,6); hold on; grid on;
  plot(t,x(:,6).*(74e3),'r');
  ylabel('DET [microg chla]')
```

Appendix 2.2: Running file to solve the set of differential equations.

```
%%%%%%%%%%%%%%%%%%%%%%%%%%%%%%%%%%%%%%%%%%%%%%%%%%%%%%%%%%%%%%%%%%%%%%%%%%%%%%%%
%%%%%
%%%%%%%%%%%%%%%%%%%%%%%%%%%%%%%%%%%%%%%%%%%%%%%%%%%%%%%%%%%%%%%%%%%%%%%%%%%%%%%%
%%%%%
% ZnPPZZD biogeochemical equation and parameters
% call by  run_template.m
% Based on the Base on Heiner Dietze work And
% oschlies & schartau 2005 Znpzd model
% modified for this PhD to integrate Zn speciation
%%%%%%%%%%%%%%%%%%%%%%%%%%%%%%%%%%%%%%%%%%%%%%%%%%%%%%%%%%%%%%%%%%%%%%%%%%%%%%%%
%%%%%
function xdot=aos_Znpzd_cte_light_2zoo(t,x)
%set of differential equations for the conceptual model built
with Zn
%inspired structure from oschlies & schartau 2005 npzd model
%Differential equation inspired from Arrigo and Tagliabue (2005)
and Fan and Dunn (2011)

global sst sra lat K w_sink


sda = 86400; %seconds in a day

%%************** parameter list *************
%Zn parameters:
kfLb =1.0e-10;              %Zn pool: [(pmol Zn m^-3)^-1 s^-1] Formation
                            constant of labile complexes
kdLb =1.0e-12;   %Zn pool: [s^-1] Rate of Dissociation constant of
                            labile complexes
kfLa = 1.0e-10;             %Zn pool: [(pmol Zn m^-3)^-1 s^-1] Formation
                            constant of non labile complexes
kdLa = 1.0e-12;             %Zn pool: [s^-1] Dissociation constant of
                            non labile complexes
La = 400;                   %Zn pool: [pmol Zn m^-3] Concentration of
                            ligands for non labile complexes
Lb = 1500;                  %Zn pool: [pmol Zn m^-3] Concentration
                            of ligands for labile complexes


%Small phytoplankton coefficients:
alpha_s = 0.25/sda;           %Phyto: [s^-1 (W m^2)] Initial slope of
                            P-I curve
par_s   = 0.43;               %Phyto:   Photosynthetically   active
                            radiation
kw_s     = 1/0.04;            %Phyto: [m] Light attenuation due to
                            water
kc_s     = 1/0.047/529);      %Phyto: [m(pmol Zn m^-3)^-1] Light att.
                            due to Phy.
a_s     = 0.1/sda;          %Phyto: [s^-1] Max. growth rate parameter
b_s     = 1.066;              %Phyto: Max. growth rate parameter
c_s     = 1.;           %Phyto: [°C ^-1] Max. growth rate parameter
Jmax_s = a_s*b_s^(c_s*sst);%Phyto: [s^-1] Specific light saturated
growth
K_s = 15;                       %Phyto: [psmol Zn s-1] Half sat.
const for Zn uptake for s phyto
morp_s   = 0.04/sda;     %Phyto: [1/s] Specific mortality rate for
small phyto
```

```
exup_s= 0.01/sda;          %Phyto: [s^-1] Exudation term from small
phyto to Zn pool

%Large phytoplankton coefficients:
alpha_l = 0.25/sda;       %Phyto: [1/s/(W/m^2)] Initial slope of P-I
curve
par_l    = 0.43;                  %Phyto: Photosynthetically active
radiation
kw_l     = 1/0.04;                %Phyto: [m] Light attenuation due
to water
kc_l     = 1/(0.047)/(529);      %Phyto: [1/m(pmol Zn m^-3)^-1] Light
att. due to Phy.
a_l        = 0.05/sda;             %Phyto: [s^-1] Max. growth rate
parameter
b_l        = 1.066;                   %Phyto: [] Max. growth rate
parameter
c_l      = 1.;                     %Phyto: [°C^-1)] Max. growth rate
parameter
Jmax_l   =  a_l*b_l^(c_l*sst);     %Phyto:  [d^-1]  Specific  light
saturated growth
 K_1l =12;                          %Phyto: [pmol Zn s^-1] Half sat.
const for Zn^2+ uptake for L phyto
 K_2l =12;                          %Phyto: [pmol Zn s^-1] Half sat.
const for ZnLb uptake for L phyto
 mup1   = 0.4;                    %Phyto: Fraction Uptake value for
Zn^2+
 morp_l  = 0.01/sda;               %Phyto: [s^-1] Specific mortality
rate for large phyto

 %Small Zooplankton coefficients:
 gam_s   = 0.975;               %Zoo: Assim. efficiency for s zoo
 g_s     = 4/sda;            %Zoo: [s^-1] Max. graz. rate
 eps_s   = 150*(529^2)/sda;             %Zoo: [((pmol Zn m^-3)^-2)s^-1]
Prey capture rate
 morz_s = (0.1*(529))/sda;              %Zoo: [(pmol Zn m^-3)^-1)s^-1]
Specific mortality rate for small zoo
 exuz_s = 0.00001/sda;             %Zoo: [s^-1] Exudation term from
small zoopk to Zn pool

 %Large zoo coefficents:
 gam_l   = 0.975;               %Zoo: Assim. efficiency for s zoo
 g_l     = 2/sda;            %Zoo: [s^-1] Max. graz. rate
 eps_l   = 150*(529^2)/sda;          %Zoo: [(pmol Zn m^3)s^-1] Prey
capture rate
 morz_l = (0.1*(529))/sda;      %Zoo: [(pmol Zn m^-3)^-1)s^-1] Specific
mortality rate for large zoo

%detrital coefficients:
 remin   = 0.0005/sda;   %Det: [s^-1] Remineralization rate
 exuzn = 0.0001/sda;            %Det: [s^-1] Exudation rate of non
labile Zn back in det
 w_sink = 20/sda;             %Det:[m s^-1] Sinking velocity
 %
%****************************************
%////////calculation of a couple of terms//////////
%Term for the light calculation for the phytoplankton:
%chd calculated length of day:
       fx1    = 2.0*pi*(K+192)./365;
       declin = 0.006918      ...
             -0.399912*cos(   fx1)+0.070257*sin(   fx1)    ...
```

```
            -0.006758*cos(2.*fx1)+0.000907*sin(2.*fx1)    ...
            -0.002697*cos(3.*fx1)+0.001480*sin(3.*fx1);
%chd   compute solar angle at noon (and assume that this is the
%equivalent
%chd daily averaged incidence angle for direct+diffuse radiation)
%chd cobeta is cos(incidence angle of solar radiation at noon)
       fx1    = pi/180. * lat;
       cobeta=max([0.sin(fx1)*sin(declin)+cos(fx1)*cos(declin)]);
       cobeta = sqrt(1.-(1.-cobeta.^2.)/1.33.^2.);

%chd   finally,length of day
       fx2    = max([-1.  min( 1.,-tan(fx1)*tan(declin))] );
       daylen = max([1.e-12 acos(fx2)/pi]);

%chd    Compute daily averaged light-limited growth rate for the
%small phytoplankton:
%chd    analytical integration over layer thickness and day
%chd    after Evans and Parslow (1985)

       rayb_s(1)= 1.0;

       rayb_s(2)= max([1e-15 exp(-50/(cobeta*kw_s))]);

          fx1_s = 0.5*daylen*daylen/alpha_s;
          radbio_s = max([1.0 par_s*sra]);
          vpbio_s = a_s*b_s.^(c_s*sst);
          fx3_s = fx1_s*vpbio_s/(radbio_s*rayb_s(1));
          fx4_s = fx1_s*vpbio_s/(radbio_s*rayb_s(2));
          fu1_s = sqrt(fx3_s.^2.+daylen.^2.);
          fu1_s = fu1_s-daylen*log((daylen+fu1_s)/fx3_s);
          fu2_s = sqrt(fx4_s.^2.+daylen.^2.);
          fu2_s = fu2_s-daylen*log((daylen+fu2_s)/fx4_s);
          mups = -1*vpbio_s./(x(7)) * cobeta*kw_s   ...
                 *(fu1_s - fu2_s - fx3_s + fx4_s);

%chd    Compute daily averaged light-limited growth rate for %the
%large phytoplankton:
%chd    analytical integration over layer thickness and day
%chd    after Evans and Parslow (1985)

       rayb_l(1)= 1.0;

       rayb_l(2)= max([1e-15 exp(-x(7)/(cobeta*kw_l))]);

          fx1_l = 0.5*daylen*daylen/alpha_l;
          radbio_l = max([1.0 par_l*sra]);
          vpbio_l = a_l*b_l.^(c_l*sst);
          fx3_l = fx1_l*vpbio_l/(radbio_l*rayb_l(1));
          fx4_l = fx1_l*vpbio_l/(radbio_l*rayb_l(2));
          fu1_l = sqrt(fx3_l.^2.+daylen.^2.);
          fu1_l = fu1_l-daylen*log((daylen+fu1_l)/fx3_l);
          fu2_l = sqrt(fx4_l.^2.+daylen.^2.);
          fu2_l = fu2_l-daylen*log((daylen+fu2_l)/fx4_l);
          mupl = -1*vpbio_l./(x(7)) * cobeta*kw_l   ...
                 *(fu1_l - fu2_l - fx3_l + fx4_l)    ;

%Calculation of growth rate as a function of light and nutrients:
```

```
%The growth rate is defined as the minimum between the light and
%the uptake of free Zn for small phyto. The uptake of free Zn
%follows a Michaelis-Menten equation.
%Limitation term for the free Zn for the small phyto:
%Unit: pmol Zn m^-3 => convert biomasse in pmol Zn m^-3 using
%convertion factor of Zn:N:
        LZn_s=(x(1)./(K_s+x(1)));%Limitation term for free Zn


%The growth rate is a bit more complicated for the large ones as
%it depends on both Zn species is able to take up, and the two
%transporters the species can take up labile Zn with. The uptake
%of free Zn follows a Michealis-Menten equation while we use the
%Hill equation in biochemistry to be able to reproduce the uptake
%of labile one.
%Limitation term for the free Zn for the large phyto:
%Unit: pmol m^-3 => convert biomasse in pmol Zn m^-3 using
%convertion factor of Zn:N:
       LZn_l=(x(1)./(K_1l+x(1)));

%Limitation term for the labile Zn for the large phyto:
%Unit: pmol m-3 => convert biomasse in pmol Zn m-3 using
convertion factor of Zn:N:
       LZnLb=(x(2).^2)'./((K_2l)^2+(x(2).^2)');  %Limitation
                                                  term for ZnLb


%HYP for the small phyto, the growth rate is limited by light and
%the free ion as they are able to only rely on free Zn:
%Unit growth:
       mup_s  = min([mups,Jmax_s*LZn_s]); %Growth term for small
phyt
o      mupS = mup_s; %Production term for the small phyto [s^-1]


%HYP for the large phyto, the growth rate is limited by the
%light, the free ion and the labile Zn as they rely on both
%chemical species:
%unit growth:
       mup_l= min([mupl,Jmax_l*LZn_l,Jmax_l*LZnLb]); %Growth term
for large phytoplankton
       mupL = mup_l;         %Production term for the large phyto


%Grazing: the grazing equation is defined by Oschlies and
%Schartau 2005 for both zooplankton. However, we increase the
%large zoo grazing by multiplying the small by a factor 1.5:
%Unit grazing: (pmol Zn m^-3 s^-1)^2
G_s=((g_s*eps_s*x(4).^2/(g_s+eps_s*x(4).^2)));

G_l=1.5*((g_l*eps_l*x(8).^2/(g_l+eps_l*x(8).^2)));


%////////////////// set of equations to be integrated /////////
%Free Zn equation, x(1):
%Free Zn =  remin from det + dissociation of complexes labile
%+ dissociation of complexes non labile - uptake from small phyto
%- fraction uptake from large - formation of complexes labile and
non labile.
```

```
%Units for each term:
%remin detritus:[nmol Zn/L/s]
%dissociation complexes labile: [nmol/L/s]
%dissociation complexes non labbile: [nmol/L/s]
%uptake small phyto: [nmol Zn/L/s]
%uptake large phyto: [?]
%formation complexes labile and non labile: [(nmol Zn/L/s)^2]
xdot(1) = remin*x(6)+ kdLb * x(2) + kdLa * x(3)...
          -mupS*x(4)-mup1*mupL*x(8)-kfLa*La*x(1)-kfLb*Lb*x(1);


%Bioavailable Zn equation, x(2):
%Bioavailble Zn = exudation from small phyto + loss from small
grazing +
%loss from large grazing + exudation from zoo + formation
complexes labile - fraction uptake from
%large-dissociation of complexes labiles
%Units for each term:
%exudation: [nmol/L/s]
%grazing: [nmol/L/s]
%exudation zoo: [nmol Zn/L/s]
%Dissociation complexes:[(nmol Zn/L/s)^2]
%uptake large phyto: [?]
%Formation complexes:[nmol/L/s]
xdot(2)    =    exup_s*x(4)+    (1-gam_s)*G_s*x(5)+    exuz_s*x(5)+
           kfLb*Lb*x(1)-(1-mup1)*mupL*x(8)-kdLb*x(2);

%Non bioavailable Zn equation, x(3):
%Non bioavailable Zn = formation complexes non labile + loss from
%large grazing- dissociation complexes non labile - remi in
%detritus
%Units for each term:
%Formation complexes: [[(nmol Zn/L/s)_2]
%Grazing: [nmol/L/s]
%formation complexes: [nmol/l/s]
%exudation Zn: [nmol/L/s]
xdot(3)= kfLa*La*x(1)+ (1-gam_l)*G_l*x(9)-kdLa*x(3);

%Phytoplankton equation, x(4):
%Phyto rate = growth term - grazing by small zoo - mortality
%phyto - exudation in Zn pools
%Units for each term:
%uptake phyto:[?]
%Grazing: [nmol Zn/L/s]
%Mortality: [nmol Zn/L/s]
%Exudation phyto: [nmol/L/s]
xdot(4) = mupS*x(4)-G_s*x(5)-morp_s*x(4)-exup_s*x(4);

%Zooplankton equation, x(5):
%Zooplankton term = assimilation small phyto - exudation in Zn
%pools -square mortality zoo
%Units for each term:
%Grazing:[nmol Zn/L/s]
%exudation zoo:[nmol Zn/L/s]
%mortalite:[nmol/L/s]
xdot(5) = gam_s*G_s*x(5)-exuz_s*(x(5))-morz_s*x(5).*x(5);

%Detritus equation, x(6):
```

```
%Det term = square mortality of zoo (L and s) + mortality phyto
%(L and s) + remin from ZnLa pool-remin in Zn pool- sinking of
%particules
%Unit for each term:
%mortality zoo l:
%mortality phyto s:[nmol Zn/L/s]
%exudation Zn: [nmol Zn/L/s]
%remin: [nmol Zn/L/s]
%mortality zoo l:[nmol Zn/L/s]
%mortality phyto l: [nmol Zn/L/s]
%sinking particules:[m/s]
xdot(6)    =    morz_s*x(5).*x(5)+    morp_s*x(4)-    remin*x(6)+
morz_l*x(9).*x(9)+ morp_l*x(8) - w_sink/x(7).*x(6);

%Mixed layer depth equation:
%Unit:[m]
xdot(7)=0;

%Phytoplankton large ones equation, x(8):
%Large phyto term = Growth rate - grazing from large zoo -
%mortality of large phyto
%Units for each term:
%Uptake
%Grazing: [nmol Zn/L/s]
%mortalite: [nmol Zn/L/s]
xdot(8) = mup_l*x(8)-G_l*x(9)-morp_l*x(8);

%Zooplankton large equation, x(8):
%Large zoo term = assimilation of large phyto - square mortality
%of large zoo
%Unit for each term:
%grazing:[nmol Zn/L/s]
%mortality:[nmol Zn/L/s]
xdot(9) = gam_l*G_l*x(9)-morz_l*x(9).*x(9);


%//////////////////////////////////////////////////////////////

xdot=xdot'; %aos_Znpzd must return a column vector
```